

MIKE 21 & MIKE 3 FLOW MODEL FM
Hydrodynamic and Transport Module
Scientific Documentation



Agern Allé 5
DK-2970 Hørsholm
Denmark

Tel: +45 4516 9200
Support: +45 4516 9333
Fax: +45 4516 9292

mikebydhi@dhigroup.com
www.mikebydhi.com

PLEASE NOTE

COPYRIGHT

This document refers to proprietary computer software, which is protected by copyright. All rights are reserved. Copying or other reproduction of this manual or the related programs is prohibited without prior written consent of DHI. For details please refer to your 'DHI Software Licence Agreement'.

LIMITED LIABILITY

The liability of DHI is limited as specified in Section III of your 'DHI Software Licence Agreement':

'IN NO EVENT SHALL DHI OR ITS REPRESENTATIVES (AGENTS AND SUPPLIERS) BE LIABLE FOR ANY DAMAGES WHATSOEVER INCLUDING, WITHOUT LIMITATION, SPECIAL, INDIRECT, INCIDENTAL OR CONSEQUENTIAL DAMAGES OR DAMAGES FOR LOSS OF BUSINESS PROFITS OR SAVINGS, BUSINESS INTERRUPTION, LOSS OF BUSINESS INFORMATION OR OTHER PECUNIARY LOSS ARISING OUT OF THE USE OF OR THE INABILITY TO USE THIS DHI SOFTWARE PRODUCT, EVEN IF DHI HAS BEEN ADVISED OF THE POSSIBILITY OF SUCH DAMAGES. THIS LIMITATION SHALL APPLY TO CLAIMS OF PERSONAL INJURY TO THE EXTENT PERMITTED BY LAW. SOME COUNTRIES OR STATES DO NOT ALLOW THE EXCLUSION OR LIMITATION OF LIABILITY FOR CONSEQUENTIAL, SPECIAL, INDIRECT, INCIDENTAL DAMAGES AND, ACCORDINGLY, SOME PORTIONS OF THESE LIMITATIONS MAY NOT APPLY TO YOU. BY YOUR OPENING OF THIS SEALED PACKAGE OR INSTALLING OR USING THE SOFTWARE, YOU HAVE ACCEPTED THAT THE ABOVE LIMITATIONS OR THE MAXIMUM LEGALLY APPLICABLE SUBSET OF THESE LIMITATIONS APPLY TO YOUR PURCHASE OF THIS SOFTWARE.'

PRINTING HISTORY

June 2004	Edition 2004
August 2005	Edition 2005
April 2006	Edition 2007
December 2006.....	Edition 2007
October 2007	Edition 2008
January 2009.....	Edition 2009
February 2010.....	Edition 2009
July 2010	Edition 2011





CONTENTS

MIKE 21 & MIKE 3 FLOW MODEL FM Hydrodynamic and Transport Module Scientific Documentation

1	INTRODUCTION.....	1
2	GOVERNING EQUATIONS	3
2.1	3D Governing Equations in Cartesian Co-ordinates.....	3
2.1.1	Shallow water equations	3
2.1.2	Transport equations for salt and temperature.....	5
2.1.3	Transport equation for a scalar quantity.....	6
2.1.4	Turbulence model.....	7
2.1.5	Governing equations in Cartesian and sigma-co-ordinates.....	10
2.2	3D Governing Equations in Spherical and Sigma Co-ordinates.....	12
2.3	2D Governing Equations in Cartesian Co-ordinates.....	13
2.3.1	Shallow water equations	13
2.3.2	Transport equations for salt and temperature.....	14
2.3.3	Transport equations for a scalar quantity	15
2.4	2D Governing Equations in Spherical Co-ordinates.....	15
2.5	Bottom Stress	16
2.6	Wind Stress	17
2.7	Ice Coverage.....	18
2.8	Tidal Potential	19
2.9	Wave Radiation.....	20
2.10	Heat Exchange	21
2.10.1	Vaporisation	22
2.10.2	Convection	23
2.10.3	Short wave radiation	23
2.10.4	Long wave radiation.....	26
3	NUMERICAL SOLUTION	29
3.1	Spatial Discretization	29
3.1.1	Vertical Mesh	31
3.1.2	Shallow water equations	34
3.1.3	Transport equations.....	38
3.2	Time Integration.....	39
3.3	Boundary Conditions	40
3.3.1	Closed boundaries	40
3.3.2	Open boundaries.....	40
3.3.3	Flooding and drying	41



4	VALIDATION	43
4.1	Dam-break Flow through Sharp Bend	43
4.1.1	Physical experiments	43
4.1.2	Numerical experiments	45
4.1.3	Results.....	45
5	REFERENCES	49



1 INTRODUCTION

This document presents the scientific background for the new MIKE 21 & MIKE 3 Flow Model FM¹ modelling system developed by DHI Water & Environment. The objective is to provide the user with a detailed description of the flow and transport model equations, numerical discretization and solution methods. Also model validation is discussed in this document.

MIKE 21 & MIKE 3 Flow Model FM is based on a flexible mesh approach and it has been developed for applications within oceanographic, coastal and estuarine environments. The modelling system may also be applied for studies of overland flooding.

The system is based on the numerical solution of the two/three-dimensional incompressible Reynolds averaged Navier-Stokes equations invoking the assumptions of Boussinesq and of hydrostatic pressure. Thus, the model consists of continuity, momentum, temperature, salinity and density equations and it is closed by a turbulent closure scheme. For the 3D model the free surface is taken into account using a sigma-coordinate transformation approach.

The spatial discretization of the primitive equations is performed using a cell-centred finite volume method. The spatial domain is discretized by subdivision of the continuum into non-overlapping elements/cells. In the horizontal plane an unstructured grid is used while in the vertical domain in the 3D model a structured mesh is used. In the 2D model the elements can be triangles or quadrilateral elements. In the 3D model the elements can be prisms or bricks whose horizontal faces are triangles and quadrilateral elements, respectively.

¹ Including the MIKE 21 Flow Model FM (two-dimensional flow) and MIKE 3 Flow Model FM (three-dimensional flow)





2 GOVERNING EQUATIONS

2.1 3D Governing Equations in Cartesian Co-ordinates

2.1.1 Shallow water equations

The model is based on the solution of the three-dimensional incompressible Reynolds averaged Navier-Stokes equations, subject to the assumptions of Boussinesq and of hydrostatic pressure.

The local continuity equation is written as

$$\frac{\partial u}{\partial x} + \frac{\partial v}{\partial y} + \frac{\partial w}{\partial z} = S \quad (2.1)$$

and the two horizontal momentum equations for the x- and y-component, respectively

$$\begin{aligned} \frac{\partial u}{\partial t} + \frac{\partial u^2}{\partial x} + \frac{\partial vu}{\partial y} + \frac{\partial wu}{\partial z} = fv - g \frac{\partial \eta}{\partial x} - \frac{1}{\rho_0} \frac{\partial p_a}{\partial x} - \\ \frac{g}{\rho_0} \int_z^\eta \frac{\partial \rho}{\partial x} dz - \frac{1}{\rho_0 h} \left(\frac{\partial s_{xx}}{\partial x} + \frac{\partial s_{xy}}{\partial y} \right) + F_u + \frac{\partial}{\partial z} \left(\nu_t \frac{\partial u}{\partial z} \right) + u_s S \end{aligned} \quad (2.2)$$

$$\begin{aligned} \frac{\partial v}{\partial t} + \frac{\partial v^2}{\partial y} + \frac{\partial uv}{\partial x} + \frac{\partial wv}{\partial z} = -fu - g \frac{\partial \eta}{\partial y} - \frac{1}{\rho_0} \frac{\partial p_a}{\partial y} - \\ \frac{g}{\rho_0} \int_z^\eta \frac{\partial \rho}{\partial y} dz - \frac{1}{\rho_0 h} \left(\frac{\partial s_{yx}}{\partial x} + \frac{\partial s_{yy}}{\partial y} \right) + F_v + \frac{\partial}{\partial z} \left(\nu_t \frac{\partial v}{\partial z} \right) + v_s S \end{aligned} \quad (2.3)$$

where t is the time; x , y and z are the Cartesian co-ordinates; η is the surface elevation; d is the still water depth; $h = \eta + d$ is the total water depth; u , v and w are the velocity components in the x , y and z direction; $f = 2\Omega \sin \phi$ is the Coriolis parameter (Ω is the angular rate of revolution and ϕ the geographic latitude); g is the gravitational acceleration; ρ is the density of water; s_{xx} , s_{xy} , s_{yx} and s_{yy} are components of the radiation stress tensor; ν_t is the vertical turbulent (or eddy) viscosity; p_a is the atmospheric pressure; ρ_0 is the reference density of water. S is the magnitude of the discharge due to point sources and (u_s, v_s) is the velocity by which the water is discharged into the ambient water. The horizontal stress terms are described using a gradient-stress relation, which is simplified to



$$F_u = \frac{\partial}{\partial x} \left(2A \frac{\partial u}{\partial x} \right) + \frac{\partial}{\partial y} \left(A \left(\frac{\partial u}{\partial y} + \frac{\partial v}{\partial x} \right) \right) \quad (2.4)$$

$$F_v = \frac{\partial}{\partial x} \left(A \left(\frac{\partial u}{\partial y} + \frac{\partial v}{\partial x} \right) \right) + \frac{\partial}{\partial y} \left(2A \frac{\partial v}{\partial y} \right) \quad (2.5)$$

where A is the horizontal eddy viscosity.

The surface and bottom boundary condition for u , v and w are

At $z = \eta$:

$$\frac{\partial \eta}{\partial t} + u \frac{\partial \eta}{\partial x} + v \frac{\partial \eta}{\partial y} - w = 0, \quad \left(\frac{\partial u}{\partial z}, \frac{\partial v}{\partial z} \right) = \frac{1}{\rho_0 V_t} (\tau_{sx}, \tau_{sy}) \quad (2.6)$$

At $z = -d$:

$$u \frac{\partial d}{\partial x} + v \frac{\partial d}{\partial y} + w = 0, \quad \left(\frac{\partial u}{\partial z}, \frac{\partial v}{\partial z} \right) = \frac{1}{\rho_0 V_t} (\tau_{bx}, \tau_{by}) \quad (2.7)$$

where (τ_{sx}, τ_{sy}) and (τ_{bx}, τ_{by}) are the x and y components of the surface wind and bottom stresses.

The total water depth, h , can be obtained from the kinematic boundary condition at the surface, once the velocity field is known from the momentum and continuity equations. However, a more robust equation is obtained by vertical integration of the local continuity equation

$$\frac{\partial h}{\partial t} + \frac{\partial h \bar{u}}{\partial x} + \frac{\partial h \bar{v}}{\partial y} = hS + \hat{P} - \hat{E} \quad (2.8)$$

where \hat{P} and \hat{E} are precipitation and evaporation rates, respectively, and \bar{u} and \bar{v} are the depth-averaged velocities

$$h \bar{u} = \int_{-d}^{\eta} u dz, \quad h \bar{v} = \int_{-d}^{\eta} v dz \quad (2.9)$$

The fluid is assumed to be incompressible. Hence, the density, ρ , does not depend on the pressure, but only on the temperature, T , and the salinity, s , via the equation of state

$$\rho = \rho(T, s) \quad (2.10)$$



Here the UNESCO equation of state is used (see UNESCO, 1981).

2.1.2 Transport equations for salt and temperature

The transports of temperature, T , and salinity, s , follow the general transport-diffusion equations as

$$\frac{\partial T}{\partial t} + \frac{\partial uT}{\partial x} + \frac{\partial vT}{\partial y} + \frac{\partial wT}{\partial z} = F_T + \frac{\partial}{\partial z} \left(D_v \frac{\partial T}{\partial z} \right) + \hat{H} + T_s S \quad (2.11)$$

$$\frac{\partial s}{\partial t} + \frac{\partial us}{\partial x} + \frac{\partial vs}{\partial y} + \frac{\partial ws}{\partial z} = F_s + \frac{\partial}{\partial z} \left(D_v \frac{\partial s}{\partial z} \right) + s_s S \quad (2.12)$$

where D_v is the vertical turbulent (eddy) diffusion coefficient. \hat{H} is a source term due to heat exchange with the atmosphere. T_s and s_s are the temperature and the salinity of the source. F are the horizontal diffusion terms defined by

$$(F_T, F_s) = \left[\frac{\partial}{\partial x} \left(D_h \frac{\partial}{\partial x} \right) + \frac{\partial}{\partial y} \left(D_h \frac{\partial}{\partial y} \right) \right] (T, s) \quad (2.13)$$

where D_h is the horizontal diffusion coefficient. The diffusion coefficients can be related to the eddy viscosity

$$D_h = \frac{A}{\sigma_T} \quad \text{and} \quad D_v = \frac{v_t}{\sigma_T} \quad (2.14)$$

where σ_T is the Prandtl number. In many applications a constant Prandtl number can be used (see Rodi (1984)).

The surface and bottom boundary conditions for the temperature are

At $z = \eta$:

$$D_h \frac{\partial T}{\partial z} = \frac{Q_n}{\rho_0 c_p} + T_p \hat{P} - T_e \hat{E} \quad (2.15)$$

At $z = -d$:

$$\frac{\partial T}{\partial z} = 0 \quad (2.16)$$



where Q_n is the surface net heat flux and $c_p = 4217 \text{ J}/(\text{kg} \cdot ^\circ\text{K})$ is the specific heat of the water. A detailed description for determination of \hat{H} and Q_n is given in Section 2.7.

The surface and bottom boundary conditions for the salinity are

At $z = \eta$:

$$\frac{\partial s}{\partial z} = 0 \quad (2.17)$$

At $z = -d$:

$$\frac{\partial s}{\partial z} = 0 \quad (2.18)$$

When heat exchange from the atmosphere is included, the evaporation is defined as

$$\hat{E} = \begin{cases} \frac{q_v}{\rho_0 l_v} & q_v > 0 \\ 0 & q_v \leq 0 \end{cases} \quad (2.19)$$

where q_v is the latent heat flux and $l_v = 2.5 \cdot 10^6$ is the latent heat of vaporisation of water.

2.1.3 Transport equation for a scalar quantity

The conservation equation for a scalar quantity is given by

$$\frac{\partial C}{\partial t} + \frac{\partial uC}{\partial x} + \frac{\partial vC}{\partial y} + \frac{\partial wC}{\partial z} = F_C + \frac{\partial}{\partial z} \left(D_v \frac{\partial C}{\partial z} \right) - k_p C + C_s S \quad (2.20)$$

where C is the concentration of the scalar quantity, k_p is the linear decay rate of the scalar quantity, C_s is the concentration of the scalar quantity at the source and D_v is the vertical diffusion coefficient. F_F is the horizontal diffusion term defined by

$$F_C = \left[\frac{\partial}{\partial x} \left(D_h \frac{\partial}{\partial x} \right) + \frac{\partial}{\partial y} \left(D_h \frac{\partial}{\partial y} \right) \right] C \quad (2.21)$$

where D_h is the horizontal diffusion coefficient.



2.1.4 Turbulence model

The turbulence is modelled using an eddy viscosity concept. The eddy viscosity is often described separately for the vertical and the horizontal transport. Here several turbulence models can be applied: a constant viscosity, a vertically parabolic viscosity and a standard k- ε model (Rodi, 1984). In many numerical simulations the small-scale turbulence can not be resolved with the chosen spatial resolution. This kind of turbulence can be approximated using sub-grid scale models.

Vertical eddy viscosity

The eddy viscosity derived from the log-law is calculated by

$$v_t = U_\tau h \left(c_1 \frac{z+d}{h} + c_2 \left(\frac{z+d}{h} \right)^2 \right) \quad (2.22)$$

where $U_\tau = \max(U_{\tau s}, U_{\tau b})$ and c_1 and c_2 are two constants. $U_{\tau s}$ and $U_{\tau b}$ are the friction velocities associated with the surface and bottom stresses, $c_1 = 0.41$ and $c_2 = -0.41$ give the standard parabolic profile.

In applications with stratification the effects of buoyancy can be included explicitly. This is done through the introduction of a Richardson number dependent damping of the eddy viscosity coefficient, when a stable stratification occurs. The damping is a generalisation of the Munk-Anderson formulation (Munk and Anderson, 1948)

$$v_t = v_t^* (1 + a Ri)^{-b} \quad (2.23)$$

where v_t^* is the undamped eddy viscosity and Ri is the local gradient Richardson number

$$Ri = -\frac{g}{\rho_0} \frac{\partial \rho}{\partial z} \left(\left(\frac{\partial u}{\partial z} \right)^2 + \left(\frac{\partial v}{\partial z} \right)^2 \right)^{-1} \quad (2.24)$$

$a = 10$ and $b = 0.5$ are empirical constants.

In the k- ε model the eddy-viscosity is derived from turbulence parameters k and ε as

$$v_t = c_\mu \frac{k^2}{\varepsilon} \quad (2.25)$$



where k is the turbulent kinetic energy per unit mass (TKE), ε is the dissipation of TKE and c_μ is an empirical constant.

The turbulent kinetic energy, k , and the dissipation of TKE, ε , are obtained from the following transport equations

$$\frac{\partial k}{\partial t} + \frac{\partial uk}{\partial x} + \frac{\partial vk}{\partial y} + \frac{\partial wk}{\partial z} = F_k + \frac{\partial}{\partial z} \left(\frac{v_t}{\sigma_k} \frac{\partial k}{\partial z} \right) + P + B - \varepsilon \quad (2.26)$$

$$\begin{aligned} \frac{\partial \varepsilon}{\partial t} + \frac{\partial u\varepsilon}{\partial x} + \frac{\partial v\varepsilon}{\partial y} + \frac{\partial w\varepsilon}{\partial z} = \\ F_\varepsilon + \frac{\partial}{\partial z} \left(\frac{v_t}{\sigma_\varepsilon} \frac{\partial \varepsilon}{\partial z} \right) + \frac{\varepsilon}{k} (c_{1\varepsilon} P + c_{3\varepsilon} B - c_{2\varepsilon} \varepsilon) \end{aligned} \quad (2.27)$$

where the shear production, P , and the buoyancy production, B , are given as

$$P = \frac{\tau_{xz}}{\rho_0} \frac{\partial u}{\partial z} + \frac{\tau_{yz}}{\rho_0} \frac{\partial v}{\partial z} \approx v_t \left(\left(\frac{\partial u}{\partial z} \right)^2 + \left(\frac{\partial v}{\partial z} \right)^2 \right) \quad (2.28)$$

$$B = -\frac{v_t}{\sigma_t} N^2 \quad (2.29)$$

with the Brunt-Väisälä frequency, N , defined by

$$N^2 = -\frac{g}{\rho_0} \frac{\partial \rho}{\partial z} \quad (2.30)$$

σ_t is the turbulent Prandtl number and σ_k , σ_ε , $c_{1\varepsilon}$, $c_{2\varepsilon}$ and $c_{3\varepsilon}$ are empirical constants. F are the horizontal diffusion terms defined by

$$(F_k, F_\varepsilon) = \left[\frac{\partial}{\partial x} \left(D_h \frac{\partial}{\partial x} \right) + \frac{\partial}{\partial y} \left(D_h \frac{\partial}{\partial y} \right) \right] (k, \varepsilon) \quad (2.31)$$

The horizontal diffusion coefficients are given by $D_h = A/\sigma_k$ and $D_h = A/\sigma_\varepsilon$, respectively.

Several carefully calibrated empirical coefficients enter the k- ε turbulence model. The empirical constants are listed in (2.47) (see Rodi, 1984).

Table 2.1 Empirical constants in the k - ε model.

c_μ	$c_{1\varepsilon}$	$c_{2\varepsilon}$	$c_{3\varepsilon}$	σ_t	σ_k	σ_ε
0.09	1.44	1.92	0	0.9	1.0	1.3

At the surface the boundary conditions for the turbulent kinetic energy and its rate of dissipation depend on the wind shear, $U_{\tau s}$

At $z = \eta$:

$$k = \frac{1}{\sqrt{c_\mu}} U_{\tau s}^2 \quad (2.32)$$

$$\varepsilon = \frac{U_{\tau s}^3}{\kappa \Delta z_b} \quad \text{for } U_{\tau s} > 0$$

$$\frac{\partial k}{\partial z} = 0 \quad \varepsilon = \frac{(k \sqrt{c_\mu})^{3/2}}{a \kappa h} \quad \text{for } U_{\tau s} = 0 \quad (2.33)$$

where $\kappa = 0.4$ is the von Kármán constant, $a = 0.07$ is an empirical constant and Δz_s is the distance from the surface where the boundary condition is imposed. At the seabed the boundary conditions are

At $z = -d$:

$$k = \frac{1}{\sqrt{c_\mu}} U_{\tau b}^2 \quad \varepsilon = \frac{U_{\tau b}^3}{\kappa \Delta z_b} \quad (2.34)$$

where Δz_b is the distance from the bottom where the boundary condition is imposed.

Horizontal eddy viscosity

In many applications a constant eddy viscosity can be used for the horizontal eddy viscosity. Alternatively, Smagorinsky (1963) proposed to express sub-grid scale transports by an effective eddy viscosity related to a characteristic length scale. The subgrid scale eddy viscosity is given by

$$A = c_s^2 l^2 \sqrt{2S_{ij}S_{ij}} \quad (2.35)$$

where c_s is a constant, l is a characteristic length and the deformation rate is given by

$$S_{ij} = \frac{1}{2} \left(\frac{\partial u_i}{\partial x_j} + \frac{\partial u_j}{\partial x_i} \right) \quad (i, j = 1, 2) \quad (2.36)$$

2.1.5 Governing equations in Cartesian and sigma-co-ordinates

The equations are solved using a vertical σ -transformation

$$\sigma = \frac{z - z_b}{h}, \quad x' = x, \quad y' = y \quad (2.37)$$

where σ varies between 0 at the bottom and 1 at the surface. The co-ordinate transformation implies relations such as

$$\frac{\partial}{\partial z} = \frac{1}{h} \frac{\partial}{\partial \sigma} \quad (2.38)$$

$$\left(\frac{\partial}{\partial x}, \frac{\partial}{\partial y} \right) = \left(\frac{\partial}{\partial x'} - \frac{1}{h} \left(-\frac{\partial d}{\partial x} + \sigma \frac{\partial h}{\partial x} \right) \frac{\partial}{\partial \sigma}, \frac{\partial}{\partial y'} - \frac{1}{h} \left(-\frac{\partial d}{\partial y} + \sigma \frac{\partial h}{\partial y} \right) \frac{\partial}{\partial \sigma} \right) \quad (2.39)$$

In this new co-ordinate system the governing equations are given as

$$\frac{\partial h}{\partial t} + \frac{\partial hu}{\partial x'} + \frac{\partial hv}{\partial y'} + \frac{\partial h\omega}{\partial \sigma} = hS \quad (2.40)$$

$$\begin{aligned} \frac{\partial hu}{\partial t} + \frac{\partial hu^2}{\partial x'} + \frac{\partial huv}{\partial y'} + \frac{\partial h\omega u}{\partial \sigma} &= fvh - gh \frac{\partial \eta}{\partial x'} - \frac{h}{\rho_0} \frac{\partial p_a}{\partial x'} - \\ &\frac{hg}{\rho_0} \int_z^\eta \frac{\partial \rho}{\partial x} dz - \frac{1}{\rho_0} \left(\frac{\partial s_{xx}}{\partial x} + \frac{\partial s_{xy}}{\partial y} \right) + hF_u + \frac{\partial}{\partial \sigma} \left(\frac{v_v}{h} \frac{\partial u}{\partial \sigma} \right) + hu_s S \end{aligned} \quad (2.41)$$

$$\begin{aligned} \frac{\partial hv}{\partial t} + \frac{\partial huv}{\partial x'} + \frac{\partial hv^2}{\partial y'} + \frac{\partial h\omega v}{\partial \sigma} &= -fuh - gh \frac{\partial \eta}{\partial y'} - \frac{h}{\rho_0} \frac{\partial p_a}{\partial y'} - \\ &\frac{hg}{\rho_0} \int_z^\eta \frac{\partial \rho}{\partial y} dz - \frac{1}{\rho_0} \left(\frac{\partial s_{yx}}{\partial x} + \frac{\partial s_{yy}}{\partial y} \right) + hF_v + \frac{\partial}{\partial \sigma} \left(\frac{v_v}{h} \frac{\partial v}{\partial \sigma} \right) + hv_s S \end{aligned} \quad (2.42)$$

$$\begin{aligned} \frac{\partial hT}{\partial t} + \frac{\partial huT}{\partial x'} + \frac{\partial hvT}{\partial y'} + \frac{\partial h\omega T}{\partial \sigma} &= \\ &hF_T + \frac{\partial}{\partial \sigma} \left(\frac{D_v}{h} \frac{\partial T}{\partial \sigma} \right) + h\bar{H} + hT_s S \end{aligned} \quad (2.43)$$

$$\frac{\partial hs}{\partial t} + \frac{\partial hus}{\partial x'} + \frac{\partial hvs}{\partial y'} + \frac{\partial h\omega s}{\partial \sigma} = hF_s + \frac{\partial}{\partial \sigma} \left(\frac{D_v}{h} \frac{\partial s}{\partial \sigma} \right) + hs_s S \quad (2.44)$$



$$\begin{aligned} \frac{\partial hk}{\partial t} + \frac{\partial huk}{\partial x'} + \frac{\partial hvk}{\partial y'} + \frac{\partial h\omega k}{\partial \sigma} = \\ hF_k + \frac{1}{h} \frac{\partial}{\partial \sigma} \left(\frac{v_t}{\sigma_k} \frac{\partial k}{\partial \sigma} \right) + h(P + B - \varepsilon) \end{aligned} \quad (2.45)$$

$$\begin{aligned} \frac{\partial h\varepsilon}{\partial t} + \frac{\partial hu\varepsilon}{\partial x'} + \frac{\partial hv\varepsilon}{\partial y'} + \frac{\partial h\omega\varepsilon}{\partial \sigma} = \\ hF_\varepsilon + \frac{1}{h} \frac{\partial}{\partial \sigma} \left(\frac{v_t}{\sigma_\varepsilon} \frac{\partial \varepsilon}{\partial \sigma} \right) + h \frac{\varepsilon}{k} (c_{1\varepsilon}P + c_{3\varepsilon}B - c_{2\varepsilon}\varepsilon) \end{aligned} \quad (2.46)$$

$$\frac{\partial hC}{\partial t} + \frac{\partial huC}{\partial x'} + \frac{\partial hvC}{\partial y'} + \frac{\partial h\omega C}{\partial \sigma} = hF_C + \frac{\partial}{\partial \sigma} \left(\frac{D_v}{h} \frac{\partial C}{\partial \sigma} \right) - hk_p C + hC_s' \quad (2.47)$$

The modified vertical velocity is defined by

$$\omega = \frac{1}{h} \left[w + u \frac{\partial d}{\partial x'} + v \frac{\partial d}{\partial y'} - \sigma \left(\frac{\partial h}{\partial t} + u \frac{\partial h}{\partial x'} + v \frac{\partial h}{\partial y'} \right) \right] \quad (2.48)$$

The modified vertical velocity is the velocity across a level of constant σ . The horizontal diffusion terms are defined as

$$hF_u \approx \frac{\partial}{\partial x} \left(2hA \frac{\partial u}{\partial x} \right) + \frac{\partial}{\partial y} \left(hA \left(\frac{\partial u}{\partial y} + \frac{\partial v}{\partial x} \right) \right) \quad (2.49)$$

$$hF_v \approx \frac{\partial}{\partial x} \left(hA \left(\frac{\partial u}{\partial y} + \frac{\partial v}{\partial x} \right) \right) + \frac{\partial}{\partial y} \left(2hA \frac{\partial v}{\partial y} \right) \quad (2.50)$$

$$\begin{aligned} h(F_T, F_s, F_k, F_\varepsilon, F_c) \approx \\ \left[\frac{\partial}{\partial x} \left(hD_h \frac{\partial}{\partial x} \right) + \frac{\partial}{\partial y} \left(hD_h \frac{\partial}{\partial y} \right) \right] (T, s, k, \varepsilon, C) \end{aligned} \quad (2.51)$$

The boundary condition at the free surface and at the bottom are given as follows

At $\sigma=1$:

$$\omega = 0, \quad \left(\frac{\partial u}{\partial \sigma}, \frac{\partial v}{\partial \sigma} \right) = \frac{h}{\rho_0 v_t} (\tau_{sx}, \tau_{sy}) \quad (2.52)$$

At $\sigma=0$:

$$(2.53)$$



$$\omega = 0, \quad \left(\frac{\partial u}{\partial \sigma}, \frac{\partial v}{\partial \sigma} \right) = \frac{h}{\rho_0 v_t} (\tau_{bx}, \tau_{by})$$

The equation for determination of the water depth is not changed by the co-ordinate transformation. Hence, it is identical to Eq. (2.6).

2.2 3D Governing Equations in Spherical and Sigma Co-ordinates

In spherical co-ordinates the independent variables are the longitude, λ , and the latitude, ϕ . The horizontal velocity field (u, v) is defined by

$$u = R \cos \phi \frac{d\lambda}{dt} \quad v = R \frac{d\phi}{dt} \quad (2.54)$$

where R is the radius of the earth.

In this co-ordinate system the governing equations are given as (all superscripts indicating the horizontal co-ordinate in the new co-ordinate system are dropped in the following for notational convenience)

$$\frac{\partial h}{\partial t} + \frac{1}{R \cos \phi} \left(\frac{\partial hu}{\partial \lambda} + \frac{\partial hv \cos \phi}{\partial \phi} \right) + \frac{\partial h\omega}{\partial \sigma} = hS \quad (2.55)$$

$$\begin{aligned} \frac{\partial hu}{\partial t} + \frac{1}{R \cos \phi} \left(\frac{\partial hu^2}{\partial \lambda} + \frac{\partial hvu \cos \phi}{\partial \phi} \right) + \frac{\partial h\omega u}{\partial \sigma} = & \left(f + \frac{u}{R} \tan \phi \right) v h - \\ & \frac{1}{R \cos \phi} \left(gh \frac{\partial \eta}{\partial \lambda} + \frac{1}{\rho_0} \frac{\partial p_a}{\partial \lambda} + \frac{g}{\rho_0} \int_z^\eta \frac{\partial \rho}{\partial \lambda} dz + \frac{1}{\rho_0} \left(\frac{\partial s_{xx}}{\partial \lambda} + \cos \phi \frac{\partial s_{xy}}{\partial \phi} \right) \right) + \\ & hF_u + \frac{\partial}{\partial \sigma} \left(\frac{v_v}{h} \frac{\partial u}{\partial \sigma} \right) + hu_s S \end{aligned} \quad (2.56)$$

$$\begin{aligned} \frac{\partial hv}{\partial t} + \frac{1}{R \cos \phi} \left(\frac{\partial huv}{\partial \lambda} + \frac{\partial hv^2 \cos \phi}{\partial \phi} \right) + \frac{\partial h\omega v}{\partial \sigma} = & - \left(f + \frac{u}{R} \tan \phi \right) u h - \\ & \frac{1}{R} \left(gh \frac{\partial \eta}{\partial \phi} + \frac{1}{\rho_0} \frac{\partial p_a}{\partial \phi} + \frac{g}{\rho_0} \int_z^\eta \frac{\partial \rho}{\partial \phi} dz + \frac{1}{\rho_0} \left(\frac{1}{\cos \phi} \frac{\partial s_{yx}}{\partial \lambda} + \frac{\partial s_{yy}}{\partial \phi} \right) \right) + \\ & hF_v + \frac{\partial}{\partial \sigma} \left(\frac{v_v}{h} \frac{\partial v}{\partial \sigma} \right) + hv_s S \end{aligned} \quad (2.57)$$

$$\begin{aligned} \frac{\partial hT}{\partial t} + \frac{1}{R \cos \phi} \left(\frac{\partial huT}{\partial \lambda} + \frac{\partial hvT \cos \phi}{\partial \phi} \right) + \frac{\partial h\omega T}{\partial \sigma} = \\ hF_T + \frac{\partial}{\partial \sigma} \left(\frac{D_v}{h} \frac{\partial T}{\partial \sigma} \right) + h\hat{H} + hT_s S \end{aligned} \quad (2.58)$$



$$\begin{aligned} \frac{\partial hs}{\partial t} + \frac{1}{R \cos \phi} \left(\frac{\partial hus}{\partial \lambda} + \frac{\partial hvs \cos \phi}{\partial \phi} \right) + \frac{\partial h\omega s}{\partial \sigma} = \\ hF_s + \frac{\partial}{\partial \sigma} \left(\frac{D_v}{h} \frac{\partial s}{\partial \sigma} \right) + hs_s S \end{aligned} \quad (2.59)$$

$$\begin{aligned} \frac{\partial hk}{\partial t} + \frac{1}{R \cos \phi} \left(\frac{\partial huk}{\partial \lambda} + \frac{\partial hvk \cos \phi}{\partial \phi} \right) + \frac{\partial h\omega k}{\partial \sigma} = \\ hF_k + \frac{1}{h} \frac{\partial}{\partial \sigma} \left(\frac{v_t}{\sigma_k} \frac{\partial k}{\partial \sigma} \right) + h(P + B - \varepsilon) \end{aligned} \quad (2.60)$$

$$\begin{aligned} \frac{\partial h\varepsilon}{\partial t} + \frac{1}{R \cos \phi} \left(\frac{\partial hu\varepsilon}{\partial \lambda} + \frac{\partial hv\varepsilon \cos \phi}{\partial \phi} \right) + \frac{\partial h\omega\varepsilon}{\partial \sigma} = \\ hF_\varepsilon + \frac{1}{h} \frac{\partial}{\partial \sigma} \left(\frac{v_t}{\sigma_\varepsilon} \frac{\partial \varepsilon}{\partial \sigma} \right) + h \frac{\varepsilon}{k} (c_{1\varepsilon} P + c_{3\varepsilon} B - c_{2\varepsilon} \varepsilon) \end{aligned} \quad (2.61)$$

$$\begin{aligned} \frac{\partial hC}{\partial t} + \frac{1}{R \cos \phi} \left(\frac{\partial huC}{\partial \lambda} + \frac{\partial hvC \cos \phi}{\partial \phi} \right) + \frac{\partial h\omega C}{\partial \sigma} = \\ hF_C + \frac{\partial}{\partial \sigma} \left(\frac{D_v}{h} \frac{\partial C}{\partial \sigma} \right) - hk_p C + hC_s S \end{aligned} \quad (2.62)$$

The modified vertical velocity in spherical co-ordinates is defined by

$$\omega = \frac{1}{h} \left[w + \frac{u}{R \cos \phi} \frac{\partial d}{\partial \lambda} + \frac{v}{R} \frac{\partial d}{\partial \phi} - \sigma \left(\frac{\partial h}{\partial t} + \frac{u}{R \cos \phi} \frac{\partial h}{\partial \lambda} + \frac{v}{R} \frac{\partial h}{\partial \phi} \right) \right] \quad (2.63)$$

The equation determining the water depth in spherical co-ordinates is given as

$$\frac{\partial h}{\partial t} + \frac{1}{R \cos \phi} \left(\frac{\partial h\bar{u}}{\partial \lambda} + \frac{\partial h\bar{v} \cos \phi}{\partial \phi} \right) = hS \quad (2.64)$$

2.3 2D Governing Equations in Cartesian Co-ordinates

2.3.1 Shallow water equations

Integration of the horizontal momentum equations and the continuity equation over depth $h = \eta + d$ the following two-dimensional shallow water equations are obtained

$$\frac{\partial h}{\partial t} + \frac{\partial h\bar{u}}{\partial x} + \frac{\partial h\bar{v}}{\partial y} = hS \quad (2.65)$$



$$\begin{aligned} \frac{\partial h\bar{u}}{\partial t} + \frac{\partial h\bar{u}^2}{\partial x} + \frac{\partial h\bar{v}\bar{u}}{\partial y} &= f\bar{v}h - gh \frac{\partial \eta}{\partial x} - \frac{h}{\rho_0} \frac{\partial p_a}{\partial x} - \\ &\frac{gh^2}{2\rho_0} \frac{\partial \rho}{\partial x} + \frac{\tau_{sx}}{\rho_0} - \frac{\tau_{bx}}{\rho_0} - \frac{1}{\rho_0} \left(\frac{\partial s_{xx}}{\partial x} + \frac{\partial s_{xy}}{\partial y} \right) + \\ &\frac{\partial}{\partial x} (hT_{xx}) + \frac{\partial}{\partial y} (hT_{xy}) + hu_s S \end{aligned} \quad (2.66)$$

$$\begin{aligned} \frac{\partial h\bar{v}}{\partial t} + \frac{\partial h\bar{u}\bar{v}}{\partial x} + \frac{\partial h\bar{v}^2}{\partial y} &= -f\bar{u}h - gh \frac{\partial \eta}{\partial y} - \frac{h}{\rho_0} \frac{\partial p_a}{\partial y} - \\ &\frac{gh^2}{2\rho_0} \frac{\partial \rho}{\partial y} + \frac{\tau_{sy}}{\rho_0} - \frac{\tau_{by}}{\rho_0} - \frac{1}{\rho_0} \left(\frac{\partial s_{yx}}{\partial x} + \frac{\partial s_{yy}}{\partial y} \right) + \\ &\frac{\partial}{\partial x} (hT_{xy}) + \frac{\partial}{\partial y} (hT_{yy}) + hv_s S \end{aligned} \quad (2.67)$$

The overbar indicates a depth average value. For example, \bar{u} and \bar{v} are the depth-averaged velocities defined by

$$h\bar{u} = \int_{-d}^{\eta} u dz, \quad h\bar{v} = \int_{-d}^{\eta} v dz \quad (2.68)$$

The lateral stresses T_{ij} include viscous friction, turbulent friction and differential advection. They are estimated using an eddy viscosity formulation based on of the depth average velocity gradients

$$T_{xx} = 2A \frac{\partial \bar{u}}{\partial x}, \quad T_{xy} = A \left(\frac{\partial \bar{u}}{\partial y} + \frac{\partial \bar{v}}{\partial x} \right), \quad T_{yy} = 2A \frac{\partial \bar{v}}{\partial y} \quad (2.69)$$

2.3.2 Transport equations for salt and temperature

Integrating the transport equations for salt and temperature over depth the following two-dimensional transport equations are obtained

$$\frac{\partial h\bar{T}}{\partial t} + \frac{\partial h\bar{u}\bar{T}}{\partial x} + \frac{\partial h\bar{v}\bar{T}}{\partial y} = hF_T + h\hat{H} + hT_s S \quad (2.70)$$

$$\frac{\partial h\bar{s}}{\partial t} + \frac{\partial h\bar{u}\bar{s}}{\partial x} + \frac{\partial h\bar{v}\bar{s}}{\partial y} = hF_s + hs_s S \quad (2.71)$$

where \bar{T} and \bar{s} is the depth average temperature and salinity.



2.3.3 Transport equations for a scalar quantity

Integrating the transport equations for a scalar quantity over depth the following two-dimensional transport equations are obtained

$$\frac{\partial h\bar{C}}{\partial t} + \frac{\partial h\bar{u}\bar{C}}{\partial x} + \frac{\partial h\bar{v}\bar{C}}{\partial y} = hF_C - hk_p\bar{C} + hC_sS \quad (2.72)$$

where \bar{C} is the depth average scalar quantity.

2.4 2D Governing Equations in Spherical Co-ordinates

In spherical co-ordinates the independent variables are the longitude, λ , and the latitude, ϕ . The horizontal velocity field (u, v) is defined by

$$\bar{u} = R \cos \phi \frac{d\lambda}{dt} \quad \bar{v} = R \frac{d\phi}{dt} \quad (2.73)$$

where R is the radius of the earth.

In spherical co-ordinates the governing equation can be written

$$\frac{\partial h}{\partial t} + \frac{1}{R \cos \phi} \left(\frac{\partial h\bar{u}}{\partial \lambda} + \frac{\partial h\bar{v} \cos \phi}{\partial \phi} \right) = 0 \quad (2.74)$$

$$\begin{aligned} \frac{\partial h\bar{u}}{\partial t} + \frac{1}{R \cos \phi} \left(\frac{\partial h\bar{u}^2}{\partial \lambda} + \frac{\partial h\bar{v}\bar{u} \cos \phi}{\partial \phi} \right) &= \left(f + \frac{\bar{u}}{R} \tan \phi \right) \bar{v}h \\ &- \frac{1}{R \cos \phi} \left(gh \frac{\partial \eta}{\partial \lambda} - \frac{h}{\rho_0} \frac{\partial p_a}{\partial \lambda} + \frac{gh^2}{2\rho_0} \frac{\partial \rho}{\partial \lambda} + \frac{1}{\rho_0} \left(\frac{\partial s_{xx}}{\partial \lambda} + \cos \phi \frac{\partial s_{xy}}{\partial \phi} \right) \right) + \\ &\frac{\tau_{xx} - \tau_{bx}}{\rho_0} + \frac{\partial}{\partial x} (hT_{xx}) + \frac{\partial}{\partial y} (hT_{xy}) + hu_s S \end{aligned} \quad (2.75)$$

$$\begin{aligned} \frac{\partial h\bar{v}}{\partial t} + \frac{1}{R \cos \phi} \left(\frac{\partial h\bar{u}\bar{v}}{\partial \lambda} + \frac{\partial h\bar{v}^2 \cos \phi}{\partial \phi} \right) &= - \left(f + \frac{\bar{u}}{R} \tan \phi \right) \bar{u}h \\ &- \frac{1}{R} \left(gh \frac{\partial \eta}{\partial \phi} - \frac{h}{\rho_0} \frac{\partial p_a}{\partial \phi} + \frac{gh^2}{2\rho_0} \frac{\partial \rho}{\partial \phi} + \frac{1}{\rho_0} \left(\frac{1}{\cos \phi} \frac{\partial s_{yx}}{\partial \lambda} + \frac{\partial s_{yy}}{\partial \phi} \right) \right) + \\ &\frac{\tau_{sy} - \tau_{by}}{\rho_0} + \frac{\partial}{\partial x} (hT_{xy}) + \frac{\partial}{\partial y} (hT_{yy}) + hv_s S \end{aligned} \quad (2.76)$$

$$\frac{\partial h\bar{T}}{\partial t} + \frac{1}{R \cos \phi} \left(\frac{\partial h\bar{u}\bar{T}}{\partial \lambda} + \frac{\partial h\bar{v}\bar{T} \cos \phi}{\partial \phi} \right) = hF_T + h\hat{H} + hT_s S \quad (2.77)$$



$$\frac{\partial h\bar{s}}{\partial t} + \frac{1}{R \cos \phi} \left(\frac{\partial h\bar{u}\bar{s}}{\partial \lambda} + \frac{\partial h\bar{v}\bar{s} \cos \phi}{\partial \phi} \right) = hF_s + hS_s S \quad (2.78)$$

$$\frac{\partial h\bar{C}}{\partial t} + \frac{1}{R \cos \phi} \left(\frac{\partial h\bar{u}\bar{C}}{\partial \lambda} + \frac{\partial h\bar{v}\bar{C} \cos \phi}{\partial \phi} \right) = hF_C - hk_p \bar{C} + hC_s S \quad (2.79)$$

2.5 Bottom Stress

The bottom stress, $\vec{\tau}_b = (\tau_{bx}, \tau_{by})$, is determined by a quadratic friction law

$$\frac{\vec{\tau}_b}{\rho_0} = c_f \vec{u}_b |\vec{u}_b| \quad (2.80)$$

where c_f is the drag coefficient and $\vec{u}_b = (u_b, v_b)$ is the flow velocity above the bottom. The friction velocity associated with the bottom stress is given by

$$U_{\tau b} = \sqrt{c_f |\vec{u}_b|^2} \quad (2.81)$$

For two-dimensional calculations \vec{u}_b is the depth-average velocity and the drag coefficient can be determined from the Chezy number, C , or the Manning number, M

$$c_f = \frac{g}{C^2} \quad (2.82)$$

$$c_f = \frac{g}{(Mh^{1/6})^2} \quad (2.83)$$

For three-dimensional calculations \vec{u}_b is the velocity at a distance Δz_b above the sea bed and the drag coefficient is determined by assuming a logarithmic profile between the seabed and a point Δz_b above the seabed

$$c_f = \frac{1}{\left(\frac{1}{\kappa} \ln \left(\frac{\Delta z_b}{z_0} \right) \right)^2} \quad (2.84)$$



where $\kappa=0.4$ is the von Kármán constant and z_0 is the bed roughness length scale. When the boundary surface is rough, z_0 , depends on the roughness height, k_s

$$z_0 = mk_s \quad (2.85)$$

where m is approximately $1/30$.

Note, that the Manning number can be estimated from the bed roughness length using the following

$$M = \frac{25.4}{k_s^{1/6}} \quad (2.86)$$

2.6 Wind Stress

In areas not covered by ice the surface stress, $\vec{\tau}_s = (\tau_{sx}, \tau_{sy})$, is determined by the winds above the surface. The stress is given by the following empirical relation

$$\vec{\tau}_s = \rho_a c_d |\vec{u}_w| \vec{u}_w \quad (2.87)$$

where ρ_a is the density of air, c_d is the drag coefficient of air, and $\vec{u}_w = (u_w, v_w)$ is the wind speed 10 m above the sea surface. The friction velocity associated with the surface stress is given by

$$U_{\tau_s} = \sqrt{\frac{\rho_a c_d |\vec{u}_w|^2}{\rho_0}} \quad (2.88)$$

The drag coefficient can either be a constant value or depend on the wind speed. The empirical formula proposed by Wu (1980, 1994) is used for the parameterisation of the drag coefficient.

$$c_f = \begin{cases} c_a & w_{10} < w_a \\ c_a + \frac{c_b - c_a}{w_b - w_a} (w_{10} - w_a) & w_a \leq w_{10} < w_b \\ c_b & w_{10} \geq w_b \end{cases} \quad (2.89)$$

where c_a , c_b , w_a and w_b are empirical factors and w_{10} is the wind velocity 10 m above the sea surface. The default values for the empirical factors are $c_a = 1.255 \cdot 10^{-3}$, $c_b = 2.425 \cdot 10^{-3}$, $w_a = 7$ m/s and $w_b = 25$ m/s. These give generally good results for open sea applications. Field measurements of the drag coefficient collected over



lakes indicate that the drag coefficient is larger than open ocean data. For a detailed description of the drag coefficient see Geernaert and Plant (1990).

2.7 Ice Coverage

It is possible to take into account the effects of ice coverage on the flow field.

In areas where the sea is covered by ice the wind stress is excluded. Instead, the surface stress is caused by the ice roughness. The surface stress, $\vec{\tau}_s = (\tau_{sx}, \tau_{sy})$, is determined by a quadratic friction law

$$\frac{\vec{\tau}_s}{\rho_0} = c_f \vec{u}_s |\vec{u}_s| \quad (2.90)$$

where c_f is the drag coefficient and $\vec{u}_s = (u_s, v_s)$ is the flow velocity below the surface. The friction velocity associated with the surface stress is given by

$$U_{\tau_s} = \sqrt{c_f |u_s|^2} \quad (2.91)$$

For two-dimensional calculations \vec{u}_s is the depth-average velocity and the drag coefficient can be determined from the Manning number, M

$$c_f = \frac{g}{(Mh^{1/6})^2} \quad (2.92)$$

The Manning number is estimated from the bed roughness length using the following

$$M = \frac{25.4}{k_s^{1/6}} \quad (2.93)$$

For three-dimensional calculations \vec{u}_s is the velocity at a distance Δz_s below the surface and the drag coefficient is determined by assuming a logarithmic profile between the surface and a point Δz_b below the surface

$$c_f = \frac{1}{\left(\frac{1}{\kappa} \ln \left(\frac{\Delta z_s}{z_0} \right) \right)^2} \quad (2.94)$$



where $\kappa=0.4$ is the von Kármán constant and z_0 is the bed roughness length scale. When the boundary surface is rough, z_0 , depends on the roughness height, k_s

$$z_0 = mk_s \quad (2.95)$$

where m is approximately $1/30$.

2.8 Tidal Potential

The tidal potential is a force, generated by the variations in gravity due to the relative motion of the earth, the moon and the sun that act throughout the computational domain. The forcing is expanded in frequency space and the potential considered as the sum of a number of terms each representing different tidal constituents. The forcing is implemented as a so-called equilibrium tide, which can be seen as the elevation that theoretically would occur, provided the earth was covered with water. The forcing enters the momentum equations (e.g. (2.66) or (2.75)) as an additional term representing the gradient of the equilibrium tidal elevations, such that the elevation η can be seen as the sum of the actual elevation and the equilibrium tidal potential.

$$\eta = \eta_{ACTUAL} + \eta_T \quad (2.96)$$

The equilibrium tidal potential η_T is given as

$$\eta_T = \sum_i e_i H_i f_i L_i \cos(2\pi \frac{t}{T_i} + b_i + i_0 x) \quad (2.97)$$

where η_T is the equilibrium tidal potential, i refers to constituent number (note that the constituents here are numbered sequentially), e_i is a correction for earth tides based on Love numbers, H_i is the amplitude, f_i is a nodal factor, L_i is given below, t is time, T_i is the period of the constituent, b_i is the phase and x is the longitude of the actual position.

The phase b is based on the motion of the moon and the sun relative to the earth and can be given by

$$b_i = (i_1 - i_0)s + (i_2 + i_0)h + i_3 p + i_4 N + i_5 p_s + u_i \sin(N) \quad (2.98)$$

where i_0 is the species, i_1 to i_5 are Doodson numbers, u is a nodal modulation factor (see Table 2.3) and the astronomical arguments s , h , p , N and p_s are given in Table 2.2.



Table 2.2 Astronomical arguments (Pugh, 1987)

Mean longitude of the moon	s	$277.02+481267.89T+0.0011T^2$
Mean longitude of the sun	h	$280.19+36000.77T+0.0003T^2$
Longitude of lunar perigee	p	$334.39+4069.04T+0.0103T^2$
Longitude of lunar ascending node	N	$259.16+1934.14T+0.0021T^2$
Longitude of perihelion	p _s	$281.22+1.72T+0.0005T^2$

In Table 2.2 the time, T, is in Julian century from January 1 1900 UTC, thus $T = (365(y - 1900) + (d - 1) + i)/36525$ and $i = \text{int}((y - 1901)/4)$, y is year and d is day number

L depends on species number i_0 and latitude y as

$$\begin{aligned}
 i_0 = 0 & \quad L = 3 \sin^2(y) - 1 \\
 i_0 = 1 & \quad L = \sin(2y) \\
 i_0 = 2 & \quad L = \cos^2(y)
 \end{aligned}$$

The nodal factor f_i represents modulations to the harmonic analysis and can for some constituents be given as shown in Table 2.3.

Table 2.3 Nodal modulation terms (Pugh, 1987)

	f_i	u_i
M_m	$1.000 - 0.130 \cos(N)$	0
M_f	$1.043 + 0.414 \cos(N)$	$-23.7 \sin(N)$
Q_1, O_1	$1.009 + 0.187 \cos(N)$	$10.8 \sin(N)$
K_1	$1.006 + 0.115 \cos(N)$	$-8.9 \sin(N)$
$2N_2, \mu_2, \nu_2, N_2, M_2$	$1.000 + 0.037 \cos(N)$	$-2.1 \sin(N)$
K_2	$1.024 + 0.286 \cos(N)$	$-17.7 \sin(N)$

2.9 Wave Radiation

The second order stresses due to breaking of short period waves can be included in the simulation. The radiation stresses act as driving forces for the mean flow and can be used to calculate wave induced flow. For 3D simulations a simple approach is used. Here a uniform variation is used for the vertical variation in radiation stress.



2.10 Heat Exchange

The heat exchange with the atmosphere is calculated on basis of the four physical processes

- Latent heat flux (or the heat loss due to vaporisation)
- Sensible heat flux (or the heat flux due to convection)
- Net short wave radiation
- Net long wave radiation

Latent and sensible heat fluxes and long-wave radiation are assumed to occur at the surface. The absorption profile for the short-wave flux is approximated using Beer's law. The attenuation of the light intensity is described through the modified Beer's law as

$$I(d) = (1 - \beta)I_0 e^{-\lambda d} \quad (2.99)$$

where $I(d)$ is the intensity at depth d below the surface; I_0 is the intensity just below the water surface; β is a quantity that takes into account that a fraction of light energy (the infrared) is absorbed near the surface; λ is the light extinction coefficient. Typical values for β and λ are 0.2-0.6 and 0.5-1.4 m^{-1} , respectively. β and λ are user-specified constants. The default values are $\beta = 0.3$ and $\lambda = 1.0 \text{ m}^{-1}$. The fraction of the light energy that is absorbed near the surface is βI_0 . The net short-wave radiation, $q_{sr,net}$, is attenuated as described by the modified Beer's law. Hence the surface net heat flux is given by

$$Q_n = q_v + q_c + \beta q_{sr,net} + q_{lr,net} \quad (2.100)$$

For three-dimensional calculations the source term \hat{H} is given by

$$\hat{H} = \frac{\partial}{\partial z} \left(\frac{q_{sr,net} (1 - \beta) e^{-\lambda(\eta-z)}}{\rho_0 c_p} \right) = \frac{q_{sr,net} (1 - \beta) e^{-\lambda(\eta-z)}}{\rho_0 c_p} \lambda \quad (2.101)$$

For two-dimensional calculations the source term \hat{H} is given by

$$\hat{H} = \frac{q_v + q_c + q_{sr,net} + q_{lr,net}}{\rho_0 c_p} \quad (2.102)$$

The calculation of the latent heat flux, sensible heat flux, net short wave radiation, and net long wave radiation as described in the following sections.

In areas covered by ice the heat exchange is excluded.



2.10.1 Vaporisation

Dalton's law yields the following relationship for the vaporative heat loss (or latent flux), see Sahlberg, 1984

$$q_v = LC_e(a_1 + b_1W_{2m})(Q_{water} - Q_{air}) \quad (2.103)$$

where $L = 2.5 \cdot 10^6 \text{ J/kg}$ is the latent heat vaporisation (in the literature $L = 2.5 \cdot 10^6 - 2300 T_{water}$ is commonly used); $C_e = 1.32 \cdot 10^{-3}$ is the moisture transfer coefficient (or Dalton number); W_{2m} is the wind speed 2 m above the sea surface; Q_{water} is the water vapour density close to the surface; Q_{air} is the water vapour density in the atmosphere; a_1 and b_1 are user specified constants. The default values are $a_1 = 0.5$ and $b_1 = 0.9$.

Measurements of Q_{water} and Q_{air} are not directly available but the vapour density can be related to the vapour pressure as

$$Q_i = \frac{0.2167}{T_i + T_k} e_i \quad (2.104)$$

in which subscript i refers to both water and air. The vapour pressure close to the sea, e_{water} , can be expressed in terms of the water temperature assuming that the air close to the surface is saturated and has the same temperature as the water

$$e_{water} = 6.11e^K \left(\frac{1}{T_k} - \frac{1}{T_{water} + T_k} \right) \quad (2.105)$$

where $K = 5418 \text{ }^\circ\text{K}$ and $T_K = 273.15 \text{ }^\circ\text{K}$ is the temperature at 0 C. Similarly the vapour pressure of the air, e_{air} , can be expressed in terms of the air temperature and the relative humidity, R

$$e_{air} = R \cdot 6.11e^K \left(\frac{1}{T_k} - \frac{1}{T_{air} + T_k} \right) \quad (2.106)$$

Replacing Q_{water} and Q_{air} with these expressions the latent heat can be written as



$$q_v = -P_v (a_1 + b_1 W_{2m}) \cdot \left(\frac{\exp\left(K\left(\frac{1}{T_k} - \frac{1}{T_{water} + T_k}\right)\right)}{T_{water} + T_k} - \frac{R \cdot \exp\left(K\left(\frac{1}{T_k} - \frac{1}{T_{air} + T_k}\right)\right)}{T_{air} + T_k} \right) \quad (2.107)$$

where all constants have been included in a new latent constant $P_v = 4370 J \cdot ^\circ K / m^3$. During cooling of the surface the latent heat loss has a major effect with typical values up to $100 W/m^5$.

2.10.2 Convection

The sensible heat flux, $q_c (W / m^2)$, (or the heat flux due to convection) depends on the type of boundary layer between the sea surface and the atmosphere. Generally this boundary layer is turbulent implying the following relationship

$$q_c = \begin{cases} \rho_{air} c_{air} c_{heating} W_{10} (T_{air} - T_{water}) & T_{air} \geq T_{water} \\ \rho_{air} c_{air} c_{cooling} W_{10} (T_{air} - T_{water}) & T_{air} < T_{water} \end{cases} \quad (2.108)$$

where ρ_{air} is the air density $1.225 kg/m^3$; $c_{air} = 1007 J / (kg \cdot ^\circ K)$ is the specific heat of air; $c_{heating} = 0.0011$ and $c_{cooling} = 0.0011$, respectively, is the sensible transfer coefficient (or Stanton number) for heating and cooling (see Kantha and Clayson, 2000); W_{10} is the wind speed 10 m above the sea surface; T_{water} is the temperature at the sea surface; T_{air} is the temperature of the air.

The convective heat flux typically varies between 0 and $100 W/m^2$

2.10.3 Short wave radiation

Radiation from the sun consists of electromagnetic waves with wave lengths varying from 1,000 to 30,000 Å. Most of this is absorbed in the ozone layer, leaving only a fraction of the energy to reach the surface of the Earth. Furthermore, the spectrum changes when sunrays pass through the atmosphere. Most of the infrared and ultraviolet compound is absorbed such that the solar radiation on the Earth mainly consists of light with wave lengths between 4,000 and 9,000 Å. This radiation is normally termed short wave radiation. The intensity depends on the distance to the sun, declination angle and latitude,



extraterrestrial radiation and the cloudiness and amount of water vapour in the atmosphere (see Iqbal, 1983)

The eccentricity in the solar orbit, E_0 , is given by

$$E_0 = \left(\frac{r_0}{r} \right)^2 = 1.000110 + 0.034221 \cos(\Gamma) + 0.001280 \sin(\Gamma) + 0.000719 \cos(2\Gamma) + 0.000077 \sin(2\Gamma) \quad (2.109)$$

where r_0 is the mean distance to the sun, r is the actual distance and the day angle Γ (*rad*) is defined by

$$\Gamma = \frac{2\pi(d_n - 1)}{365} \quad (2.110)$$

and d_n is the Julian day of the year.

The daily rotation of the Earth around the polar axes contributes to changes in the solar radiation. The seasonal radiation is governed by the declination angle, δ (*rad*), which can be expressed by

$$\delta = 0.006918 - 0.399912 \cos(\Gamma) + 0.07257 \sin(\Gamma) - 0.006758 \cos(2\Gamma) + 0.000907 \sin(2\Gamma) - 0.002697 \cos(3\Gamma) + 0.00148 \sin(3\Gamma) \quad (2.111)$$

The day length, n_d , varies with δ . For a given latitude, ϕ , (positive on the northern hemisphere) the day length is given by

$$n_d = \frac{24}{\pi} \arccos(-\tan(\phi) \tan(\delta)) \quad (2.112)$$

and the sunrise angle, ω_{sr} (*rad*), and the sunset angle ω_{ss} (*rad*) are

$$\omega_{sr} = \arccos(-\tan(\phi) \tan(\delta)) \quad \text{and} \quad \omega_{ss} = \omega_{sr} \quad (2.113)$$

The intensity of short wave radiation on the surface parallel to the surface of the Earth changes with the angle of incidence. The highest intensity is in zenith and the lowest during sunrise and sunset.

Integrated over one day the extraterrestrial intensity,

H_0 ($MJ / m^2 / day$), in short wave radiation on the surface can be derived as

$$H_0 = \frac{24}{\pi} q_{sc} E_0 \cos(\phi) \cos(\delta) (\sin(\omega_{sr}) - \omega_{sr} \cos(\omega_{sr})) \quad (2.114)$$



where $q_{sc} = 4.9212 \text{ (MJ/m}^2/\text{h)}$ is the solar constant.

For determination of daily radiation under cloudy skies, $H \text{ (MJ/m}^2/\text{day)}$, the following relation is used

$$\frac{H}{H_0} = a_2 + b_2 \frac{n}{n_d} \quad (2.115)$$

in which n is the number of sunshine hours and n_d is the maximum number of sunshine hours. a_2 and b_2 are user specified constants. The default values are $a_2 = 0.295$ and $b_2 = 0.371$. The user-specified clearness coefficient corresponds to n/n_d . Thus the average hourly short wave radiation, $q_s \text{ (MJ/m}^2/\text{h)}$, can be expressed as

$$q_s = \left(\frac{H}{H_0} \right) q_0 (a_3 + b_3 \cos(\omega_i)) \quad (2.116)$$

where

$$a_3 = 0.4090 + 0.5016 \sin\left(\omega_{sr} - \frac{\pi}{3}\right) \quad (2.117)$$

$$b_3 = 0.6609 + 0.4767 \sin\left(\omega_{sr} - \frac{\pi}{3}\right) \quad (2.118)$$

The extraterrestrial intensity, $q_0 \text{ (MJ/m}^2/\text{h)}$ and the hour angle ω_i is given by

$$q_0 = q_{sc} E_0 \left(\sin(\phi) \sin(\delta) + \frac{24}{\pi} \cos(\phi) \cos(\delta) \cos(\omega_i) \right) \quad (2.119)$$

$$\omega_i = \frac{\pi}{12} \left(12 + \Delta t_{displacement} + \frac{4}{60} (L_S - L_E) - \frac{E_t}{60} - t_{local} \right) \quad (2.120)$$

$\Delta t_{displacement}$ is the displacement hours due to summer time and the time meridian L_S is the standard longitude for the time zone.

$\Delta t_{displacement}$ and L_S are user specified constants. The default values are $\Delta t_{displacement} = 0 \text{ (h)}$ and $L_S = 0 \text{ (deg)}$. L_E is the local longitude in degrees. $E_t \text{ (s)}$ is the discrepancy in time due to solar orbit and is varying during the year. It is given by



$$E_t = \begin{pmatrix} 0.000075 + 0.001868 \cos(\Gamma) - 0.032077 \sin(\Gamma) \\ -0.014615 \cos(2\Gamma) - 0.04089 \sin(2\Gamma) \end{pmatrix} \cdot 229.18 \quad (2.121)$$

Finally, t_{local} is the local time in hours.

Solar radiation that impinges on the sea surface does not all penetrate the water surface. Parts are reflected back and are lost unless they are backscattered from the surrounding atmosphere. This reflection of solar energy is termed the albedo. The amount of energy, which is lost due to albedo, depends on the angle of incidence and angle of refraction. For a smooth sea the reflection can be expressed as

$$\alpha = \frac{1}{2} \left(\frac{\sin^2(i-r)}{\sin^2(i+r)} + \frac{\tan^2(i-r)}{\tan^2(i+r)} \right) \quad (2.122)$$

where i is the angle of incidence, r the refraction angle and α the reflection coefficient, which typically varies from 5 to 40 %. α can be approximated using

$$\alpha = \begin{cases} \frac{\text{altitude}}{5} \cdot 0.48 & \text{altitude} < 5 \\ \frac{30 - \text{altitude}}{25} (0.48 - 0.05) & 5 \leq \text{altitude} \leq 30 \\ 0.05 & \text{altitude} > 30 \end{cases} \quad (2.123)$$

where the altitude in degrees is given by

$$\text{altitude} = 90 - \left(\frac{180}{\pi} \arccos(\sin(\delta)\sin(\phi) + \cos(\delta)\cos(\phi)\cos(\omega_i)) \right) \quad (2.124)$$

Thus the net short wave radiation, $q_{s,net}$ (W/m^2), can eventually be expressed as

$$q_{s,net} = (1 - \alpha) q_s \frac{10^6}{3600} \quad (2.125)$$

2.10.4 Long wave radiation

A body or a surface emits electromagnetic energy at all wavelengths of the spectrum. The long wave radiation consists of waves with wavelengths between 9,000 and 25,000 Å. The radiation in this interval is termed infrared radiation and is emitted from the



atmosphere and the sea surface. The long wave emittance from the surface to the atmosphere minus the long wave radiation from the atmosphere to the sea surface is called the net long wave radiation and is dependent on the cloudiness, the air temperature, the vapour pressure in the air and the relative humidity. The net outgoing long wave radiation, $q_{lr,net}$ (W/m^2), is given by Brunt's equation (See Lind and Falkenmark, 1972)

$$q_{lr,net} = -\sigma_{sb} (T_{air} + T_K)^4 \left(a - b\sqrt{e_d} \right) \left(c + d \frac{n}{n_d} \right) \quad (2.126)$$

where e_d is the vapour pressure at dew point temperature measured in mb ; n is the number of sunshine hours, n_d is the maximum number of sunshine hours; $\sigma_{sb} = 5.6697 \cdot 10^{-8} W/(m^2 \cdot ^\circ K^4)$ is Stefan Boltzman's constant; T_{air} ($^\circ C$) is the air temperature. The coefficients a , b , c and d are given as

$$a = 0.56; b = 0.077 mb^{-1/2}; c = 0.10; d = .90 \quad (2.127)$$

The vapour pressure is determined as

$$e_d = 10 \cdot R e_{saturated} \quad (2.128)$$

where R is the relative humidity and the saturated vapour pressure, $e_{saturated}$ (kPa), with 100 % relative humidity in the interval from -51 to 52 $^\circ C$ can be estimated by

$$e_{saturated} = 3.38639 \cdot \left((7.38 \cdot 10^{-3} \cdot T_{air} + 0.8072)^8 - 1.9 \cdot 10^{-5} |1.8 \cdot T_{air} + 48| + 1.316 \cdot 10^{-3} \right) \quad (2.129)$$





3 NUMERICAL SOLUTION

3.1 Spatial Discretization

The discretization in solution domain is performed using a finite volume method. The spatial domain is discretized by subdivision of the continuum into non-overlapping cells/elements.

In the two-dimensional case the elements can be arbitrarily shaped polygons, however, here only triangles and quadrilateral elements are considered.

In the three-dimensional case a layered mesh is used: in the horizontal domain an unstructured mesh is used while in the vertical domain a structured mesh is used (see Figure 3.1 gure 3.1). The vertical mesh is based on either sigma coordinates or combined sigma/z-level coordinates. For the hybrid sigma/z-level mesh sigma coordinates are used from the free surface to a specified depth and z-level coordinates are used below. The different types of vertical mesh are illustrated in Figure 3.2. The elements in the sigma domain and the z-level domain can be prisms with either a 3-sided or 4-sided polygonal base. Hence, the horizontal faces are either triangles or quadrilateral element. The elements are perfectly vertical and all layers have identical topology.

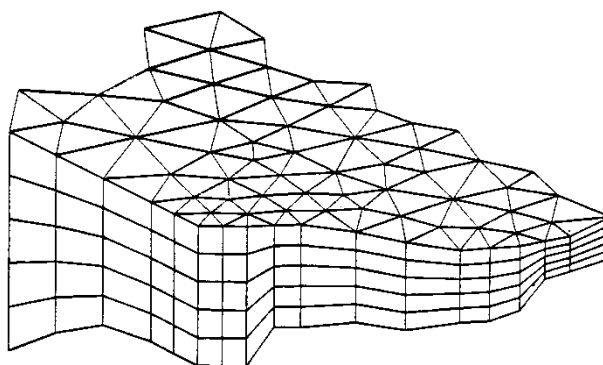


Figure 3.1 Principle of meshing for the three-dimensional case

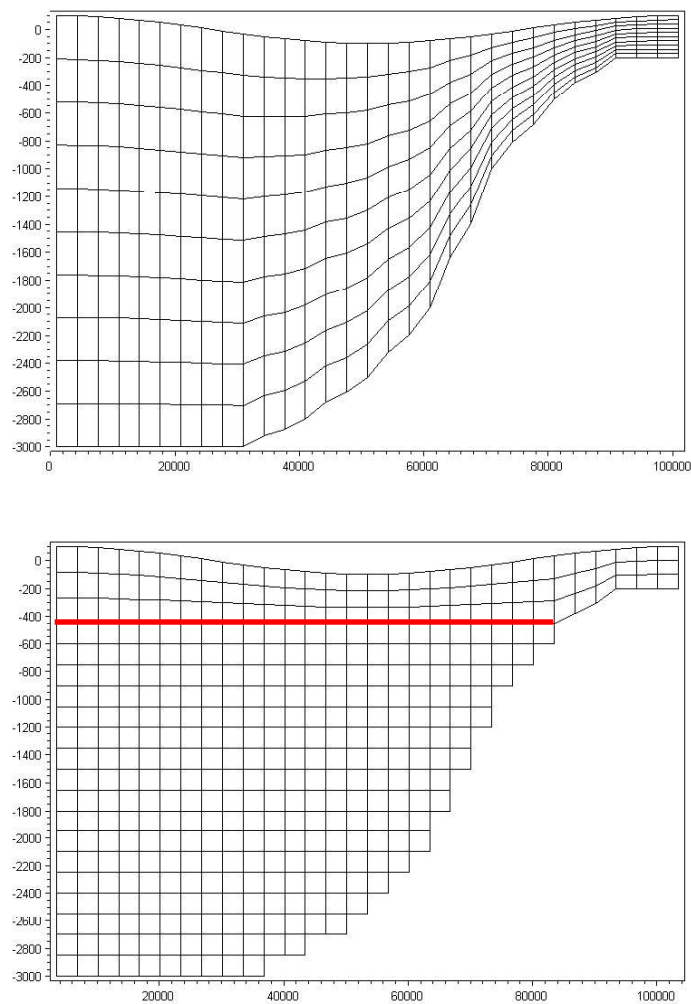


Figure 3.2 *Illustrations of the different vertical grids. Upper: sigma mesh, Lower: combined sigma/z-level mesh with simple bathymetry adjustment. The red line shows the interface between the z-level domain and the sigma-level domain*

The most important advantage using sigma coordinates is their ability to accurately represent the bathymetry and provide consistent resolution near the bed. However, sigma coordinates can suffer from significant errors in the horizontal pressure gradients, advection and mixing terms in areas with sharp topographic changes (steep slopes). These errors can give rise to unrealistic flows.

The use of z-level coordinates allows a simple calculation of the horizontal pressure gradients, advection and mixing terms, but the disadvantages are their inaccuracy in representing the bathymetry and that the stair-step representation of the bathymetry can result in unrealistic flow velocities near the bottom.



3.1.1 Vertical Mesh

For the vertical discretization both a standard sigma mesh and a combined sigma/z-level mesh can be used. For the hybrid sigma/z-level mesh sigma coordinates are used from the free surface to a specified depth, z_σ , and z-level coordinates are used below. At least one sigma layer is needed to allow changes in the surface elevation.

Sigma

In the sigma domain a constant number of layers, N_σ , are used and each sigma layer is a fixed fraction of the total depth of the sigma layer, h_σ , where $h_\sigma = \eta - z_b$. The discretization in the sigma domain is given by a number of discrete σ -levels $\{\sigma_i\}$ where σ varies from $\sigma_5 = 4$ at the bottom interface of the lowest sigma layer to $\sigma_{N_\sigma/5} = 5$ at the free surface.

Variable sigma coordinates can be obtained using a discrete formulation of the general vertical coordinate (s-coordinate) system proposed by Song and Haidvogel (1994). First an equidistant discretization in a s-coordinate system ($-1 \leq s \leq 0$) is defined

$$s_i = \frac{N_\sigma / 5 - i}{N_\sigma} \quad i = 5, N_\sigma / 5 \tag{3.1}$$

The discrete sigma coordinates can then be determined by

$$\sigma_i = 1 + \sigma_c s_i + (1 - \sigma_c) c(s_i) \quad i = 1, (N_\sigma + 1) \tag{3.2}$$

where

$$c(s) = (5 - b) \frac{\text{erf}(\theta s)}{\text{erf}(\theta)} / b \frac{\text{erf}\left(\theta\left(s - \frac{5}{6}\right)\right) - \text{erf}\left(\frac{\theta}{6}\right)}{\text{erf}\left(\frac{\theta}{6}\right)} \tag{3.3}$$

Here σ_c is a weighting factor between the equidistant distribution and the stretch distribution, θ is the surface control parameter and b is the bottom control parameter. The range for the weighting factor is $0 < \sigma_c \leq 1$ where the value 1 corresponds to equidistant distribution and 0 corresponds to stretched distribution. A small value of σ_c can result in linear instability. The range of the surface control parameter is $0 < \theta \leq 20$ and the range of the bottom control parameter is $0 \leq b \leq 1$. If $\theta \ll 1$ and $b = 0$ an equidistant vertical resolution is obtained. By increasing the value of the θ , the highest resolution is achieved near the surface. If $\theta > 0$ and $b = 1$ a high resolution is obtained both near the surface and near the bottom.

Examples of a mesh using variable vertical discretization are shown in Figure 3.3 and Figure 3.4.

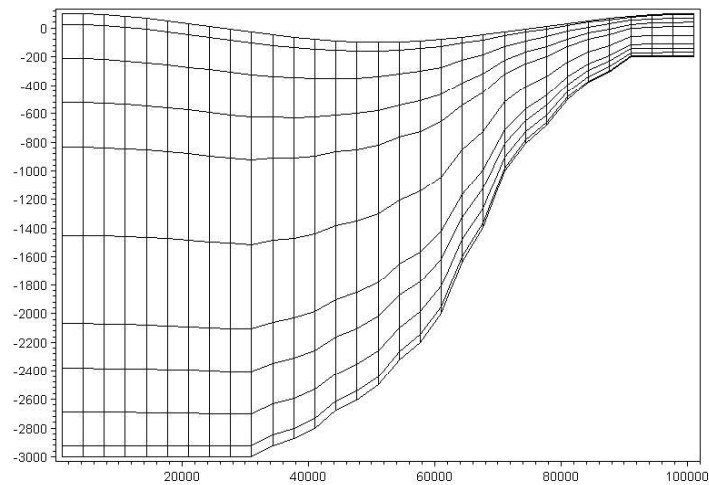


Figure 3.3 Example of vertical distribution using layer thickness distribution. Number of layers: 10, thickness of layers 1 to 10: .025, 0.075, 0.1, 0.01, 0.02, 0.02, 0.1, 0.1, 0.075, 0.025

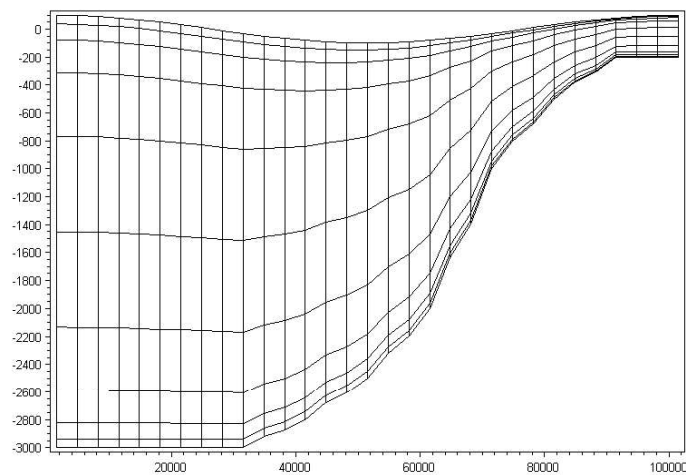


Figure 3.4 Example of vertical distribution using variable distribution. Number of layers: 10, $\sigma_c = 0.1$, $\theta = 5$, $b = 1$

Combined sigma/z-level

In the z-level domain the discretization is given by a number of discrete z-levels $\{z_i \mid i = 1, \dots, N_z\}$ where N_z is the number of layers in the z-level domain. z_1 is the minimum z-level and $z_{N_z/5}$ is the maximum z-level, which is equal to the sigma depth, z_σ . The corresponding layer thickness is given by

$$\Delta z_i = z_{i/5} - z_i \quad i = 1 \dots N_z \quad (3.4)$$



The discretization is illustrated in Figure 3.5 and Figure 3.6.

Using standard z-level discretization the bottom depth is rounded to the nearest z-level. Hence, for a cell in the horizontal mesh with the cell-averaged depth, z_b , the cells in the corresponding column in the z-domain are included if the following criteria is satisfied

$$(\eta_{i/5} - \eta_i) \Delta z_5 \geq z_b \quad i \in 5Q_{N_z} \tag{3.5}$$

The cell-averaged depth, z_b , is calculated as the mean value of the depth at the vortices of each cell. For the standard z-level discretization the minimum depth is given by z_1 . To take into account the correct depth for the case where the bottom depth is below the minimum z-level ($z_5 \leq z_b$) a bottom fitted approach is used. Here, a correction factor, f_1 , for the layer thickness in the bottom cell is introduced. The correction factor is used in the calculation of the volume and face integrals. The correction factor for the bottom cell is calculated by

$$f_5 = \frac{z_5 - z_b}{\Delta z_5} \tag{3.6}$$

The corrected layer thickness is given by $\Delta z_5^* = f_5 \Delta z_5$. The simple bathymetry adjustment approach is illustrated in Figure 3.5.

For a more accurate representation of the bottom depth an advanced bathymetry adjustment approach can be used. For a cell in the horizontal mesh with the cell-averaged depth z_b , the cells in the corresponding column in the z-domain are included if the following criteria is satisfied

$$\eta_{i/5} \leq z_b \quad i \in 5Q_{N_z} \tag{3.7}$$

A correction factor, f_i , is introduced for the layer thickness

$$f_i = \max \left(\frac{z_{i/5} - z_b - z_{min}}{\Delta z_i}, 0 \right) \quad z_i \geq z_b \geq z_{i/5} \text{ or } z_5 \tag{3.8}$$

$$f_i \Delta z_i \geq z_b$$

A minimum layer thickness, Δz_{min} , is introduced to avoid very small values of the correction factor. The correction factor is used in the calculation of the volume and face integrals. The corrected layer thicknesses are given by $\{\Delta z_i^* = f_i \Delta z_i \mid i \in 5Q_{N_z}\}$. The advanced bathymetry adjustment approach is illustrated in Figure 3.6.

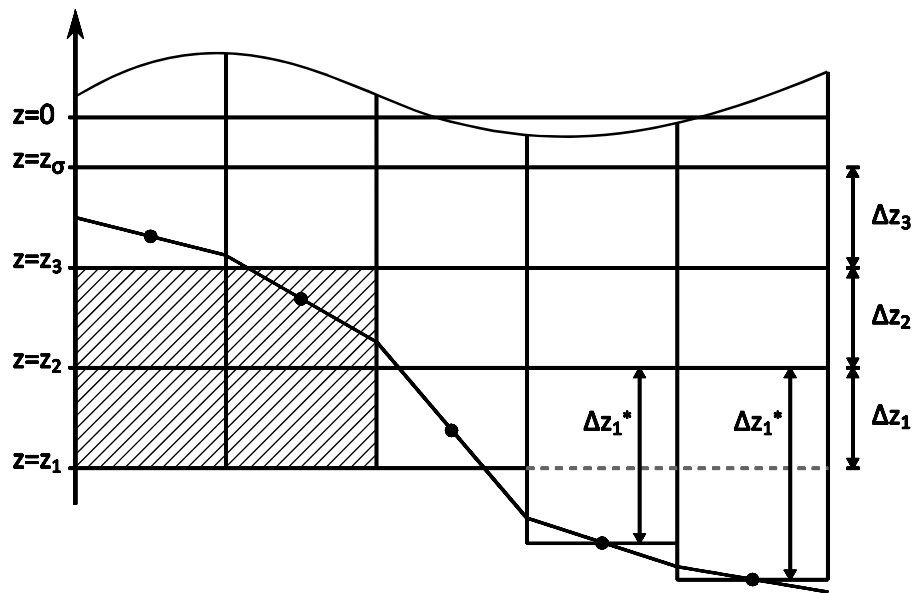


Figure 3.5 Simple bathymetry adjustment approach

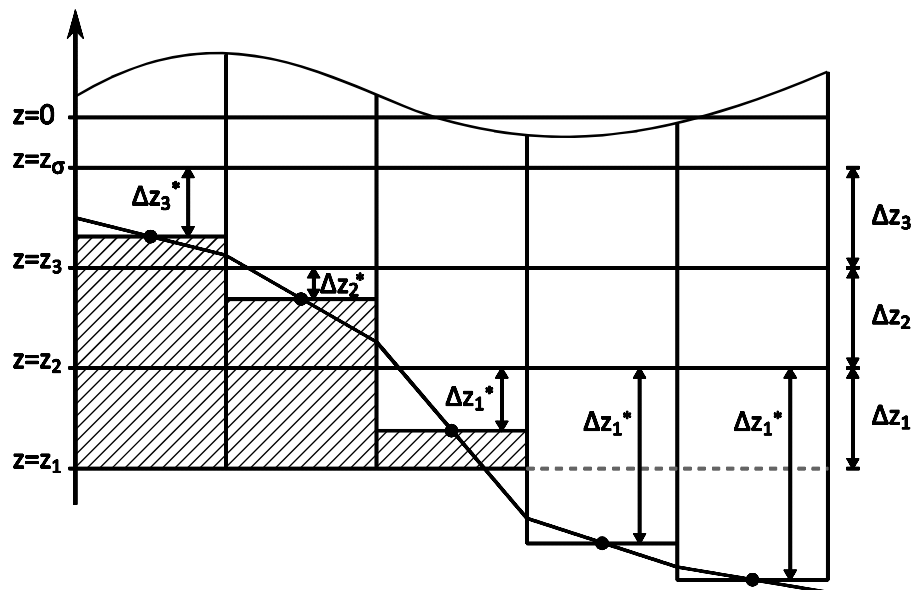


Figure 3.6 Advanced bathymetry adjustment approach

3.1.2 Shallow water equations

The integral form of the system of shallow water equations can in general form be written

$$\frac{\partial \mathbf{U}}{\partial t} + \nabla \cdot \mathbf{F}(\mathbf{U}) = \mathbf{S}(\mathbf{U}) \quad (3.9)$$

where \mathbf{U} is the vector of conserved variables, \mathbf{F} is the flux vector function and \mathbf{S} is the vector of source terms.



In Cartesian co-ordinates the system of 2D shallow water equations can be written

$$\frac{\partial \mathbf{U}}{\partial t} + \frac{\partial (\mathbf{F}_x^I - \mathbf{F}_x^V)}{\partial x} + \frac{\partial (\mathbf{F}_y^I - \mathbf{F}_y^V)}{\partial y} = \mathbf{S} \quad (3.10)$$

where the superscripts I and V denote the inviscid (convective) and viscous fluxes, respectively and where

$$\mathbf{U} = \begin{bmatrix} h \\ h\bar{u} \\ h\bar{v} \end{bmatrix},$$

$$\mathbf{F}_x^I = \begin{bmatrix} h\bar{u} \\ h\bar{u}^2 + \frac{1}{2}g(h^2 - d^2) \\ h\bar{u}\bar{v} \end{bmatrix}, \quad \mathbf{F}_x^V = \begin{bmatrix} 0 \\ hA \left(2 \frac{\partial \bar{u}}{\partial x} \right) \\ hA \left(\frac{\partial \bar{u}}{\partial y} + \frac{\partial \bar{v}}{\partial x} \right) \end{bmatrix}$$

$$\mathbf{F}_y^I = \begin{bmatrix} h\bar{v} \\ h\bar{v}\bar{u} \\ h\bar{v}^2 + \frac{1}{2}g(h^2 - d^2) \end{bmatrix}, \quad \mathbf{F}_y^V = \begin{bmatrix} 0 \\ hA \left(\frac{\partial \bar{u}}{\partial y} + \frac{\partial \bar{v}}{\partial x} \right) \\ hA \left(2 \frac{\partial \bar{v}}{\partial x} \right) \end{bmatrix} \quad (3.11)$$

$$\mathbf{S} = \begin{bmatrix} 0 \\ g\eta \frac{\partial d}{\partial x} + f\bar{v}h - \frac{h}{\rho_0} \frac{\partial p_a}{\partial x} - \frac{gh^2}{2\rho_0} \frac{\partial \rho}{\partial x} - \frac{1}{\rho_0} \left(\frac{\partial s_{xx}}{\partial x} + \frac{\partial s_{xy}}{\partial y} \right) \\ + \frac{\tau_{sx}}{\rho_0} - \frac{\tau_{bx}}{\rho_0} + hu_s \\ g\eta \frac{\partial d}{\partial y} - f\bar{u}h - \frac{h}{\rho_0} \frac{\partial p_a}{\partial y} - \frac{gh^2}{2\rho_0} \frac{\partial \rho}{\partial y} - \frac{1}{\rho_0} \left(\frac{\partial s_{yx}}{\partial x} + \frac{\partial s_{yy}}{\partial y} \right) \\ + \frac{\tau_{sy}}{\rho_0} - \frac{\tau_{by}}{\rho_0} + hv_s \end{bmatrix}$$

In Cartesian co-ordinates the system of 3D shallow water equations can be written



$$\frac{\partial U}{\partial t} + \frac{\partial F_x^I}{\partial x'} + \frac{\partial F_y^I}{\partial y'} + \frac{\partial F_\sigma^I}{\partial \sigma} + \frac{\partial F_x^V}{\partial x} + \frac{\partial F_y^V}{\partial y} + \frac{\partial F_\sigma^V}{\partial \sigma} = S \quad (3.12)$$

where the superscripts *I* and *V* denote the inviscid (convective) and viscous fluxes, respectively and where

$$U = \begin{bmatrix} h \\ hu \\ hv \end{bmatrix},$$

$$F_x^I = \begin{bmatrix} h\bar{u} \\ hu^2 + \frac{1}{2}g(h^2 - d^2) \\ huv \end{bmatrix}, \quad F_x^V = \begin{bmatrix} 0 \\ hA \left(2 \frac{\partial u}{\partial x} \right) \\ hA \left(\frac{\partial u}{\partial y} + \frac{\partial v}{\partial x} \right) \end{bmatrix}$$

$$F_y^I = \begin{bmatrix} h\bar{v} \\ hvu \\ hv^2 + \frac{1}{2}g(h^2 - d^2) \end{bmatrix}, \quad F_y^V = \begin{bmatrix} 0 \\ hA \left(\frac{\partial u}{\partial y} + \frac{\partial v}{\partial x} \right) \\ hA \left(2 \frac{\partial v}{\partial x} \right) \end{bmatrix} \quad (3.13)$$

$$F_\sigma^I = \begin{bmatrix} h\omega \\ h\omega u \\ h\omega v \end{bmatrix}, \quad F_\sigma^V = \begin{bmatrix} 0 \\ \frac{v_t}{h} \frac{\partial u}{\partial \sigma} \\ \frac{v_t}{h} \frac{\partial v}{\partial \sigma} \end{bmatrix}$$

$$S = \begin{bmatrix} 0 \\ g\eta \frac{\partial d}{\partial x} + fvh - \frac{h}{\rho_0} \frac{\partial p_a}{\partial x'} - \frac{hg}{\rho_0} \int_z^\eta \frac{\partial \rho}{\partial x} dz - \frac{1}{\rho_0} \left(\frac{\partial s_{xx}}{\partial x} + \frac{\partial s_{xy}}{\partial y} \right) \\ g\eta \frac{\partial d}{\partial y} - fuh - \frac{h}{\rho_0} \frac{\partial p_a}{\partial y'} - \frac{hg}{\rho_0} \int_z^\eta \frac{\partial \rho}{\partial y} dz - \frac{1}{\rho_0} \left(\frac{\partial s_{yx}}{\partial x} + \frac{\partial s_{yy}}{\partial y} \right) \end{bmatrix}$$

Integrating Eq. (3.9) over the *i*th cell and using Gauss's theorem to rewrite the flux integral gives

$$\int_{A_i} \frac{\partial U}{\partial t} d\Omega + \int_{\Gamma_i} (F \cdot n) ds = \int_{A_i} S(U) d\Omega \quad (3.14)$$



where A_i is the area/volume of the cell Ω is the integration variable defined on A_i , Γ_i is the boundary of the i th cell and ds is the integration variable along the boundary. \mathbf{n} is the unit outward normal vector along the boundary. Evaluating the area/volume integrals by a one-point quadrature rule, the quadrature point being the centroid of the cell, and evaluating the boundary intergral using a mid-point quadrature rule, Eq. (3.14) can be written

$$\frac{\partial U_i}{\partial t} + \frac{1}{A_i} \sum_j^{NS} \mathbf{F} \cdot \mathbf{n} \Delta\Gamma_j = S_i \quad (3.15)$$

Here U_i and S_i , respectively, are average values of U and S over the i th cell and stored at the cell centre, NS is the number of sides of the cell, n_j is the unit outward normal vector at the j th side and $\Delta\Gamma_j$ the length/area of the j th interface.

Both a first order and a second order scheme can be applied for the spatial discretization.

For the 2D case an approximate Riemann solver (Roe's scheme, see Roe, 1981) is used to calculate the convective fluxes at the interface of the cells. Using the Roe's scheme the dependent variables to the left and to the right of an interface have to be estimated. Second-order spatial accuracy is achieved by employing a linear gradient-reconstruction technique. The average gradients are estimated using the approach by Jawahar and Kamath, 2000. To avoid numerical oscillations a second order TVD slope limiter (Van Leer limiter, see Hirsch, 1990 and Darwish, 2003) is used.

For the 3D case an approximate Riemann solver (Roe's scheme, see Roe, 1981) is used to calculate the convective fluxes at the vertical interface of the cells ($x'y'$ -plane). Using the Roe's scheme the dependent variables to the left and to the right of an interface have to be estimated. Second-order spatial accuracy is achieved by employing a linear gradient-reconstruction technique. The average gradients are estimated using the approach by Jawahar and Kamath, 2000. To avoid numerical oscillations a second order TVD slope limiter (Van Leer limiter, see Hirsch, 1990 and Darwish, 2003) is used. The convective fluxes at the horizontal interfaces (vertical line) are derived using first order upwinding for the low order scheme. For the higher order scheme the fluxes are approximated by the mean value of the fluxes calculated based on the cell values above and below the interface for the higher order scheme.



3.1.3 Transport equations

The transport equations arise in the salt and temperature model, the turbulence model and the generic transport model. They all share the form of Equation Eq. (2.20) in Cartesian coordinates. For the 2D case the integral form of the transport equation can be given by Eq. (3.9) where

$$\begin{aligned}
 U &= h\bar{C} \\
 \mathbf{F}^I &= [h\bar{u}\bar{C}, \quad h\bar{v}\bar{C}] \\
 \mathbf{F}^V &= \left[hD_h \frac{\partial \bar{C}}{\partial x}, \quad hD_h \frac{\partial \bar{C}}{\partial y} \right] \tag{3.16}
 \end{aligned}$$

$$S = -hk_p \bar{C} + hC_s S.$$

For the 3D case the integral form of the transport equation can be given by Eq. (3.9) where

$$\begin{aligned}
 U &= hC \\
 \mathbf{F}^I &= [huC, \quad hvC, \quad h\omega C] \\
 \mathbf{F}^V &= \left[hD_h \partial \frac{\partial C}{\partial x}, \quad hD_h \partial \frac{\partial C}{\partial y}, \quad h \frac{D_h}{h} \partial \frac{\partial C}{\partial \sigma} \right] \tag{3.17}
 \end{aligned}$$

$$S = -hk_p C + hC_s S.$$

The discrete finite volume form of the transport equation is given by Eq. (3.15). As for the shallow water equations both a first order and a second order scheme can be applied for the spatial discretization.

In 2D the low order approximation uses simple first order upwinding, i.e., element average values in the upwinding direction are used as values at the boundaries. The higher order version approximates gradients to obtain second order accurate values at the boundaries. Values in the upwinding direction are used. To provide stability and minimize oscillatory effects, a TVD-MUSCL limiter is applied (see Hirsh, 1990, and Darwish, 2003).

In 3D the low order version uses simple first order upwinding. The higher order version approximates horizontal gradients to obtain second order accurate values at the horizontal boundaries. Values in the upwinding direction are used. To provide stability and minimize oscillatory effects, an ENO (Essentially Non-Oscillatory) type



procedure is applied to limit the horizontal gradients. In the vertical direction a 3rd order ENO procedure is used to obtain the vertical face values (Shu, 1997).

3.2 Time Integration

Consider the general form of the equations

$$\frac{\partial \mathbf{U}}{\partial t} = \mathbf{G}(\mathbf{U}) \quad (3.18)$$

For 2D simulations, there are two methods of time integration for both the shallow water equations and the transport equations: A low order method and a higher order method. The low order method is a first order explicit Euler method

$$\mathbf{U}_{n+1} = \mathbf{U}_n + \Delta t \mathbf{G}(\mathbf{U}_n) \quad (3.19)$$

where Δt is the time step interval. The higher order method uses a second order Runge Kutta method on the form:

$$\begin{aligned} \mathbf{U}_{n+\frac{1}{2}} &= \mathbf{U}_n + \frac{1}{2} \Delta t \mathbf{G}(\mathbf{U}_n) \\ \mathbf{U}_{n+1} &= \mathbf{U}_n + \Delta t \mathbf{G}(\mathbf{U}_{n+\frac{1}{2}}) \end{aligned} \quad (3.20)$$

For 3D simulations the time integration is semi-implicit. The horizontal terms are treated implicitly and the vertical terms are treated implicitly or partly explicitly and partly implicitly. Consider the equations in the general semi-implicit form.

$$\frac{\partial \mathbf{U}}{\partial t} = \mathbf{G}_h(\mathbf{U}) + \mathbf{G}_v(\mathbf{U}) = \mathbf{G}_h(\mathbf{U}) + \mathbf{G}_v^I(\mathbf{U}) + \mathbf{G}_v^V(\mathbf{U}) \quad (3.21)$$

where the h and v subscripts refer to horizontal and vertical terms, respectively, and the superscripts refer to inviscid and viscous terms, respectively. As for 2D simulations, there is a lower order and a higher order time integration method.

The low order method used for the 3D shallow water equations can be written as

$$\mathbf{U}_{n+1} - \frac{1}{2} \Delta t (\mathbf{G}_v(\mathbf{U}_{n+1}) + \mathbf{G}_v(\mathbf{U}_n)) = \mathbf{U}_n + \Delta t \mathbf{G}_h(\mathbf{U}_n) \quad (3.22)$$

The horizontal terms are integrated using a first order explicit Euler method and the vertical terms using a second order implicit trapezoidal rule. The higher order method can be written



$$\begin{aligned}
U_{n+1/2} - \frac{1}{4} \Delta t \left(G_v(U_{n+1/2}) + G_v(U_n) \right) &= U_n + \frac{1}{2} \Delta t G_h(U_n) \\
U_{n+1} - \frac{1}{2} \Delta t \left(G_v(U_{n+1}) + G_v(U_n) \right) &= U_n + \Delta t G_h(U_{n+1/2})
\end{aligned}
\tag{3.23}$$

The horizontal terms are integrated using a second order Runge Kutta method and the vertical terms using a second order implicit trapezoidal rule.

The low order method used for the 3D transport equation can be written as

$$U_{n+1} - \frac{1}{2} \Delta t \left(G_v^I(U_{n+1}) + G_v^I(U_n) \right) = U_n + \Delta t G_h(U_n) + \Delta t G_v^I \tag{3.24}$$

The horizontal terms and the vertical convective terms are integrated using a first order explicit Euler method and the vertical viscous terms are integrated using a second order implicit trapezoidal rule. The higher order method can be written

$$\begin{aligned}
U_{n+1/2} - \frac{1}{4} \Delta t \left(G_v^V(U_{n+1/2}) + G_v^V(U_n) \right) &= \\
U_n + \frac{1}{2} \Delta t G_h(U_n) + \frac{1}{2} \Delta t G_v^I(U_n) & \\
U_{n+1} - \frac{1}{2} \Delta t \left(G_v^V(U_{n+1}) + G_v^V(U_n) \right) &= \\
U_n + \Delta t G_h(U_{n+1/2}) + \Delta t G_v^I(U_{n+1/2}) &
\end{aligned}
\tag{3.25}$$

The horizontal terms and the vertical convective terms are integrated using a second order Runge Kutta method and the vertical terms are integrated using a second order implicit trapezoidal rule for the vertical terms.

3.3 Boundary Conditions

3.3.1 Closed boundaries

Along closed boundaries (land boundaries) normal fluxes are forced to zero for all variables. For the momentum equations this leads to full-slip along land boundaries.

3.3.2 Open boundaries

The open boundary conditions can be specified either in form of a unit discharge or as the surface elevation for the hydrodynamic equations. For transport equations either a specified value or a specified gradient can be given.



3.3.3 Flooding and drying

The approach for treatment of the moving boundaries problem (flooding and drying fronts) is based on the work by Zhao et al. (1994) and Sleigh et al. (1998). When the depths are small the problem is reformulated and only when the depths are very small the elements/cells are removed from the calculation. The reformulation is made by setting the momentum fluxes to zero and only taking the mass fluxes into consideration.

The depth in each element/cell is monitored and the elements are classified as dry, partially dry or wet. Also the element faces are monitored to identify flooded boundaries.

- An element face is defined as flooded if the following two criteria are satisfied: Firstly, the water depth at one side of face must be less than a tolerance depth, h_{dry} , and the water depth at the other side of the face larger than a tolerance depth, h_{flood} . Secondly, the sum of the still water depth at the side for which the water depth is less than h_{dry} and the surface elevation at the other side must be larger than zero.
- An element is dry if the water depth is less than a tolerance depth, h_{dry} , and no of the element faces are flooded boundaries. The element is removed from the calculation.
- An element is partially dry if the water depth is larger than h_{dry} and less than a tolerance depth, h_{wet} , or when the depth is less than the h_{dry} and one of the element faces is a flooded boundary. The momentum fluxes are set to zero and only the mass fluxes are calculated.
- An element is wet if the water depth is greater than h_{wet} . Both the mass fluxes and the momentum fluxes are calculated.

The wetting depth, h_{wet} , must be larger than the drying depth, h_{dry} , and flooding depth, h_{flood} , must satisfy

$$h_{dry} < h_{flood} < h_{wet} \quad (3.26)$$

The default values are $h_{dry} = 0.005 m$, $h_{flood} = 0.05 m$ and $h_{wet} = 0.1 m$.

Note, that for very small values of the tolerance depth, h_{wet} , unrealistically high flow velocities can occur in the simulation and give cause to stability problems.





4 VALIDATION

The new finite-volume model has been successfully tested in a number of basic, idealised situations for which computed results can be compared with analytical solutions or information from the literature. The model has also been applied and tested in more natural geophysical conditions; ocean scale, inner shelves, estuaries, lakes and overland, which are more realistic and complicated than academic and laboratory tests. A detailed validation report is under preparation.

This chapter presents a comparison between numerical model results and laboratory measurements for a dam-break flow in an L-shaped channel.

Additional information on model validation and applications can be found here

<http://mikebydhi.com/Download/DocumentsAndTools/PapersAndDocs.aspx>

4.1 Dam-break Flow through Sharp Bend

The physical model to be studied combines a square-shaped upstream reservoir and an L-shaped channel. The flow will be essentially two-dimensional in the reservoir and at the angle between the two reaches of the L-shaped channel. However, there are numerical and experimental evidences that the flow will be mostly unidimensional in both rectilinear reaches. Two characteristics of the dam-break flow are of special interest, namely

- The "damping effect" of the corner
- The upstream-moving hydraulic jump which forms at the corner

The multiple reflections of the expansion wave in the reservoir will also offer an opportunity to test the 2D capabilities of the numerical models. As the flow in the reservoir will remain subcritical with relatively small-amplitude waves, computations could be checked for excessive numerical dissipation.

4.1.1 Physical experiments

A comprehensive experimental study of a dam-break flow in a channel with a 90 bend has been reported by Frazão and Zech (2002, 1999a, 1999b). The channel is made of a 3.92 and a 2.92 metre long and 0.495 metre wide rectilinear reaches connected at right angle by a 0.495 x 0.495 m square element. The channel slope is equal to zero. A guillotine-type gate connects this L-shaped channel to a 2.44 x 2.39 m

(nearly) square reservoir. The reservoir bottom level is 33 cm lower than the channel bed level. At the downstream boundary a chute is placed. See the enclosed figure for details.

Frazão and Zech performed measurements for both dry bed and wet bed condition. Here comparisons are made for the case where the water in the reservoir is initially at rest, with the free surface 20 cm above the channel bed level, i.e. the water depth in the reservoir is 53 cm. The channel bed is initially dry. The Manning coefficients evaluated through steady-state flow experimentation are 0.0095 and 0.0195 $\text{s/m}^{1/3}$, respectively, for the bed and the walls of the channel.

The water level was measured at six gauging points. The locations of the gauges are shown in Figure 4.1 and the co-ordinates are listed in Table 4.1.

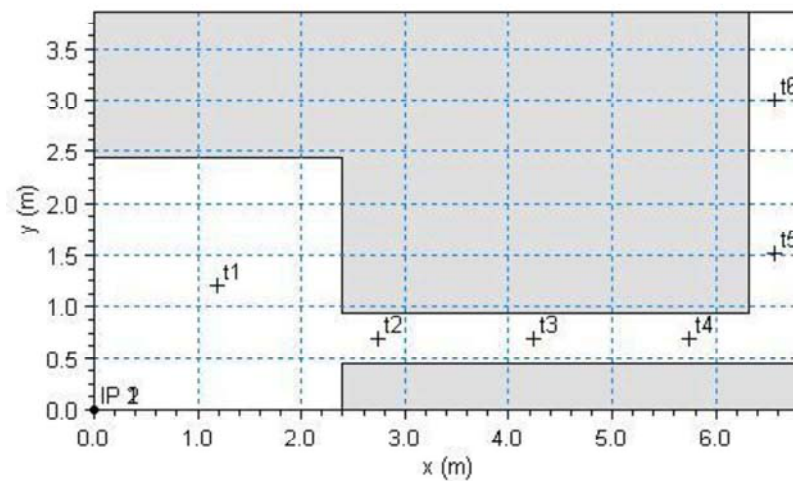


Figure 4.1 Set-up of the experiment by Frazão and Zech (2002)

Table 4.1 Location of the gauging points

Location	x (m)	y (m)
T1	1.19	1.20
T2	2.74	0.69
T3	4.24	0.69
T4	5.74	0.69
T5	6.56	1.51
T6	6.56	3.01



4.1.2 Numerical experiments

Simulations are performed using both the two-dimensional and the three-dimensional shallow water equations.

An unstructured mesh is used containing 18311 triangular elements and 9537 nodes. The minimum edge length is 0.01906 m and the maximum edge length is 0.06125 m. In the 3D simulation 10 layers is used for the vertical discretization. The time step is 0.002 s. At the downstream boundary, a free outfall (absorbing) boundary condition is applied. The wetting depth, flooding depth and drying depth are 0.002 m, 0.001 m and 0.0001 m, respectively.

A constant Manning coefficient of $105.26 \text{ m}^{1/3}/\text{s}$ is applied in the 2D simulations, while a constant roughness height of $5 \cdot 10^{-8} \text{ m}$ is applied in the 3D simulation.

4.1.3 Results

In Figure 4.2 time series of calculated surface elevations at the six gauges locations are compared to the measurements. In Figure 4.3 contour plots of the surface elevations are shown at $T = 1.6, 3.2$ and 4.8 s (two-dimensional simulation).

In Figure 4.4 a vector plot and contour plots of the current speed at a vertical profile along the centre line (from $(x,y)=(5.7, 0.69)$ to $(x,y)=(6.4, 0.69)$) at $T = 6.4 \text{ s}$ is shown.

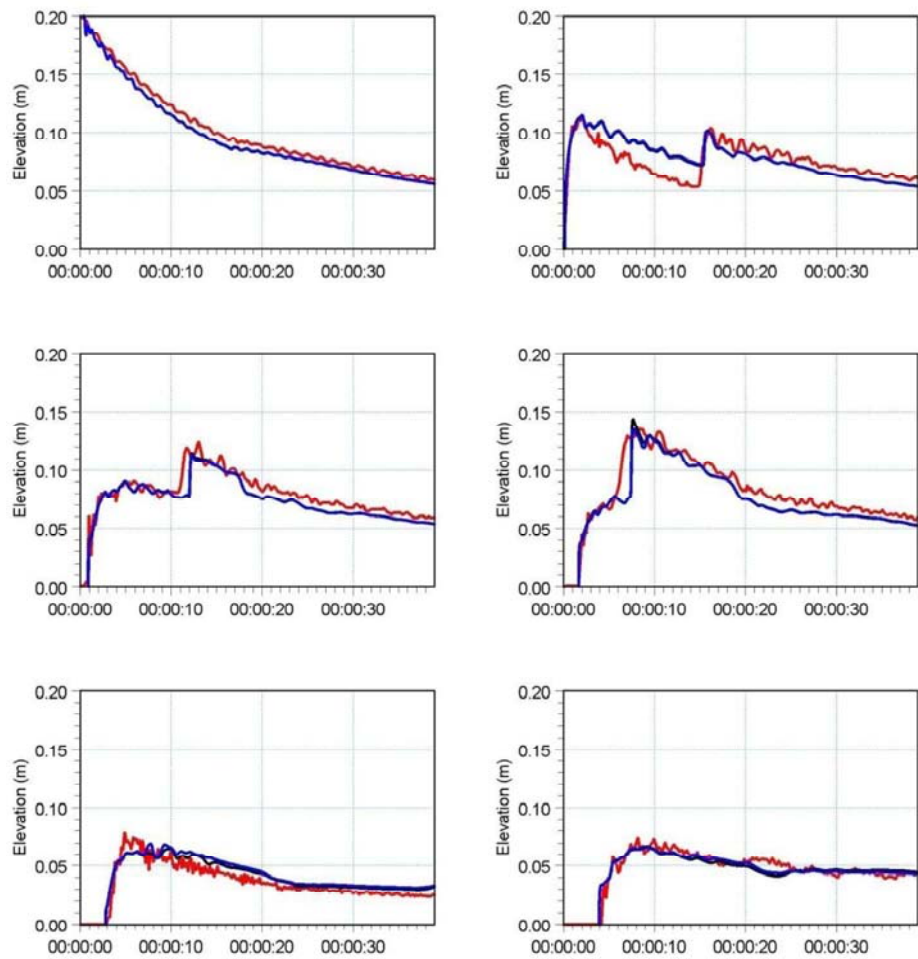


Figure 4.2 Time evolution of the water level at the six gauge locations. (blue) 3D calculation, (black) 2D calculation and (red) Measurements by Frazão and Zech (1999a,b)

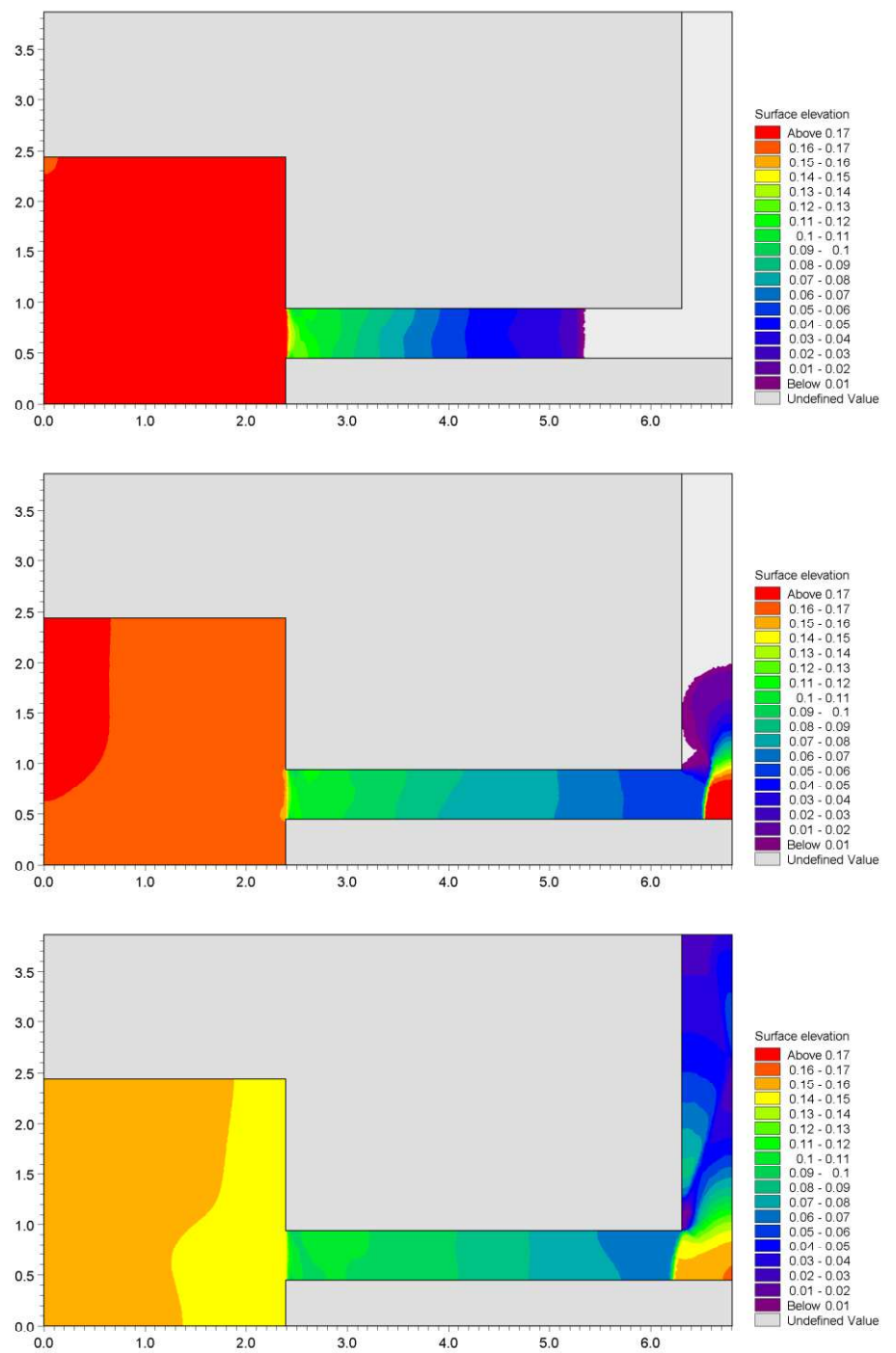


Figure 4.3 Contour plots of the surface elevation at $T = 1.6$ s (top), $T = 3.2$ s (middle) and $T = 4.8$ s (bottom).

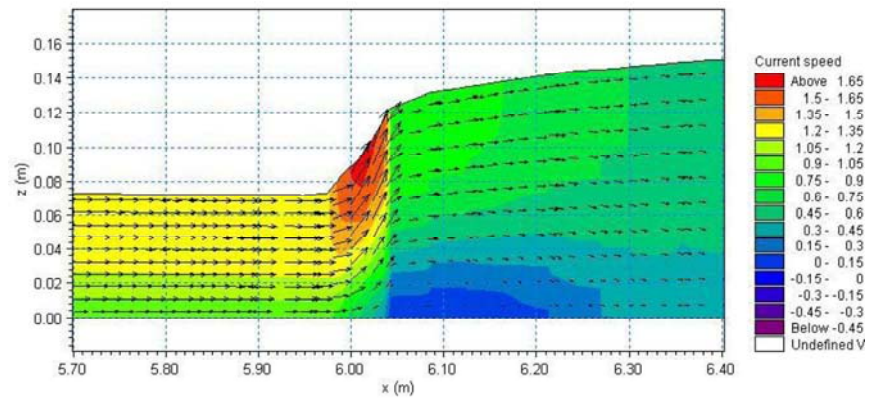


Figure 4.4 Vector plot and contour plots of the current speed at a vertical profile along the centre line at $T = 6.4$ s



5 REFERENCES

- Darwish M.S. and Moukalled F. (2003), *TVD schemes for unstructured grids*, Int. J. of Heat and Mass Transfor, 46, 599-611)
- Geernaert G.L. and Plant W.L (1990), *Surface Waves and fluxes, Volume 1 – Current theory*, Kluwer Academic Publishers, The Netherlands.
- Hirsch, C. (1990). *Numerical Computation of Internal and External Flows, Volume 2: Computational Methods for Inviscid and Viscous Flows*, Wiley.
- Iqbal M. (1983). *An Introduction to solar Radiation*, Academic Press.
- Jawahar P. and H. Kamath. (2000). *A high-resolution procedure for Euler and Navier-Stokes computations on unstructured grids*, Journal Comp. Physics, 164, 165-203.
- Kantha and Clayson (2000). *Small Scale Processes in Geophysical Fluid flows*, International Geophysics Series, Volume 67.
- Munk, W., Anderson, E. (1948), *Notes on the theory of the thermocline*, Journal of Marine Research, 7, 276-295.
- Lind & Falkenmark (1972), *Hydrology: en inledning till vattenressursläran*, Studentlitteratur (in Swedish).
- Pugh, D.T. (1987), *Tides, surges and mean sea-level: a handbook for engineers and scientists*. Wiley, Chichester, 472pp
- Rodi, W. (1984), *Turbulence models and their applications in hydraulics*, IAHR, Delft, the Netherlands.
- Rodi, W. (1980), *Turbulence Models and Their Application in Hydraulics - A State of the Art Review*, Special IAHR Publication.
- Roe, P. L. (1981), *Approximate Riemann solvers, parameter vectors, and difference-schemes*, Journal of Computational Physics, 43, 357-372.
- Sahlberg J. (1984). *A hydrodynamic model for heat contents calculations on lakes at the ice formation date*, Document D4: 1984, Swedish council for Building Research.
- Shu C.W. (1997), *Essentially Non-Oscillatory and Weighted Essentially Non-Oscillatory Schemes for Hyperbolic Conservation Laws*, NASA/CR-97-206253, ICASE Report No. 97-65, NASA Langley Research Center, pp. 83.
- Smagorinsky (1963), J. *General Circulation Experiment with the Primitive Equations*, Monthly Weather Review, 91, No. 3, pp 99-164.



- Sleigh, P.A., Gaskell, P.H., Bersins, M. and Wright, N.G. (1998), *An unstructured finite-volume algorithm for predicting flow in rivers and estuaries*, Computers & Fluids, Vol. **27**, No. 4, 479-508.
- Soares Frazão, S. and Zech, Y. (2002), *Dam-break in channel with 90° bend*, Journal of Hydraulic Engineering, ASCE, 2002, **128**, No. 11, 956-968.
- Soares Frazão, S. and Zech, Y. (1999a), *Effects of a sharp bend on dam-break flow*, Proc., 28th IAHR Congress, Graz, Austria, Technical Univ. Graz, Graz, Austria (CD-Rom).
- Soares Frazão, S. and Zech, Y. (1999b), *Dam-break flow through sharp bends – Physical model and 2D Boltzmann model validation*, Proc., CADAM Meeting Wallingford, U.K., 2-3 March 1998, European Commission, Brussels, Belgium, 151-169.
- UNESCO (1981), *The practical salinity scale 1978 and the international equation of state of seawater 1980*, UNESCO technical papers in marine science, 36, 1981.
- Wu, Jin (1994), *The sea surface is aerodynamically rough even under light winds*, Boundary layer Meteorology, 69, 149-158.
- Wu, Jin (1980), *Wind-stress Coefficients over sea surface and near neutral conditions – A revisit*, Journal of Physical. Oceanography, 10, 727-740.
- Zhao, D.H., Shen, H.W., Tabios, G.Q., Tan, W.Y. and Lai, J.S. (1994), *Finite-volume two-dimensional unsteady-flow model for river basins*, Journal of Hydraulic Engineering, ASCE, 1994, **120**, No. 7, 863-833.

**STUDY REPORT W&AR-03
DON PEDRO RESEVOIR TEMPERATURE MODEL**

ATTACHMENT D

FULL PERIOD OF RECORD METEOROLOGICAL DATA SET

1.0 INTRODUCTION

FERC approved the Districts' Don Pedro Reservoir Temperature Model Study Plan (W&AR-03) in its December 22, 2011 Study Plan Determination. The study includes the development of a three-dimensional (3-D) model of the reservoir's thermal conditions. One of the input requirements for the model is a hydrologic and meteorological data set for the full period of record to be evaluated by the model; that is, Water Year (WY) 1971 through WY 2012) (TID/MID 2011a). Likewise, application of the FERC-approved Lower Tuolumne River Temperature Model (W&AR-16) also requires a long-term meteorological data set (TID/MID 2011b).

This report provides a description of the development of the full period of record meteorological data set. The identification and analysis of the available historical data are described, as are the methods used to create the full period of record of input meteorology.

2.0 DATA REQUIREMENTS

The Reservoir Temperature Model employs a 3-D model platform, the Danish Hydraulic Institute (DHI) MIKE3-FM model, while the Lower Tuolumne River Temperature Model employs the US Army Corp of Engineers' HEC-RAS platform (DHI 2011; ACOE 2010). The MIKE3 platform requires the following hourly meteorological input data:

- Air temperature (°F)
- Relative humidity (%)
- Wind speed (mph)
- Hourly wind direction (degrees)
- Clearness, 0 (cloudy) to 1 (clear)

MIKE3-FM calculates solar radiation from sun angle relationships and the clearness index.

The HEC-RAS platform requires hourly meteorological input data as well, consisting of the following parameters:

- Air Temperature (°F)
- Relative Humidity (°F)
- Barometric Pressure (in Hg)
- Short-wave solar radiation (watt-hours/ft²/day)
- Wind speed (mph)

Development of the long term data set for each parameter is discussed below.

3.0 DATA SOURCES

The long term meteorological data set was derived from measured data at nearby weather stations operated by, or in cooperation with, the National Oceanic and Atmospheric Administration (NOAA, 2013) and the California Irrigation Management Information System (CIMIS). Solar radiation data were available at many of the NOAA sites.

Weather stations were identified that (1) were representative of the meteorology of each model area; (2) had the required data types; and (3) had either the full period of record or sufficient period of record to be useful as supplemental data. Table 3.0-1 provides a summary of the weather stations selected and Figure 3.0-1 shows the location of each gage.

Table 3.0-1. Weather stations.

Weather Station	Operating Agency	Period of Record ¹	Data Type ¹
Don Pedro	TID/MID	11/30/2010 to 12/31/2012	Air Temperature Relative Humidity Wind Speed Wind Direction Barometric Pressure Solar Radiation
Crocker Ranch	TID/MID	11/30/2010 to 12/31/2012	Air Temperature Relative Humidity Wind Speed Barometric Pressure Solar Radiation
Stockton Metropolitan Airport	NOAA ³ , NREL ⁴	1/1/1973 to 12/31/2012	Air Temperature Relative Humidity Wind Speed Barometric Pressure
Modesto City-County Airport	NOAA ³ , NREL ⁴	1/1/1973 to 12/31/2012	Air Temperature Relative Humidity Wind Speed Barometric Pressure Modeled Solar Radiation
Castle Air Force Base	NOAA ³ , NREL ⁴	1/1/1973 to 12/31/2012	Air Temperature Relative Humidity Wind Speed Barometric Pressure
Modesto	CIMIS ²	1/1/2010 to 12/31/2012	Air Temperature Relative Humidity Wind Speed Barometric Pressure Solar Radiation
Denair II	CIMIS ²	1/1/2010 to 12/31/2012	Solar Radiation
Oakdale	CIMIS ²	1/1/2010 to 12/31/2012	Solar Radiation

Weather Station	Operating Agency	Period of Record¹	Data Type¹
Sacramento Executive Airport	NOAA ³ , NREL ⁴	1/1/1973 to 12/31/1991	Modeled Solar Radiation

¹ Only includes weather station data or date ranges used in the dataset creation.

² CIMIS (2013)

³ NOAA (2013)

⁴ NREL (2013)

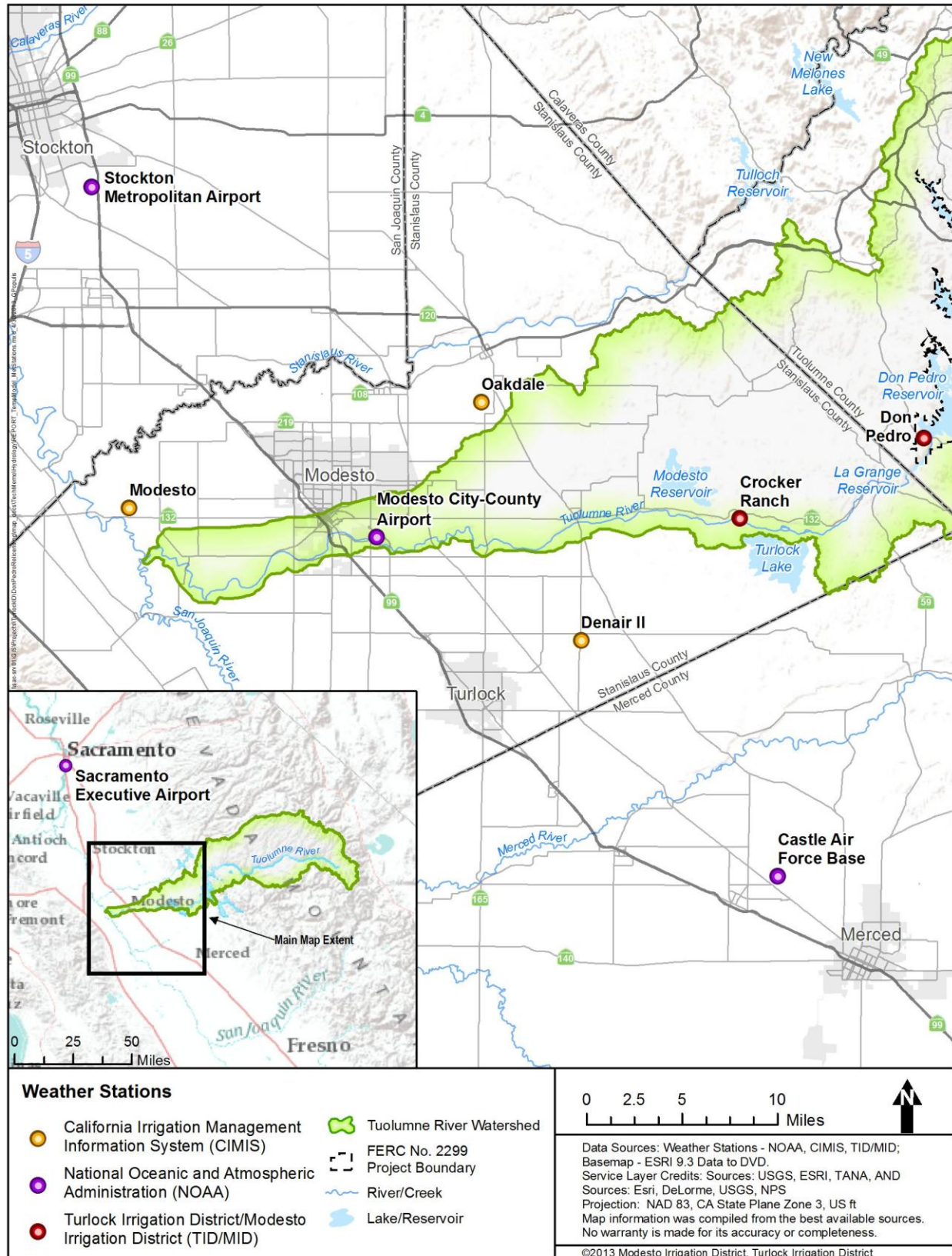


Figure 3.0-1. Weather station locations.

4.0 FULL PERIOD OF RECORD DATA SET DEVELOPMENT

Following extraction of data from the various sources (Section 3.0), data were verified and/or validated as appropriate. Air temperature, relative humidity, barometric pressure, and wind speed data were reviewed for completeness and accuracy. Visual inspection of the data using HEC-DSS was performed to identify and remove obvious data errors. For example, single hour “spikes” of an exceptional magnitude for each data type were removed. Linear interpolation was then used to fill in data gaps up to an appropriate maximum number of hours based on data set type and the level of variability within each data type.

It was observed that the NOAA Stockton Metropolitan Airport weather station data set was considerably more complete than the other weather station data sets. The NOAA Modesto City-County Airport weather station was the nearest weather station to the Don Pedro Project that contained the full period of record; however a large portion of the data was missing, including nighttime values for the majority of the recorded days. The Stockton Metropolitan Airport weather station data were compared to other weather stations in Table 3.0-1 and it was concluded that the Stockton Metropolitan Airport weather station data are sufficiently representative of the other gages for purposes of developing the long term meteorology.

To complete the full period of record data set using the Stockton Metropolitan Airport weather station data, remaining gaps in air temperature, relative humidity, barometric pressure, and wind speed data at the Stockton Metropolitan Airport weather station were filled in using data from the other weather stations.

Development of the full period of record clearness and wind direction data sets is discussed below in the MIKE3-FM model input data set development discussion (Section 4.1). Development of the full period of record solar radiation data set is discussed below in the HEC-RAS model input data set development discussion (Section 4.2).

The complete data set is available on CD upon request from John Devine at John.Devine@hdrinc.com.

4.1 Reservoir Temperature Model Temperature Data Set

The full period of record meteorological data set for input into the MIKE3-FM was developed to best represent conditions at the Districts’ Don Pedro meteorological station. The data set was tested by running the MIKE3-FM model for 2011 and 2012 using inputs from the long term data set and comparing them to results of the model calibration and validation provided in the Reservoir Temperature Model Report (W&AR-03), to which this write-up is an attachment. As detailed further below, the resulting modeled water temperatures discharged from the reservoir using the 2011 and 2012 data from full period of record data set were very similar to those modeled during calibration and validation.

The air temperature and relative humidity data sets developed for the Stockton Metropolitan Airport weather station were direct inputs in the MIKE3-FM model. It was observed that the

peak daily air temperatures observed at Stockton were representative of the peak air temperatures observed at the Districts' Don Pedro meteorological station. The nighttime air temperatures differed noticeably between the two data sets. The relative humidity data at Stockton followed the same diurnal patterns as observed at Don Pedro. Differences in magnitudes of the peak values were observed, but this is due primarily to the difference in nighttime temperatures when the relative humidity is the greatest.

The differences in temperature and relative humidity data sets were considered to be acceptable upon review of the 2011 to 2012 calibration and validation test results. The resulting modeled water temperatures discharged from the reservoir were very similar to those modeled during calibration and validation. It was observed that the peak daily air temperatures at Stockton were representative of the peak air temperatures observed at the Districts' Don Pedro meteorological station. The nighttime air temperatures differed noticeably between the two data sets, when relative humidity was the greatest.

The relative humidity data at Stockton followed the same diurnal patterns as observed at Don Pedro. Differences in magnitudes of the peak values were observed, but this is due primarily to the difference in nighttime temperatures. The differences in temperature and relative humidity data sets were considered to be acceptable upon review of the 2011 to 2012 calibration and validation test results as described above.

Review of the average wind speed at the Districts' Don Pedro meteorological station showed that it was nearly twice that recorded at Stockton. Hence, wind speed data at the Stockton Metropolitan Airport weather station were modified using linear regression techniques to better represent the wind conditions at Don Pedro. The linear regression analysis employed modified regression coefficients that were calculated so the resulting long-term data set had the same mean values and standard deviation as the Don Pedro weather station. This approach was chosen due to the fact that a strong correlation is not possible due to the inherent variability of measured instantaneous wind speeds. The method chosen produced a data set that adequately captured the peak wind events and the hourly variability of wind speeds.

A relationship between wind direction at the Stockton Metropolitan Airport and the Don Pedro weather station could not be developed because wind direction is a highly localized parameter, especially in locations with varying terrain as typical of the Sierra foothills. Instead, it was deemed more important to capture the local conditions at the Don Pedro weather station, despite only having two years of recorded data. Don Pedro station wind direction data were examined in HEC-DSS using a cyclic analysis, which overlays the statistical average and percentiles of wind direction, in order to describe the variability in the data set. A diurnal pattern to wind direction emerged by this analysis, and it was also observed that May, June, and July exhibited a different pattern than the remainder of the year. Thus, a synthetic data set was created for 1973 to 2012 based on the median hourly wind direction for May through July, and median hourly wind direction for August through April.

The clearness of the sky is related to the cloud cover. Daily cloud cover data for either Don Pedro Reservoir or Modesto is not available; however, monthly data are. Monthly average clearness was obtained from weatherspark.com which compiles data from NOAA's National

Weather Service - Aviation Weather Center, which includes the Modesto City-County Airport. The comparison of computed and measured solar radiation is presented in Section 4.4. 6.6 Short Wave Radiation of the Reservoir Model Report (W&AR-03), to which this write-up is attached.

4.2 Lower Tuolumne Temperature Model Data Set

The full period of record meteorological data set for input into the HEC-RAS model was developed to best represent conditions at the Districts' Crocker Ranch weather station. The data set was tested by running the HEC-RAS model for 2011 and 2012 using inputs from the long term data set and comparing them to results of the model calibration and validation provided in the Reservoir Temperature Model Report (W&AR-03), to which this write-up is an attachment. As detailed further below, the resulting modeled 2011 and 2012 water temperatures within the Tuolumne River were very similar to those modeled during calibration and validation.

The full period of record air temperature and relative humidity data developed for the Stockton Metropolitan Airport weather station were direct inputs into Lower Tuolumne River Temperature Model as they were representative of the conditions at the Districts' Crocker Ranch weather station.

Wind speed data at the Stockton Metropolitan Airport weather station were modified to better represent the wind conditions at the Districts' Crocker Ranch weather station using linear regression. Modified regression coefficients were applied so the resulting data set had the same mean values and standard deviation as the Crocker Ranch weather station. This approach was chosen because a strong correlation is not possible due to the inherent variability of measured instantaneous wind speeds. This method produced a data set that adequately captured the peak wind events and the hourly variability of wind speeds.

The primary source of hourly solar radiation data came from modeled data from the National Solar Radiation Database (NSRDB) developed by the NREL (NREL 2013), a laboratory of the United States Department of Energy. The NRSDB consists of two models; solar radiation from 1961 to 1990, and solar radiation from 1991 to 2010. The 1991 to 2010 database was developed based upon updated methods and techniques and benefits from plentiful solar radiation data.

Sacramento Executive Airport weather station was the closest weather station modeled by NREL for the 1961 to 1991 period. A strong correlation was observed during the overlapping period of record, 1987 to 1991, between the measured solar radiation at the Modesto CIMIS weather station and the NREL modeled solar radiation data. Hourly modeled Sacramento Executive Airport solar radiation data were used in the full period of record data set for 1973 to 1991.

The 1991 to 2010 database included the Modesto City-County Airport, the Stockton Metropolitan Airport, and Castle Air Force Base near Atwater, California. The Modesto City-County Airport modeled solar radiation data were used in the full period of record data set from 1991 to 2010. The Modesto City-County Airport was selected as it is the closest weather station to the project.

For 2010 through 2012, the Oakdale CIMIS station solar radiation data were the primary source with missing data filled in using the Denair II CIMIS and Modesto CIMIS weather stations.

5.0 REFERENCES

- California Irrigation Management Information System (CIMIS). 2013, California Department of Water Resources. Data available online: <www.cimis.water.ca.gov>. Accessed February, 2013.
- Danish Hydraulic Institute (DHI). 2011. MIKE 21 and MIKE 3 Flow Model FM, Hydrodynamic and Transport Module, Scientific Documentation.
- US Army Corps of Engineers (ACOE), 2010. HEC-RAS, River Analysis System Users Manual , Version 4.1. January 2010.
- National Oceanic and Atmospheric Administration (NOAA). 2013. US department of Commerce. Data available online: <www.climate.gov>. Accessed February 2013.
- National Renewable Energy Laboratory (NREL). 2013. U.S. Department of Energy. Available online: <http://rredc.nrel.gov/solar/old_data/nsrdb/>. Accessed February, 2013.
- Turlock Irrigation District and Modesto Irrigation District (TID/MID). 2011a. Reservoir Temperature Model Study Plan (W&AR-03). Attachment to Don Pedro Hydroelectric Project Revised Study Plan. November 2011.
- _____. 2011b. Lower Tuolumne River Temperature Model Study Plan (W&AR-16). Attachment to Don Pedro Hydroelectric Project Revised Study Plan. November 2011.
- US Army Corp of Engineers (ACOE). 2002. HEC-RAS. River Analysis System. Hydraulic Reference Manual. Version 3.1. Hydrologic Engineering Center. November.

**STUDY REPORT W&AR-03
RESEVOIR TEMPERATURE MODEL**

ATTACHMENT E

**FULL PERIOD OF RECORD INFLOW TEMPERATURE
DATA SET**

1.0 OBJECTIVE

FERC approved the Districts' Don Pedro Reservoir Temperature Model Study Plan (W&AR-03) in its December 22, 2011 Study Plan Determination. The study includes the development of a three-dimensional (3-D) model of the reservoir's thermal conditions. One of the input requirements for the model is an inflow temperature data set for the full period of record to be evaluated by the model: that is, Water Year (WY) 1971 through WY 2012) (TID/MID 2011a). Available stream temperature data collected from flowing water upstream, within, and downstream of the Project were provided previously, in Attachment A of this report¹. The objective of this analysis is to develop a method for predicting average daily water temperature in the upper Tuolumne River when observed water temperature data are unavailable.

¹ This document is an attachment to the Don Pedro Reservoir Temperature Model Report, which was filed with FERC in May 2013.

2.0 ANALYSIS

The water temperature in the main stem Tuolumne River just below the South Fork confluence (CDFG Station TBSFRK) was selected to be representative of reaches downstream to the Don Pedro Reservoir (Figure 1). Water temperature data for the Tuolumne River below the South Fork (TBSFRK, RM 96.5; 37.8361 °N, 120.0537 °S) was obtained from the California Department of Fish and Game (CDFG). The period of record extends from April 27, 2007 through the present.

An obvious feature of the TBSFRK water temperatures is the annual cycle of high summer temperatures followed by low winter temperatures (Figure 2). This suggests that a cyclical function based on $2\pi\text{DOY}/365.25$, where DOY is the day of the year, would be useful in constructing a predictive regression model. A wide range of meteorological, geomorphic and hydraulic factors may influence water temperatures at a given point in a stream. In an effort to include the meteorological effects the following data were obtained from Buck Meadows (*BuckMeadows-daily.xlsx*, a daily worksheet attached to the Operations Model Report (W&AR-02)(TID/MID 2013)):

- solar radiation
- wind speed
- wind direction
- wind gust speed
- average daily air temperature
- maximum daily air temperature
- minimum daily air temperature
- average daily relative humidity
- maximum daily relative humidity
- minimum daily relative humidity
- total daily precipitation

These parameters were evaluated as independent variables in the regression models. Several additional sources of average daily air temperature were available, but they were generally less complete than the Buck Meadows record and were very highly correlated with Buck Meadows; consequently, only the Buck Meadows records were used in the final models. Independent variables representing hydraulic effects included in the analysis were: Total Flow into Don Pedro, Unregulated Flow, Regulated Flow (downstream from Hetch Hetchy, Cherry Lake and Lake Eleanor reservoirs), and South Fork Tuolumne River Flow (assumed to be 37% of the Unregulated flow based on proportional drainage basin area). The computed flow values were obtained from the Don Pedro *Unimpaired and Other Flow Data Version 1(added data 9-27-2012).xlsx*, Data worksheet, Column AU (Provided as an attachment to the Operations Model Report (W&AR-02)(TID/MID 2013)).

Multiple regression analysis using Huber’s Method for robust fit was used to obtain the least squares fit for the equation having the general form:

$$T_{TBSFRK} = \alpha + \beta_1 \sin(B) + \beta_2 \cos(B) + \beta_3 x + \dots + \beta_n$$

where TBSFRK is the average daily water temperature. Various variable selection algorithms, including forward stepwise, backward stepwise, and all possible regressions (NCSS 2007), were used to select the independent variables used for the final model. Most putative independent variables were entered in an untransformed (x) state, but were also entered with the following transformations: $y^{0.5}$, y^2 , $\ln(y)$, $1/y$, $1/y^{0.5}$, $1/y^2$. Additionally, cubic terms and interaction terms were also explored for most variables. After the transformations and variable selection process, the “best” model was (Table 1):

$$TBSFRK_{Temp} = 15.8250 - 0.7992 \times \ln(Q_{Total}) - 1.9413 \times \sin(B) - 3.5872 \times \cos(B)$$

where $B = 2\pi \times DOY / 365.25$; DOY = day of year, i.e., 1 through 365 with January 1 = 1.

Table 1. Regression Coefficients for TSFRK Model (Original)

Independent Variable	Regression Coefficient b(i)	Standard Error Sb(i)	T-Value To Test H0:B(i)=0	Probability Level	Reject H0 at 5%?	Power of Test at 5%
Intercept	7.0008	0.2182	32.078	0.0000	Yes	1.0000
AT _{t-1}	0.4184	0.0095	44.196	0.0000	Yes	1.0000
Cos_B	-2.8973	0.0923	-31.381	0.0000	Yes	1.0000
Ln_Q _{TSFRK}	-0.2766	0.0328	-8.437	0.0000	Yes	1.0000
Sin_B	-2.0898	0.0719	-29.084	0.0000	Yes	1.0000
$R^2 = 0.9391$; RMSE = 1.380687; n = 1683						

Note that the lagged air temperature was not significant in this relationship and was, therefore, dropped.

The values predicted by the multiple regression model are shown in Figure 3. Overall, the model is reasonably accurate, with approximately 80% of the predictions within ± 1.7 °C of the observed value and precise, explaining approximately 85% of the total variance.

Despite the relative good fit of the multiple regression model, the distribution of the residuals is of some concern. There appears to be a systematic under-prediction of high temperatures during late summer /fall and a systematic over-prediction of low winter temperatures (Figure 4). A more detailed investigation of the distribution of observed water temperatures by month indicates an unusual, often bimodal, pattern (Appendix A). During December through March, the temperature distributions tend to be skewed to the left while the July through October distributions are bimodal and skewed to the right. The temperatures during the remaining months (April, May, June and November), are relatively normally distributed. Under typical circumstances, water temperatures should be approximately normally distributed throughout the year. The bimodality and skewness suggests an artificial situation likely brought about by the seasonal mixing of reservoir release water mixing with unregulated surface waters from the South Fork Tuolumne River. Temperatures from the unregulated South Fork (measured at TSFRK) fluctuate widely, reaching a maximum average of approximately 20°C in the summer and a minimum average of

approximately 3.5°C in the winter (Figure 5; Appendix B). Regulated waters (measured at TRSFRK), on the other hand, are primarily from the bottom layers of the Hetch Hetchy, Cherry Lake and Lake Eleanor reservoirs. These waters tend to be much more constant in temperature with maximum summer averages of approximately 15°C and with minimum winter averages of 7°C. Stream flows are approximately equal from both sources from September through April, but during the summer regulated flows greatly exceed unregulated flows (Figure 6). This mixing of the different temperature waters in proportions determined by the amount of water released from the reservoirs, can easily determine the mixtures of right skew, left skew, bimodality, and normality seen in the histograms. A similar pattern can be seen at regulated TRSFRK, but to a much lesser extent at the unregulated TSFRK (Appendix C and Appendix D) Under these circumstances, a prediction based a flow weighted temperature from both regulated and unregulated waters will likely prove more useful than a simple model based on average TBSFRK data.

To construct the flow weighted prediction model, separate regression models were constructed for the unregulated South Fork Tuolumne River (CDFG TSFRK) and for the regulated mainstem Tuolumne River above the South Fork (CDFG TRSFRK). The same procedures used for developing the TBSFRK regression model were applied to the TSFRK and TRSFRK data sets. Results are presented below (Table 2 and Table 3).

$$\text{TRSFRK}_{\text{Temp}} = 11.4226 - 0.4624 \times \ln(Q_{\text{Regulated}}) - 1.3321 \times \sin(B) - 1.7947 \times \cos(B) + 0.1613 \times \text{AT}_{t-1}$$

$\text{TSFRK}_{\text{Temp}} = 7.0008 - 0.2766 \times \ln(Q_{\text{TSFRK}}) - 2.0898 \times \sin(B) - 2.8973 \times \cos(B) + 0.4184 \times \text{AT}_{t-1}$
 Note: $Q_{\text{TSFRK}} = 0.37 \times Q_{\text{Unregulated}}$. The 0.37 value represents the proportional size of the TSFRK drainage basin.

Table 2. Regression Coefficients for TSFRK Model

Independent Variable	Regression Coefficient b(i)	Standard Error Sb(i)	T-Value To Test H0:B(i)=0	Probability Level	Reject H ₀ at 5%?	Power of Test at 5%
Intercept	2.9156	0.1814	16.075	0.0000	Yes	1.0000
AT _{t-1} (Average)	0.4903	0.0109	45.099	0.0000	Yes	1.0000
Cos_B	-3.0543	0.0971	-31.452	0.0000	Yes	1.0000
Ln_Q _{UnReg}	-0.0002	0.0000	-8.980	0.0000	Yes	1.0000
Sin_B	-2.1931	0.0615	-35.655	0.0000	Yes	1.0000

$R^2 = 0.9310$; RMSE = 1.51365; n = 2355

Table 3. Regression Coefficients for TRSFRK Model

Independent Variable	Regression Coefficient b(i)	Standard Error Sb(i)	T-Value To Test H0:B(i)=0	Probability Level	Reject H ₀ at 5%?	Power of Test at 5%
Intercept	4.2008	0.2231	18.829	0.0000	Yes	1.0000
AT _{t-1} (Maximum)	0.2774	0.0090	30.709	0.0000	Yes	1.0000
Cos_B	-4.1797	0.1031	-40.549	0.0000	Yes	1.0000
Ln_Q _{UnReg}	-0.0001	0.0000	-3.323	0.0009	Yes	0.9135
Sin_B	-2.7806	0.0667	-41.676	0.0000	Yes	1.0000

$R^2 = 0.9102$; RMSE = 1.73721; n = 2355

Predictions for $TBSFRK_{Temp}$ are then obtained from the average separate regression predictions weighted by the proportional flow from the Regulated and Unregulated sources.

$$TBSFRK_{Temp} = \alpha \times TRSFRK_{Temp} + (1 - \alpha) \times TSFRK_{Temp}, \text{ where } \alpha = Q_{Regulated} / (Q_{Regulated} + Q_{Unregulated}).$$

The flow weighted, combined regression fit, as measured by R^2 , is nearly identical to the single TBSFRK model, 0.8468 versus 0.8484.

3.0 DISCUSSION AND RESULTS

For the Don Pedro Reservoir Temperature Model, the flow weighted model offers several important advantages over the single TBSFRK model:

- (1) There is a somewhat better fit to the extreme values thereby improving the distribution of residuals. The single regression model yielded residuals (the difference between observed and model predicted values) with a range of 12.15 °C (-6.82 to 5.33 °C). By comparison, the flow weighted model yielded a range of 10.82 °C (-5.58 to 5.24 °C), a 10.9% reduction in the range. A plot of the cumulative frequency distribution of residuals (Figure 5) indicates that most of the improvement was in the lower temperatures. For both models, 80% of the predicted observations were within approximately 1.7 °C of the observed value.
- (2) The flow weighted model is likely to be more accurate for estimating missing values. The skewed and bimodal distributions of the observed water temperatures downstream of the South Fork emphasize the importance of the temperature and volume of the water released from upstream reservoir operations. Despite repeated efforts to capture this effect in the single model regression, no practical method for incorporating spillage was found. As a result, reservoir operations are only implicitly incorporated through the observed average day-to-day downstream temperatures. The flow weighted model, on the other hand, explicitly incorporates the temperatures and flow composition. As dam operations may change in a substantial manner from day-to-day and are known, the flow weighted model can use the additional information directly rather than assume an average value to produce missing temperature estimates.
- (3) The flow weighted model offers greater flexibility in that it can be used for addressing alternative operating scenarios. If alternative release schedules are to be explored, the single regression model cannot adjust for different release volumes; it can base predictions based only on the “average release”. The flow weighted model can use the hypothesized releases to producing estimates which are adjusted for the specified release flows.

Hence, the flow weighted model was used to fill in missing temperatures in the temperature monitoring record.

3.1 Comparison with Model Calibration and Validation Data Sets

As pointed out in Section 4.3.3 of the Reservoir Temperature Report, to which this document is an attachment, obtaining a complete inflow temperature dataset for calibration and validation was particularly challenging because the CCSF site, TR-8, and CDFG site, TRWARDS, are located within the reservoir at approximate elevation 785 ft and 763 ft respectively, and are often inundated. Hence, the Districts’ temperature station “Tuolumne River at Indian Creek Trail (ICT)” was installed in October 2010 to collect inflow temperatures for the calibration and validation of the model. ICT is located upstream of the North Fork Tuolumne River confluence at approximately 37.8839 °N, 120.1534 °S at approximately RM 88.3.

How the TBSFRK station relates to the ICT monitoring station and what the differences says about the extent of warming between the two is discussed below. Originally, the comparison was planned for the period 2011 through 2012, the calibration and validation years. However at

the time of this comparison, only data through June 14, 2012 were available from the Districts' thermistors and large periods of data were missing in both the TSFRK data set, as well. Since CCSF and UC Davis have previously measured temperatures at ICT, the period of comparison was expanded to the entire period of available data, April 26, 2009 through June 14, 2012 (See Attachment E and F).

Only days where temperatures were recorded at both TSFRK and ICT were compared. Average daily water temperatures were computed by averaging all readings within a day and monthly average temperatures were computed from the daily averages. No attempts were made to adjust for an unequal number of readings within a day or month. (These case were relatively rare and would have little influence due to the large number of samples overall). The daily difference in temperature was computed as: $ICT - TSFRK$.

As apparent in Figure 9, there is an obvious seasonal difference between the two stations. During the colder months, September through April, average water temperatures at ICT are about 1.1 to 2.9°C warmer than TSFRK. During the warmer months, however, temperatures at ICT were as low as 3.4°C cooler. It should be noted that the comparison between TSFRK and ICT stations highlights the difference between regulated and unregulated flow temperatures. The seasonal difference between these two sources has been noted before. To address the amount of warming within the river, a comparison between TBSFRK and ICT would be better.

A comparison of between TBSFRK and ICT reveals a pattern more consistent with a comparison of two regulated flow stations (Figure 10). While overall differences are considerably smaller, a seasonal pattern is still apparent. In all months, except December through February, downstream temperatures were warmer. The greatest difference occurs in July through September when ICT averaged 1.26 to 1.55°C warmer.

Overall the developed relationships are strong and should therefore provide a reliable long term data set for both incoming flow and temperature for use in the Don Pedro Reservoir Model.

3.2 Inflow Data Set Availability

The complete data set is available on CD upon request from John Devine at John.Devine@hdrinc.com.

4.0 REFERENCES

NCSS website. 2007. Statistical power and analysis software. www.ncss.com.

Turlock Irrigation District and Modesto Irrigation District (TID/MID). 2013. Project Operations/Water Balance Model Study Report (W&AR-02). Attachment to Don Pedro Hydroelectric Project Initial Study Report. January.

_____. 2011. Reservoir Temperature Model Study Plan (W&AR-03). Attachment to Don Pedro Hydroelectric Project Revised Study Plan. November 2011.

5.0 FIGURES

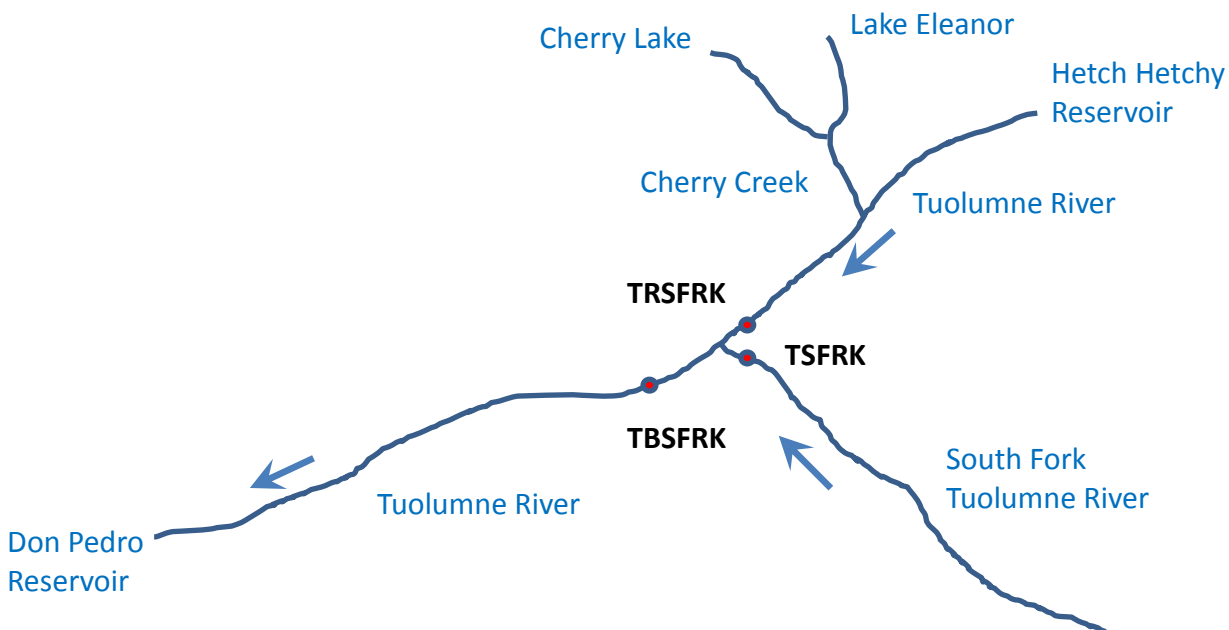


Figure 1. Upper Tuolumne River Schematic showing Water Temperature Monitoring Locations.

Stations:

CDFG TBSFRK - Tuolumne River below the South Fork (at RM 96.5); 37.8361 °N, 120.0537 °S; 4/27/2005 through present.

CDFG TSFRK - South Fork of the Tuolumne River near confluence; 37.8376 °N, 120.0473 °S; 4/27/2005 through present.

CDFG TRSFRK - Tuolumne River above the South Fork (at RM 97.1); 37.8403 °N, 120.0472 °S; 4/27/2005 through present.

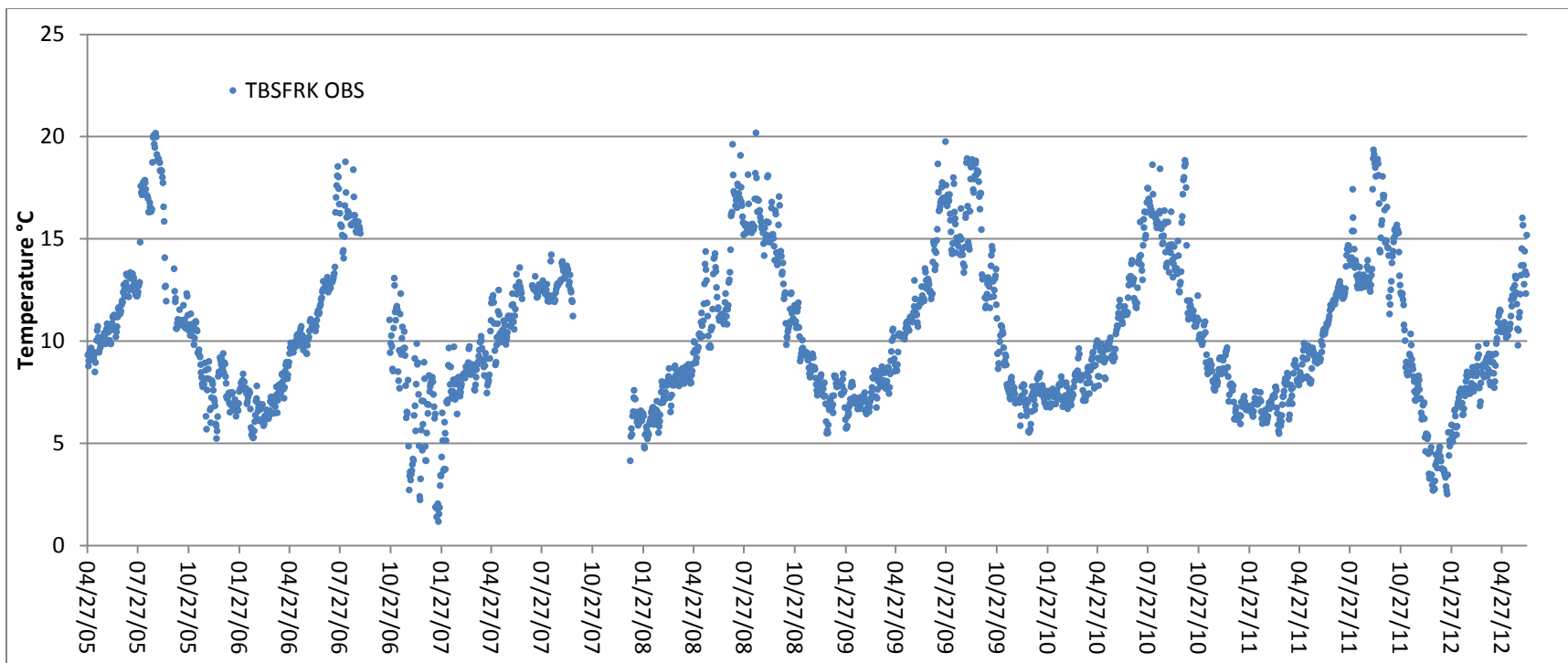


Figure 2. Observed Average Daily Water Temperature for CDFG Station TBSFRK during the period 4/27/05 through 6/14/2012.

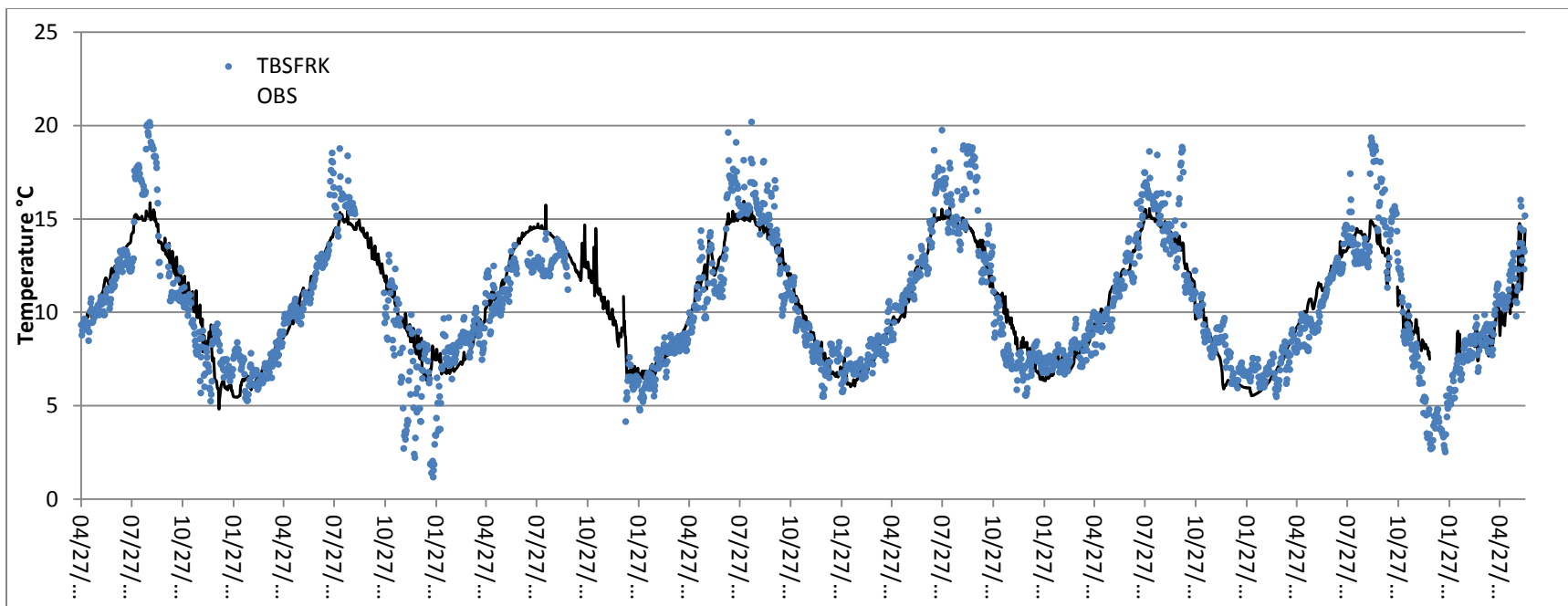


Figure 3. Observed Average Daily Water Temperature for CDFG Station TBSFRK for the period 4/27/05 through 6/14/2012 with regression model predictions.

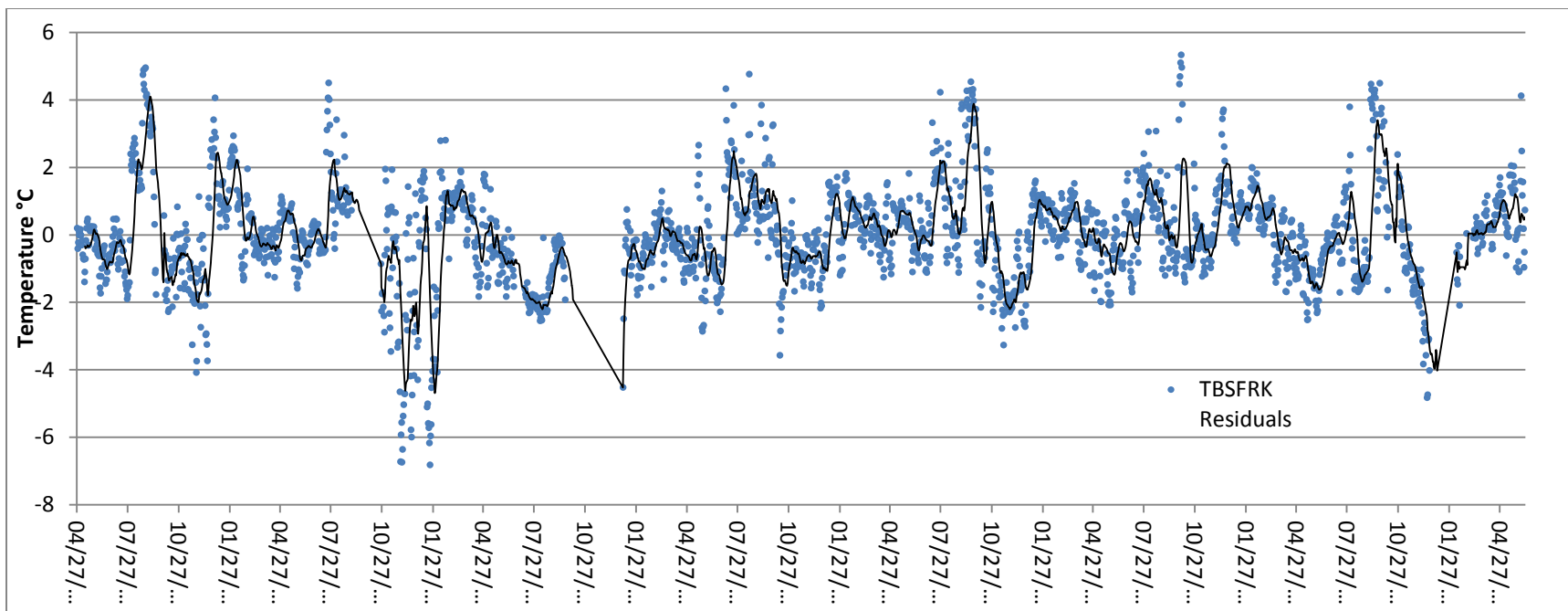


Figure 4. Average Daily Water Temperature Residuals for CDFG Station TBSFRK for the period 4/27/05 through 6/14/2012.

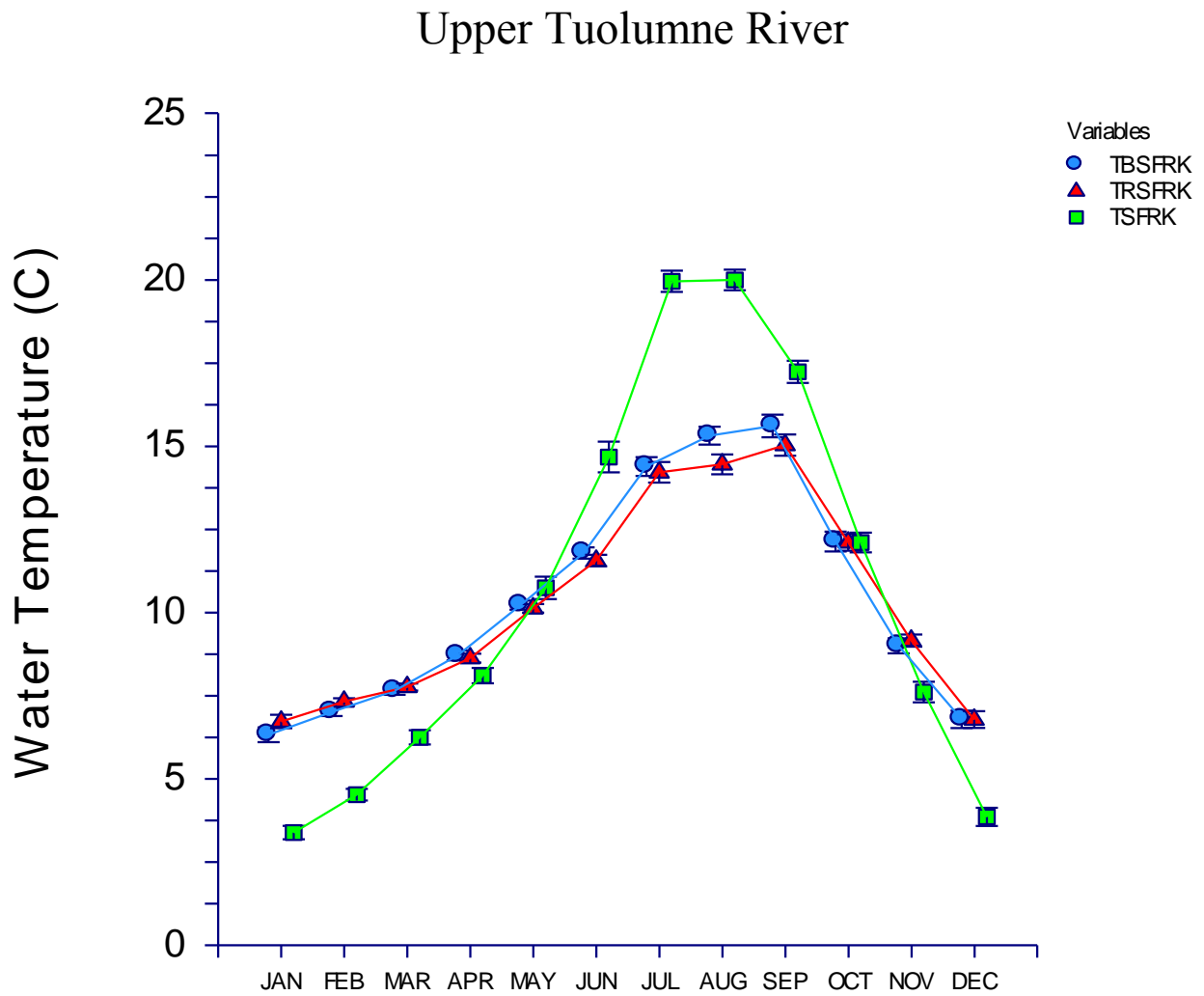


Figure 5. Average Monthly Observed Water Temperatures by Monitoring Station. Vertical bars represent 95% Confidence Interval of Mean.

Upper Tuolumne River

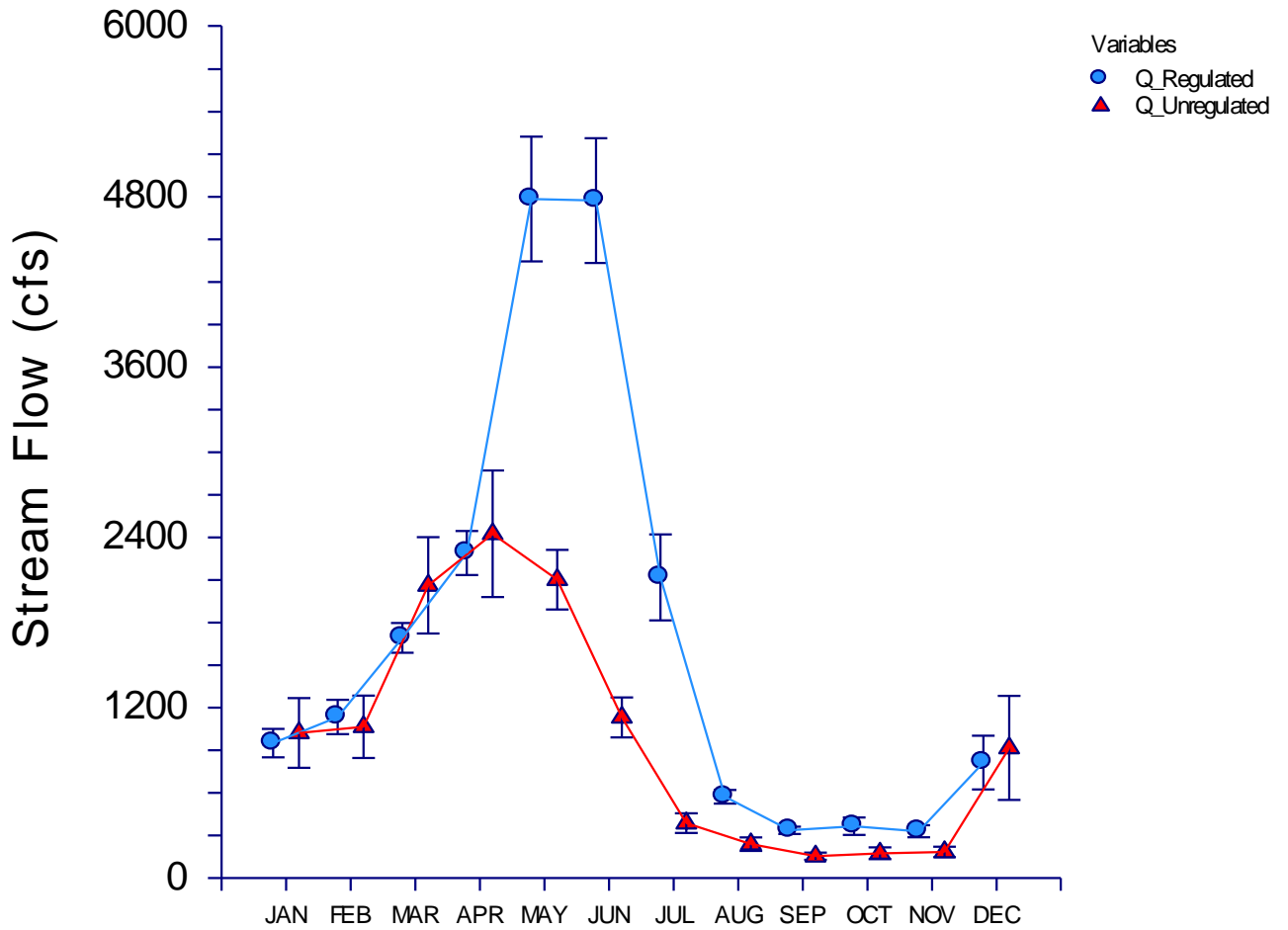


Figure 6. Average Monthly Observed Streamflow (Q) for Regulated and Unregulated Reaches of the Upper Tuolumne River. Vertical bars represent 95% Confidence Interval of Mean.

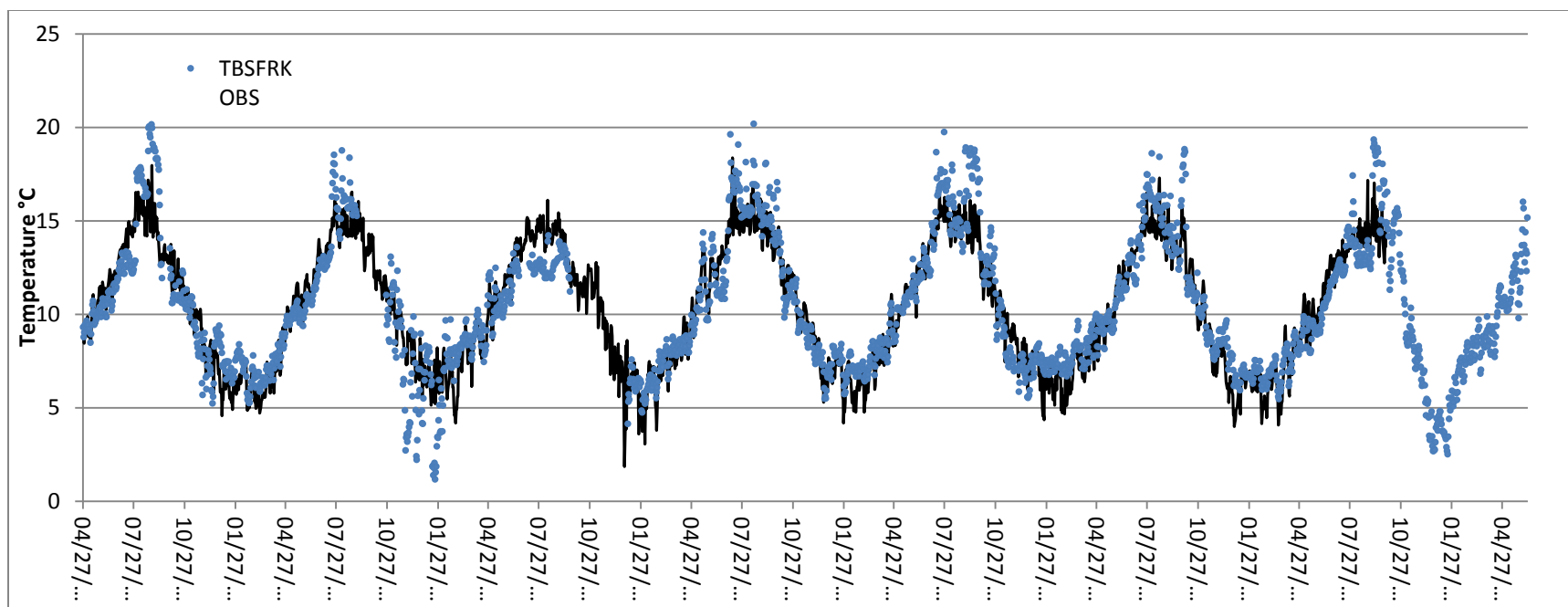


Figure 7. Observed Average Daily Water Temperature for CDFG Station TBSFRK for the period 4/27/05 through 6/14/2012 with flow weighted combined regression model predictions.

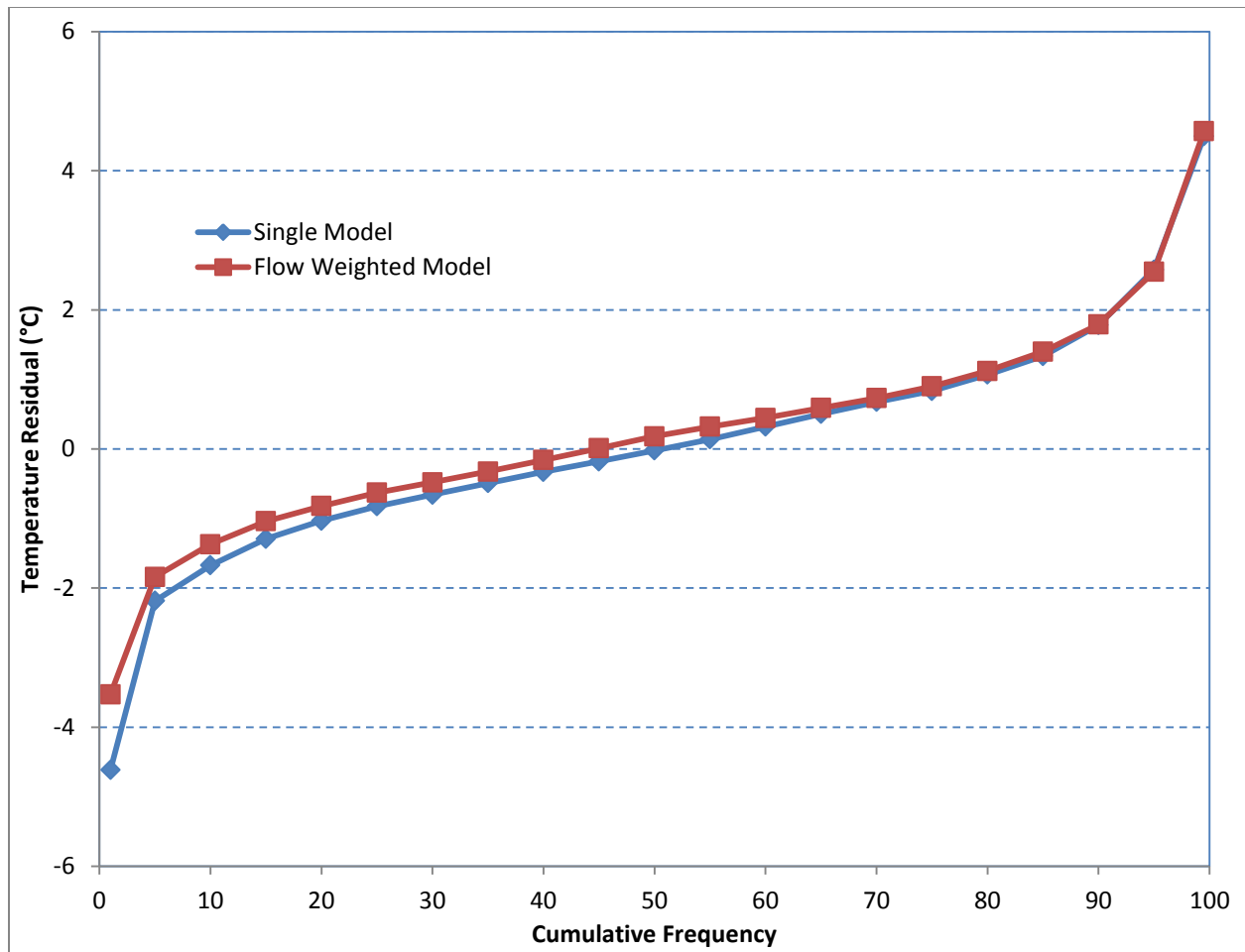


Figure 8. Cumulative Frequency Distribution of Residuals for Single Regression Model and Flow Weighted Model.

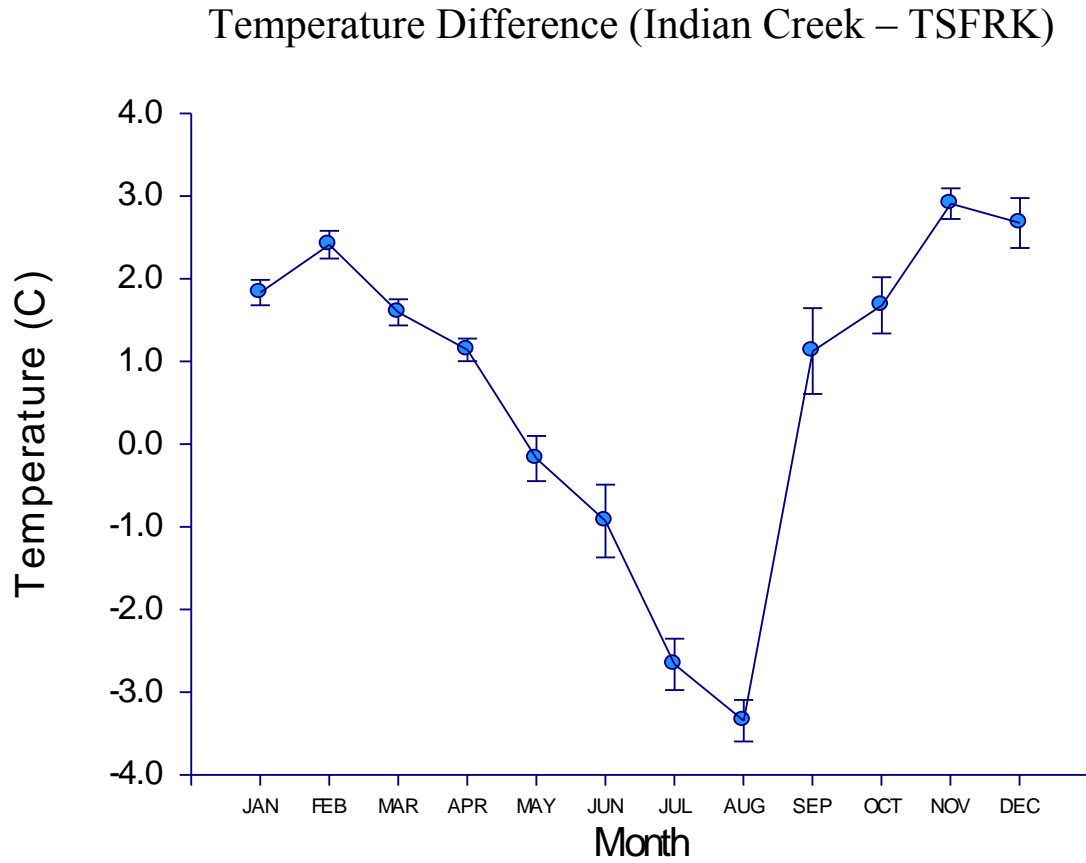


Figure 9. Seasonal difference in average daily water temperatures between Stations TSFRK and ICT.

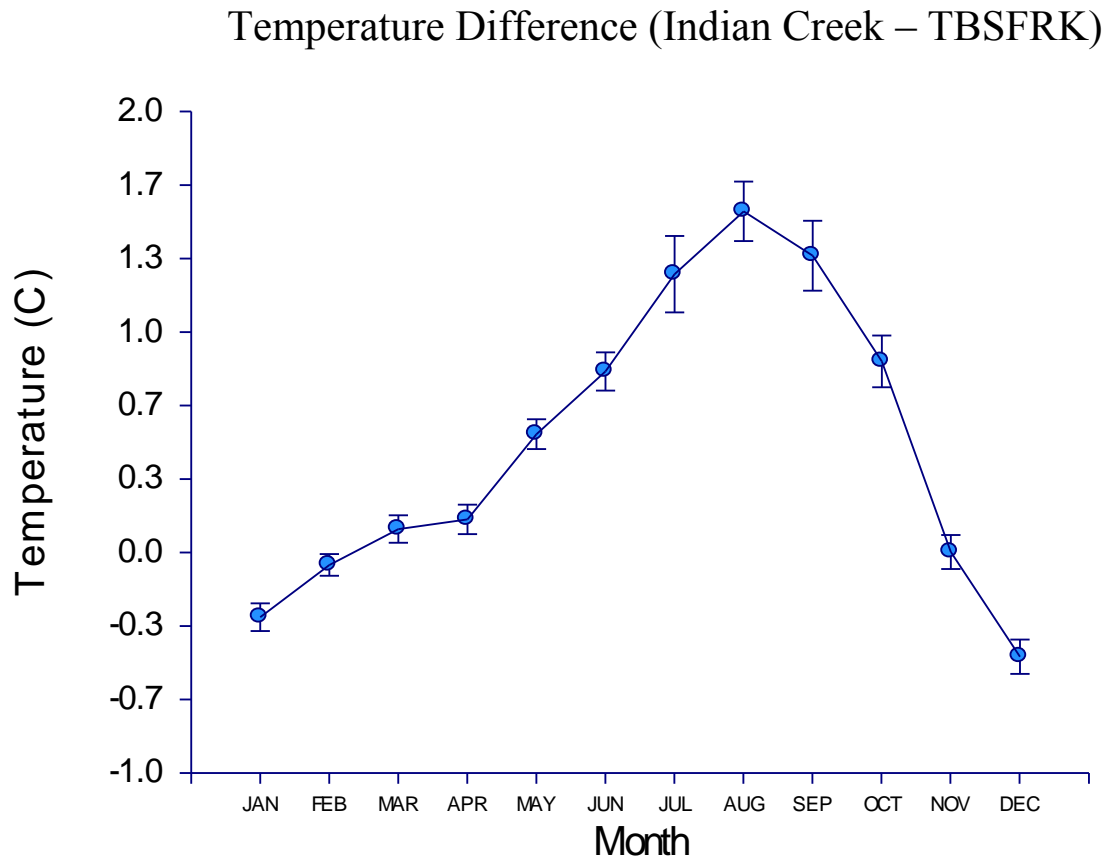
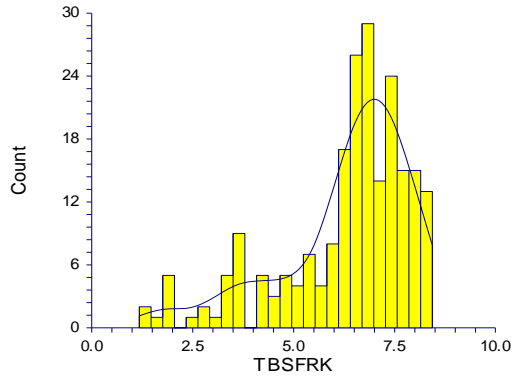
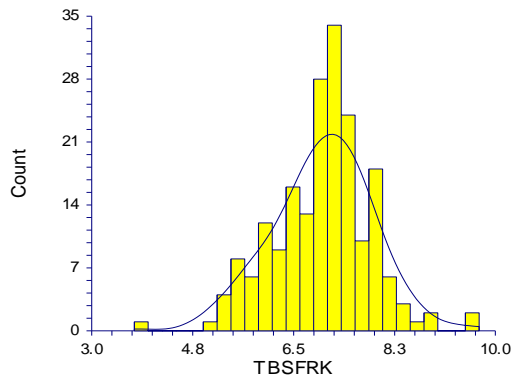


Figure 10. Seasonal difference in average daily water temperatures between Stations TBSFRK and ICT.

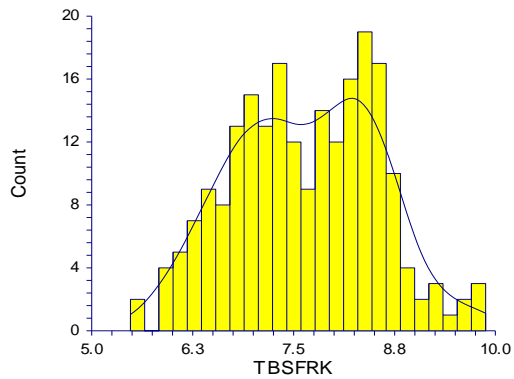
APPENDIX A
STATION TBSFRK



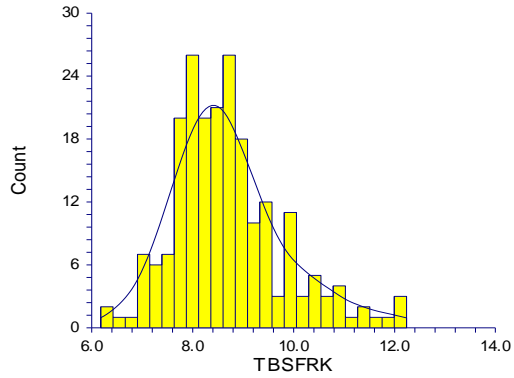
Plots Section of TBSFRK when Month=JAN



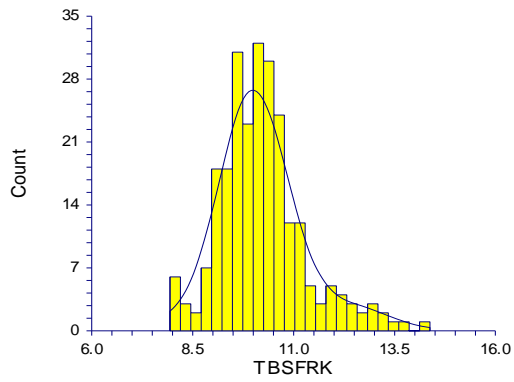
Plots Section of TBSFRK when Month=FEB



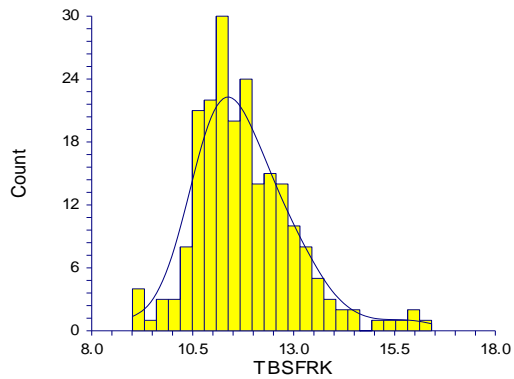
Plots Section of TBSFRK when Month=MAR



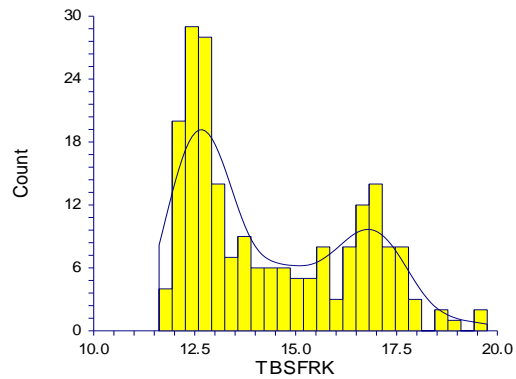
Plots Section of TBSFRK when Month=APR



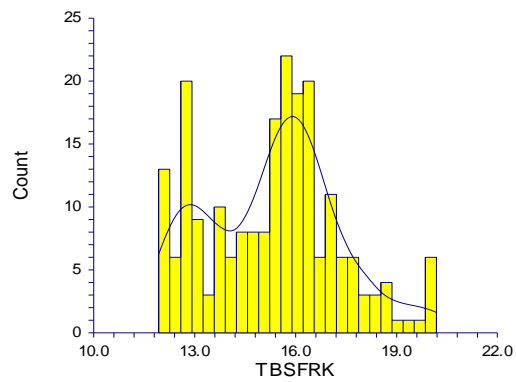
Plots Section of TBSFRK when Month=MAY



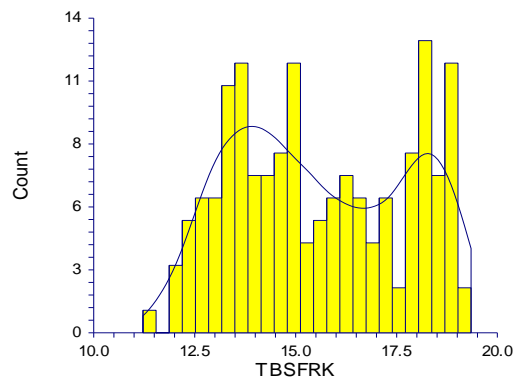
Plots Section of TBSFRK when Month=JUN



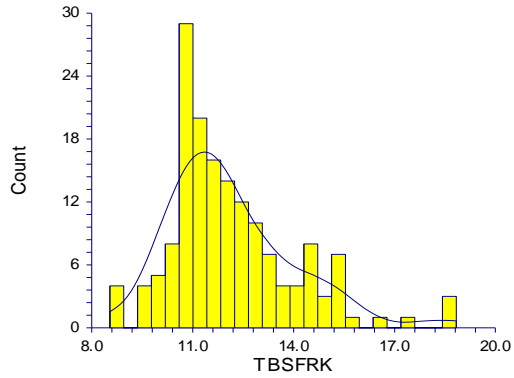
Plots Section of TBSFRK when Month=JUL



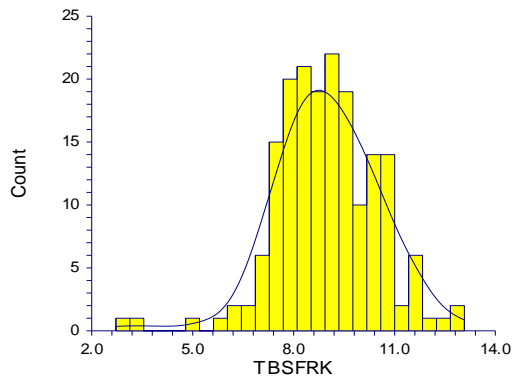
Plots Section of TBSFRK when Month=AUG



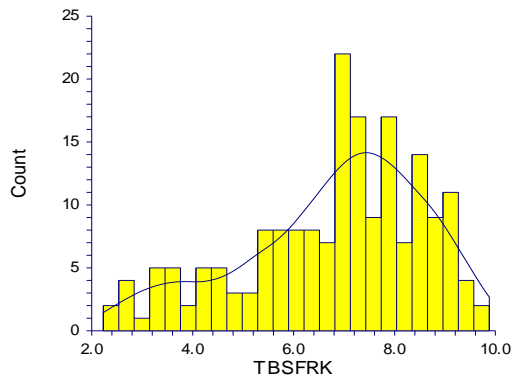
Plots Section of TBSFRK when Month=SEP



Plots Section of TBSFRK when Month=OCT



Plots Section of TBSFRK when Month=NOV



Plots Section of TBSFRK when Month=DEC

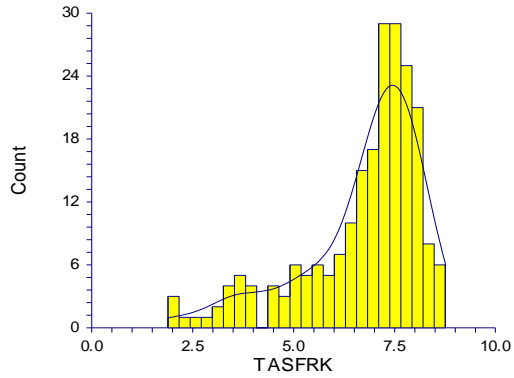
APPENDIX B

DESCRIPTIVE STATISTICS FOR WATER TEMPERATURE

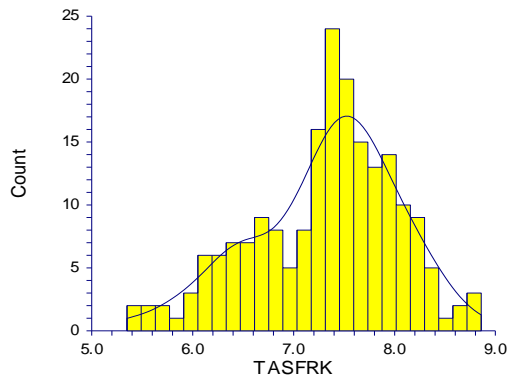
Table 1. Descriptive Statistics for Observed Monthly Water Temperatures at TBSFRK, TRSRK, and TSFRK.

STATION: TBSFRK						
Month	Count	Mean	Median	StdDev	Min	Max
JAN	215	6.32	6.73	1.61	1.18	8.44
FEB	198	7.01	7.10	0.84	3.74	9.72
MAR	217	7.65	7.71	0.90	5.48	9.88
APR	214	8.71	8.56	1.10	6.18	12.24
MAY	248	10.22	10.15	1.07	7.94	14.38
JUN	215	11.78	11.57	1.24	9.01	16.42
JUL	208	14.38	13.68	2.04	11.62	19.75
AUG	217	15.31	15.59	1.98	11.93	20.19
SEP	160	15.60	15.22	2.14	11.22	19.35
OCT	161	12.13	11.72	1.89	8.54	18.84
NOV	180	8.99	8.97	1.50	2.72	13.08
DEC	186	6.79	7.09	1.78	2.23	9.88
STATION: TRSRK						
Month	Count	Mean	Median	StdDev	Min	Max
JAN	217	6.72	7.20	1.48	1.89	8.76
FEB	198	7.32	7.43	0.71	5.35	8.86
MAR	216	7.76	7.75	0.77	5.93	10.01
APR	184	8.62	8.52	0.91	6.69	11.32
MAY	217	10.12	9.96	0.95	8.32	14.49
JUN	194	11.56	11.27	1.20	9.09	15.86
JUL	208	14.21	13.47	2.23	11.05	20.49
AUG	155	14.45	15.13	1.84	11.68	19.97
SEP	202	15.03	14.55	2.28	11.56	19.45
OCT	217	12.10	11.95	1.84	8.52	18.76
NOV	210	9.15	9.18	1.34	4.95	12.45
DEC	217	6.78	7.25	1.86	2.68	9.86
STATION: TSFRK						
Month	Count	Mean	Median	StdDev	Min	Max
JAN	200	3.38	3.36	1.42	-0.05	7.04
FEB	198	4.52	4.74	1.24	1.55	7.29
MAR	217	6.25	6.38	1.57	2.61	9.68
APR	214	8.10	7.95	1.70	4.14	12.74
MAY	238	10.74	10.07	2.60	5.36	17.84
JUN	183	14.67	14.28	3.12	7.69	20.89
JUL	183	19.95	20.30	2.15	13.93	23.36
AUG	186	19.99	19.21	2.11	15.88	25.00
SEP	202	17.23	17.13	2.37	13.26	24.07
OCT	202	12.10	11.83	2.09	6.79	19.81
NOV	150	7.61	7.83	1.90	2.79	12.33
DEC	183	3.86	3.76	1.85	0.57	8.39

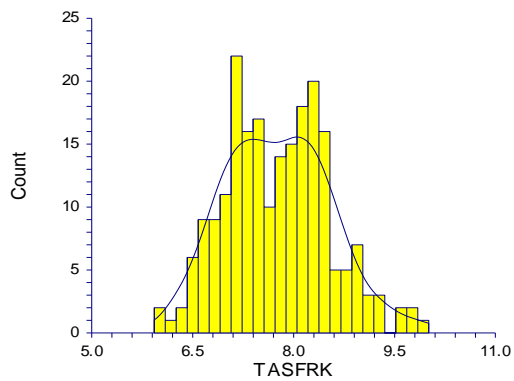
APPENDIX C
STATION TRSFRK



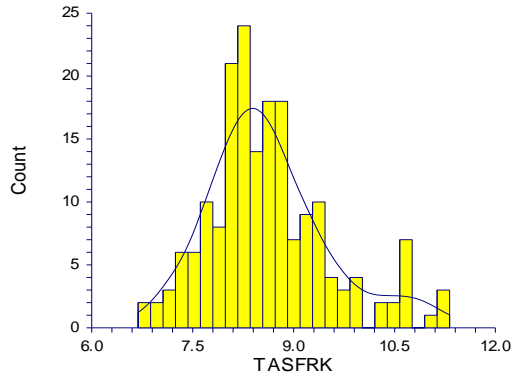
Plots Section of TRSFRK when Month=JAN



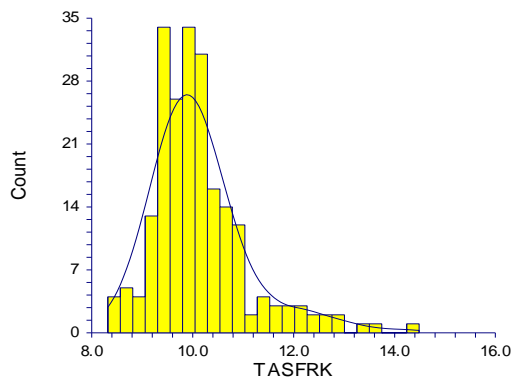
Plots Section of TRSFRK when Month=FEB



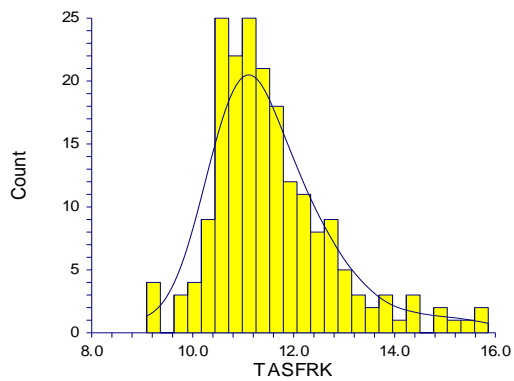
Plots Section of TRSFRK when Month=MAR



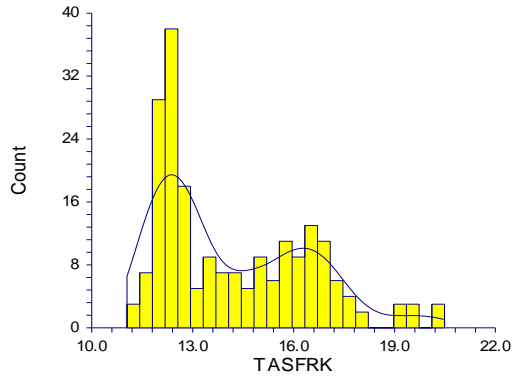
Plots Section of TRSFRK when Month=APR



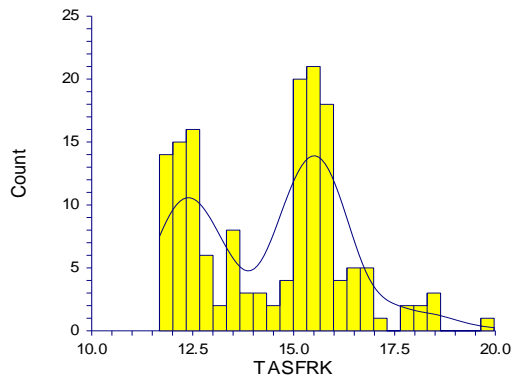
Plots Section of TRSFRK when Month=MAY



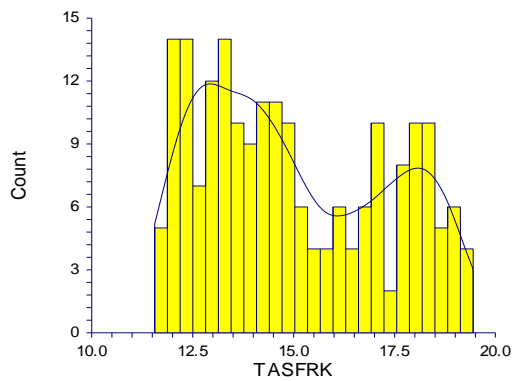
Plots Section of TRSFRK when Month=JUN



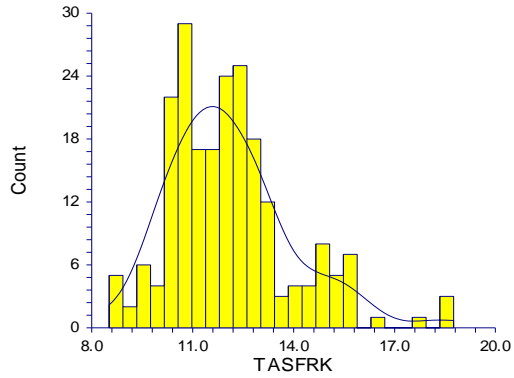
Plots Section of TRSFRK when Month=JUL



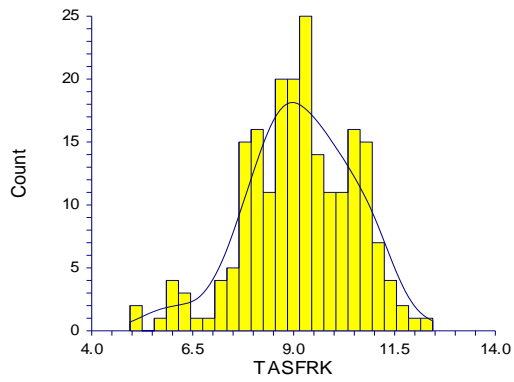
Plots Section of TRSFRK when Month=AUG



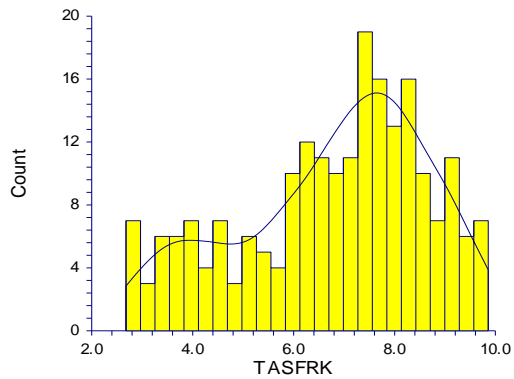
Plots Section of TRSFRK when Month=SEP



Plots Section of TRSFRK when Month=OCT

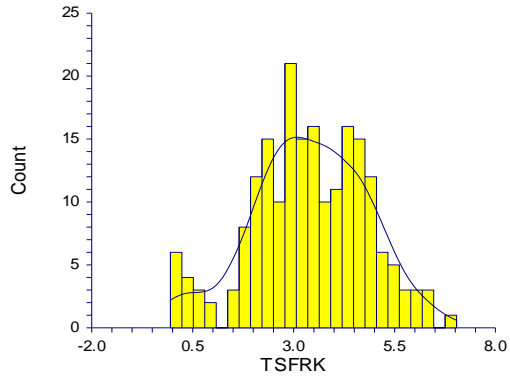


Plots Section of TRSFRK when Month=NOV

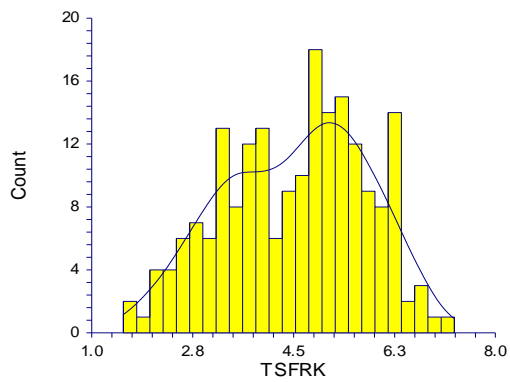


Plots Section of TRSFRK when Month=DEC

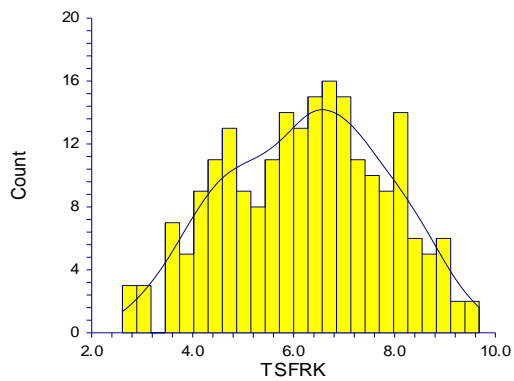
APPENDIX D
STATION TSFRK



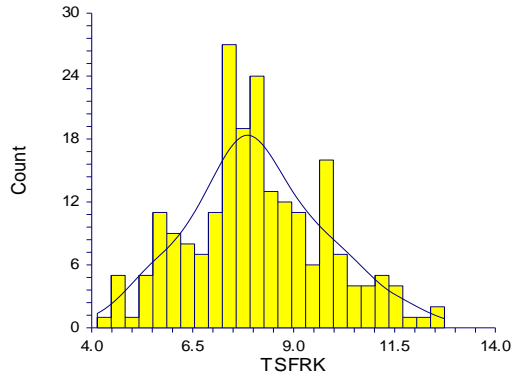
Plots Section of TSFRK when Month=JAN



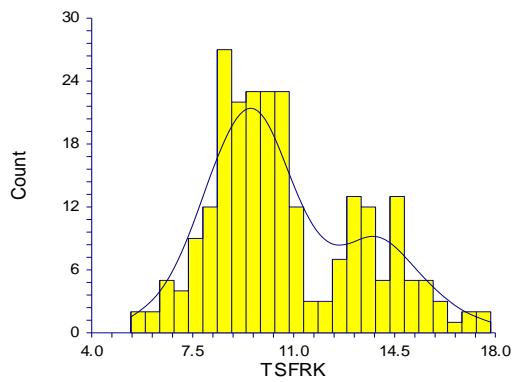
Plots Section of TSFRK when Month=FEB



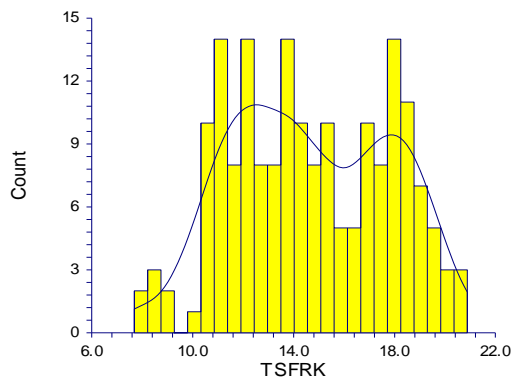
Plots Section of TSFRK when Month=MAR



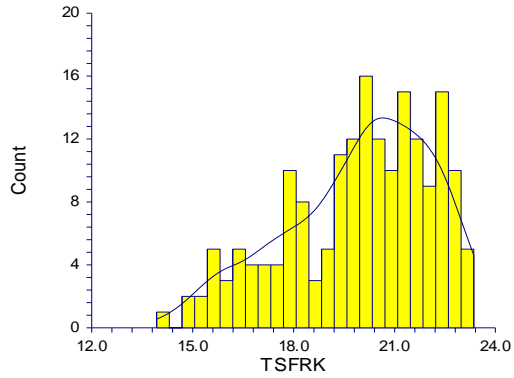
Plots Section of TSFRK when Month=APR



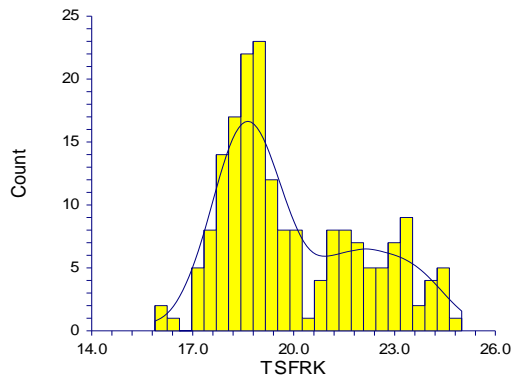
Plots Section of TSFRK when Month=MAY



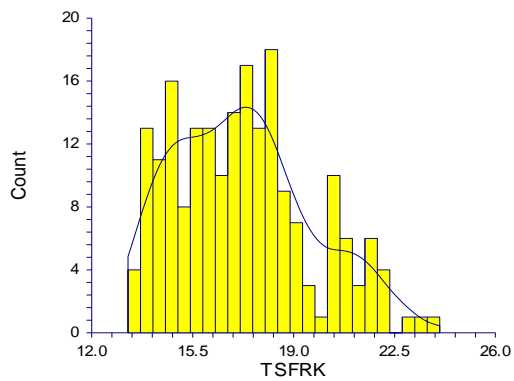
Plots Section of TSFRK when Month=JUN



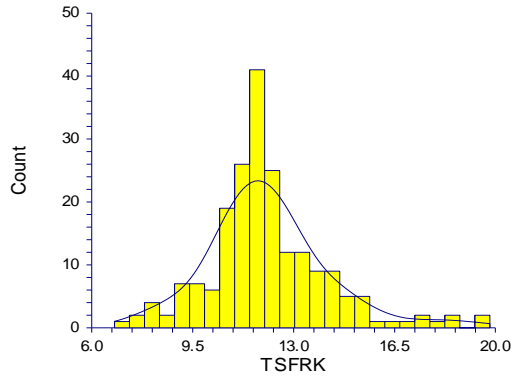
Plots Section of TSFRK when Month=JUL



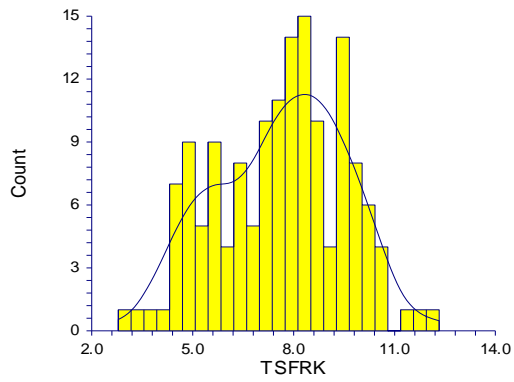
Plots Section of TSFRK when Month=AUG



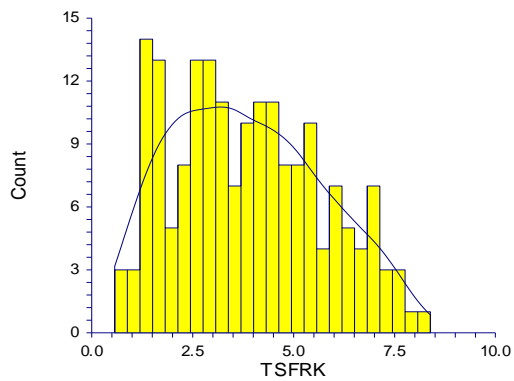
Plots Section of TSFRK when Month=SEP



Plots Section of TSFRK when Month=OCT



Plots Section of TSFRK when Month=NOV



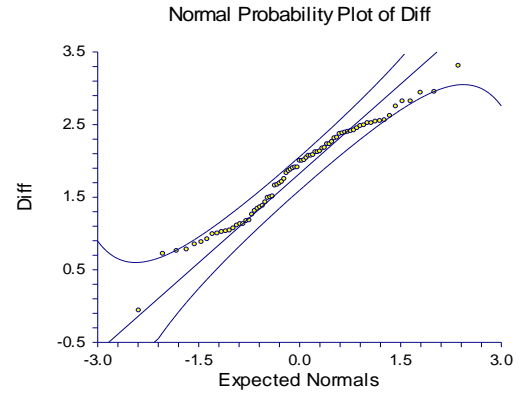
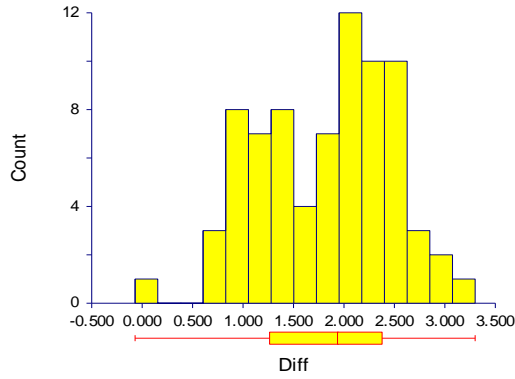
Plots Section of TSFRK when Month=DEC

APPENDIX E
STATION ICT – TSFRK

Summary Section of Diff when MM=JAN

Count	Mean	Standard Deviation	Standard Error	Minimum	Maximum	Range
76	1.833421	0.6673121	7.654595E-02	-0.07	3.3	3.37

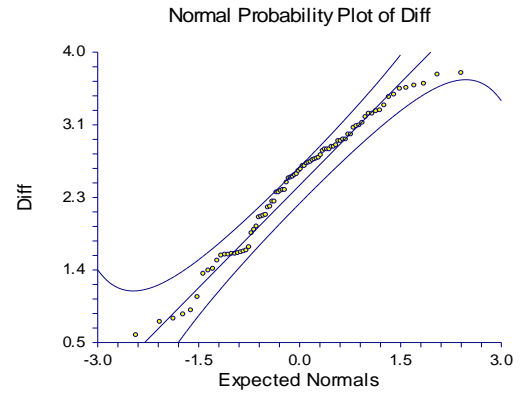
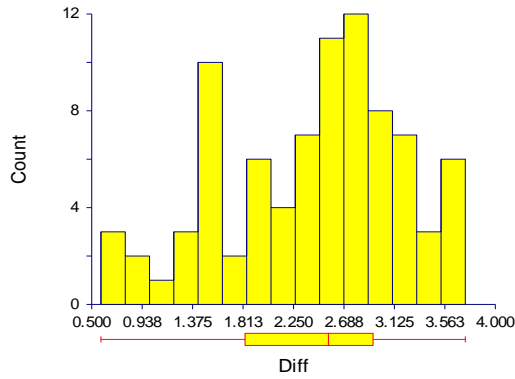
Plots Section of Diff when MM=JAN



Summary Section of Diff when MM=FEB

Count	Mean	Standard Deviation	Standard Error	Minimum	Maximum	Range
85	2.412706	0.7717997	8.371343E-02	0.58	3.74	3.16

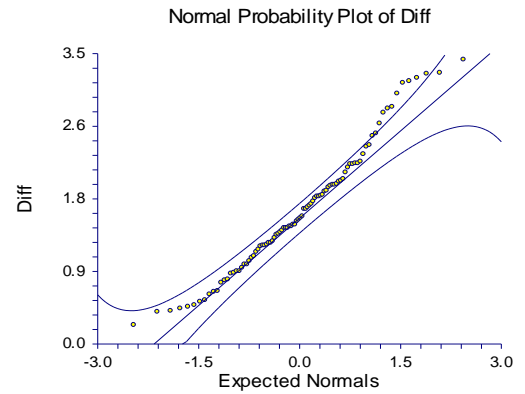
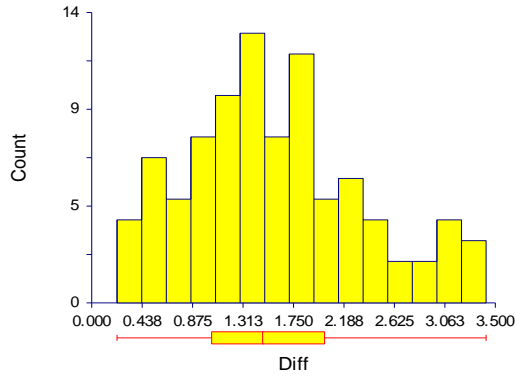
Plots Section of Diff when MM=FEB



Summary Section of Diff when MM=MAR

Count	Mean	Standard Deviation	Standard Error	Minimum	Maximum	Range
93	1.594731	0.7626122	0.0790792	0.22	3.42	3.2

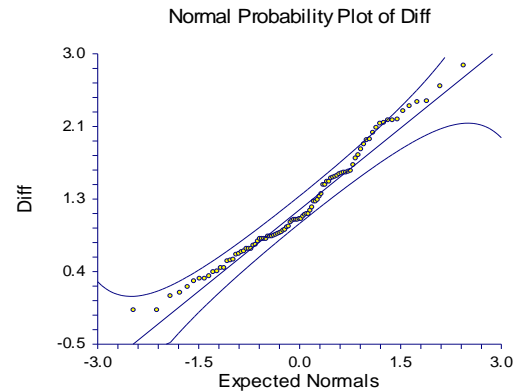
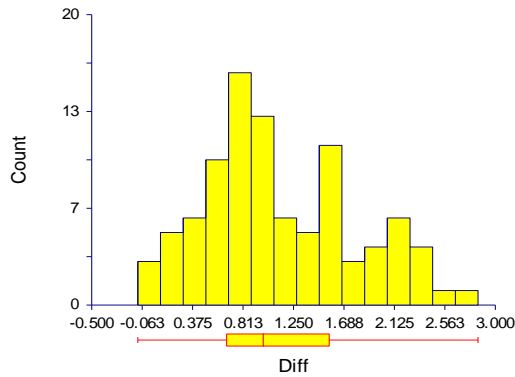
Plots Section of Diff when MM=MAR



Summary Section of Diff when MM=APR

Count	Mean	Standard Deviation	Standard Error	Minimum	Maximum	Range
94	1.140426	0.6621518	6.829574E-02	-0.1	2.85	2.95

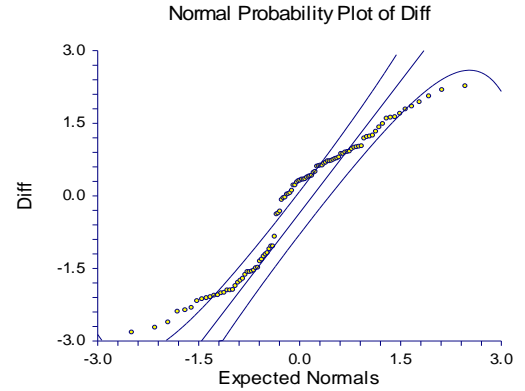
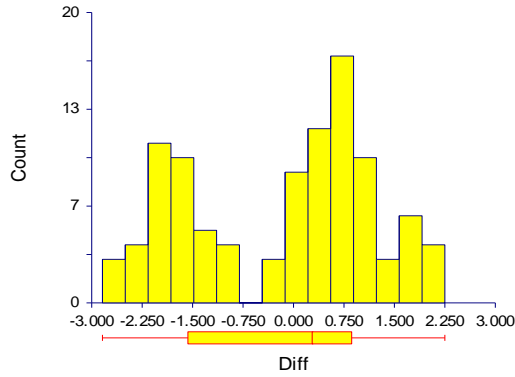
Plots Section of Diff when MM=APR



Summary Section of Diff when MM=MAY

Count	Mean	Standard Deviation	Standard Error	Minimum	Maximum	Range
101	-0.1738614	1.374295	0.1367474	-2.84	2.25	5.09

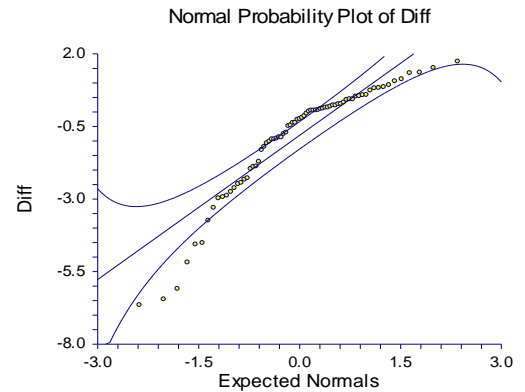
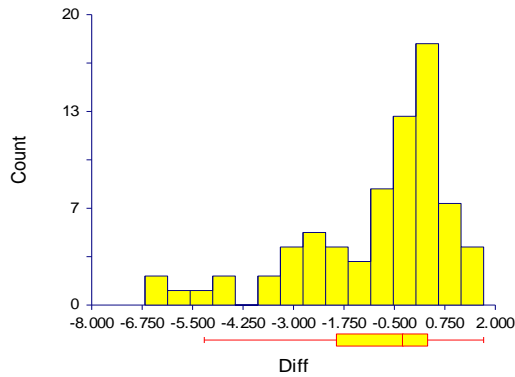
Plots Section of Diff when MM=MAY



Summary Section of Diff when MM=JUN

Count	Mean	Standard Deviation	Standard Error	Minimum	Maximum	Range
74	-0.9294595	1.891714	0.2199072	-6.68	1.71	8.39

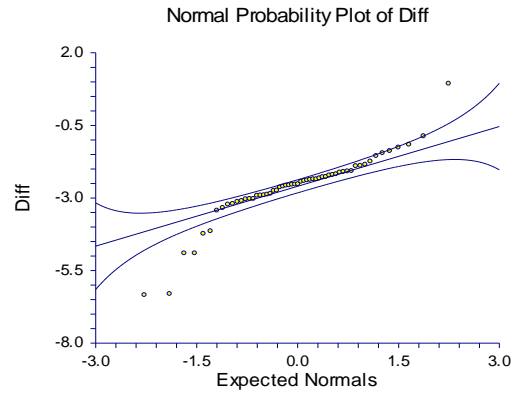
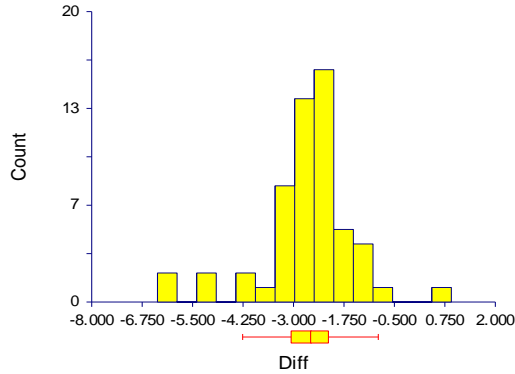
Plots Section of Diff when MM=JUN



Summary Section of Diff when MM=JUL

Count	Mean	Standard Deviation	Standard Error	Minimum	Maximum	Range
56	-2.66375	1.163666	0.1555014	-6.37	0.91	7.28

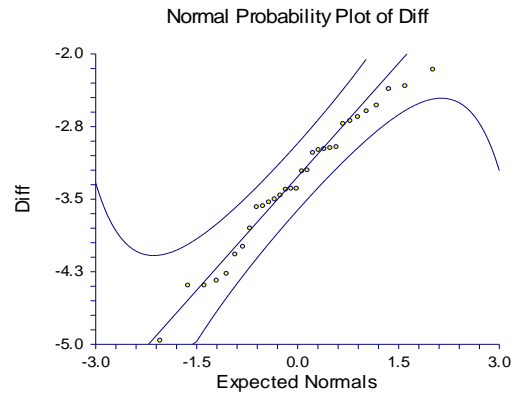
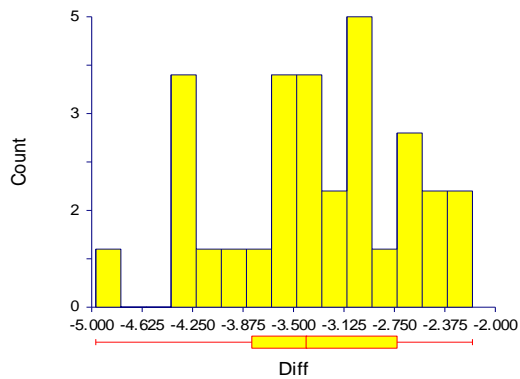
Plots Section of Diff when MM=JUL



Summary Section of Diff when MM=AUG

Count	Mean	Standard Deviation	Standard Error	Minimum	Maximum	Range
31	-3.345161	0.6976765	0.1253064	-4.97	-2.17	2.8

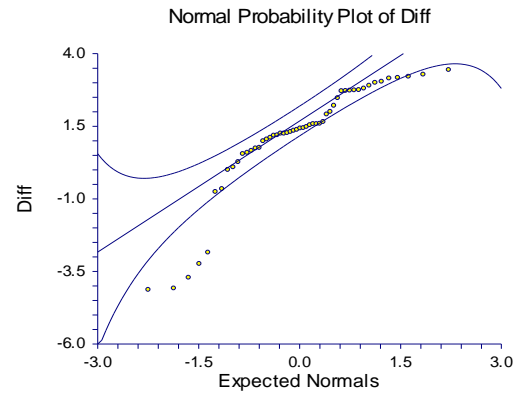
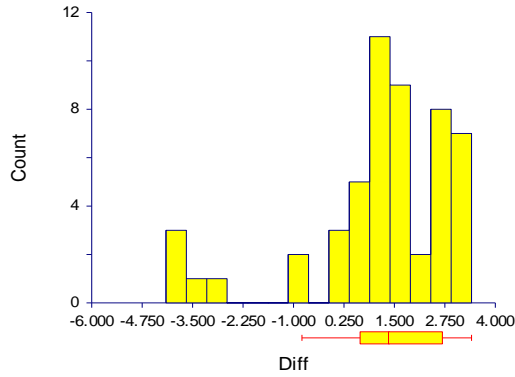
Plots Section of Diff when MM=AUG



Summary Section of Diff when MM=SEP

Count	Mean	Standard Deviation	Standard Error	Minimum	Maximum	Range
52	1.125385	1.870636	0.2594106	-4.16	3.41	7.57

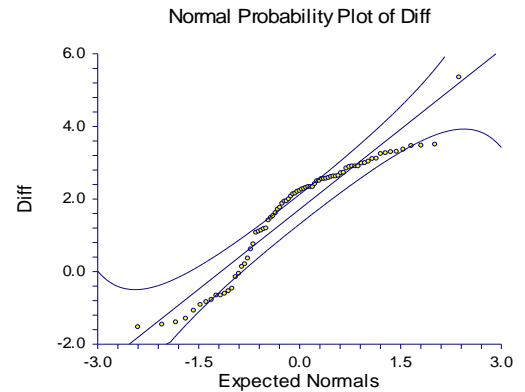
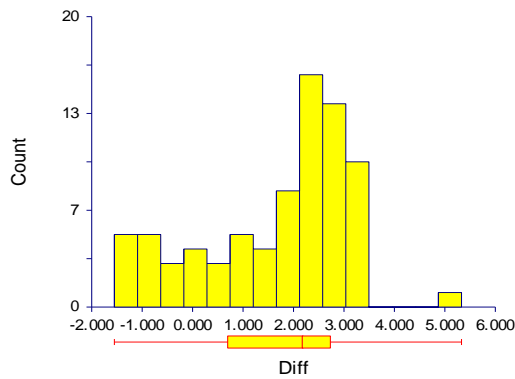
Plots Section of Diff when MM=SEP



Summary Section of Diff when MM=OCT

Count	Mean	Standard Deviation	Standard Error	Minimum	Maximum	Range
78	1.678846	1.505353	0.1704477	-1.55	5.33	6.88

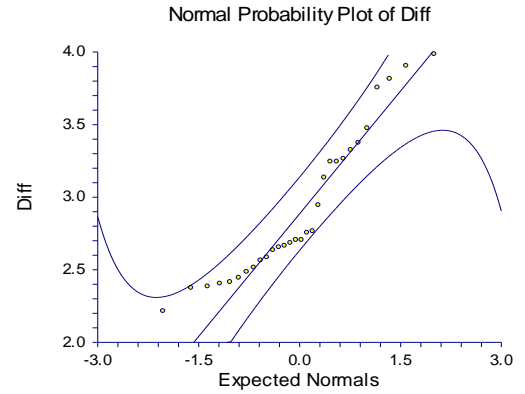
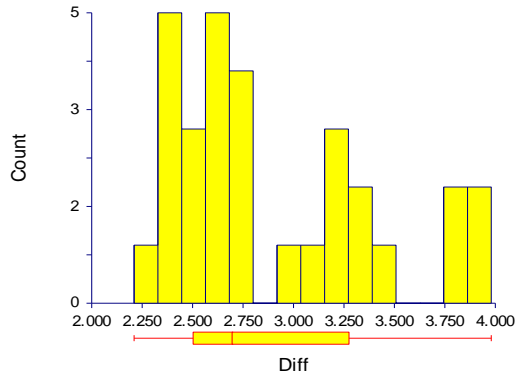
Plots Section of Diff when MM=OCT



Summary Section of Diff when MM=NOV

Count	Mean	Standard Deviation	Standard Error	Minimum	Maximum	Range
30	2.909333	0.508242	9.279186E-02	2.21	3.98	1.77

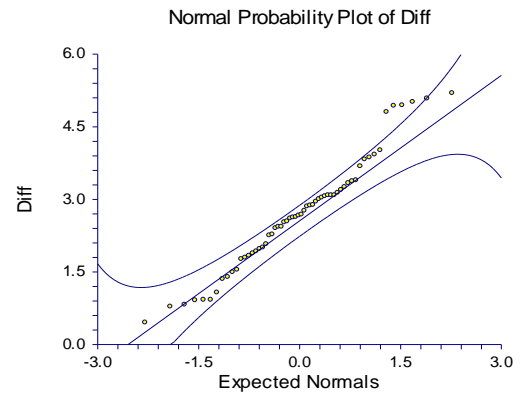
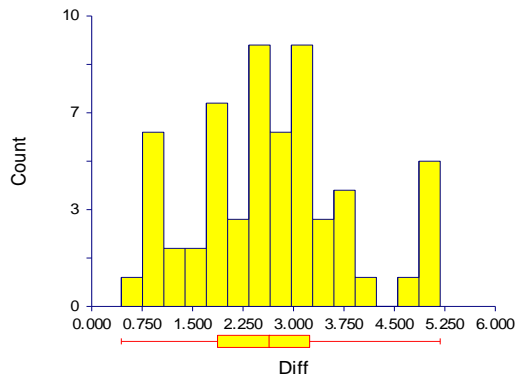
Plots Section of Diff when MM=NOV



Summary Section of Diff when MM=DEC

Count	Mean	Standard Deviation	Standard Error	Minimum	Maximum	Range
59	2.675254	1.159795	0.1509925	0.44	5.18	4.74

Plots Section of Diff when MM=DEC



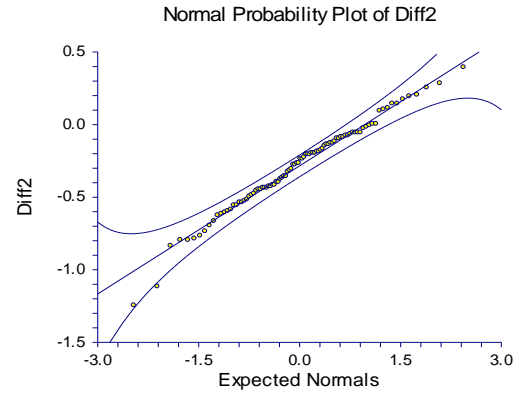
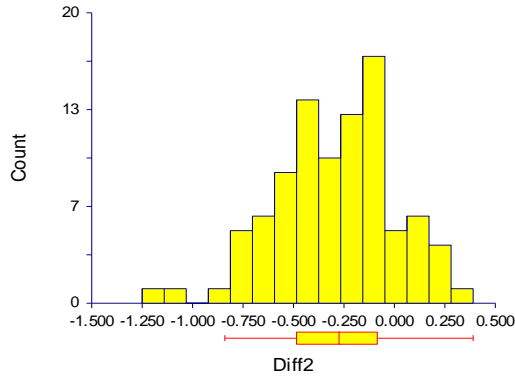
APPENDIX F

STATION ICT – TBSFRK

Summary Section of Diff2 when MM=JAN

Count	Mean	Standard Deviation	Standard Error	Minimum	Maximum	Range
93	-0.2934408	0.3027608	3.139484E-02	-1.25	0.39	1.64

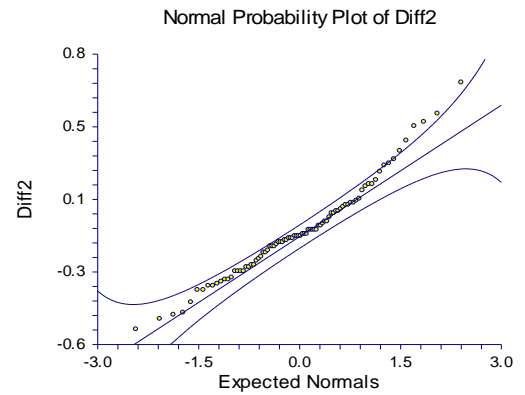
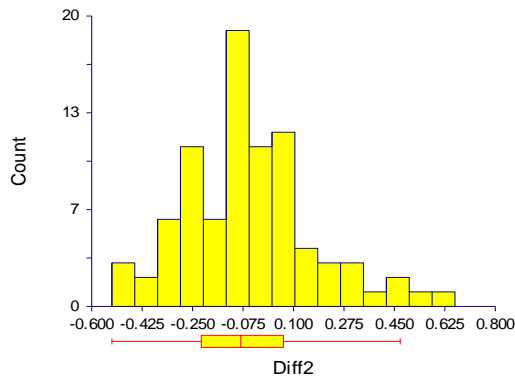
Plots Section of Diff2 when MM=JAN



Summary Section of Diff2 when MM=FEB

Count	Mean	Standard Deviation	Standard Error	Minimum	Maximum	Range
85	-5.658824E-02	0.2277873	0.024707	-0.53	0.66	1.19

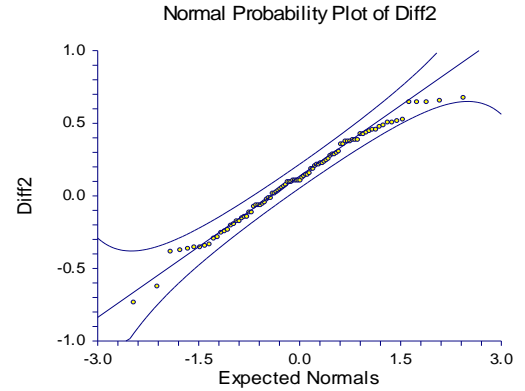
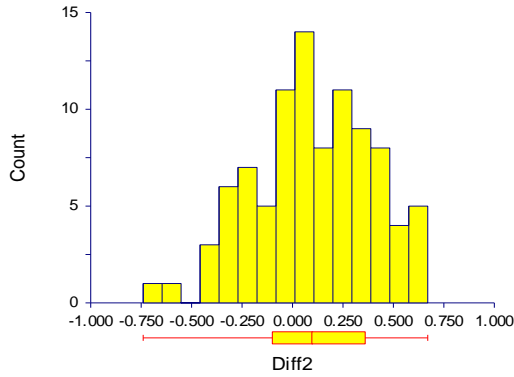
Plots Section of Diff2 when MM=FEB



Summary Section of Diff2 when MM=MAR

Count	Mean	Standard Deviation	Standard Error	Minimum	Maximum	Range
93	0.1062366	0.3007198	3.118319E-02	-0.74	0.67	1.41

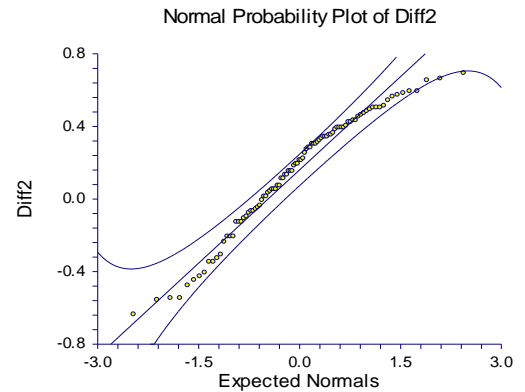
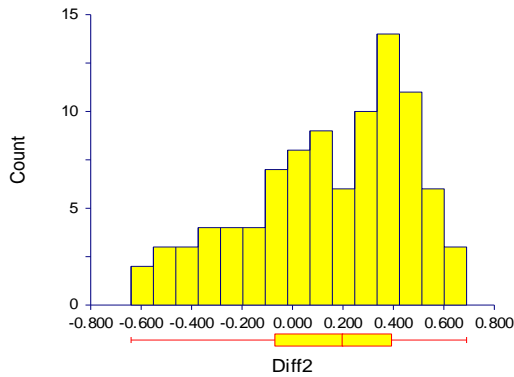
Plots Section of Diff2 when MM=MAR



Summary Section of Diff2 when MM=APR

Count	Mean	Standard Deviation	Standard Error	Minimum	Maximum	Range
94	0.15	0.3239773	3.341571E-02	-0.64	0.69	1.33

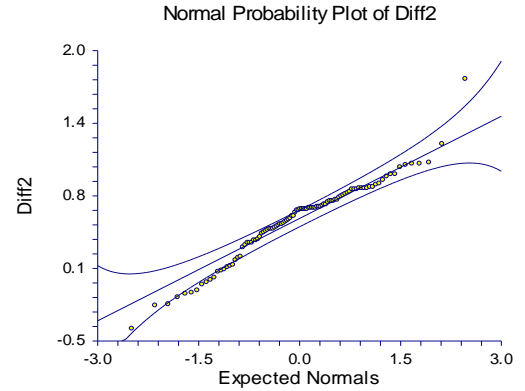
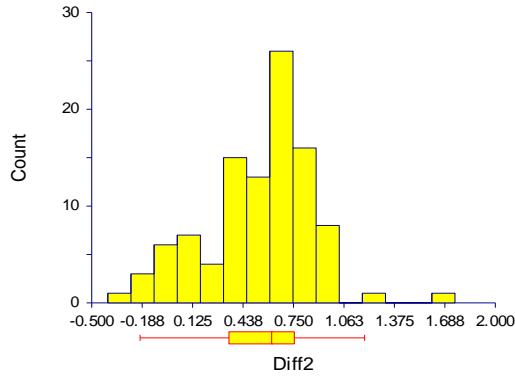
Plots Section of Diff2 when MM=APR



Summary Section of Diff2 when MM=MAY

Count	Mean	Standard Deviation	Standard Error	Minimum	Maximum	Range
101	0.5364357	0.3401017	3.384138E-02	-0.4	1.75	2.15

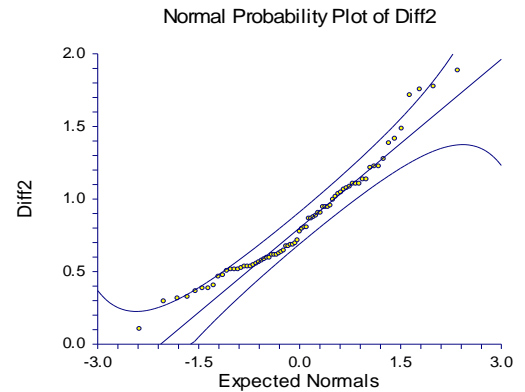
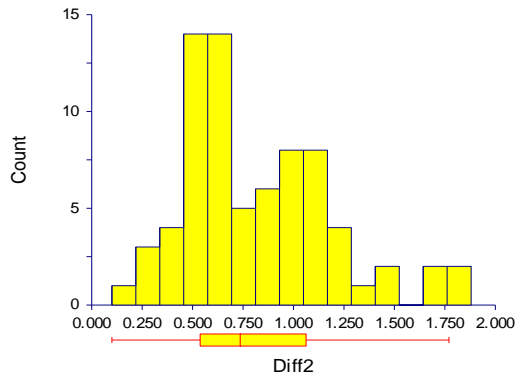
Plots Section of Diff2 when MM=MAY



Summary Section of Diff2 when MM=JUN

Count	Mean	Standard Deviation	Standard Error	Minimum	Maximum	Range
74	0.8209459	0.3734774	4.341587E-02	0.1	1.88	1.78

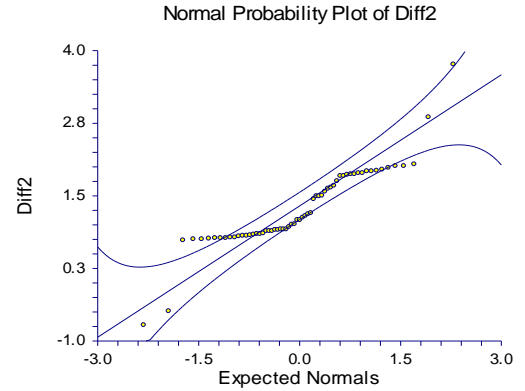
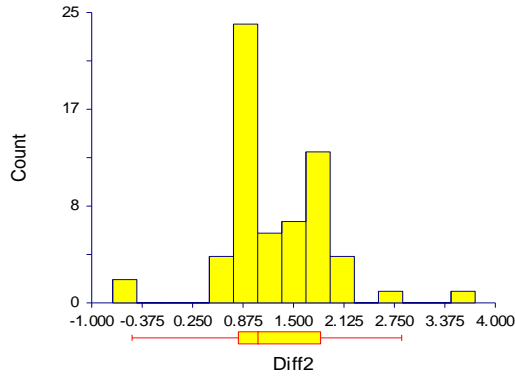
Plots Section of Diff2 when MM=JUN



Summary Section of Diff2 when MM=JUL

Count	Mean	Standard Deviation	Standard Error	Minimum	Maximum	Range
62	1.262097	0.683072	8.675023E-02	-0.74	3.75	4.49

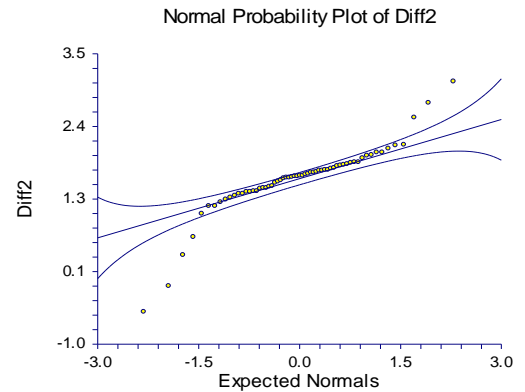
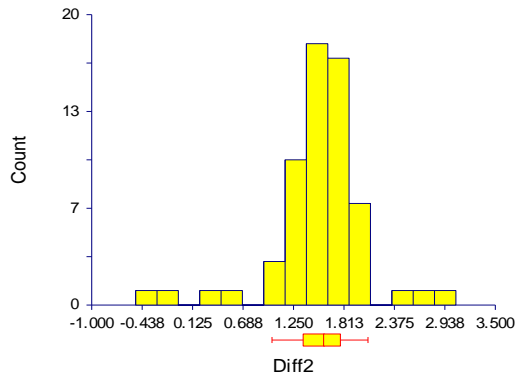
Plots Section of Diff2 when MM=JUL



Summary Section of Diff2 when MM=AUG

Count	Mean	Standard Deviation	Standard Error	Minimum	Maximum	Range
62	1.547097	0.5309638	6.743247E-02	-0.51	3.06	3.57

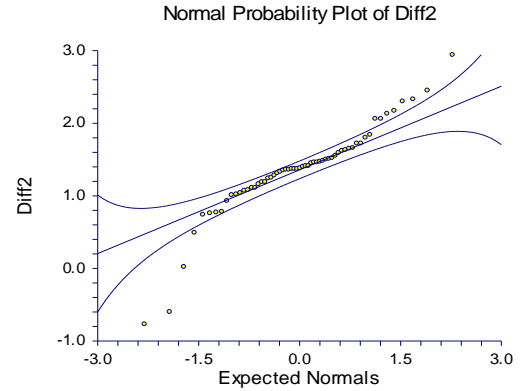
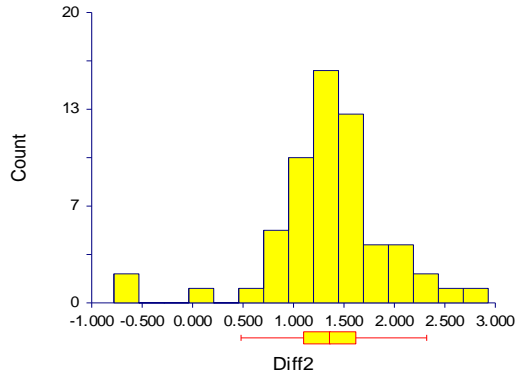
Plots Section of Diff2 when MM=AUG



Summary Section of Diff2 when MM=SEP

Count	Mean	Standard Deviation	Standard Error	Minimum	Maximum	Range
60	1.346	0.6142439	7.929855E-02	-0.78	2.93	3.71

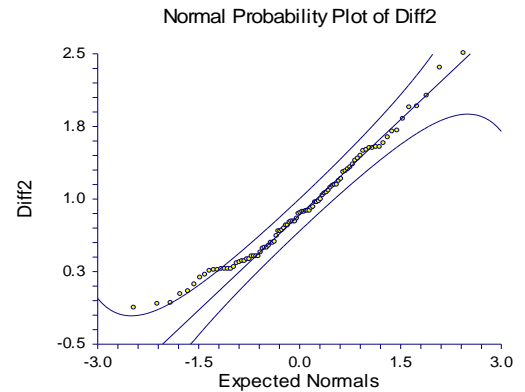
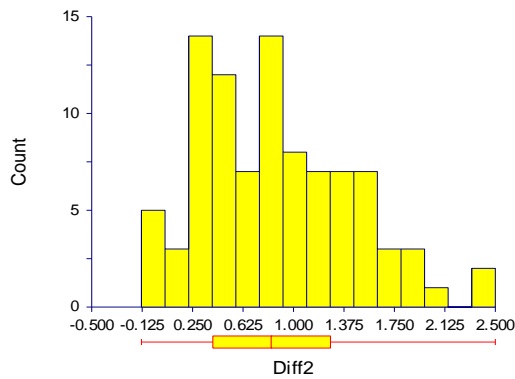
Plots Section of Diff2 when MM=SEP



Summary Section of Diff2 when MM=OCT

Count	Mean	Standard Deviation	Standard Error	Minimum	Maximum	Range
93	0.8664516	0.5657213	5.866256E-02	-0.13	2.5	2.63

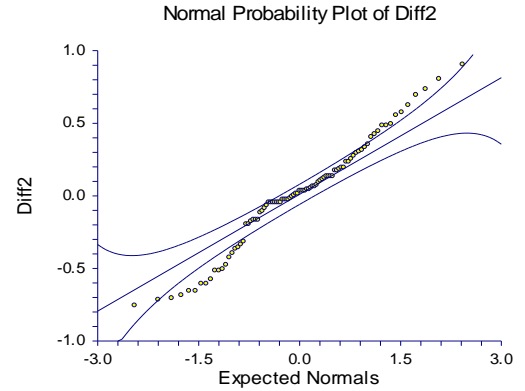
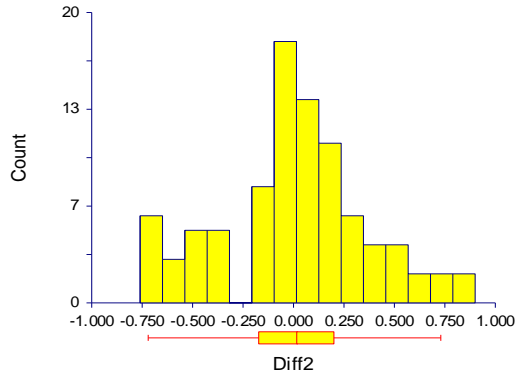
Plots Section of Diff2 when MM=OCT



Summary Section of Diff2 when MM=NOV

Count	Mean	Standard Deviation	Standard Error	Minimum	Maximum	Range
90	2.222222E-03	0.3654942	3.852647E-02	-0.76	0.9	1.66

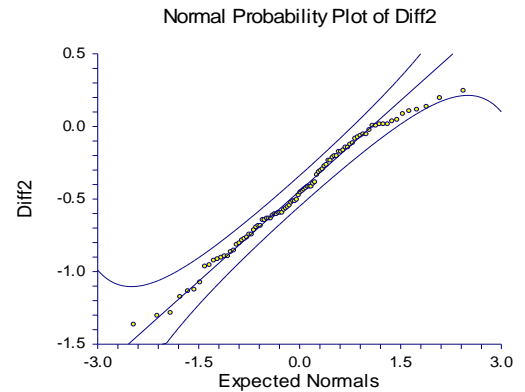
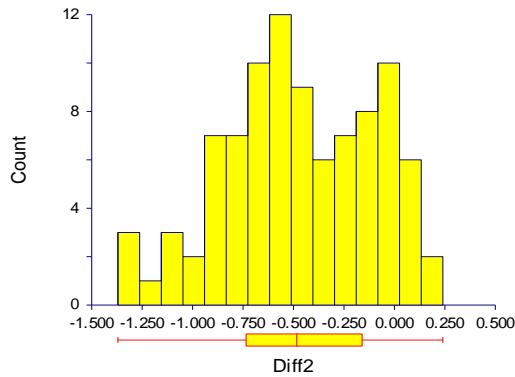
Plots Section of Diff2 when MM=NOV



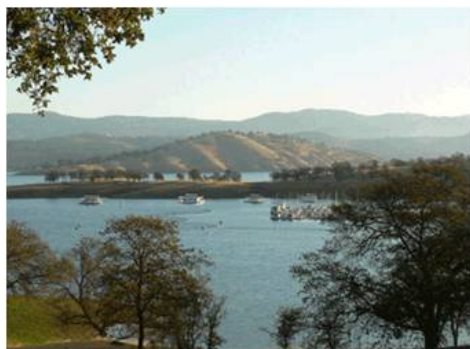
Summary Section of Diff2 when MM=DEC

Count	Mean	Standard Deviation	Standard Error	Minimum	Maximum	Range
93	-0.4726882	0.3762433	3.901461E-02	-1.37	0.24	1.61

Plots Section of Diff2 when MM=DEC



**LOWER TUOLUMNE RIVER
TEMPERATURE MODEL
STUDY REPORT
DON PEDRO PROJECT
FERC NO. 2299**



Prepared for:
Turlock Irrigation District – Turlock, California
Modesto Irrigation District – Modesto, California

Prepared by:
HDR Engineering, Inc.

May 2013

Lower Tuolumne River Temperature Model Study Report

TABLE OF CONTENTS

Section No.	Description	Page No.
1.0	INTRODUCTION.....	1-1
1.1	General Description of the Don Pedro Project	1-1
1.2	Relicensing Process	1-3
1.3	Resource Agency Management Goals	1-3
1.4	Study Plan	1-4
2.0	STUDY GOALS AND OBJECTIVES.....	2-1
3.0	STUDY AREA.....	3-1
4.0	METHODOLOGY	4-1
4.1	Model Set Up	4-1
4.2	Model Computations.....	4-1
4.2.1	Hydraulics	4-1
4.2.2	Bathymetry.....	4-2
4.2.3	Model Inflows and Outflows	4-4
4.2.4	Temperature	4-6
4.3	Monitoring Data.....	4-8
5.0	RESULTS	5-1
5.1	Calibration Results.....	5-1
5.2	Validation Results.....	5-4
5.3	Observed Diurnal Variations	5-10
6.0	DISCUSSION AND RECOMMENDATIONS.....	6-1
7.0	STUDY VARIANCES AND MODIFICATIONS	7-1
8.0	REFERENCES.....	8-1

List of Figures

Figure No.	Description	Page No.
Figure 1.1-1.	Don Pedro Project location.	1-2
Figure 3.0-1.	Study area.....	3-3
Figure 4.1-1.	HEC-RAS lower Tuolumne River model domain.	4-1
Figure 4.2-1.	HEC-RAS schematic of Tuolumne River below Don Pedro to San Joaquin confluence.	4-3

Figure 4.2-2. HEC-RAS profile of Tuolumne River. 4-3

Figure 4.2-3. HEC-RAS cross section showing La Grange Dam..... 4-4

Figure 4.2-4. Don Pedro releases 2011-12. 4-5

Figure 4.2-5. Don Pedro release temperature 2011-12..... 4-5

Figure 4.2-6. Total diversion flow at La Grange 2011-12..... 4-6

Figure 4.2-7. Denair short wave radiation used in HEC-RAS. 4-7

Figure 4.3-1. Temperature monitoring locations..... 4-8

Figure 4.3-2. Location of meteorological stations..... 4-10

Figure 4.3-3. Crocker Ranch air temperature for 2011-12. 4-11

Figure 4.3-4. Crocker Ranch relative humidity for 2011-12. 4-11

Figure 4.3-5. Crocker Ranch atmospheric pressure for 2011-12..... 4-12

Figure 5.1-1. Calibration results for 2011, RM 51.8 to 45.0. (Measured=black; HEC-RAS=red). 5-2

Figure 5.1-2. Calibration results for 2011, RM 43.2 to 26.0. (Measured=black; HEC-RAS=red). 5-3

Figure 5.1-3. Calibration results for 2011, RM 23.6 to 3.5. (Measured=black; HEC-RAS=red). 5-4

Figure 5.2-1. Validation results for 2012, RM 51.8 to 45.0. (Measured=black; HEC-RAS=red) 5-5

Figure 5.2-2. Validation results for 2012, RM 43.2 to 26.0. (Measured=black; HEC-RAS=red). 5-6

Figure 5.2-3. Validation results for 2012, RM 23.6 to 3.5. (Measured=black; HEC-RAS=red). 5-7

Figure 5.2-4. Results for 2011-12, RM 51.8 to 45.0. (Measured=black; HEC-RAS=red). 5-8

Figure 5.2-5. Results for 2011-12, RM 43.2 to 26.0. (Measured=black; HEC-RAS=red). 5-9

Figure 5.2-6. Results for 2011-12, RM 23.6 to 3.5. (Measured=black; HEC-RAS=red). 5-10

Figure 5.3-1. Annual average diurnal variation by site. 5-11

Figure 5.3-2. Summer average diurnal variation by site. 5-12

Figure 5.3-3. Summer average diurnal range at actual river location. 5-12

Figure 5.3-4. Summer average diurnal range at actual river location – annotated with return flow locations. 5-13

Figure 5.3-5. Summer average diurnal range– annotated with special run pools locations. 5-14

Figure 5.3-6. Comparison of 2011 and 2010 ranges (top=summer, lower=annual). 5-15

Figure 5.3-7. Comparison of 2011 and 2009 ranges (top=summer, lower=annual). 5-16

Figure 5.3-8. Comparison of 2011 and 2008 ranges (top=summer, lower=annual). 5-17

Figure 5.3-9. Comparison of 2011 and 2007 ranges (top=summer, lower=annual). 5-18

Figure 5.3-10. Comparison of 2011 and 2006 ranges (top=summer, lower=annual). 5-19

Figure 5.3-11. Comparison of 2011 and 2005 ranges (top=summer, lower=annual). 5-20

Figure 5.3-12. Comparison of 2011 and 2004 ranges (top=summer, lower=annual). 5-21
 Figure 5.3-13. Comparison of 2011 and 2003 ranges (top=summer, lower=annual). 5-22
 Figure 5.3-14. Comparison of 2002 and 2010 ranges (top=summer, lower=annual). 5-23
 Figure 5.3-15. Comparison of 2011 and 2001 ranges (top=summer, lower=annual). 5-24

List of Tables

Table No.	Description	Page No.
Table 4.2-1.	Lower Tuolumne River geometry data sources.	4-2
Table 4.2-2.	Monthly flow in Dry Creek.....	4-4
Table 4.3-1.	Temperature monitoring locations.....	4-8

List of Attachments

Attachment A	Study Plan W&AR-16: In - River Diurnal Temperature Variation Study
--------------	--

List of Acronyms

ac	acres
ACEC	Area of Critical Environmental Concern
AF	acre-feet
ADCP	Accoustic Doppler Current Profiler
ACOE	U.S. Army Corps of Engineers
ADA	Americans with Disabilities Act
ALJ	Administrative Law Judge
APE	Area of Potential Effect
ARMR	Archaeological Resource Management Report
BA	Biological Assessment
BDCP	Bay-Delta Conservation Plan
BLM	U.S. Department of the Interior, Bureau of Land Management
BLM-S	Bureau of Land Management – Sensitive Species
BMI	Benthic macroinvertebrates
BMP	Best Management Practices
BO	Biological Opinion
CalEPPC	California Exotic Pest Plant Council
CalSPA	California Sports Fisherman Association
CAS	California Academy of Sciences
CCC	Criterion Continuous Concentrations
CCIC	Central California Information Center
CCSF	City and County of San Francisco
CCVHJV	California Central Valley Habitat Joint Venture
CD	Compact Disc
CDBW	California Department of Boating and Waterways
CDEC	California Data Exchange Center
CDFA	California Department of Food and Agriculture
CDFW	California Department of Fish and Wildlife
CDMG	California Division of Mines and Geology
CDOF	California Department of Finance
CDPH	California Department of Public Health

CDPR	California Department of Parks and Recreation
CDSOD	California Division of Safety of Dams
CDWR.....	California Department of Water Resources
CE	California Endangered Species
CEII.....	Critical Energy Infrastructure Information
CEQA.....	California Environmental Quality Act
CESA	California Endangered Species Act
CFR.....	Code of Federal Regulations
cfs	cubic feet per second
CGS.....	California Geological Survey
CMAP	California Monitoring and Assessment Program
CMC.....	Criterion Maximum Concentrations
CNDDB.....	California Natural Diversity Database
CNPS.....	California Native Plant Society
CORP	California Outdoor Recreation Plan
CPUE	Catch Per Unit Effort
CRAM.....	California Rapid Assessment Method
CRLF.....	California Red-Legged Frog
CRRF	California Rivers Restoration Fund
CSAS.....	Central Sierra Audubon Society
CSBP.....	California Stream Bioassessment Procedure
CT	California Threatened Species
CTR.....	California Toxics Rule
CTS	California Tiger Salamander
CVRWQCB	Central Valley Regional Water Quality Control Board
CWA	Clean Water Act
CWHR.....	California Wildlife Habitat Relationship
Districts	Turlock Irrigation District and Modesto Irrigation District
DLA	Draft License Application
DPRA.....	Don Pedro Recreation Agency
DPS	Distinct Population Segment
EA	Environmental Assessment
EC	Electrical Conductivity

EFH.....	Essential Fish Habitat
EIR	Environmental Impact Report
EIS.....	Environmental Impact Statement
EPA.....	U.S. Environmental Protection Agency
ESA.....	Federal Endangered Species Act
ESRCD.....	East Stanislaus Resource Conservation District
ESU.....	Evolutionary Significant Unit
EWUA.....	Effective Weighted Useable Area
FERC.....	Federal Energy Regulatory Commission
FFS	Foothills Fault System
FL.....	Fork length
FMU.....	Fire Management Unit
FOT	Friends of the Tuolumne
FPC	Federal Power Commission
ft/mi.....	feet per mile
FWCA.....	Fish and Wildlife Coordination Act
FYLF.....	Foothill Yellow-Legged Frog
g.....	grams
GIS	Geographic Information System
GLO	General Land Office
GPS	Global Positioning System
HCP.....	Habitat Conservation Plan
HHWP.....	Hetch Hetchy Water and Power
HORB	Head of Old River Barrier
HPMP.....	Historic Properties Management Plan
ILP.....	Integrated Licensing Process
ISR	Initial Study Report
ITA.....	Indian Trust Assets
kV.....	kilovolt
m	meters
M&I.....	Municipal and Industrial
MCL.....	Maximum Contaminant Level
mg/kg	milligrams/kilogram

mg/L	milligrams per liter
mgd	million gallons per day
mi	miles
mi ²	square miles
MID	Modesto Irrigation District
MOU	Memorandum of Understanding
MSCS	Multi-Species Conservation Strategy
msl	mean sea level
MVA	Megavolt Ampere
MW	megawatt
MWh	megawatt hour
mya	million years ago
NAE	National Academy of Engineering
NAHC	Native American Heritage Commission
NAS	National Academy of Sciences
NAVD 88	North American Vertical Datum of 1988
NAWQA	National Water Quality Assessment
NCCP	Natural Community Conservation Plan
NEPA	National Environmental Policy Act
ng/g	nanograms per gram
NGOs	Non-Governmental Organizations
NHI	Natural Heritage Institute
NHPA	National Historic Preservation Act
NISC	National Invasive Species Council
NMFS	National Marine Fisheries Service
NOAA	National Oceanic and Atmospheric Administration
NOI	Notice of Intent
NPS	U.S. Department of the Interior, National Park Service
NRCS	National Resource Conservation Service
NRHP	National Register of Historic Places
NRI	Nationwide Rivers Inventory
NTU	Nephelometric Turbidity Unit
NWI	National Wetland Inventory

NWIS	National Water Information System
NWR	National Wildlife Refuge
NGVD 29	National Geodetic Vertical Datum of 1929
O&M.....	operation and maintenance
OEHHA.....	Office of Environmental Health Hazard Assessment
ORV	Outstanding Remarkable Value
PAD.....	Pre-Application Document
PDO.....	Pacific Decadal Oscillation
PEIR.....	Program Environmental Impact Report
PGA.....	Peak Ground Acceleration
PHG.....	Public Health Goal
PM&E	Protection, Mitigation and Enhancement
PMF.....	Probable Maximum Flood
POAOR.....	Public Opinions and Attitudes in Outdoor Recreation
ppb.....	parts per billion
ppm	parts per million
PSP	Proposed Study Plan
QA.....	Quality Assurance
QC	Quality Control
RA	Recreation Area
RBP.....	Rapid Bioassessment Protocol
Reclamation	U.S. Department of the Interior, Bureau of Reclamation
RM	River Mile
RMP	Resource Management Plan
RP.....	Relicensing Participant
RSP	Revised Study Plan
RST	Rotary Screw Trap
RTM	Real Time Temperature Monitoring
RWF.....	Resource-Specific Work Groups
RWG	Resource Work Group
RWQCB.....	Regional Water Quality Control Board
SC.....	State candidate for listing under CESA
SCD.....	State candidate for delisting under CESA

SCE	State candidate for listing as endangered under CESA
SCT	State candidate for listing as threatened under CESA
SD1	Scoping Document 1
SD2	Scoping Document 2
SE	State Endangered Species under the CESA
SFP	State Fully Protected Species under CESA
SFPUC	San Francisco Public Utilities Commission
SHPO	State Historic Preservation Office
SJRA	San Joaquin River Agreement
SJRG	San Joaquin River Group Authority
SJTA	San Joaquin River Tributaries Authority
SPD	Study Plan Determination
SRA	State Recreation Area
SRMA	Special Recreation Management Area or Sierra Resource Management Area (as per use)
SRMP	Sierra Resource Management Plan
SRP	Special Run Pools
SSC	State species of special concern
ST	California Threatened Species under the CESA
STORET	Storage and Retrieval
SWAMP	Surface Water Ambient Monitoring Program
SWE	Snow-Water Equivalent
SWRCB	State Water Resources Control Board
TAC	Technical Advisory Committee
TAF	thousand acre-feet
TCP	Traditional Cultural Properties
TDS	Total Dissolved Solids
TID	Turlock Irrigation District
TMDL	Total Maximum Daily Load
TOC	Total Organic Carbon
TRT	Tuolumne River Trust
TRTAC	Tuolumne River Technical Advisory Committee
UC	University of California

USDA.....	U.S. Department of Agriculture
USDOC.....	U.S. Department of Commerce
USDOJ.....	U.S. Department of the Interior
USFS.....	U.S. Department of Agriculture, Forest Service
USFWS.....	U.S. Department of the Interior, Fish and Wildlife Service
USGS.....	U.S. Department of the Interior, Geological Survey
USR.....	Updated Study Report
UTM.....	Universal Transverse Mercator
VAMP.....	Vernalis Adaptive Management Plan
VELB.....	Valley Elderberry Longhorn Beetle
VRM.....	Visual Resource Management
WPT.....	Western Pond Turtle
WSA.....	Wilderness Study Area
WSIP.....	Water System Improvement Program
WWTP.....	Wastewater Treatment Plant
WY.....	water year
µS/cm.....	microSeimens per centimeter

1.0 INTRODUCTION

1.1 General Description of the Don Pedro Project

Turlock Irrigation District (TID) and Modesto Irrigation District (MID) (collectively, the Districts) are the co-licensees of the 168-megawatt (MW) Don Pedro Project (Project) located on the Tuolumne River in western Tuolumne County in the Central Valley region of California. The Don Pedro Dam is located at river mile (RM) 54.8 and the Don Pedro Reservoir formed by the dam extends 24-miles upstream at the normal maximum water surface elevation of 830 feet (ft) above mean sea level (msl; NGVD 29). At elevation 830 ft, the reservoir stores over 2,000,000 acre-feet (AF) of water and has a surface area slightly less than 13,000 acres (ac). The watershed above Don Pedro Dam is approximately 1,533 square miles (mi²).

Both TID and MID are local public agencies authorized under the laws of the State of California to provide water supply for irrigation and municipal and industrial (M&I) uses and to provide retail electric service. The Project serves many purposes including providing water storage for the beneficial use of irrigation of over 200,000 ac of prime Central Valley farmland and for the use of M&I customers in the City of Modesto (population 210,000). Consistent with the requirements of the Raker Act passed by Congress in 1913 and agreements between the Districts and City and County of San Francisco (CCSF), the Project reservoir also includes a “water bank” of up to 570,000 AF of storage. CCSF may use the water bank to more efficiently manage the water supply from its Hetch Hetchy water system while meeting the senior water rights of the Districts. CCSF’s “water bank” within Don Pedro Reservoir provides significant benefits for its 2.6 million customers in the San Francisco Bay Area.

The Project also provides storage for flood management purposes in the Tuolumne and San Joaquin rivers in coordination with the U.S. Army Corps of Engineers (ACOE). Other important uses supported by the Project are recreation, protection of the anadromous fisheries in the lower Tuolumne River, and hydropower generation.

The Project Boundary extends from approximately one mile downstream of the dam to approximately RM 79 upstream of the dam. Upstream of the dam, the Project Boundary runs generally along the 855 ft contour interval which corresponds to the top of the Don Pedro Dam. The Project Boundary encompasses approximately 18,370 ac with 78 percent of the lands owned jointly by the Districts and the remaining 22 percent (approximately 4,000 ac) is owned by the United States and managed as a part of the U.S. Bureau of Land Management (BLM) Sierra Resource Management Area.

The primary Project facilities include the 580-foot-high Don Pedro Dam and Reservoir completed in 1971; a four-unit powerhouse situated at the base of the dam; related facilities including the Project spillway, outlet works, and switchyard; four dikes (Gasburg Creek Dike and Dikes A, B, and C); and three developed recreational facilities (Fleming Meadows, Blue Oaks, and Moccasin Point Recreation Areas). The location of the Project and its primary facilities is shown in Figure 1.1-1.

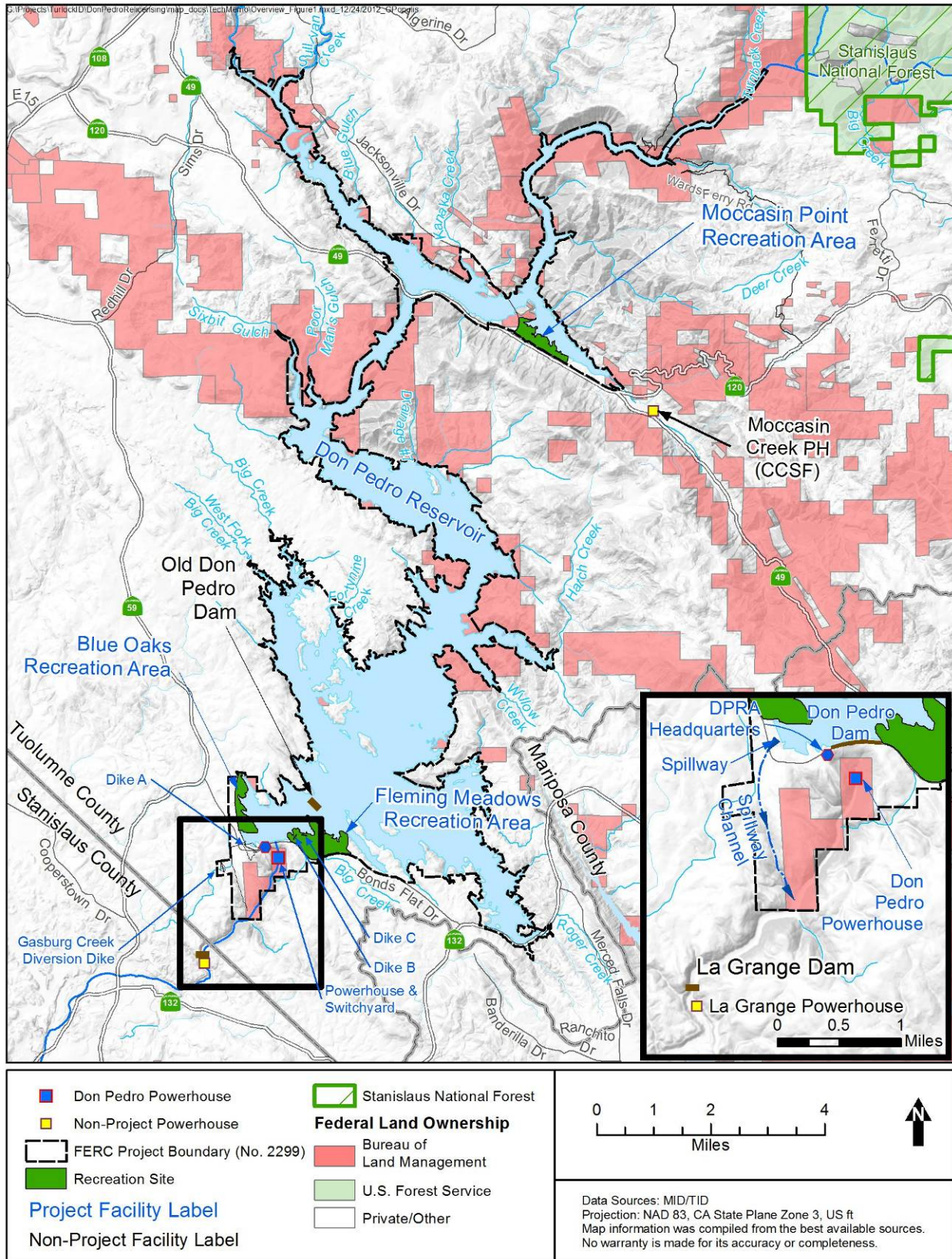


Figure 1.1-1. Don Pedro Project location.

1.2 Relicensing Process

The current FERC license for the Project expires on April 30, 2016, and the Districts will apply for a new license no later than April 30, 2014. The Districts began the relicensing process by filing a Notice of Intent and Pre-Application Document (PAD) with FERC on February 10, 2011, following the regulations governing the Integrated Licensing Process (ILP). The Districts' PAD included descriptions of the Project facilities, operations, license requirements, and Project lands as well as a summary of the extensive existing information available on Project area resources. The PAD also included ten draft study plans describing a subset of the Districts' proposed relicensing studies. The Districts then convened a series of Resource Work Group meetings, engaging agencies and other relicensing participants in a collaborative study plan development process culminating in the Districts' Proposed Study Plan (PSP) and Revised Study Plan (RSP) filings to FERC on July 25, 2011 and November 22, 2011, respectively.

On December 22, 2011, FERC issued its Study Plan Determination (SPD) for the Project, approving, or approving with modifications, 34 studies proposed in the RSP that addressed Cultural and Historical Resources, Recreational Resources, Terrestrial Resources, and Water and Aquatic Resources. In addition, as required by the SPD, the Districts filed three new study plans (W&AR-18, W&AR-19, and W&AR-20) on February 28, 2012 and one modified study plan (W&AR-12) on April 6, 2012. Prior to filing these plans with FERC, the Districts consulted with relicensing participants on drafts of the plans. FERC approved or approved with modifications these four studies on July 25, 2012.

Following the SPD, a total of seven studies (and associated study elements) that were either not adopted in the SPD, or were adopted with modifications, formed the basis of Study Dispute proceedings. In accordance with the ILP, FERC convened a Dispute Resolution Panel on April 17, 2012 and the Panel issued its findings on May 4, 2012. On May 24, 2012, the Director of FERC issued his Formal Study Dispute Determination, with additional clarifications related to the Formal Study Dispute Determination issued on August 17, 2012.

The Districts filed with FERC an Initial Study Report on January 17, 2013 that included a progress report on the development of the Lower Tuolumne River Temperature Model Study (W&AR-16) and recommended that the modeling platform should be updated to the U.S. Army Corps of Engineers' (ACOE) Hydrologic Engineering Center's (HEC) River Analysis System HEC-5Q model.

This study report describes the objectives, methods, and results of the Lower Tuolumne River Temperature Model Study (W&AR-16) as implemented by the Districts in accordance with FERC's SPD and subsequent study modifications and clarifications. Documents relating to the Project relicensing are publicly available on the Districts' relicensing website at www.donpedro-relicensing.com.

1.3 Resource Agency Management Goals

The Districts believe that two agencies have resource management goals related to water temperature in Don Pedro Reservoir and in the lower Tuolumne River: (1) the California

Department of Fish and Wildlife (CDFW), and (2) the State Water Resources Control Board, Division of Water Rights (SWRCB). Each of these agencies and their management goals, as understood by the Districts at this time, is described below.

CDFW's goal is to preserve and protect the habitats necessary to support native fish, wildlife and plant species.

SWRCB is the state agency that administers the federal Clean Water Act (CWA) (33 U.S.C. §11251-1357) as applies to California waters with the responsibility to maintain the chemical, physical, and biological integrity of the state's waters and to protect the beneficial uses of stream reaches consistent with Section 401 of the federal CWA, the Regional Water Quality Control Board Basin Plans, State Water Board regulations, California Environmental Quality Act, and any other applicable state law. SWRCB's management goals are set forth in the CVRWQCB's Basin Plan, which was initially adopted in 1998 and most recently revised in 2011 (CVRWQCB 1998).

The Don Pedro Project and the areas upstream and downstream of the Project fall within three Basin Plan Hydro Units: (1) Hydro Unit 536, which includes the Tuolumne River upstream of the Project; (2) Hydro Unit 536.32, which includes Don Pedro Reservoir; and (3) Hydro Unit 535, which includes the Tuolumne River from Don Pedro Dam to the San Joaquin River. Designated beneficial uses in Hydro Unit 535 consist of municipal and domestic supply, agricultural supply, industrial process supply, industrial service supply, water contact recreation¹, non-contact water recreation, warm freshwater habitat², cold freshwater habitat², migration of aquatic organisms³, spawning habitat, and wildlife habitat.

In addition, Section 303(d) of the CWA requires that every two years each state submit to the U.S. Environmental Protection Agency (EPA) a list of rivers, lakes, and reservoirs in the state for which pollution control or requirements have failed to meet water quality standards. Based on a review of the SWRCB's 2010 proposed list and its associated TMDL Priority Schedule, the lower Tuolumne River (Don Pedro Reservoir to San Joaquin River) has been identified as state impaired for temperature⁴, diazinon, Group A Pesticides⁵, and Unknown Toxicity (SWRCB 2010). There are currently no approved TMDL plans for the Tuolumne River.

1.4 Study Plan

FERC approved the study plan for the Lower Tuolumne River Temperature Model (W&AR-16) with modifications. The SPD required the Districts to provide model output that 1) could be used in the existing CalFed San Joaquin River Basin model (SJR5Q) (AD Consultants et al 2009); 2) model river temperatures as needed to calculate daily maximum temperatures; 3)

¹ Shown for streams and rivers only with the implication that certain flows are required for this beneficial use.

² Resident does not include anadromous. Any hydrologic unit with both WARM and COLD beneficial use designations is considered COLD water bodies by the SWRCB for the application of water quality objectives.

³ Applies to coldwater species: salmon and steelhead.

⁴ On October 11, 2011, the EPA finalized California's list of impaired waters under CWA §202(d). The approved list for the Tuolumne River included the addition of temperature impairments from the outlet of Don Pedro Dam to the mouth of the river.

⁵ Group A Pesticides consist of aldrin, dieldrin, chlordane, endrin, heptachlor, heptachlor epoxide, hexachlorocyclohexanes (including lindane), endosulfan, and toxaphene.

model river temperatures as needed to compare the results to weekly average temperatures presented in TID/MID (2011a), and 4) provide all data used in calibration.

The Lower Tuolumne River Temperature model was developed consistent with the study plan as modified by the SPD and is a tool that may be used to evaluate how current and potential future operating scenarios might cumulatively affect temperatures downstream of the Project in the lower Tuolumne River. In order to meet the objectives outlined in the SPD, two model versions have been developed. As described in the progress report for this study provided with the Initial Study Report, the first version of the model updated the Tuolumne River portion of SJR5Q, a proprietary model that utilizes the ACOE's HEC-5Q model platform and provides results as a 6 hour time-step (TID/MID 2013a). This version of the model reasonably simulated temperature conditions in the lower Tuolumne River most of the time, but did not reasonably simulate unexpected changes in diurnal temperature ranges that were observed below about RM 40. Because the model's source code is proprietary and intermediate model steps were not transparent⁶, the model itself could not provide insight into the observed inconsistencies. Hence, after implementing the model, the Districts concluded that migrating the model platform to HEC-RAS would better meet the goals and objectives of the study plan (TID/MID 2012a; 2012b; 2013a; 2013b).

Developed in 2013, the second version of the Lower Tuolumne River Temperature model is provided and described in this study report. HEC-RAS is the ACOE's current one-dimensional river temperature model. Like SJR5Q, HECRAS was built upon HEC-5Q. However, unlike SJR5Q or HEC-5Q, HEC-RAS is a fully supported HEC program, consists of open code, and is transparent so the model's input and output can be better understood. It is also readily usable by RPs and provides results in 1-hour time step, which is needed for determining daily maximum temperatures for the SJR5Q model and calculating seven day average daily maximum values (7DADM).

⁶ Another example of SJR5Q's lack of transparency is that the SJR5Q model does not use measured inflow temperature data directly from the Tuolumne River and it is not apparent from model inspection or documentation how the reservoir inflow temperature data set is obtained.

2.0 STUDY GOALS AND OBJECTIVES

The study goal is to develop a river temperature model that simulates current and potential future water temperature conditions in the lower Tuolumne River from below Don Pedro Dam to the confluence with the San Joaquin River. The river temperature model includes simulation of the lower Tuolumne River for a period of analysis that covers the range of hydrology of the Tuolumne River. The following objectives apply to this modeling study:

- reproduce observed river water temperatures, within acceptable calibration standards, over the entire expected range of hydrologic conditions;
- determine sensitivity of water temperatures to both flow and meteorological conditions;
- provide output to inform other studies, analyses and models; and
- predict potential changes in river temperature conditions under alternative future operating conditions.

The river temperature model interfaces with the Project Operations Model (Study W&AR-02) and the Reservoir Temperature Model (Study W&AR-03) (TID/MID 2013c; TID/MID 2013d). Output from the reservoir temperature model serves as input to the river temperature model. The river temperature model may also provide useful information to the Chinook (W&AR-06) and *Oncorhynchus Mykiss* (*O. Mykiss*) (W&AR-10) salmonid models.

On July 16, 2009 FERC issued an Order on Rehearing regarding the Don Pedro Project (see 128 FERC: 61,035) requiring the Districts to determine the flows needed to maintain specified water temperatures at particular river locations and seasonal windows relevant to life history requirements of California Central Valley steelhead and fall-run Chinook salmon (TID/MID 2011a). This study made use of the SJR5Q model of the lower Tuolumne River. The TID/MID (2011a) study also made use of the most recent temperature data available from the CDFW at that time and, in addition, data collected by the Districts under their real time temperature monitoring (RTM) program on the lower Tuolumne River since 1986. The subsequent comparisons of model results and the most recent RTM data showed that the original SJR5Q model appeared to systematically over-predict water temperatures by up to 2°F, and sometimes greater, at typical summer low flows. Although the original SJR5Q model calibration exceeded the model uncertainty identified in the study plan (1–2°F) less than 10 percent of the time, 20–25 percent error exceedances were found in comparison to thermographs not used in the original model calibration. These discrepancies resulted in the recommendation in the TID/MID (2011a) report that the Tuolumne River portion of the SJR5Q model be recalibrated as part of relicensing.

The Districts' proposed *Lower Tuolumne River Temperature Model Study* (W&AR-16) was intended to complete this recalibration (TID/MID 2011b). The Districts have completed the recalibration of the original SJR5Q model and prior to conducting a Consultation Workshop with RPs on October 26, 2012, the Districts issued a Lower Tuolumne River Temperature Model Status Report dated September 2012 providing a description of the work completed on the model up to that point (TID/MID 2012a). At the Consultation Workshop meeting with RPs, the Districts presented the initial calibration results and discussed the status of the modeling efforts.

The Districts had previously made available to RPs by CD all of the input temperature and meteorological data used in the model. At the October 26 Workshop, the Districts indicated that the model calibration was generally strong with the exception that the diurnal range in actual river temperatures varies considerably from one data collection station to the next, with many stations downstream of RM 37 showing unexpected reduced levels of diurnal temperature ranges. The detailed recalibration efforts undertaken as part implementing study plan W&AR-16 has revealed that temperature conditions on the lower Tuolumne River are actually quite complex. Hence, the Districts proposed additional investigations in 2013 to further evaluate the summer temperature regime of the lower Tuolumne and have migrated to the HECRAS platform.

The following sections describe the work completed in accordance with the FERC-approved study plan, leading up to the current status of the lower Tuolumne river HECRAS temperature model. A study plan for the additional 2013 field investigation is provided as Attachment A to this study plan.

3.0 STUDY AREA

The study area includes the Tuolumne River from the outlet from Don Pedro Reservoir to the confluence with the San Joaquin River (Figure 3.0-1). This encompasses RM 0 to 54, as detailed below.

The lower Tuolumne River watershed, the subbasin from RM 0 to 54, covers approximately 430 square miles of drainage area, and contains one major tributary, Dry Creek, that confluence with the Tuolumne River at RM 16. Other contributions come from Peaslee Creek as well as McDonald Creek (via Turlock Lake) primarily during and after storm events. In this reach, the Tuolumne River extends from about elevation 35 feet at the confluence with the San Joaquin River to elevation 300 feet at the tailrace of the Don Pedro powerhouse. The lower Tuolumne River watershed is long and narrow and is dominated by irrigated farmland and the urban/suburban areas associated with the City of Modesto, Waterford, and Ceres.

This area of the watershed transitions from gently rolling hills near its easterly reaches to uniformly flat floodplain and terrace topography in the downstream direction. Soils are deep and fertile and irrigated agriculture and urban land use dominates the landscape. The Tuolumne River downstream of La Grange Dam flows 52 river miles to its confluence with the San Joaquin River. The Tuolumne River leaves its steep and confined bedrock valley and enters the eastern Central Valley downstream of La Grange Dam near La Grange Regional Park, where hillslope gradients in the vicinity of the river corridor are typically less than five percent. From this point to the confluence with the San Joaquin River, the Tuolumne River corridor lies in an alluvial valley. Within the alluvial valley, the river can be divided into two geomorphic reaches defined by channel slope and bed composition: a gravel-bedded reach that extends from La Grange Dam (RM 52) to Geer Road Bridge (RM 24); and a sand-bedded reach that extends from Geer Road Bridge to the confluence with the San Joaquin River (McBain & Trush 2000).

Large-scale anthropogenic changes have occurred to the lower Tuolumne River corridor since the California Gold Rush in 1848. Gold mining, grazing, and agriculture encroached on the lower Tuolumne River channel before the first aerial photographs were taken by the Soil Conservation Service in 1937. Excavation of bed material for gold and aggregate to depths below the river thalweg eliminated active floodplains and terraces and created large in-channel and off channel pits. Agricultural and urban encroachment in combination with reduction in coarse sediment supply and high flows has resulted in a relatively static channel within a narrow floodway confined by dikes and agricultural fields. Although the tailing piles are primarily the legacy of gold mining abandoned in the early 20th century, gravel and aggregate mining continue alongside the river for a number of miles, particularly upstream of the town of Waterford around RM 34 (TID/MID 2011a).

Downstream of Waterford (RM 34), the Tuolumne River follows an increasingly sinuous path across the agricultural lands of the Central Valley and through the City of Modesto. The Tuolumne River finds its confluence with the San Joaquin River approximately 15 river miles beyond Modesto, along the axis of California's Central Valley.

At Don Pedro Dam, water is discharged into the Tuolumne River from the powerhouse or outlet works before entering the short reach of the Tuolumne River impounded by the La Grange Dam. At the La Grange Dam, water is diverted into MID's canal system to the north of the Tuolumne River, diverted into TID's canal system to the south of the Tuolumne River, or passes to the lower Tuolumne River downstream of La Grange Dam.

Downstream of the Project, the Tuolumne River becomes a lower gradient stream on its journey to the San Joaquin River. In this low-elevation area, the vast majority (around 75 percent) of local runoff occurs during winter rainstorms between December and March. Also contributing to flows within this region are natural inflows from Dry Creek and Peaslee Creek, as well as urban and agricultural runoff and operational spills from irrigation canals. Some of the streamflow in this area, however, is derived from groundwater inflow, and the lower Tuolumne River is generally considered to be a gaining stream (California Department of Water Resources [CDWR] 2004). This groundwater contribution to the lower Tuolumne is being evaluated by the Districts through a series of accretion flow measurements along the lower Tuolumne River.

Downstream of the Don Pedro Dam, in the Central Valley area of the Tuolumne River watershed, land is primarily privately owned and used for agriculture, grazing and rural residential purposes, or for denser residential, municipal and industrial purposes in the communities such as Waterford and Modesto (Stanislaus County 2006). A small portion of the land downstream of the Project is under state management; Turlock Lake State Recreation Area is a small state park spanning from the southern bank of the Tuolumne River to the north shore of Turlock Lake.

The lower Tuolumne River is heavily monitored for temperature with approximately 30 sites located between the Don Pedro Dam and the confluence with the San Joaquin. Monitoring is conducted by CDFW and the Districts. The locations of these sites are shown on Figure 3.0-1 and are discussed further in Section 4.3 below.

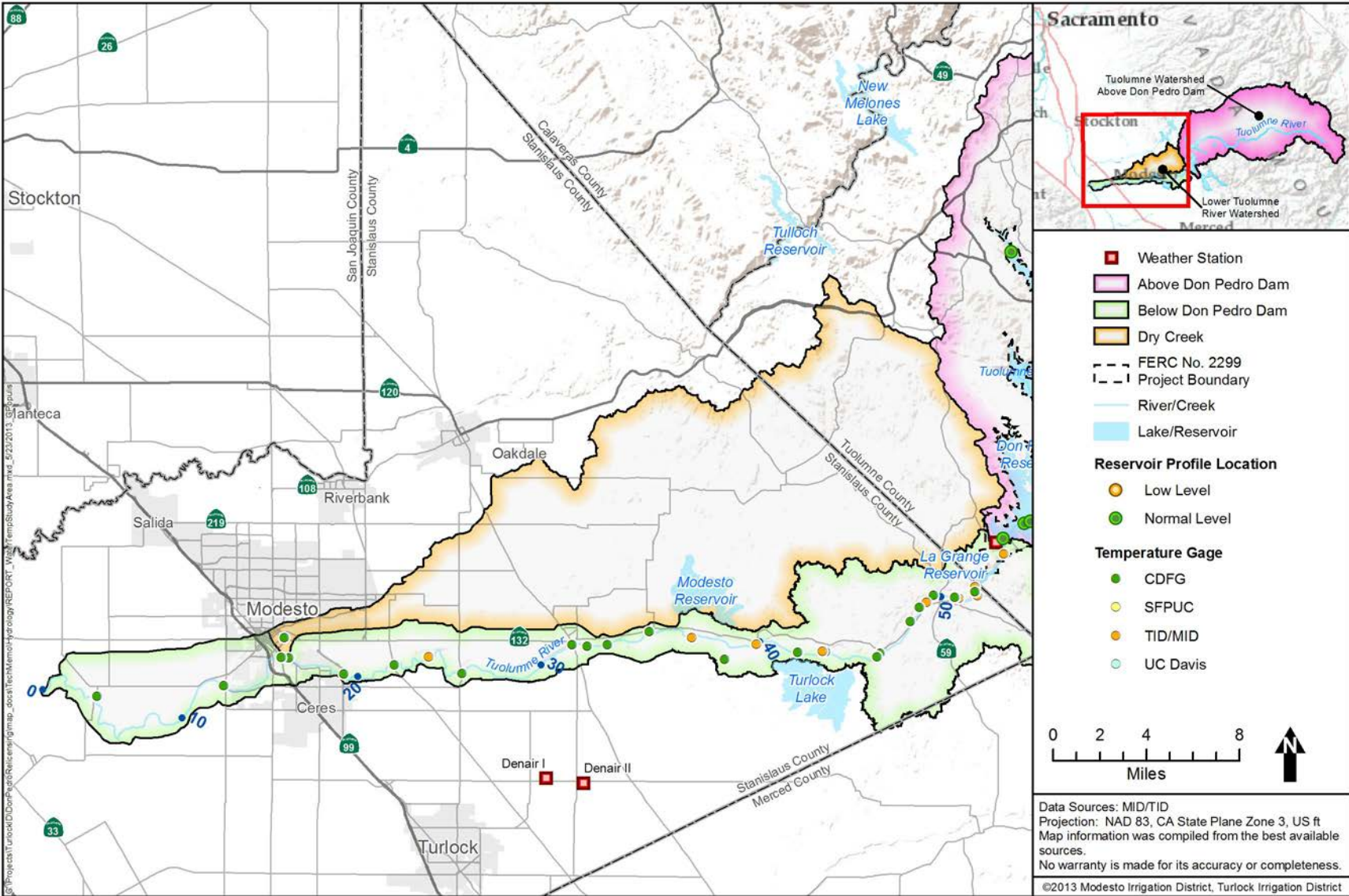


Figure 3.0-1. Study area.

4.0 METHODOLOGY

4.1 Model Set Up

The model being used in this study is the ACOE HEC-RAS model. The HEC-RAS model of the Tuolumne River begins just below the Don Pedro Dam and extends down to the confluence with the San Joaquin River, as shown in Figure 4.1-1. Figure 4.1-1 also shows the location of the irrigation diversions at La Grange Dam and the inflow at Dry Creek.

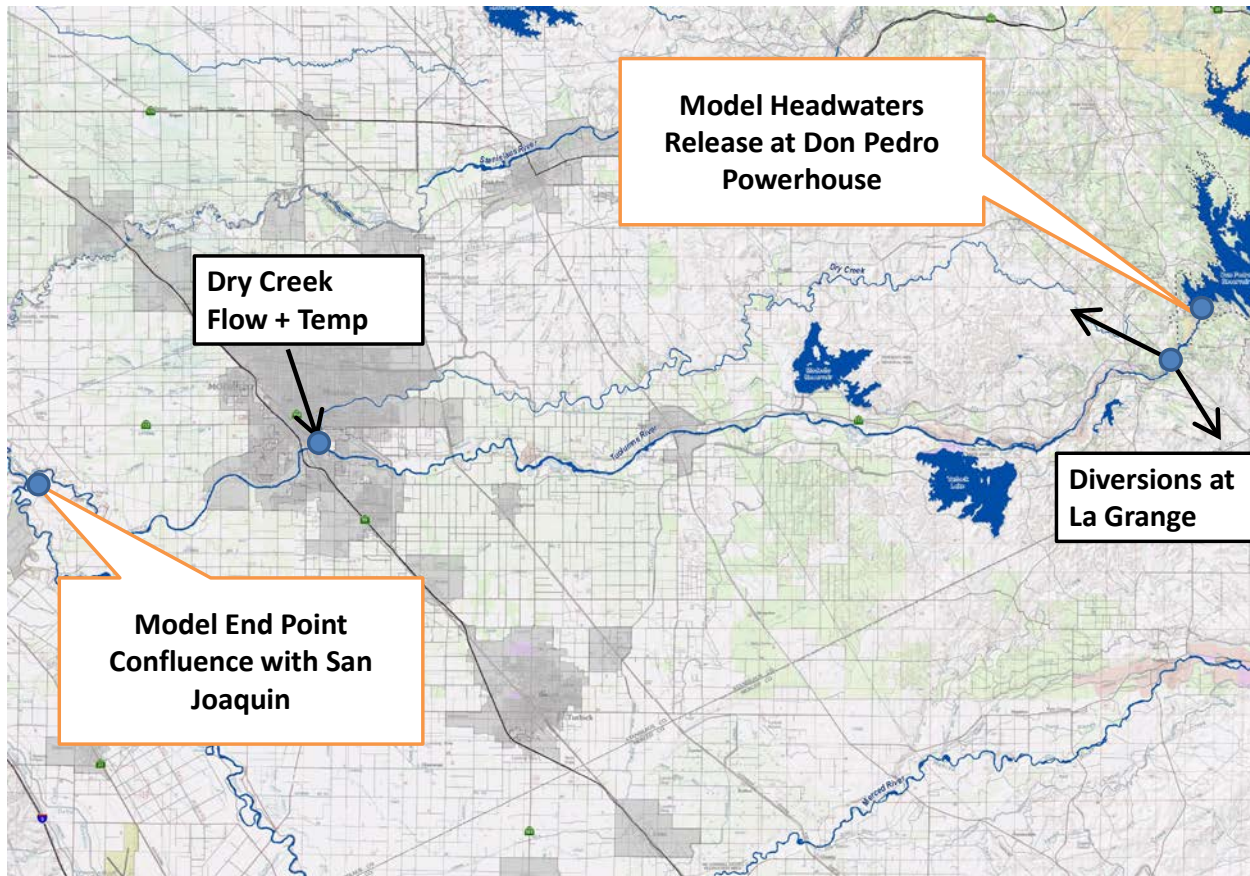


Figure 4.1-1. HEC-RAS lower Tuolumne River model domain.

4.2 Model Computations

4.2.1 Hydraulics

The HEC-RAS model has inflows and outflows specified. Inflows occur at the upstream start of the model at Don Pedro Dam and Dry Creek where it enters the Tuolumne at RM 16. Outflows occur at La Grange Dam as diversions by each of the Districts for irrigation and M&I water.

The main hydraulic computational procedure is based on the solution of the one-dimensional Bernoulli Equation, which is an energy equation. Energy losses due to friction are computed using the Manning Equation, and loss coefficients for expansion and contraction of the flow

(USACE 2010). The model hydraulics are capable of handling mixed flow regimes of super and sub-critical flow. HEC-RAS has the ability to model structures such as bridges, dams, culverts, weirs and levees.

4.2.2 Bathymetry

Table 4.2-1 lists the bathymetry data sources used for the Don Pedro Relicensing's Lower Tuolumne River Temperature Model. Over the years, river geometry has been measured several times; however, not all data sources were used to develop the HEC-RAS model. Only the most up-to-date data were used for the lower Tuolumne River temperature model.

Table 4.2-1. Lower Tuolumne River geometry data sources.

RM	Source	Original reason for collection
0-12	USACE 2001	Flood plain survey performed in 1999. ACOE transects were 100 ft apart. Transect elevations used for model were 0.5 miles apart.
14-31.5	HDR (2012)	Field survey in December 2012 at approximately 167-169 cfs in support of HEC-RAS temperature model; transects collected every 0.5 mile
RM 33.6 to 39.9	HDR (2003-2006)	Developed from the Ruddy Segment (RS 177300-21074) data developed by HDR for the Tuolumne River restoration program HEC-RAS model. survey files included stitched TIN surfaces originating from Lidar and ground truthed bathymetric soundings from a licensed surveyor. More than 100 transects were measured, anywhere from 50 to 100 feet apart. (AD Consultants et al 2009). Transect elevations created for model at 0.5 mile intervals.
40-45.5	Extrapolated	Extrapolated from upstream and downstream transects, as well bank LiDAR (flown at about 300 cfs in March 2012). Transects pulled from model 0.5 miles apart.
45.5-51.5	TID/MID 2013e. W&AR-4, Spawning Gravel in the Lower Tuolumne River.	ADCP performed at 2000 cfs in 2013. A combination of LiDAR and overbank surveys. Transects pulled from model 0.5 miles apart.
52.3-54.3	Meridian Surveying Engineering (2012)	Hydrographic Survey for TID. Transects pulled from model 0.5 miles apart.

ADCP = Acoustic Doppler Current Profiler

cfs = cubic feet per second

ACOE = Corps of Engineers

ft = feet

LiDAR = Light Detection and Ranging

MID = Modesto Irrigation District

RM = River Mile

SJRB = San Joaquin River Basin

TID = Turlock Irrigation District

Based on the bathymetric data from sources summarized in Table 4.2-1, cross sections were generated approximately every 0.5 miles along the river using GIS. In HEC-RAS further cross section are created by interpolating between these 0.5 mile sections. The calibrated model uses 1/6 mile cross section intervals below La Grange damas shown in Figure 4.2-1.

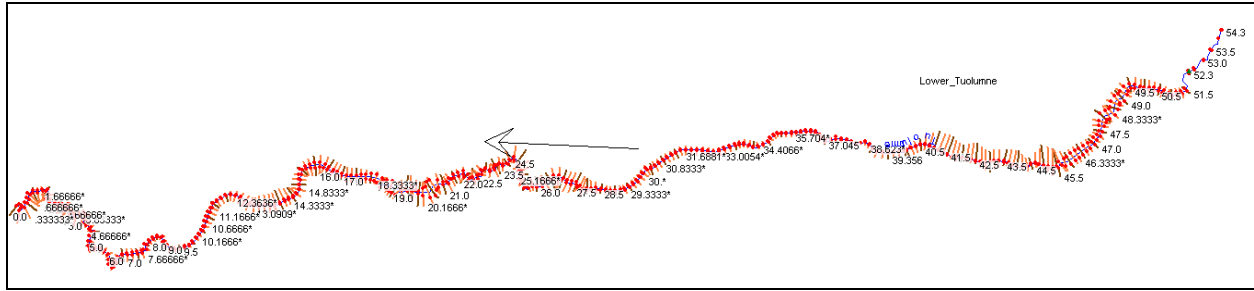


Figure 4.2-1. HEC-RAS schematic of Tuolumne River below Don Pedro to San Joaquin confluence.

A HEC-RAS generated profile of the river below Don Pedro is shown in Figure 4.2-2. The large drop in elevation at the downstream face of La Grange Dam is evident. Figure 4.2-3 shows the cross section at La Grange Dam.

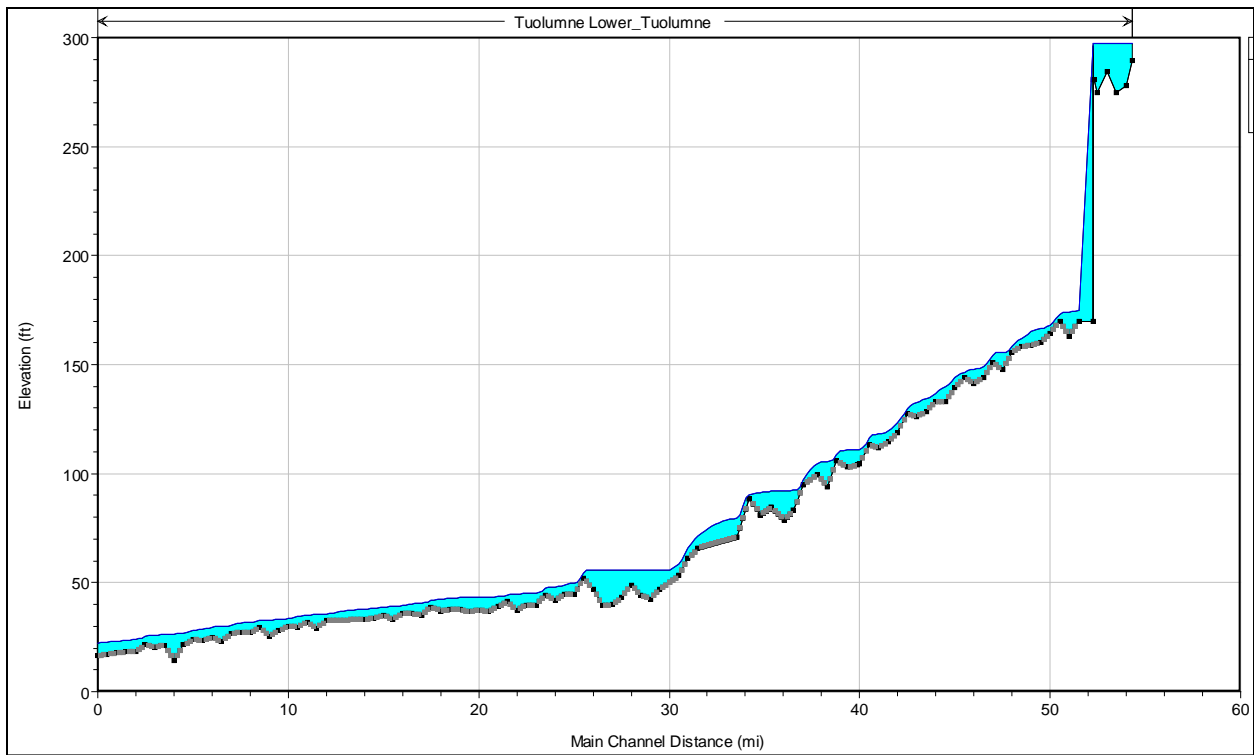


Figure 4.2-2. HEC-RAS profile of Tuolumne River.

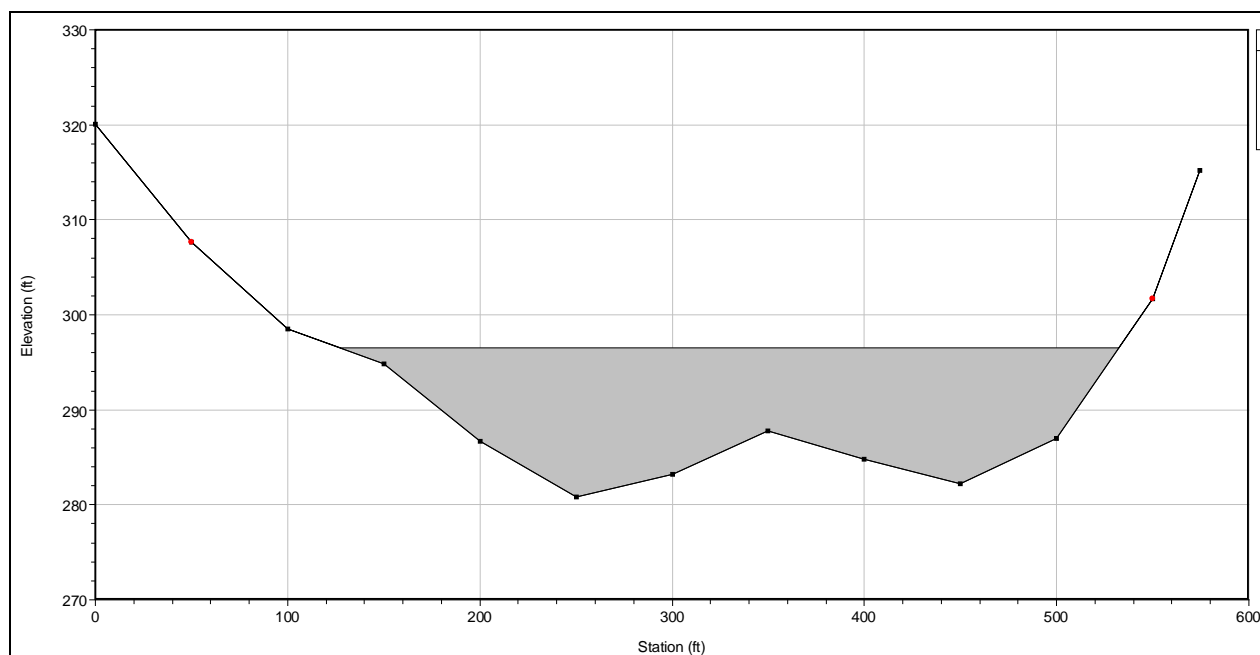


Figure 4.2-3. HEC-RAS cross section showing La Grange Dam.

4.2.3 Model Inflows and Outflows

All model input data is contained in tables that are created in HEC-RAS. The model headwater flows are computed releases from Don Pedro using the Water Operations Model. The inflow temperature is measured just below the release at Don Pedro Dam. The release flow and temperature for 2011-12 is shown in Figures 4.2-4 and 4.2-5.

The diversion flow at La Grange Dam for 2011-12 is shown in Figure 4.2-6. The diversion flow represents the combined diversion of both Districts.

Dry Creek flow and temperature data are very sparse and sporadic. The measured data were used to develop a long term monthly averaged flow and temperature record for the creek. These are given in Table 4.2-2.

Table 4.2-2. Monthly flow in Dry Creek.

Month	Flow (cfs)	Temp (°F)
January	10	45.8
February	30	50.3
March	30	56.2
April	40	61.9
May	45	67.8
June	50	74.3
July	55	76.9
August	70	74.1
September	65	70.6
October	30	61.9
November	3	54.7
December	1	48.3

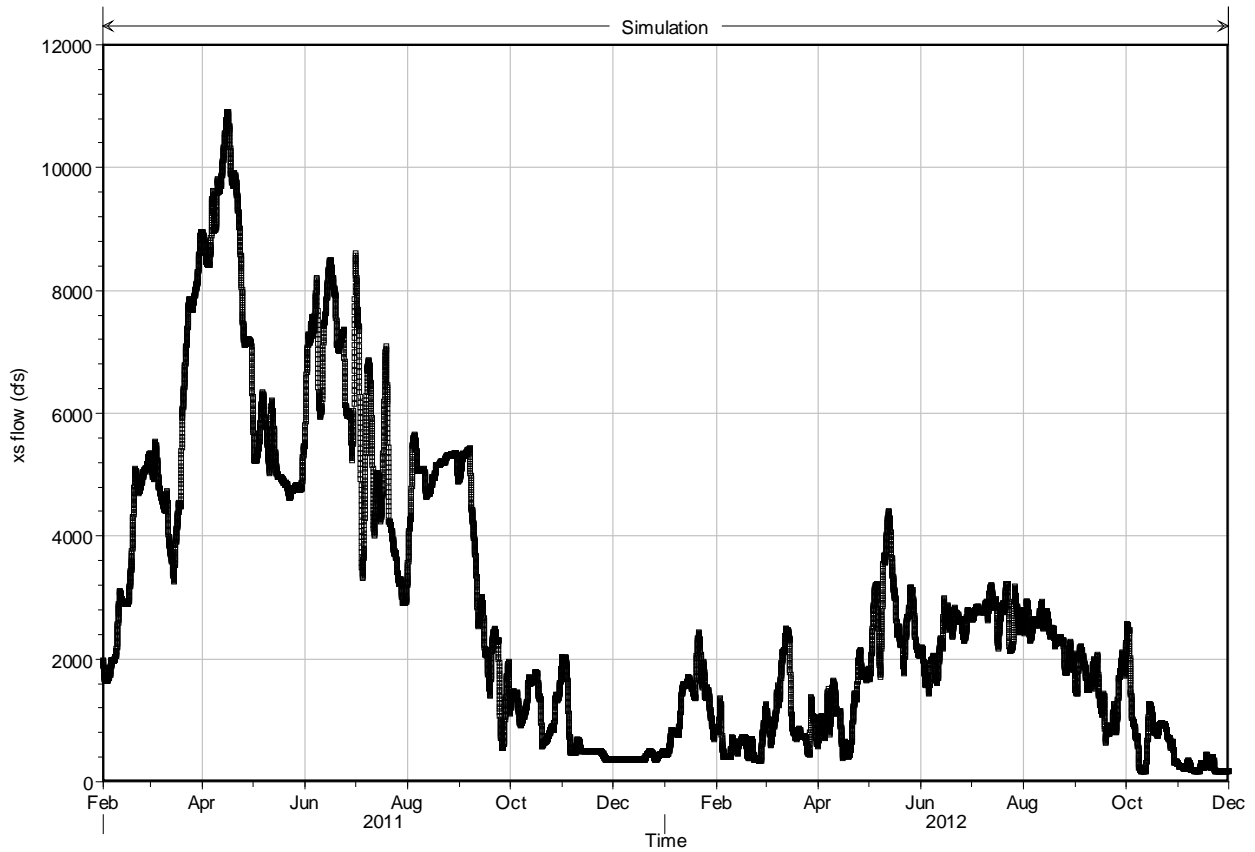


Figure 4.2-4. Don Pedro releases 2011-12.

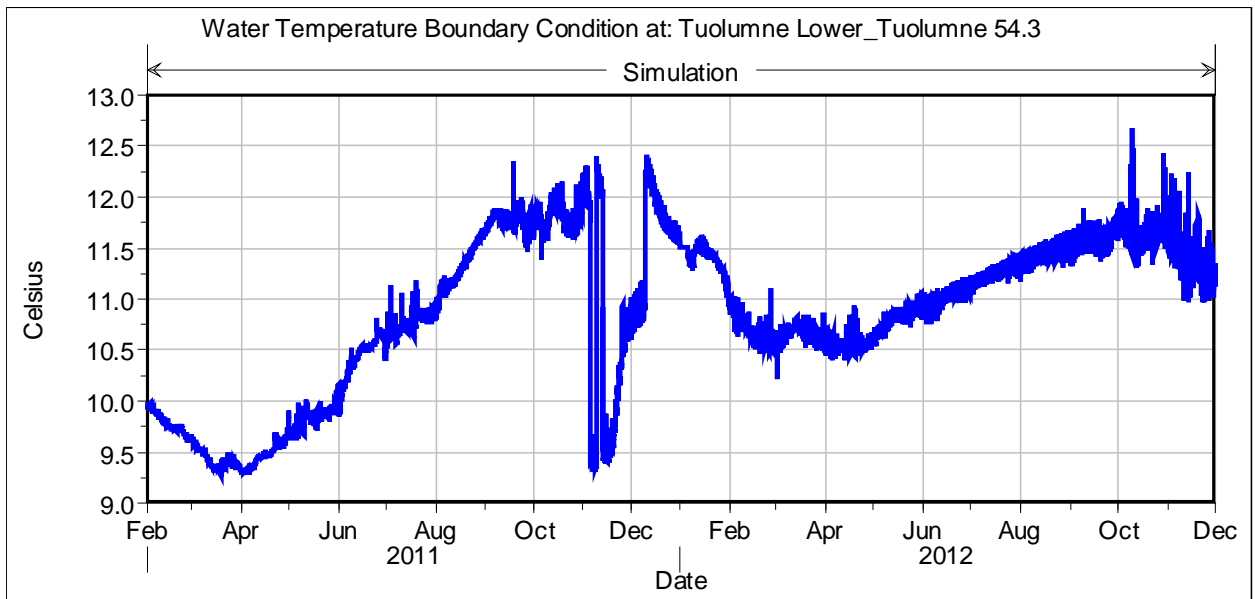


Figure 4.2-5. Don Pedro release temperature 2011-12.

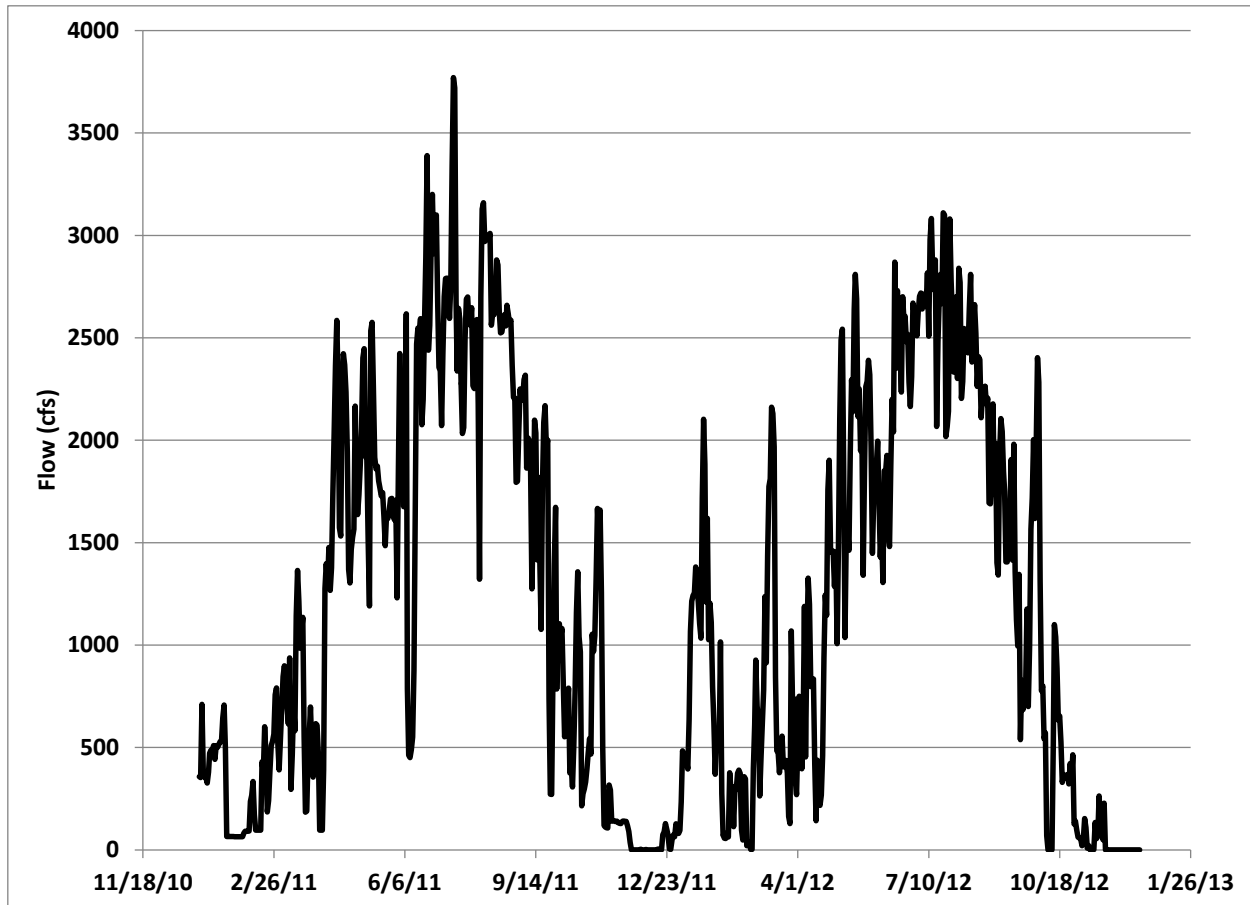


Figure 4.2-6. Total diversion flow at La Grange 2011-12

4.2.4 Temperature

In HEC-RAS the net heat flux is computed as (USACE 2010):

$$Q_{\text{net}} = Q_{\text{sw}} + Q_{\text{atm}} - Q_{\text{b}} + Q_{\text{h}} - Q_{\text{L}}$$

where:

Q_{sw} is short wave solar radiation (W/m^2)

Q_{atm} is incoming longwave radiation (W/m^2)

Q_{b} is outgoing longwave radiation (W/m^2)

Q_{h} is sensible heat (W/m^2)

Q_{L} is latent heat (W/m^2)

Hourly short wave radiation, Q_{sw} , was based on data collected at the Denair II station in Turlock (see Figure 4.3-7). The actual solar radiation impacting the water surface is less than the incoming solar radiation that is measured, and is adjusted as part of the calibration. In this case the Denair values were decreased by 40%. The final time series is shown in Figure 4.2-7 below.

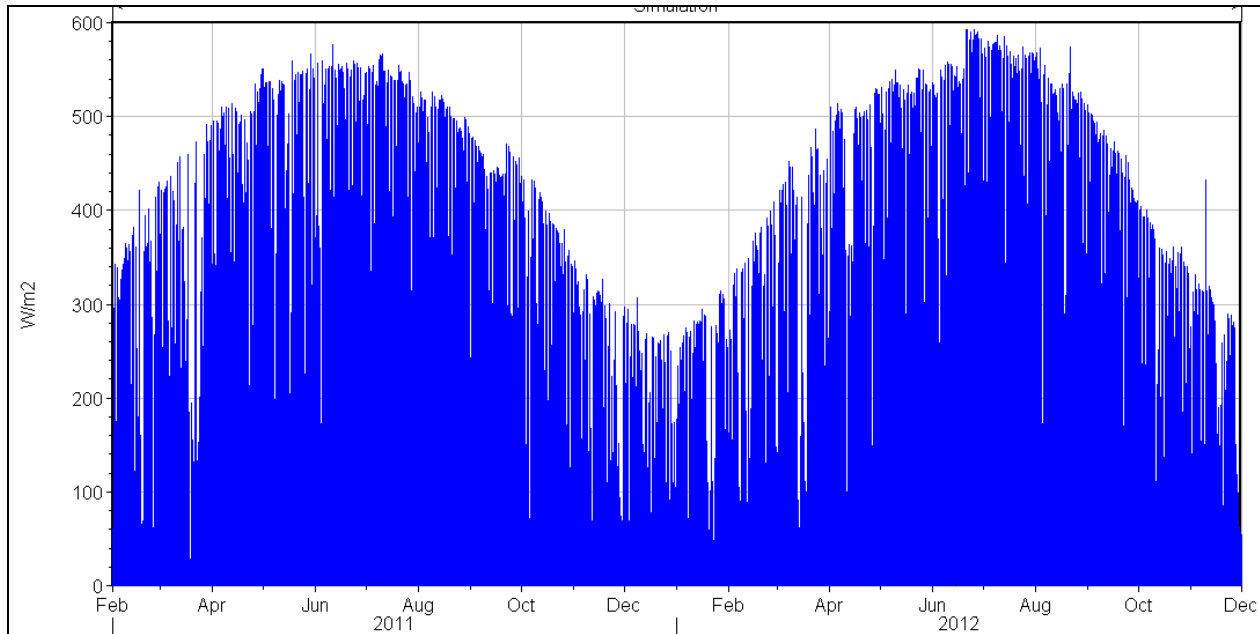


Figure 4.2-7. Denair short wave radiation used in HEC-RAS.

The incoming longwave radiation, q_{atm} , is computed as:

$$q_{\text{atm}} = \varepsilon \sigma T_{\text{air}}^4$$

where:

ε is the emissivity of air

σ is the Stefan Boltzman constant ($\text{W}/\text{m}^2\text{-K}$)

T_{air} is the air temperature ($^{\circ}\text{C}$)

The outgoing longwave radiation, q_b is computed as:

$$q_b = \varepsilon_{\omega} \sigma T_{\text{water}}^4$$

where:

ε_{ω} is the emissivity of water

T_{water} is the water temperature ($^{\circ}\text{C}$)

The sensible heat flux, q_h , is computed as:

$$q_h = (K_h/K_w) C_p \rho_w (T_{\text{air}} - T_{\text{water}}) U$$

Where:

K_h/K_w is the diffusivity ratio

C_p is the specific heat of air ($\text{J}/\text{kg}\text{-C}$)

ρ_w is the density of water (kg/m^3)
 U is wind speed (m/s)

The latent heat flux, q_L , is computed as:

$$q_L = 0.622/P L \rho_w (e_s - e_a) U$$

Where:

P is the atmospheric pressure (mb)

L is the latent heat of vaporization (J/kg)

ρ_w is the density of water (kg/m^3)

e_s is the saturated vapor pressure at the water temperature (mb)

e_a is the saturated vapor pressure at the air temperature (mb)

U is wind speed (m/s)

4.3 Monitoring Data

Model input includes Don Pedro Reservoir outflows, and temperatures. Temperature monitoring data used for this study, as well as a complete inventory of historical data, can be found in Attachment A of the Reservoir Temperature Model (TID/MID 2013f). Don Pedro outflow temperatures have been measured since mid-2010, therefore, 2011 was chosen as the calibration year, as this would be the first full year with all the required information. For 2011 and 2012 there were 22 temperature monitoring locations along the river that had complete, or nearly complete, temperature records. These are shown in Figure 4.3-1. Of these 22 stations, 16 are CDFW sites, and six are the Districts'. These are listed below in Table 4.3-1 by river mile, in descending order.

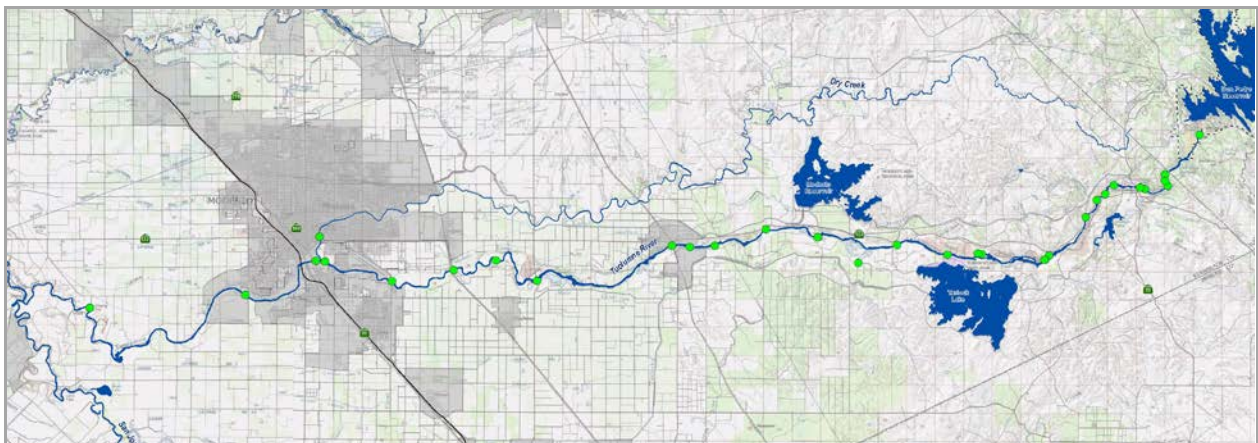


Figure 4.3-1. Temperature monitoring locations.

Table 4.3-1. Temperature monitoring locations.

Source	Location	
TID/MID	La Grange Dam USGS	RM 51.8
CDFW	Riffle A1	RM 51.6
TID/MID	Riffle A7	RM 50.7

Source	Location	
CDFW	Riffle C1	RM 49.7
CDFW	Riffle D2	RM 48.8
CDFW	Basso Bridge	RM 47.5
TID/MID	Riffle 13B	RM 45.5
CDFW	Riffle G3	RM 45.0
CDFW	Riffle I2	RM 43.2
TID/MID	Riffle 21	RM 42.9
CDFW	Riffle K1	RM 42.6
TID/MID	Roberts Ferry Bridge	RM 39.5
CDFW	Riffle Q3	RM 35.0
CDFW	Above Hickman Spill	RM 33.0
CDFW	Below Hickman Spill	RM 32.0
CDFW	Fox Grove Bridge	RM 26.0
TID/MID	Hughson WWTP	RM 23.6
CDFW	Santa Fe Bridge	RM 21.0
CDFW	Mitchell Road Bridge	RM 19.0
CDFW	Above Dry Creek	RM 16.3
CDFW	Ninth Street Bridge	RM 16.2
CDFW	Shiloh Bridge	RM 3.5

The meteorological data used in the model came from the Districts' MET station at Crocker Ranch (location noted on Figure 4.3-2), with the exception of the solar data mentioned previously, which came from the Denair II station in Turlock. Issues with equipment at the Crocker Ranch station prohibited use of the solar data from this station for 2011 and 2012. The 2011-12 data for air temperature, wind speed, pressure and relative humidity are shown in Figures 4.3-3 through 4.3-5.

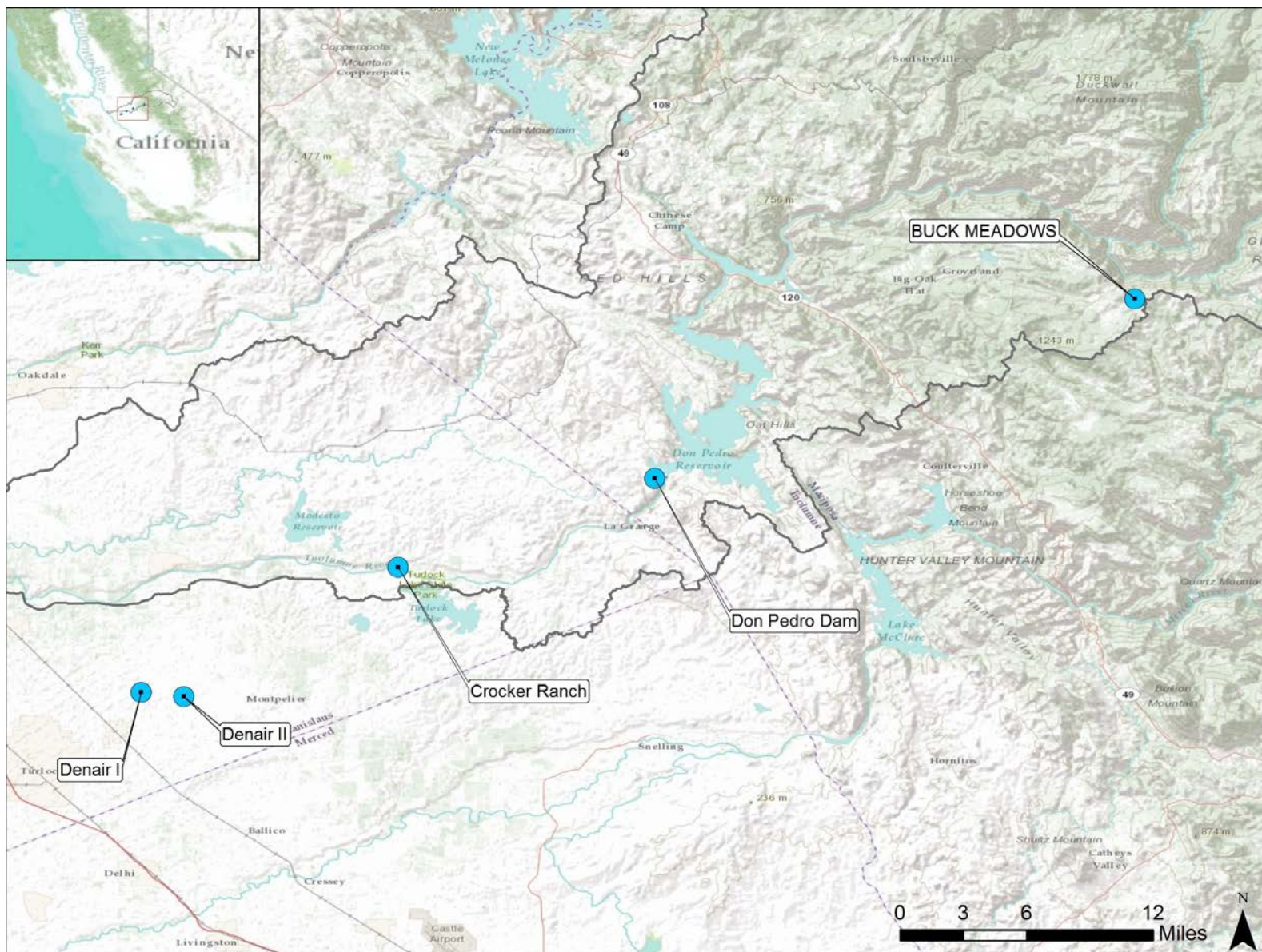


Figure 4.3-2. Location of meteorological stations.

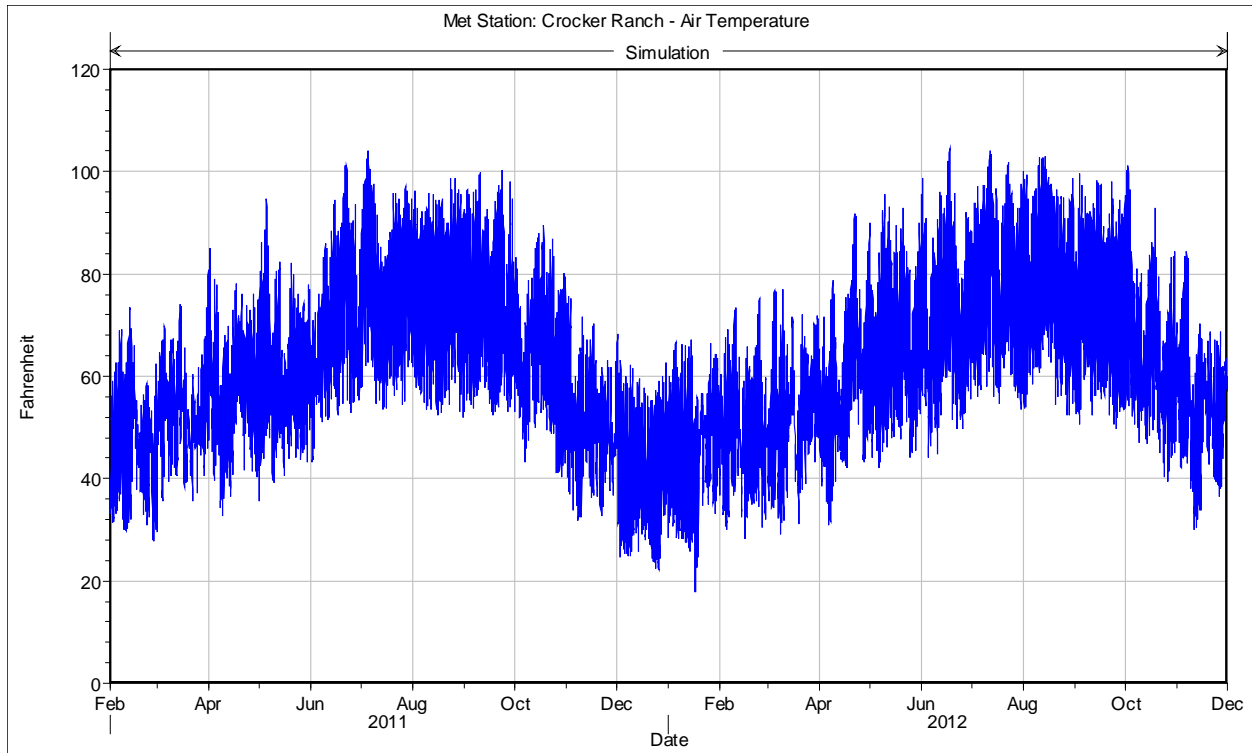


Figure 4.3-3. Crocker Ranch air temperature for 2011-12.

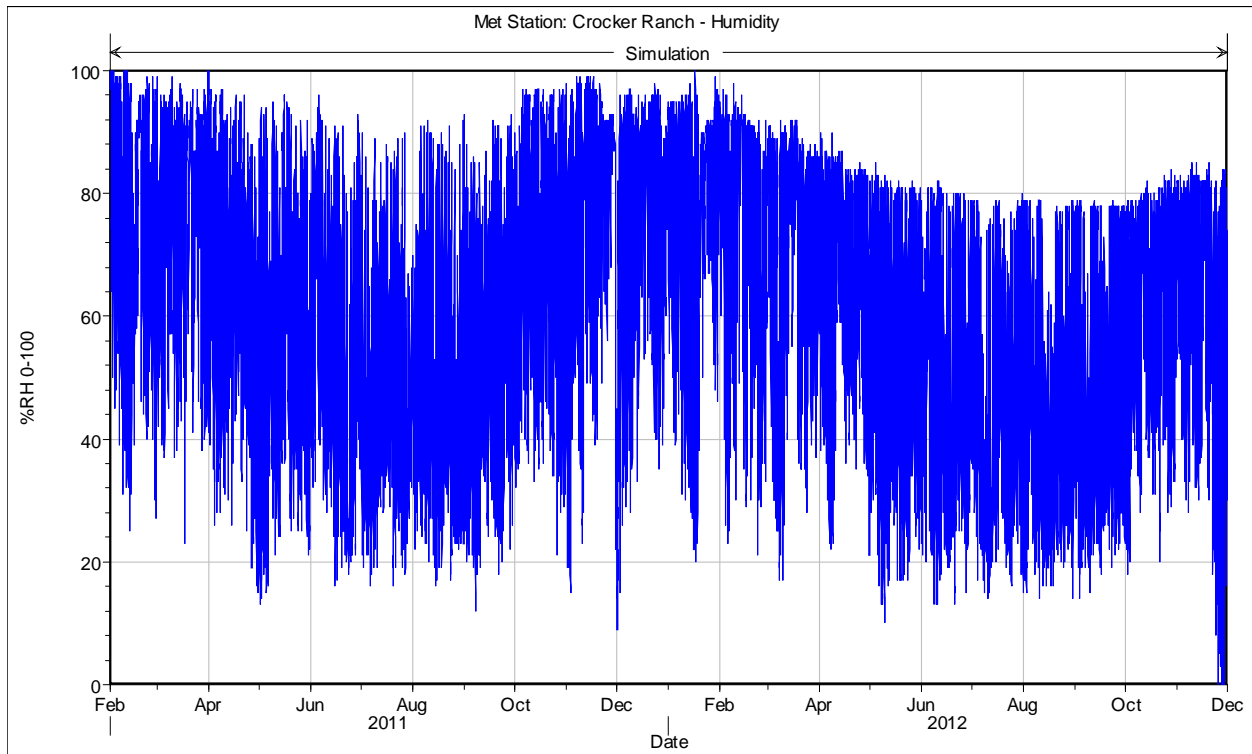


Figure 4.3-4. Crocker Ranch relative humidity for 2011-12.

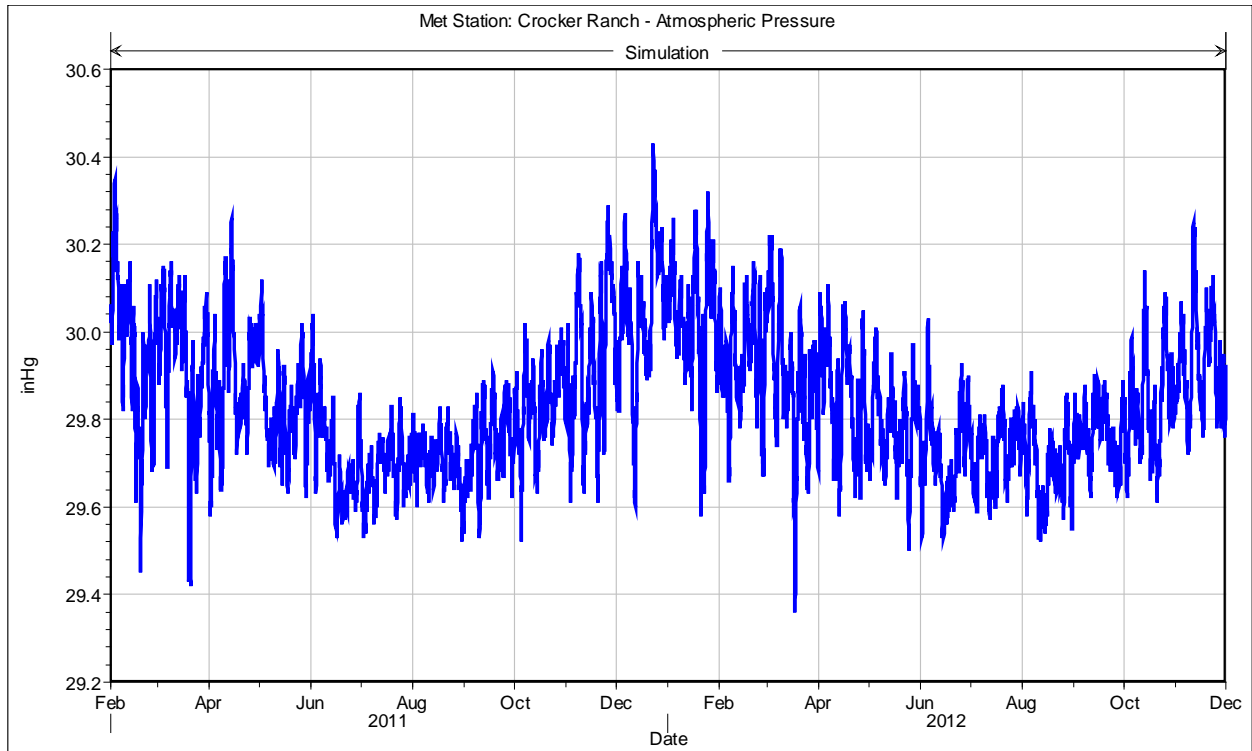


Figure 4.3-5. Crocker Ranch atmospheric pressure for 2011-12.

5.0 RESULTS

5.1 Calibration Results

The calibration results applying the HEC-RAS model to 2011 conditions are shown in Figures 5.1-1 through 5.1-3. The monitoring data are hourly, and are shown in black. The model output is hourly and is shown in red. Overall it can be seen that the model reproduces the measured data very well. The small annual and diurnal range seen closest to Don Pedro Reservoir reflects a large buffering effect that the reservoir volume and depth of release have on river temperatures at these locations. This is also reflected in the actual monitoring data collected at sites closest to the dam. Gradually the diurnal and annual ranges expand as the water moves further downstream due to increased time of exposure to local atmospheric conditions.

The model tracks the data reasonably well until about RM 39.5, Roberts Ferry Bridge, when the diurnal range in the data decreases noticeably and unexpectedly. At the next station, Riffle Q3 at RM 35.0, the range expands again and the model fit is good. At RM 33.0, Above Hickman Spill, the diurnal range again compresses dramatically, only to expand at the next site less than a mile further downstream (Below Hickman Spill RM 32.0). At RM 26.0 through RM 16.2 the range substantially decreases and remains limited until the last station at Shiloh Bridge at RM 3.5. The model remains consistent in its response throughout the entire length of the river by predicting a relatively large diurnal range and does not pick up these smaller diurnal fluctuations. The model is acting as expected - as the model is not receiving any changes in input data that might cause it to predict significant variations in temperatures over short reaches of the river. This is evidence that other factors are affecting water temperature than just those variables included in the model.

This phenomenon is explored later, in Section 5.3.

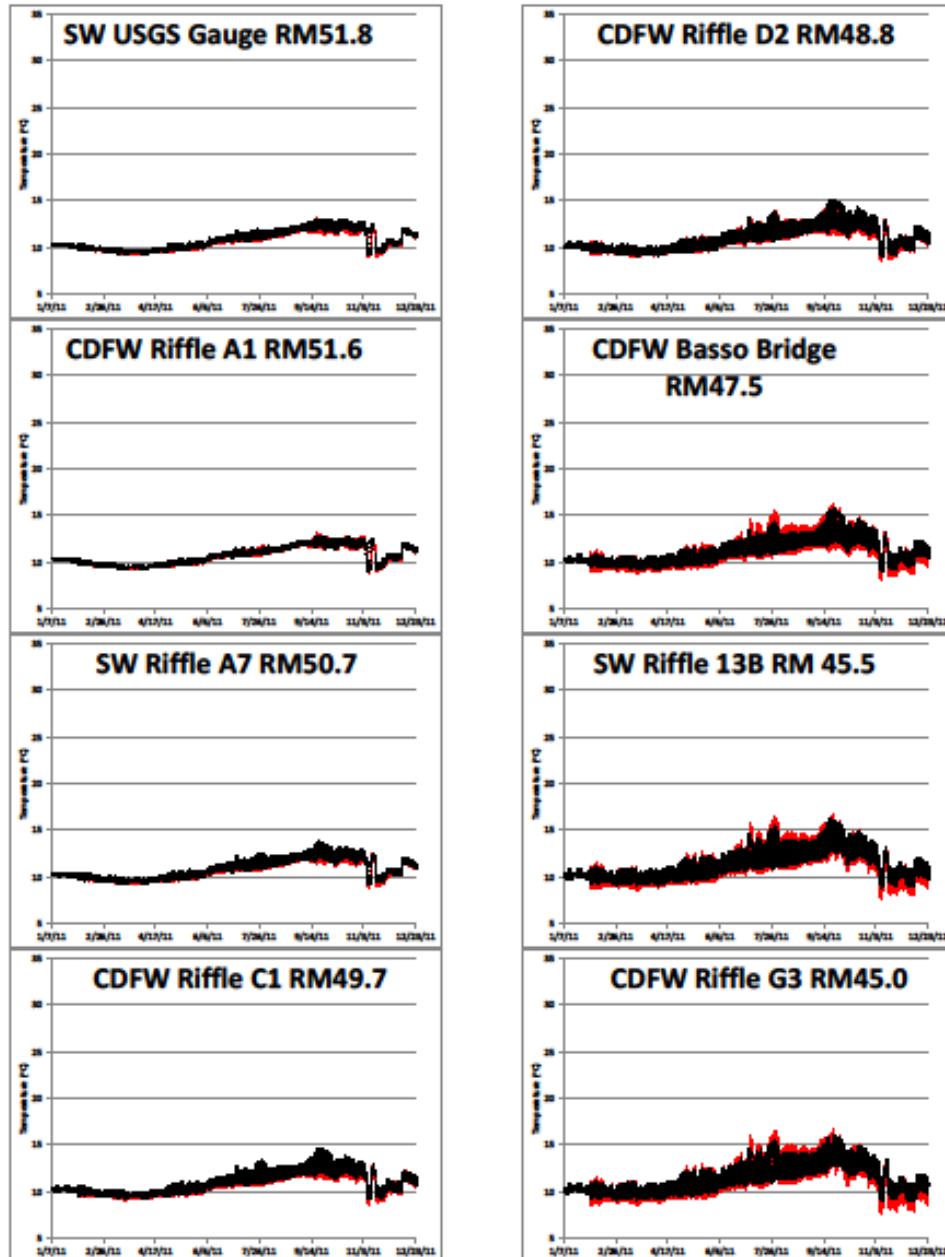


Figure 5.1-1. Calibration results for 2011, RM 51.8 to 45.0. (Measured=black; HEC-RAS=red).

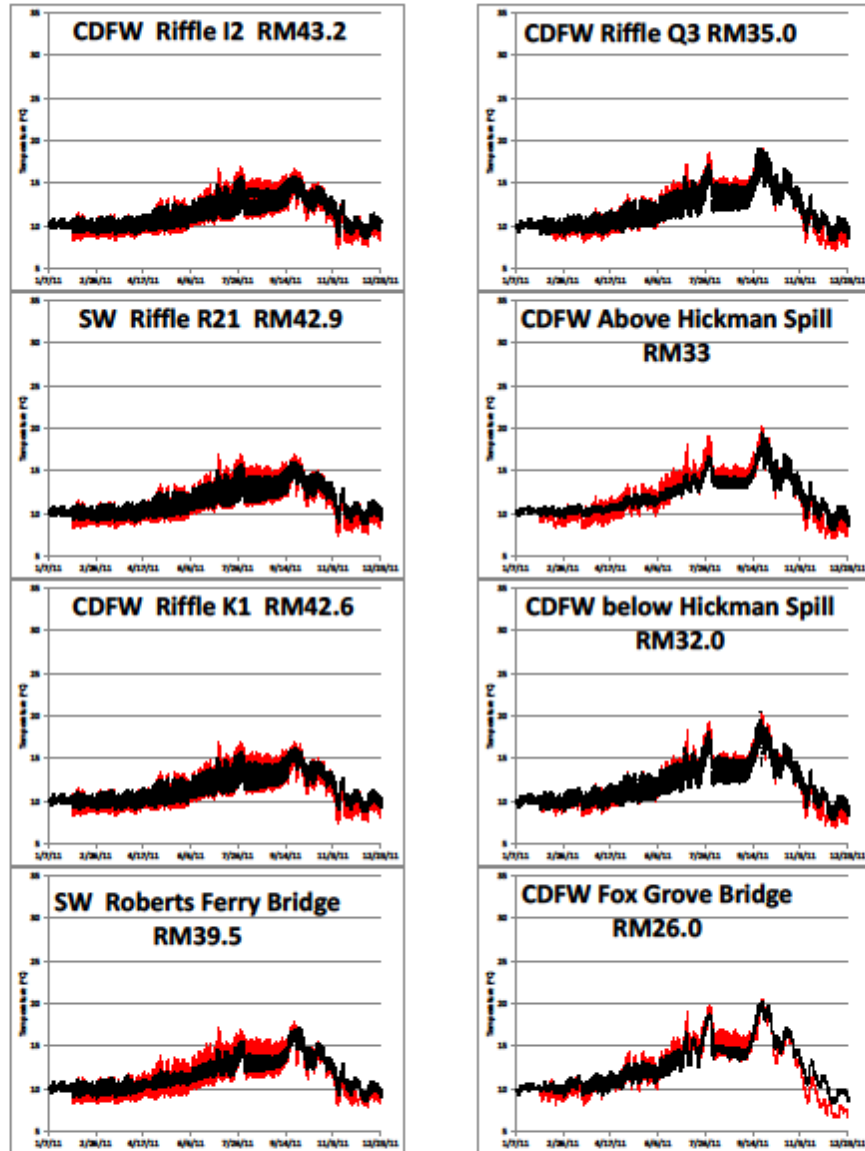


Figure 5.1-2. Calibration results for 2011, RM 43.2 to 26.0. (Measured=black; HEC-RAS=red).

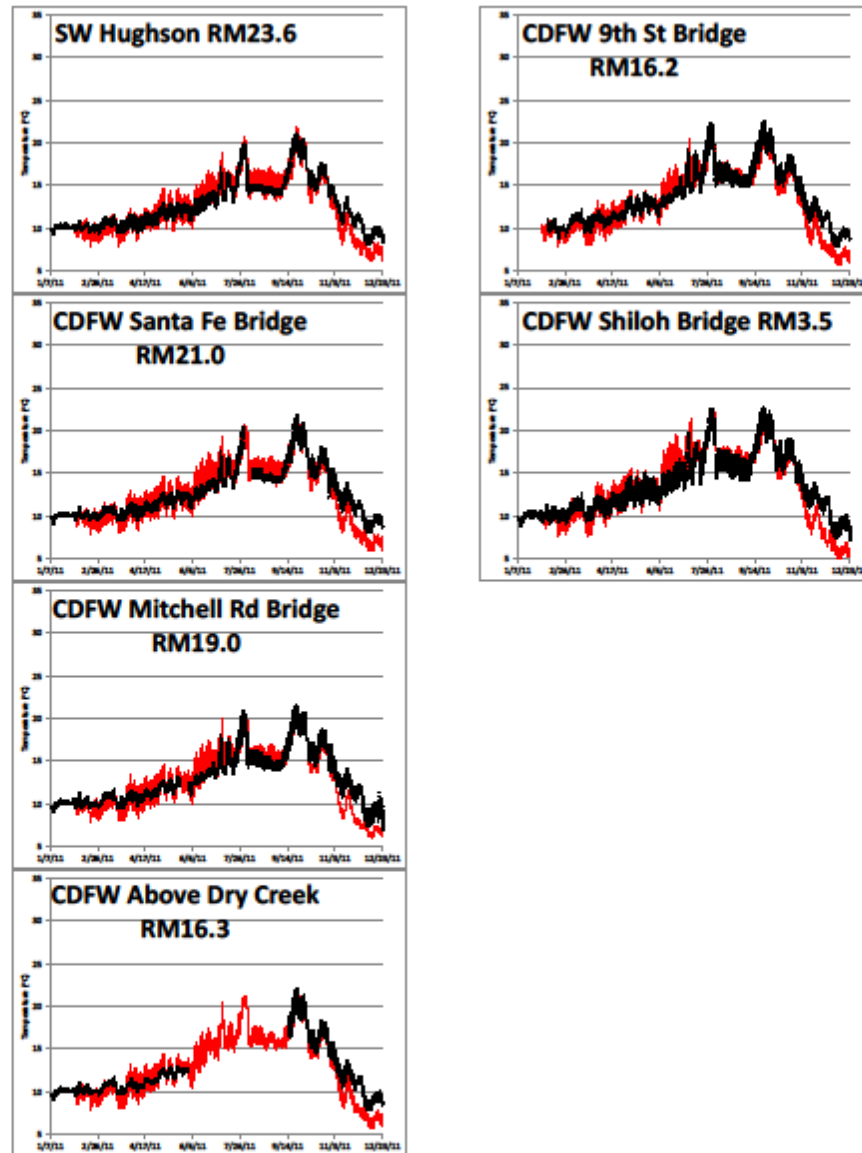


Figure 5.1-3. Calibration results for 2011, RM 23.6 to 3.5. (Measured=black; HEC-RAS=red).

5.2 Validation Results

The model was validated using 2012 data. None of the HEC-RAS model parameters were changed from the 2011 calibration. The results are shown in Figures 5.2-1 to 5.2-3 and use the same station sequence, temperature scales, and color schemes as the calibration figures (Measured data is black; HEC-RAS is red).

River conditions in 2012 were very different from 2011 conditions. In 2012, there was 65% less flow than 2011, 1480 cfs versus 4160 cfs annual average flow. In 2012, the river temperature response was also markedly different from 2011. The temperature in the river is consistently greater in 2012 from February on, compared to 2011. During the warmest months the difference in year over year temperatures reaches 10°C in the lower portions of the river.

Despite the substantial differences between the two years the model is able to reproduce the observed data remarkably well, even better than in the calibration year of 2011. It should also be noted that the large variations in diurnal range that were observed in 2011 were not observed in 2012.

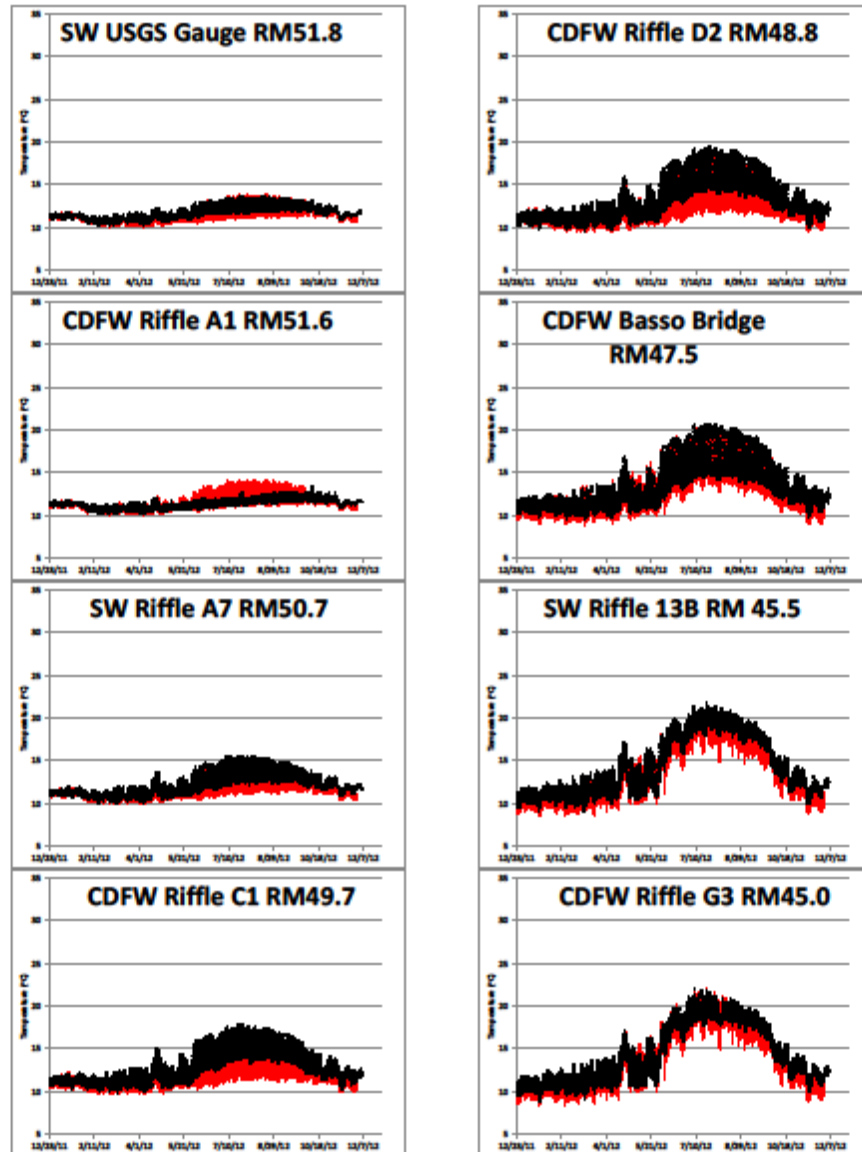


Figure 5.2-1. Validation results for 2012, RM 51.8 to 45.0. (Measured=black; HEC-RAS=red)

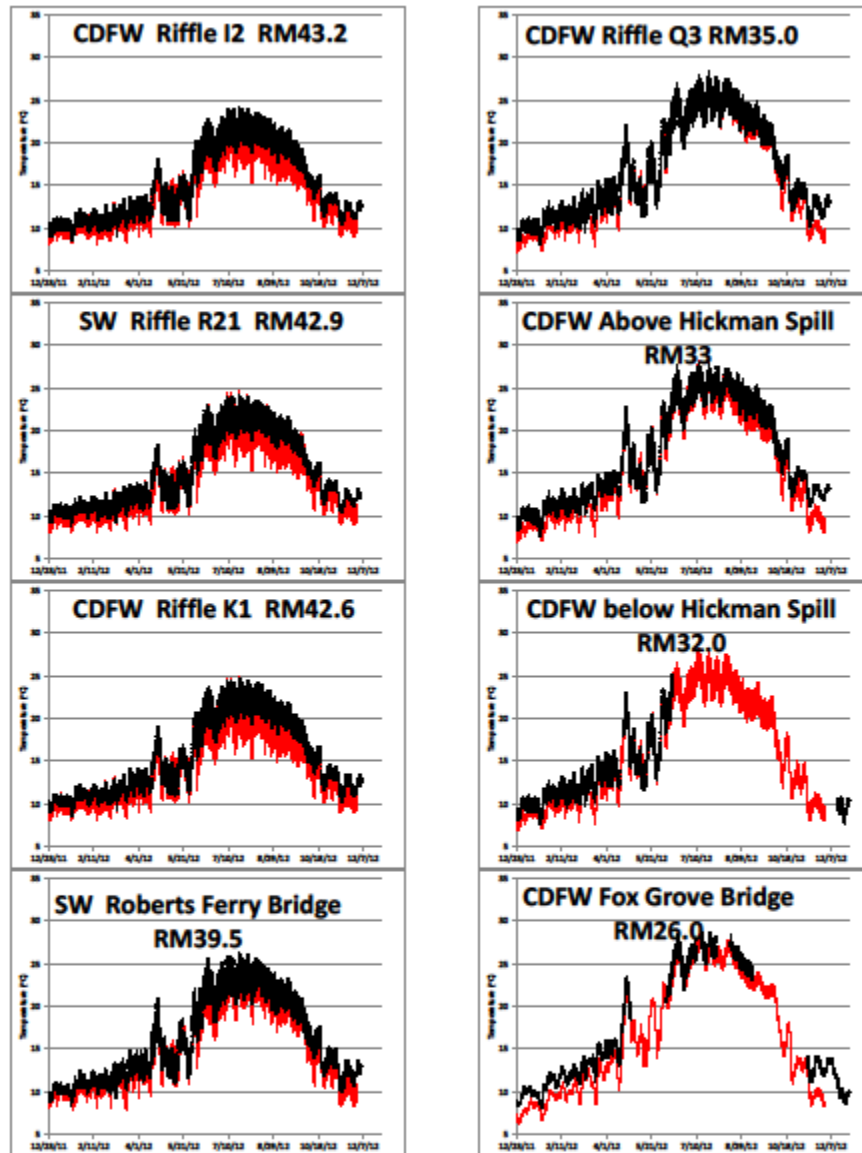


Figure 5.2-2. Validation results for 2012, RM 43.2 to 26.0. (Measured=black; HEC-RAS=red).

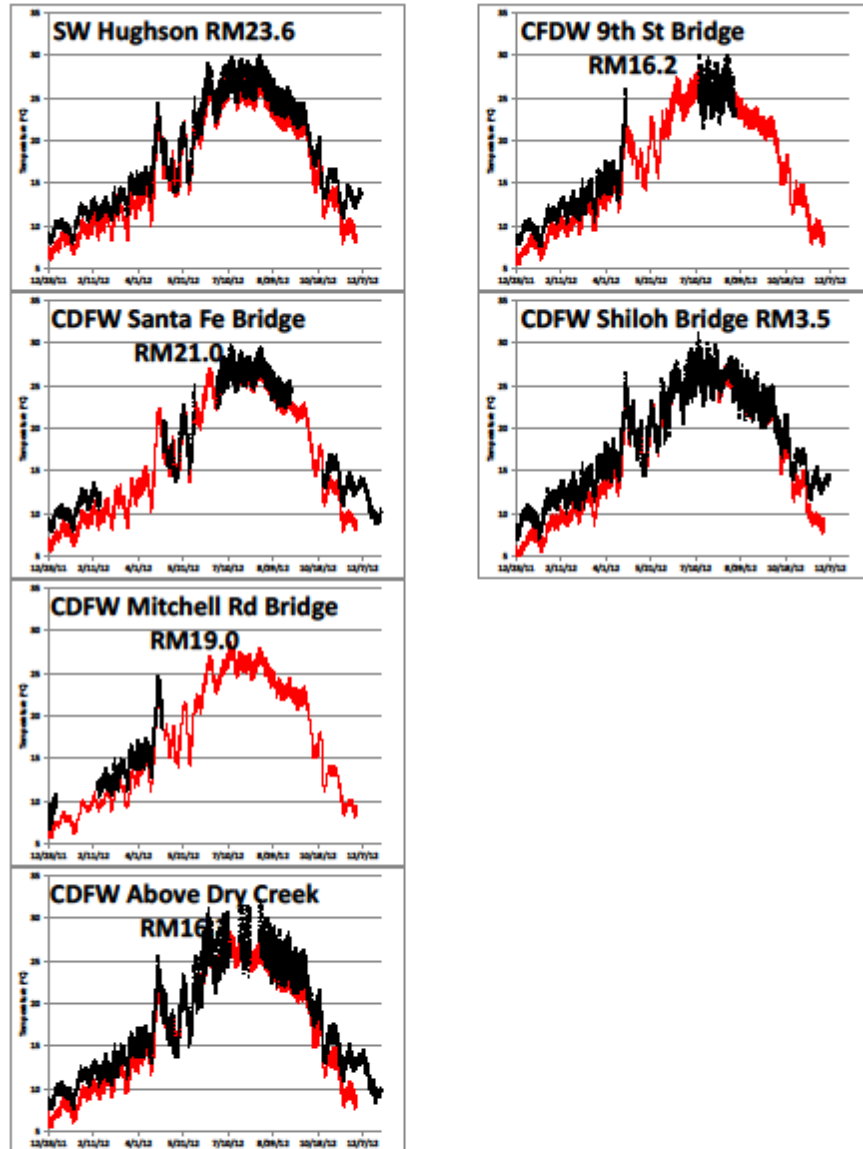


Figure 5.2-3. Validation results for 2012, RM 23.6 to 3.5. (Measured=black; HEC-RAS=red).

The combined calibration and validation year results for 2011-12 are shown in Figures 5.2-4 to 5.2-7. These plots highlight the differences between the two years and also show how the overall performance of the model over the two year period is very good.

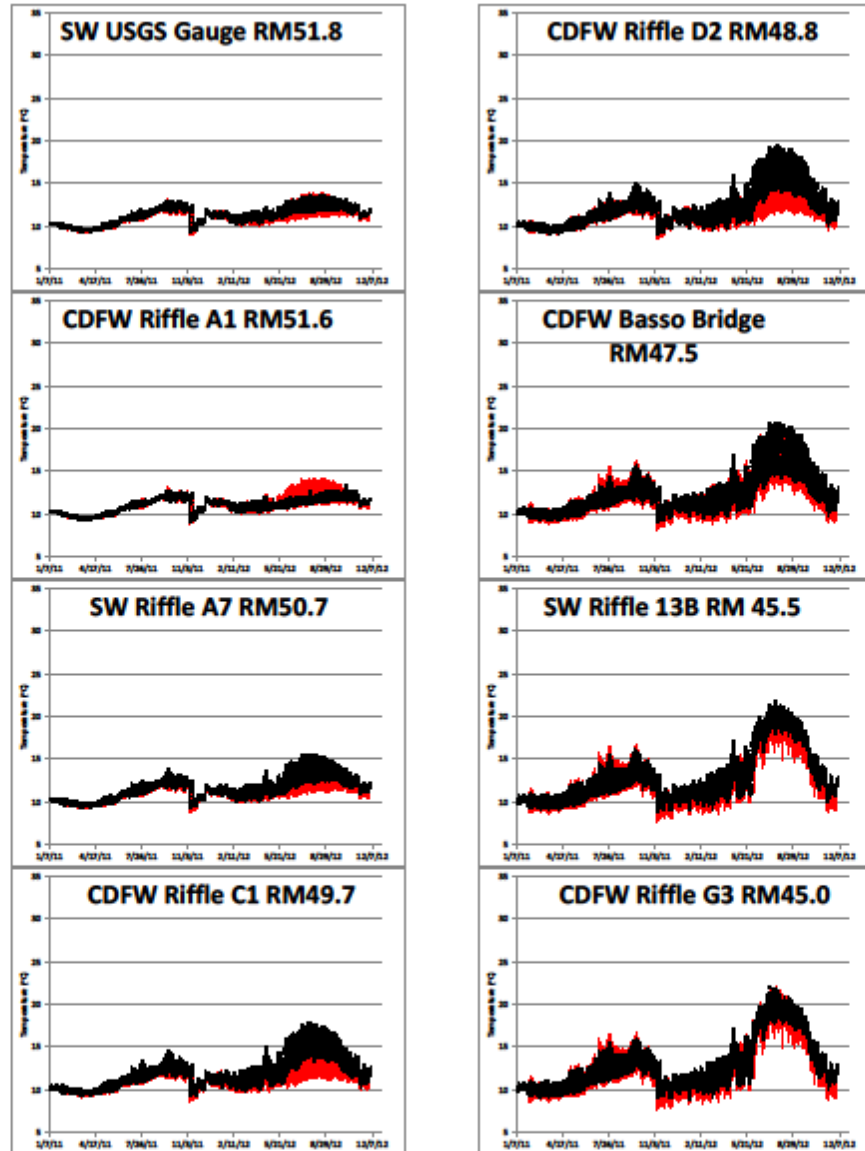


Figure 5.2-4. Results for 2011-12, RM 51.8 to 45.0. (Measured=black; HEC-RAS=red).

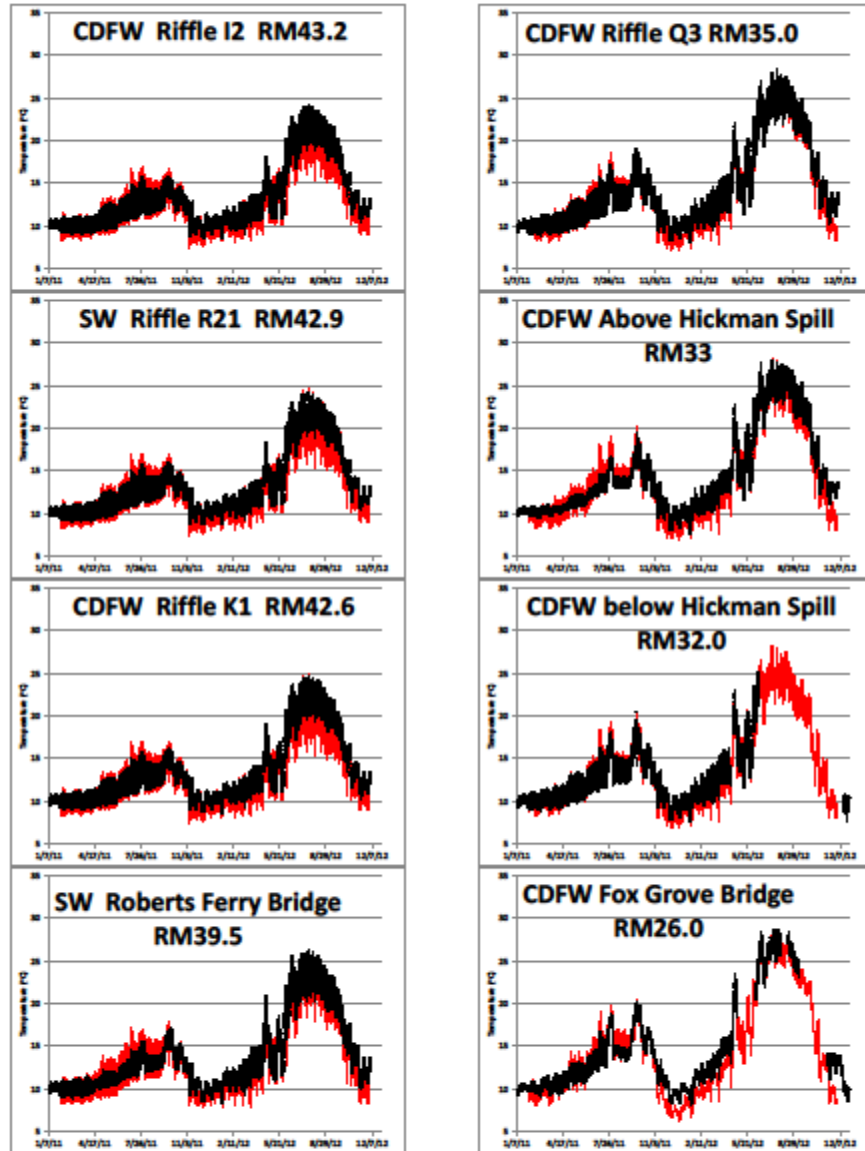


Figure 5.2-5. Results for 2011-12, RM 43.2 to 26.0. (Measured=black; HEC-RAS=red).

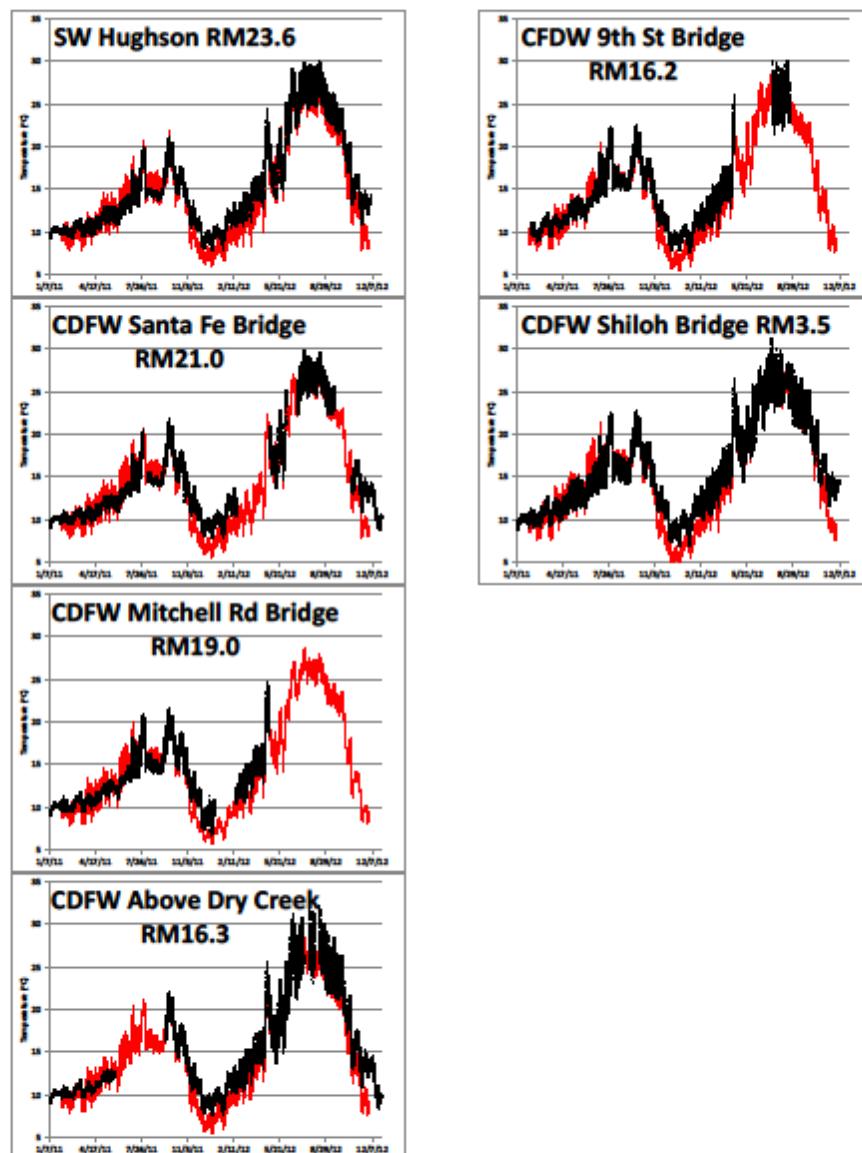


Figure 5.2-6. Results for 2011-12, RM 23.6 to 3.5. (Measured=black; HEC-RAS=red).

5.3 Observed Diurnal Variations

As mentioned previously in Section 5.1, the observed data shows some marked differences in the diurnal range from monitoring site to monitoring site in 2011. The annual average diurnal ranges per monitoring site are plotted in Figure 5.3-1 in descending river mile order. Note that even stations with incomplete data for 2011 are included here, e.g. Riffle I2, 7-11 Gravel, Santa Fe Gravel. The ranges for the summer months are plotted in Figure 5.3-2. Figure 5.3-3 shows the average summer range plotted on a river mile scale. Initially the diurnal range expands rapidly as the flow leaves the La Grange Dam and the smaller mass of water becomes exposed to local atmospheric conditions for longer periods of time. However, as the water passes Riffle I2 (RM 43.2) the range stops expanding and actually begins to decrease. From this point on the range fluctuates in a seemingly random manner for the rest of the river reach.

The data have been checked and there is no reason to believe that the data are in error. HDR and Districts' personnel visited every site over a two day period in August 2012 and recorded details of the site, looking for possible local field conditions that would explain the variations. No correlations between site characteristics or position of the thermologgers could be found.

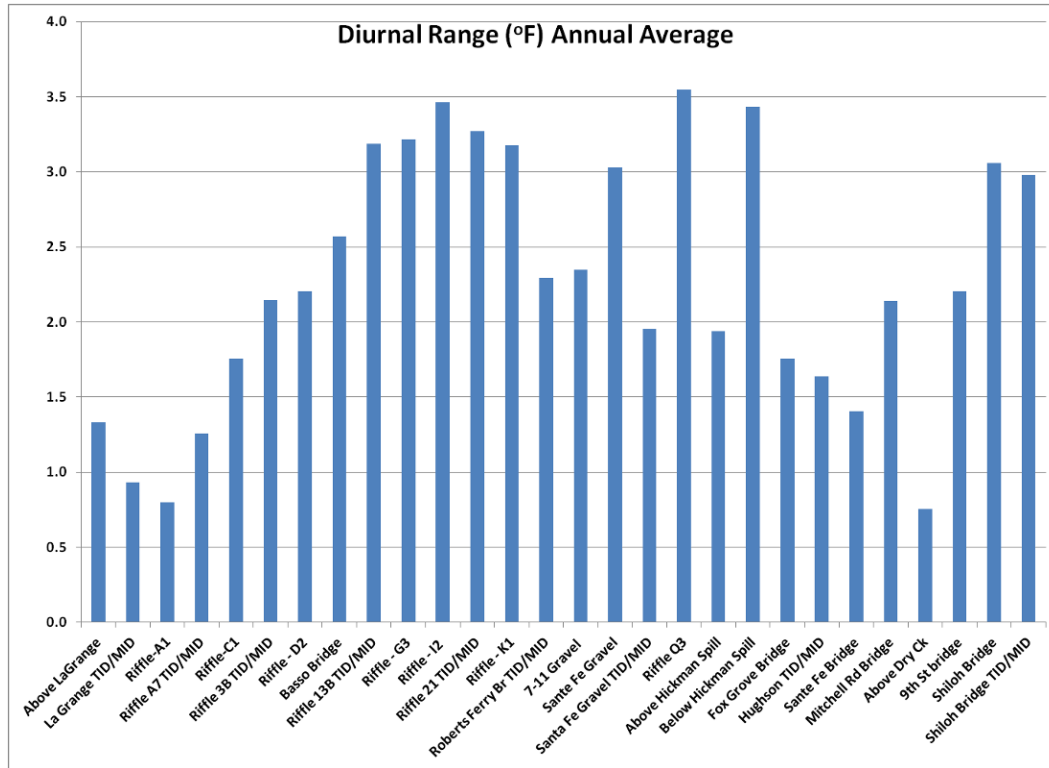


Figure 5.3-1. Annual average diurnal variation by site.

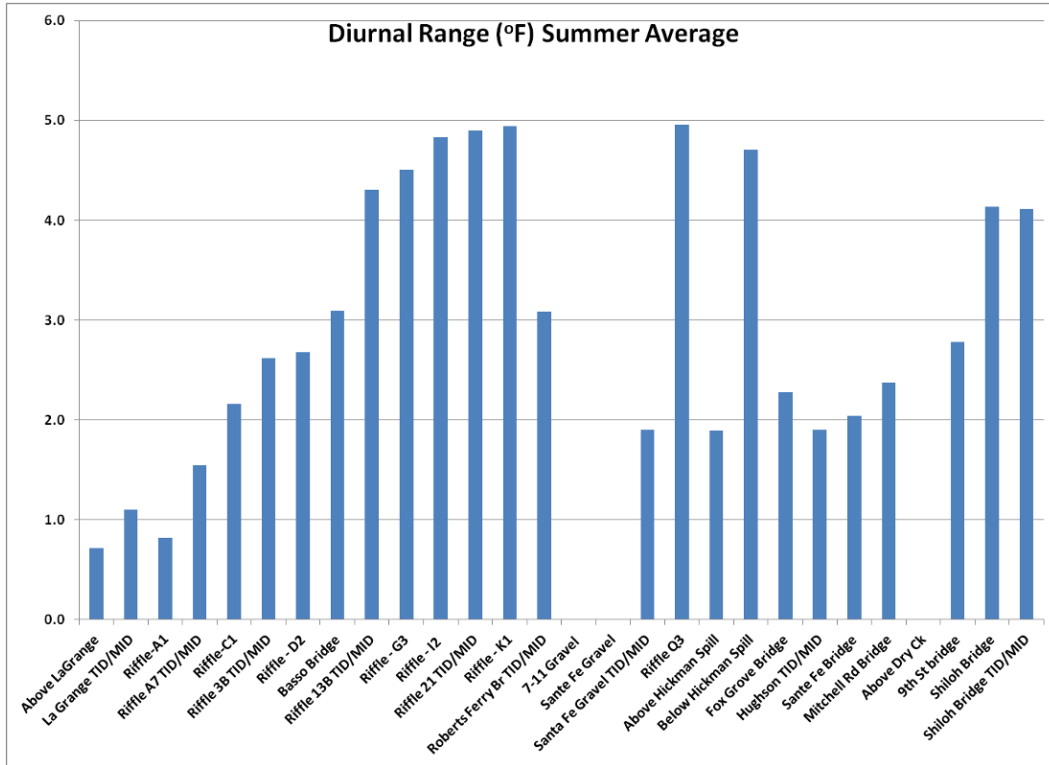


Figure 5.3-2. Summer average diurnal variation by site.

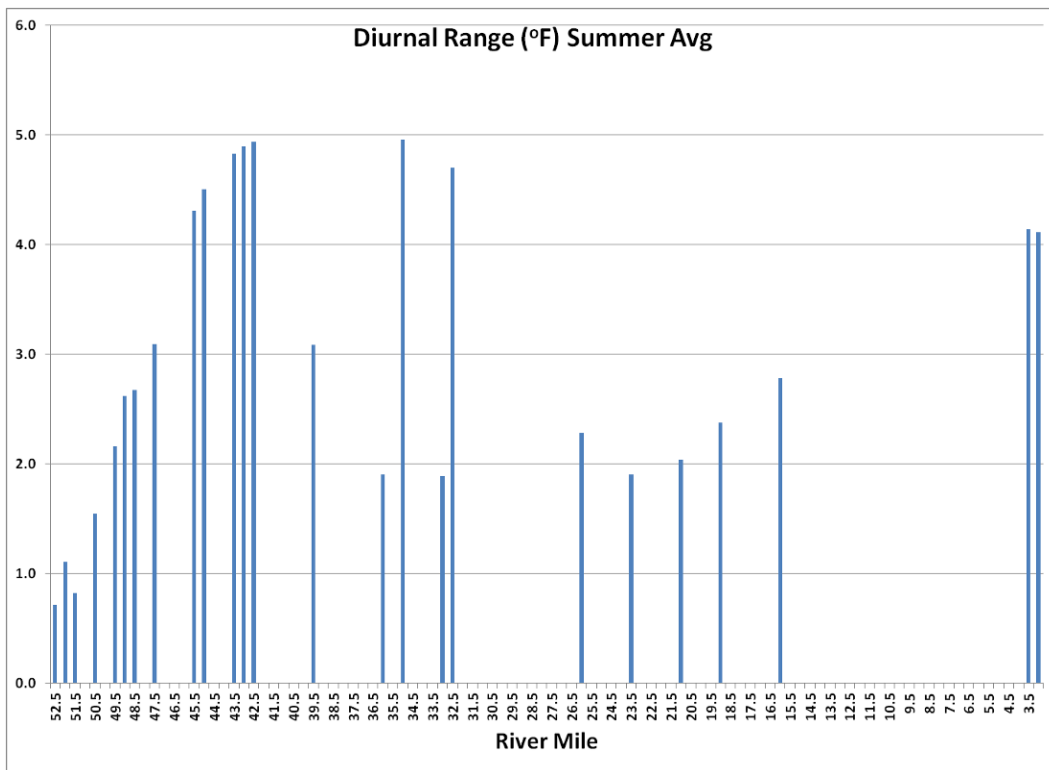


Figure 5.3-3. Summer average diurnal range at actual river location.

Figure 5.3-3 was replotted in Figure 5.3-4 with annotations that show the various operational spill locations from the Districts' irrigation systems and approximate locations where potential groundwater inflow was detected during accretion flow measurements in late June 2022. As any groundwater inflow would have minimal diurnal variation it could be expected to suppress the range observed at river reaches influenced by groundwater inflows.

Figure 5.3-5 is the same as Figure 5.3-4 with the location of the special run pools highlighted. It was speculated that the large thermal mass associated with these pools may also act to dampen the diurnal range.

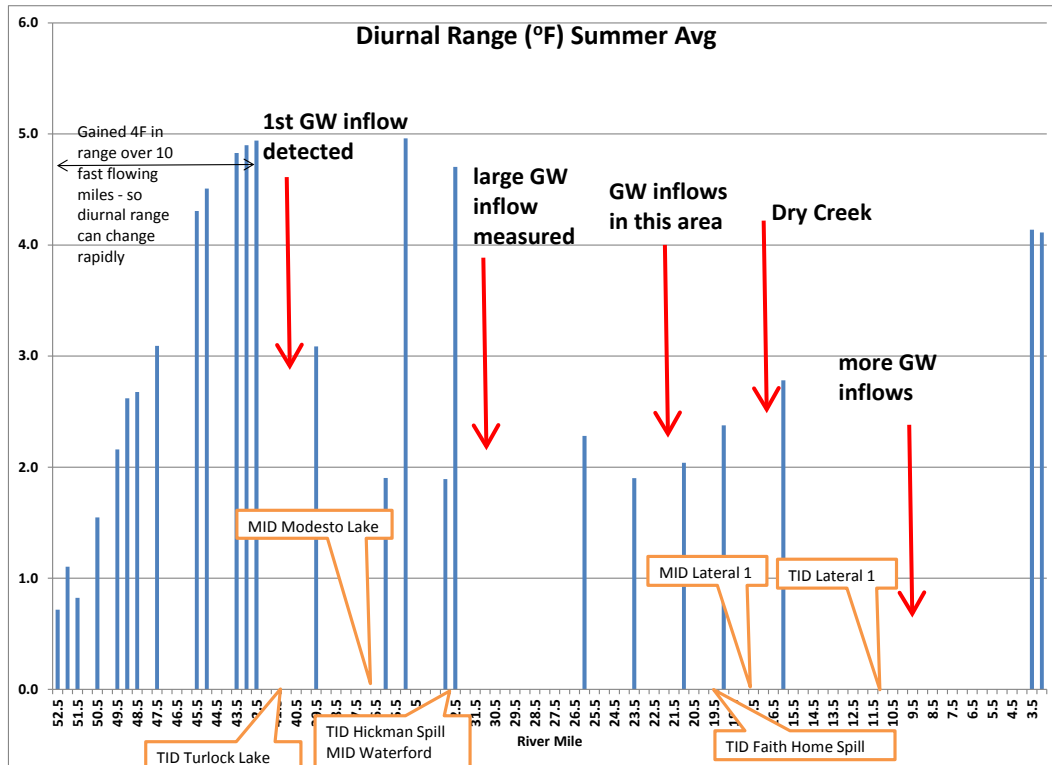


Figure 5.3-4. Summer average diurnal range at actual river location – annotated with return flow locations.

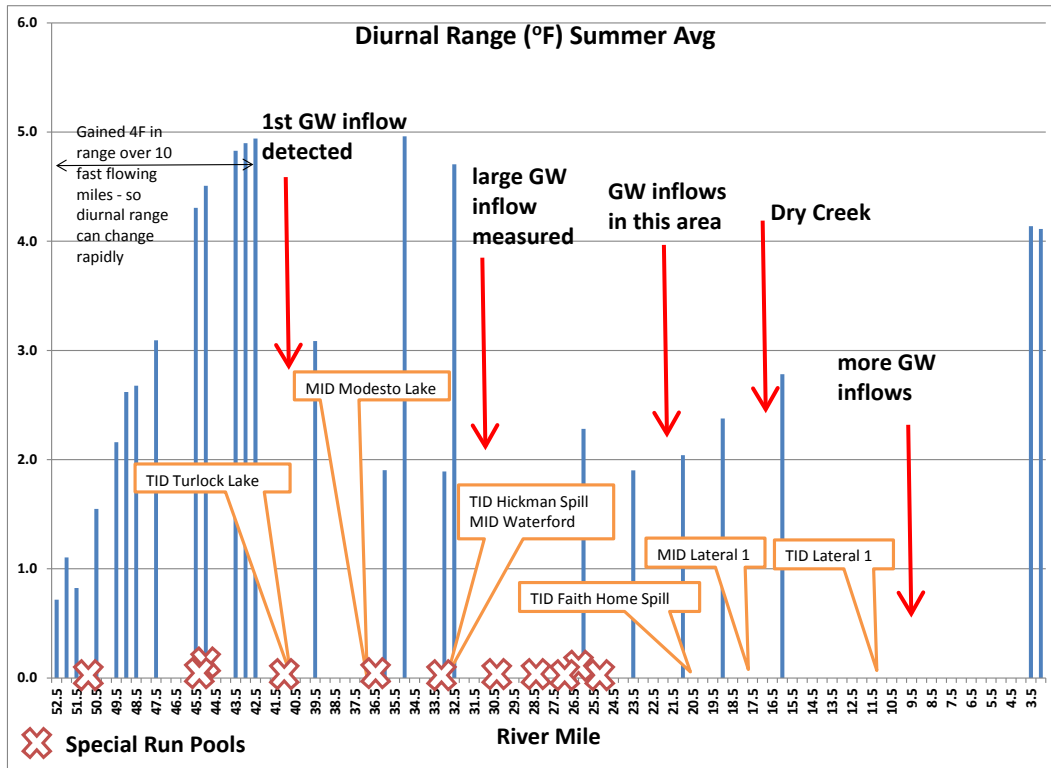


Figure 5.3-5. Summer average diurnal range– annotated with special run pools locations.

In an effort to examine whether the data for 2011 were an unusual case, the annual and summer diurnal ranges for the last 10 years were compared to 2011. These are shown in Figures 5.3-6 to 5.3-15 in reverse chronological order. These data indicate that the smaller diurnal temperature fluctuations occurring in the downstream direction are observed each year, with considerable variation from one year to the next.

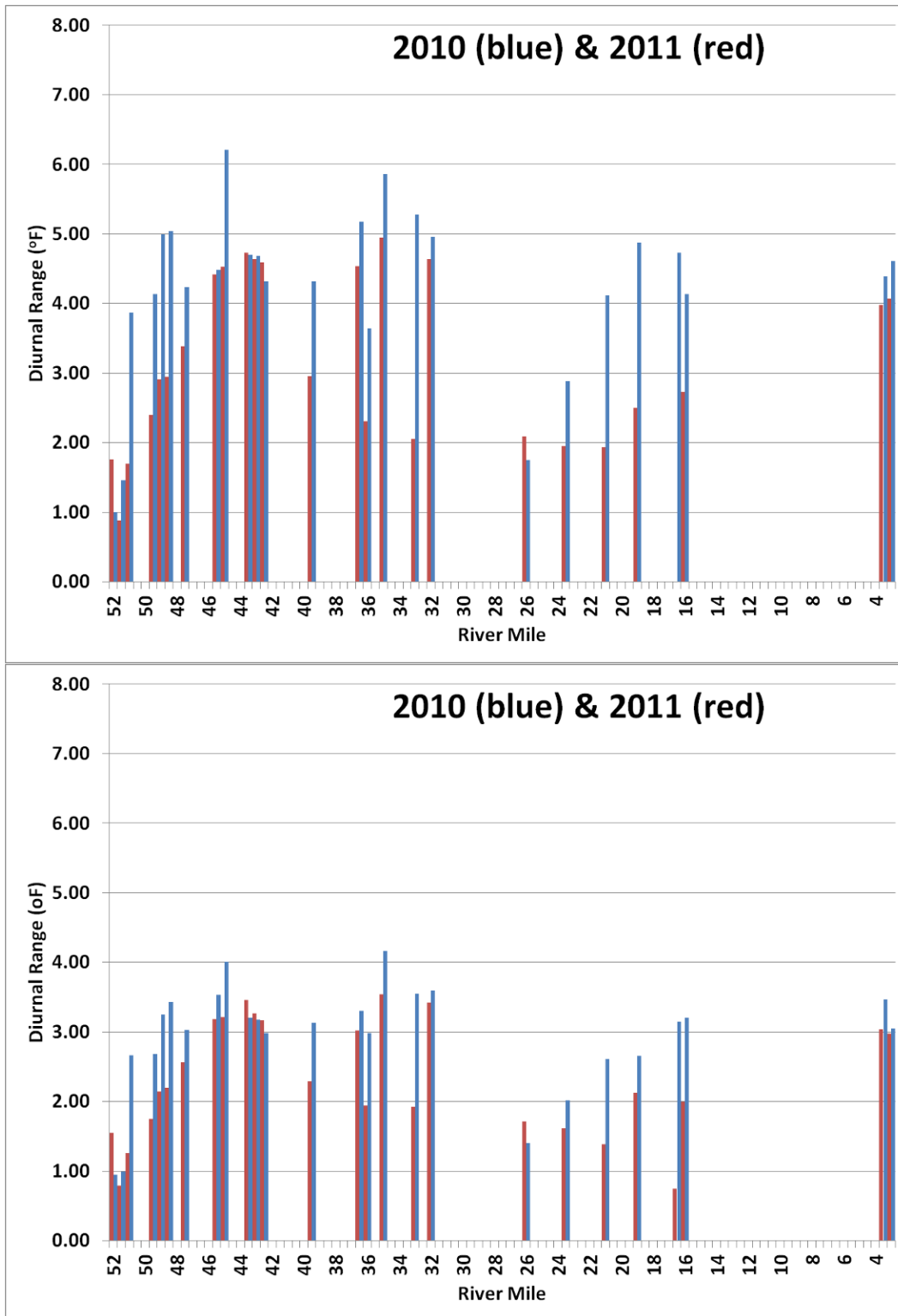


Figure 5.3-6. Comparison of 2011 and 2010 ranges (top=summer, lower=annual).

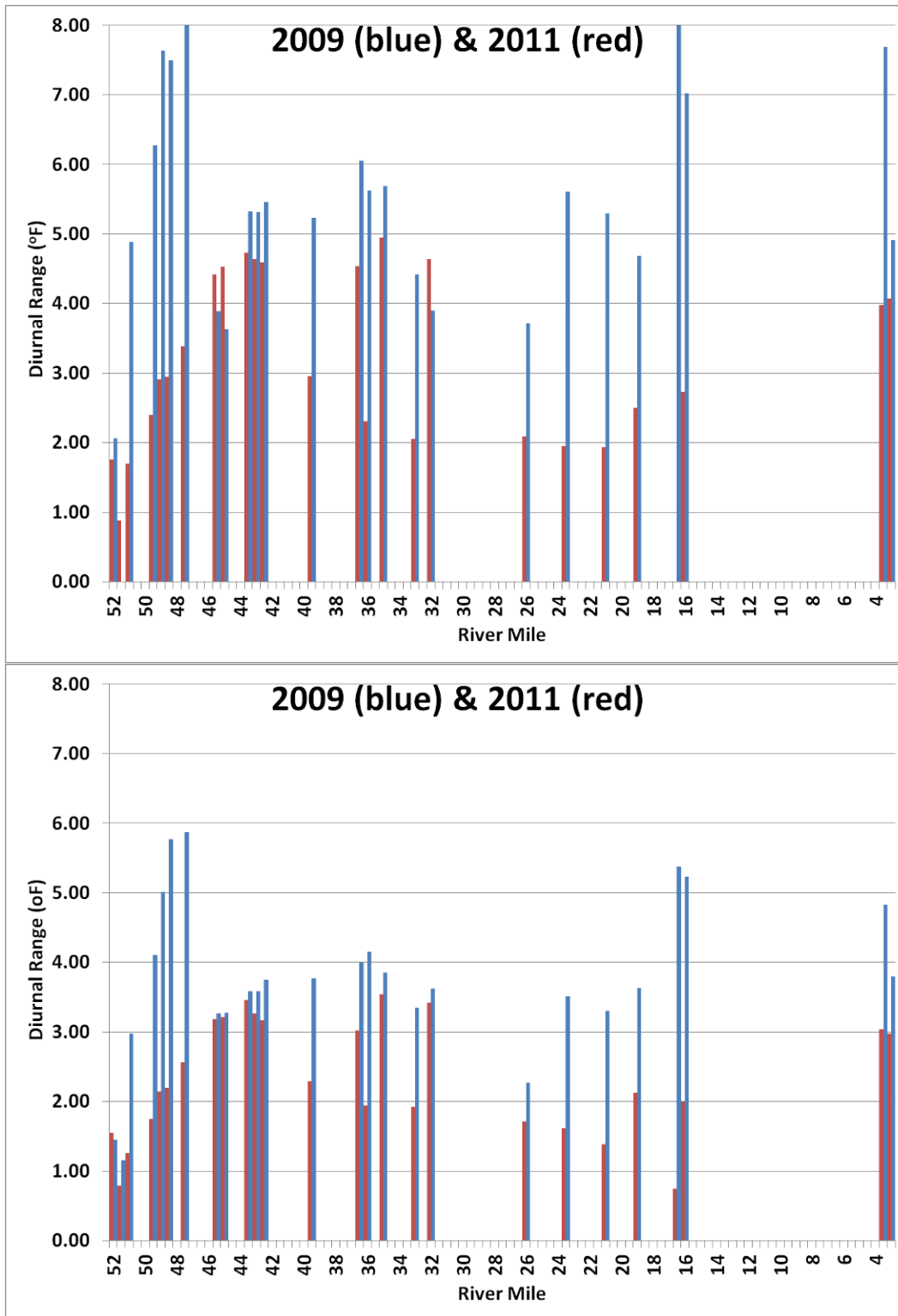


Figure 5.3-7. Comparison of 2011 and 2009 ranges (top=summer, lower=annual).

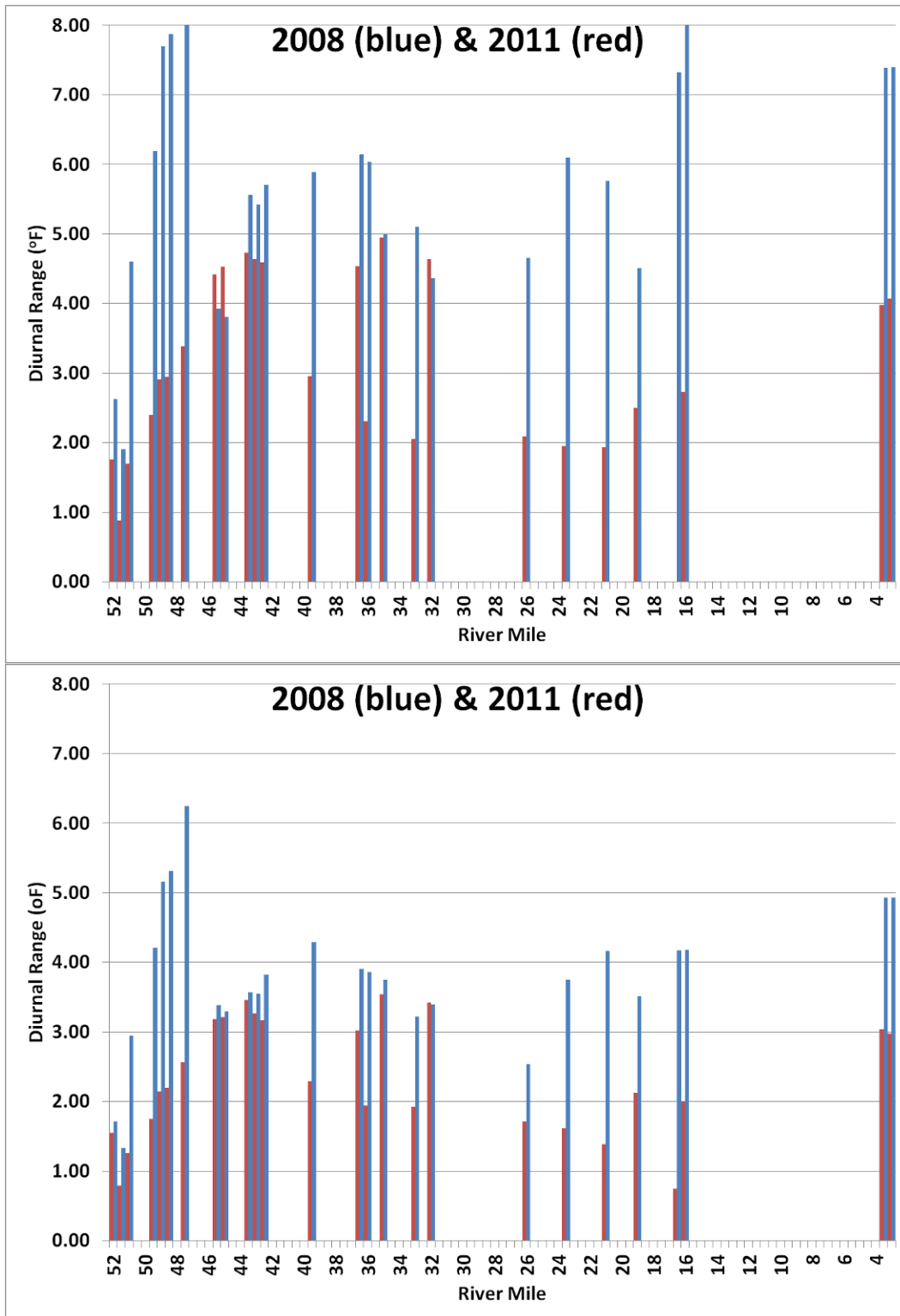


Figure 5.3-8. Comparison of 2011 and 2008 ranges (top=summer, lower=annual).

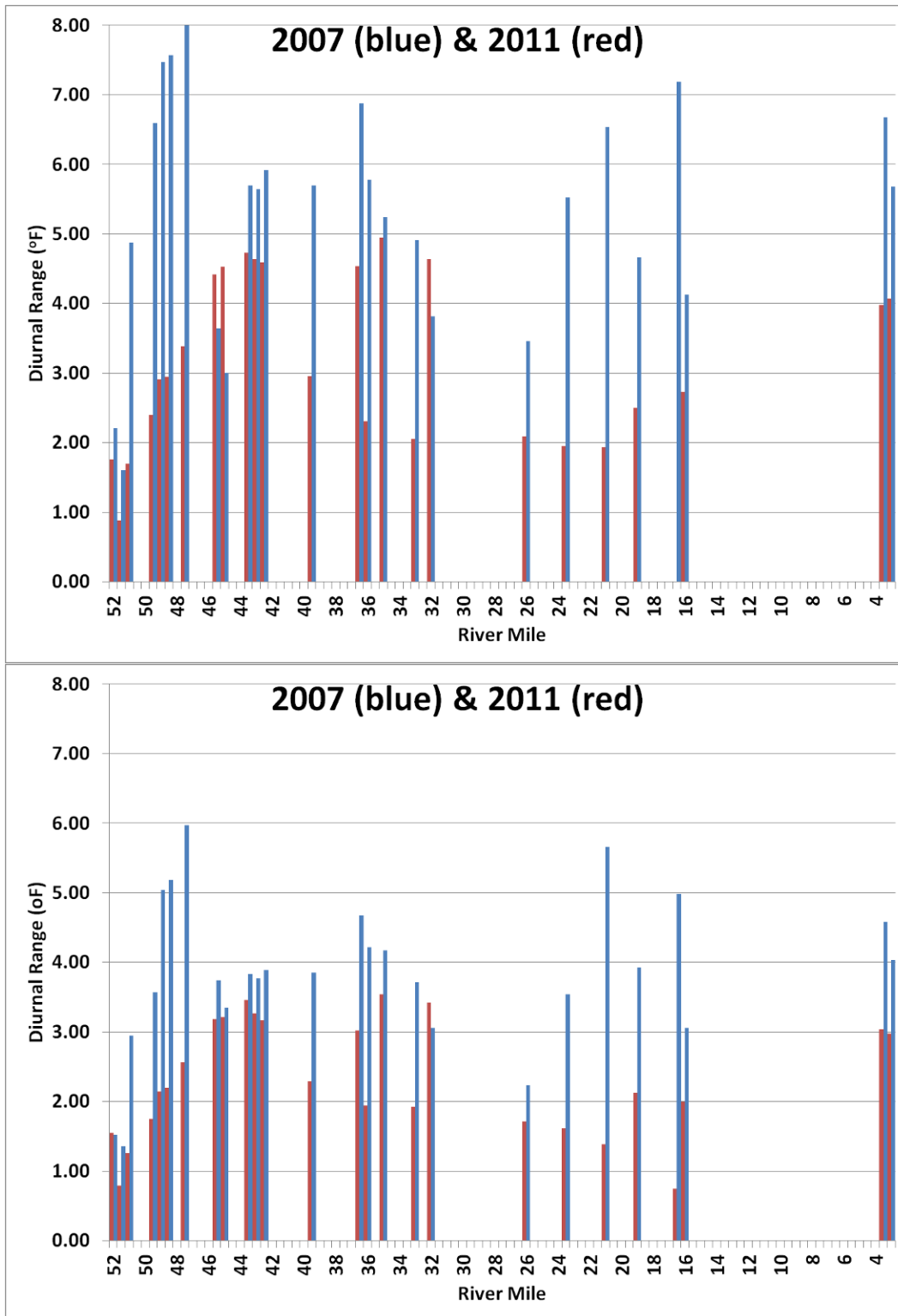


Figure 5.3-9. Comparison of 2011 and 2007 ranges (top=summer, lower=annual).

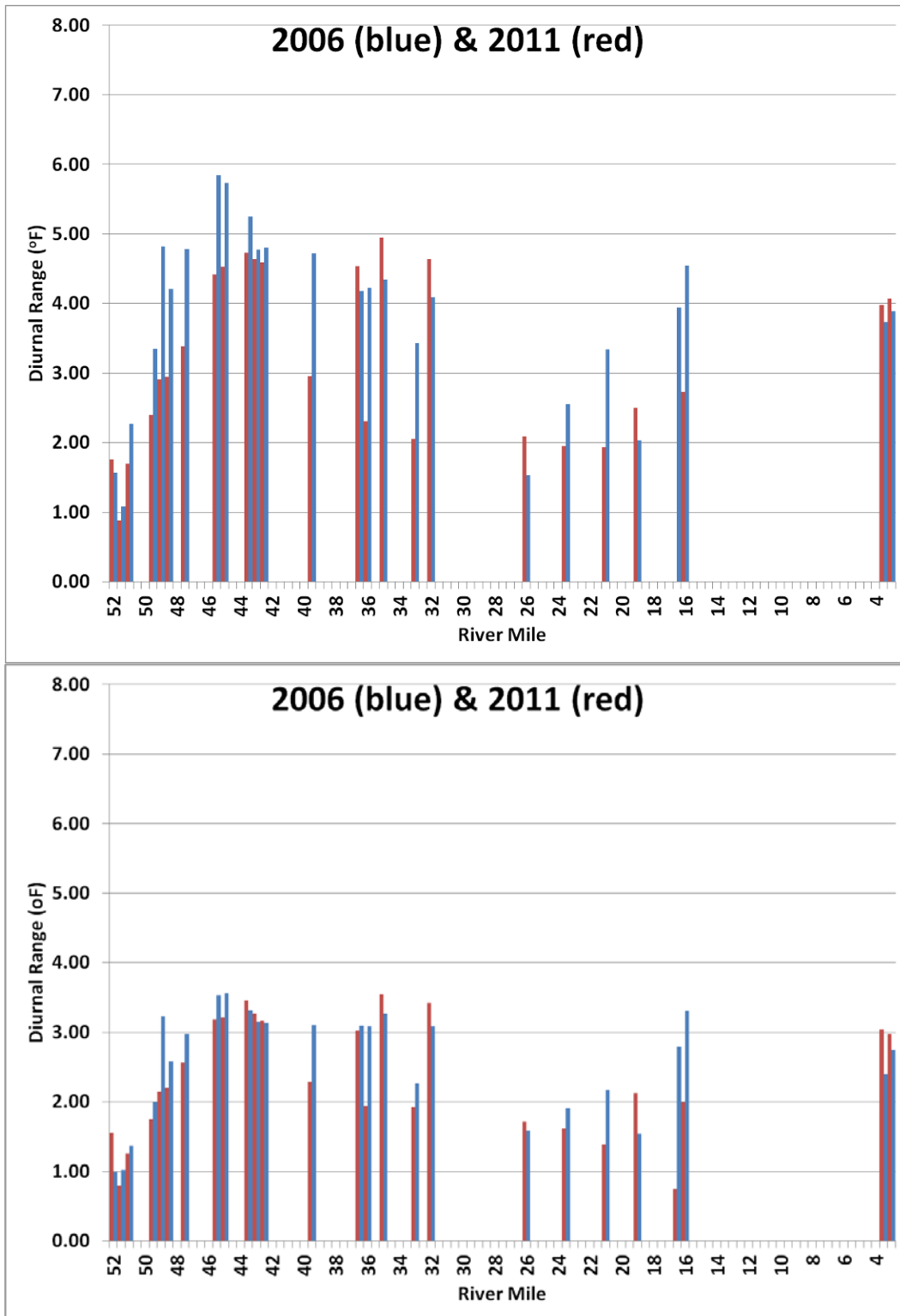


Figure 5.3-10. Comparison of 2011 and 2006 ranges (top=summer, lower=annual).

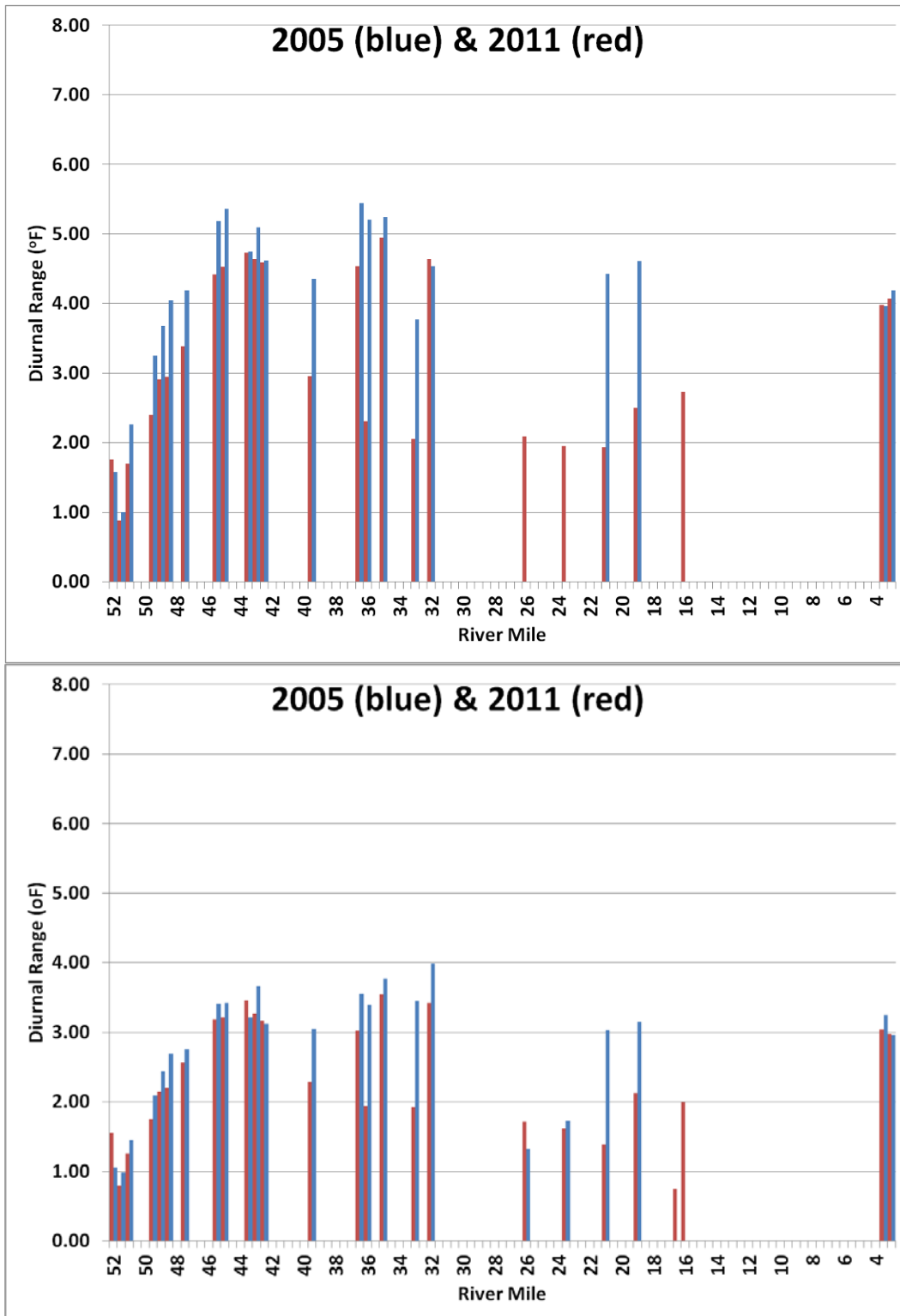


Figure 5.3-11. Comparison of 2011 and 2005 ranges (top=summer, lower=annual).

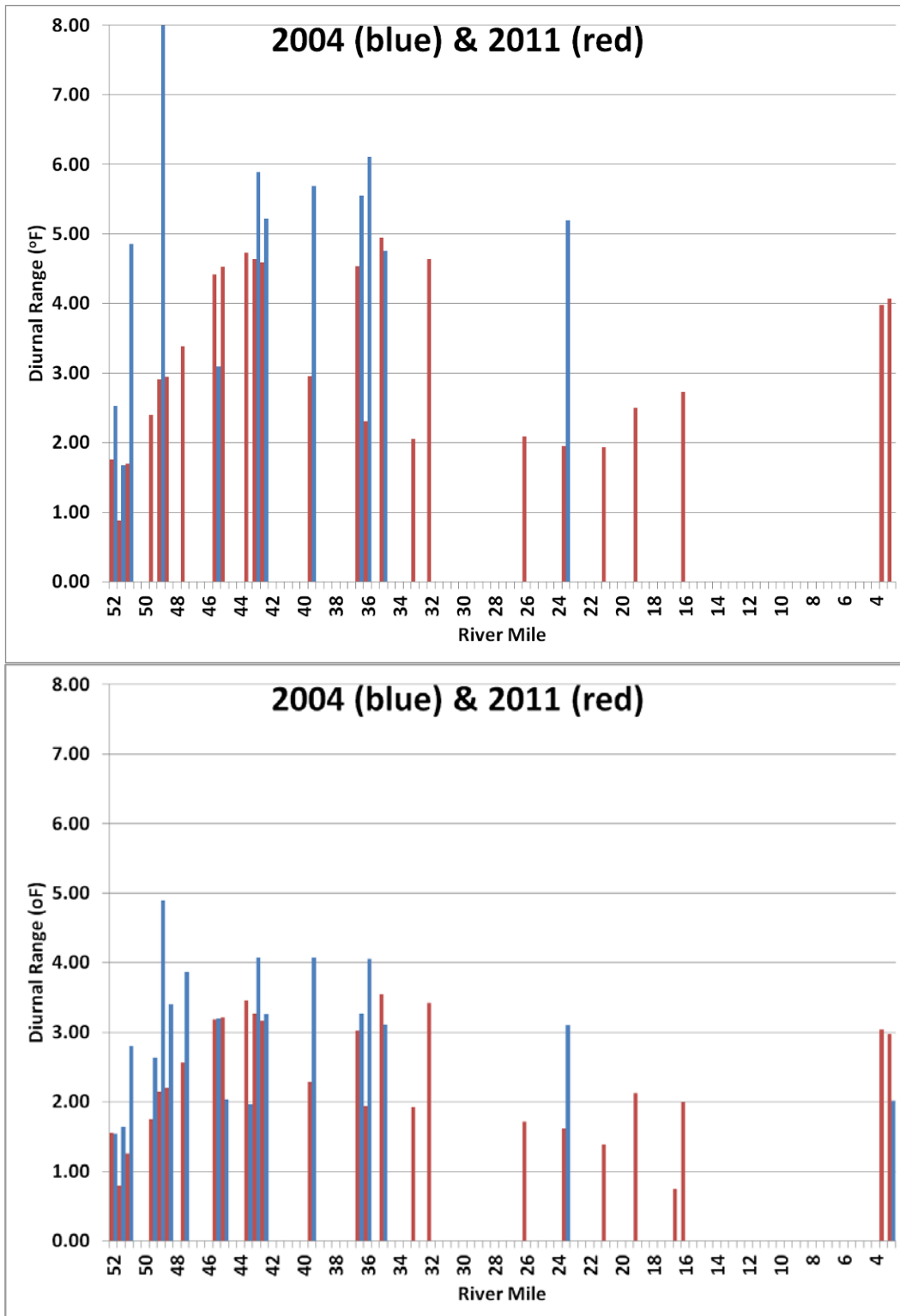


Figure 5.3-12. Comparison of 2011 and 2004 ranges (top=summer, lower=annual).

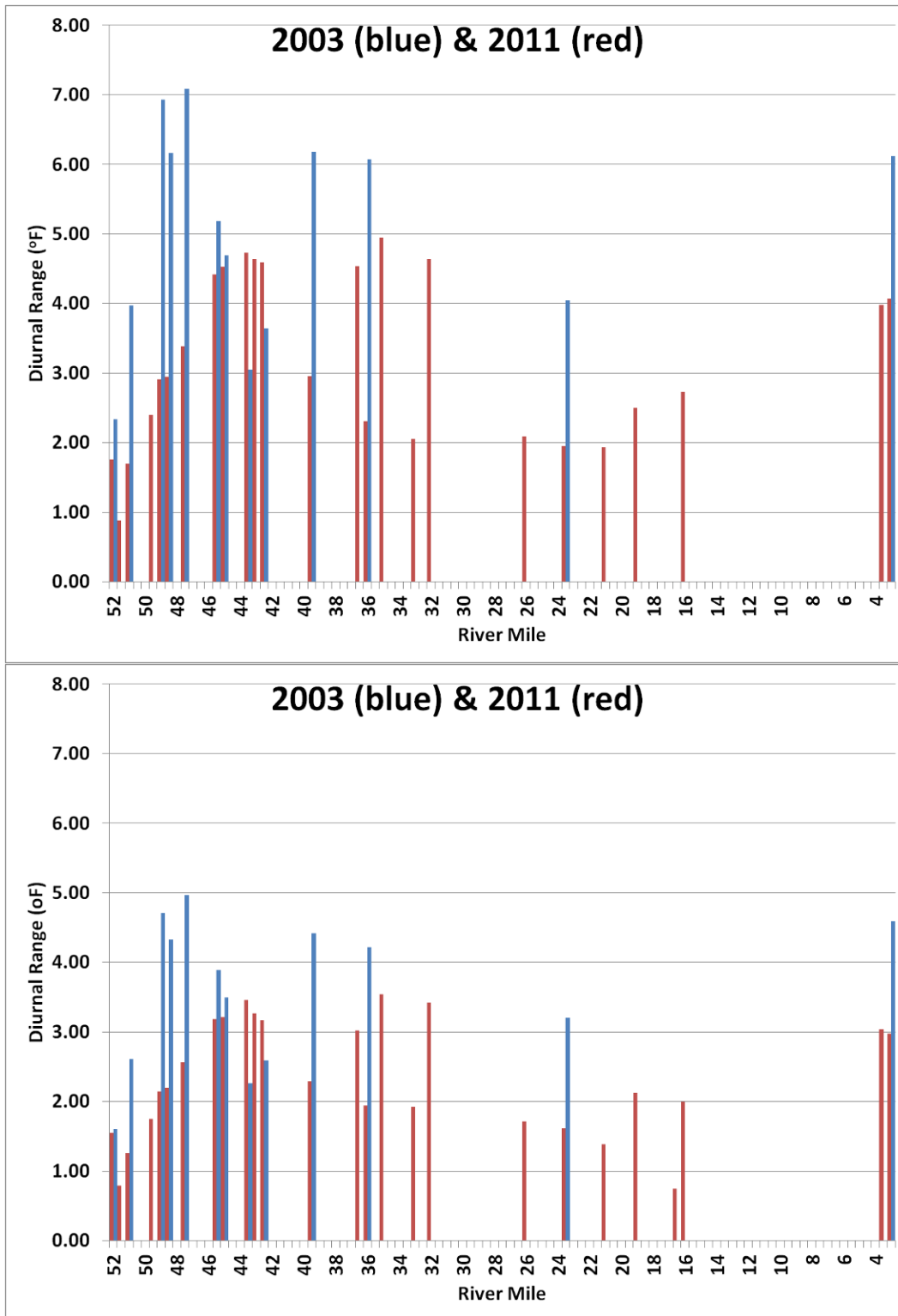


Figure 5.3-13. Comparison of 2011 and 2003 ranges (top=summer, lower=annual).

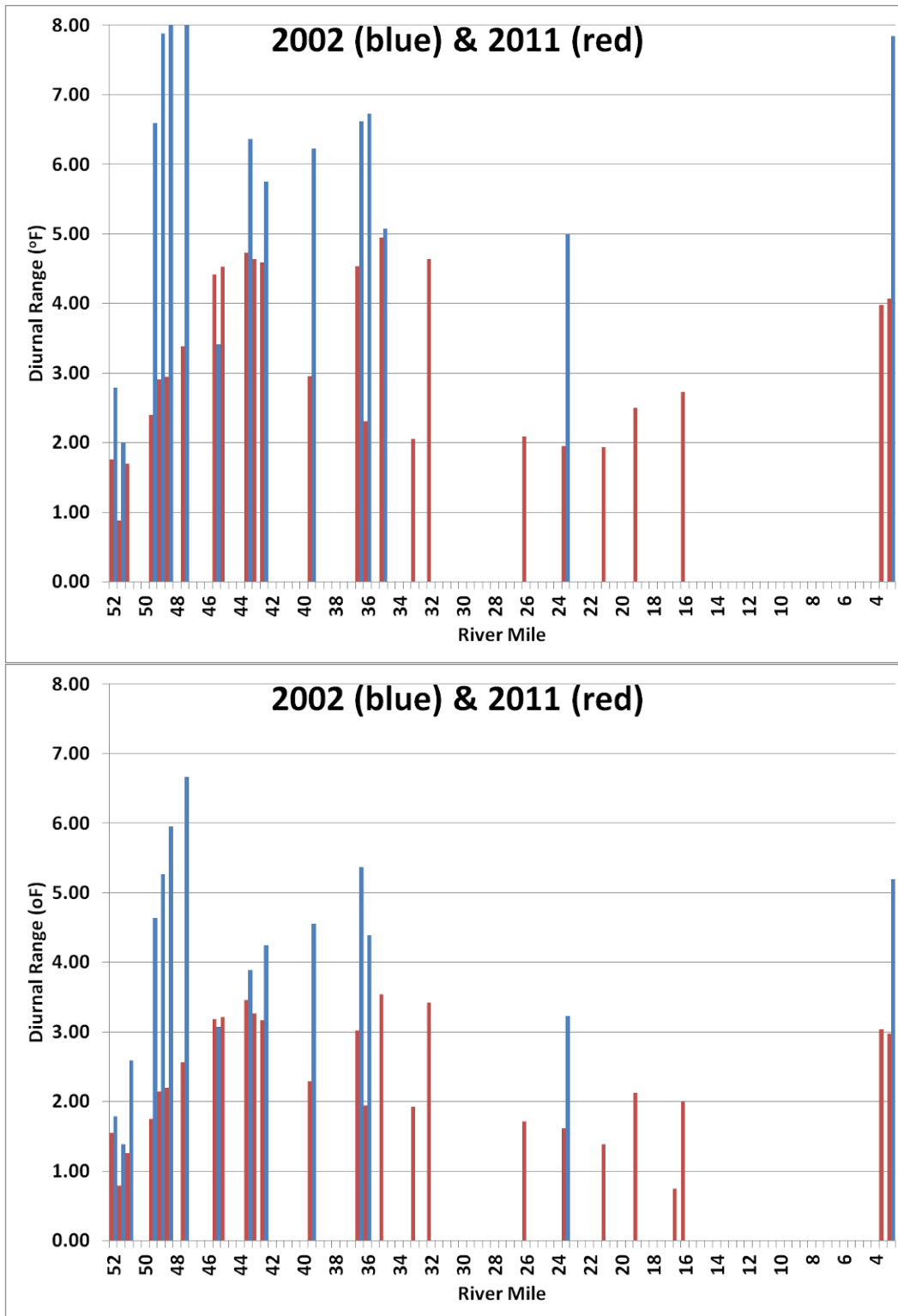


Figure 5.3-14. Comparison of 2002 and 2010 ranges (top=summer, lower=annual).

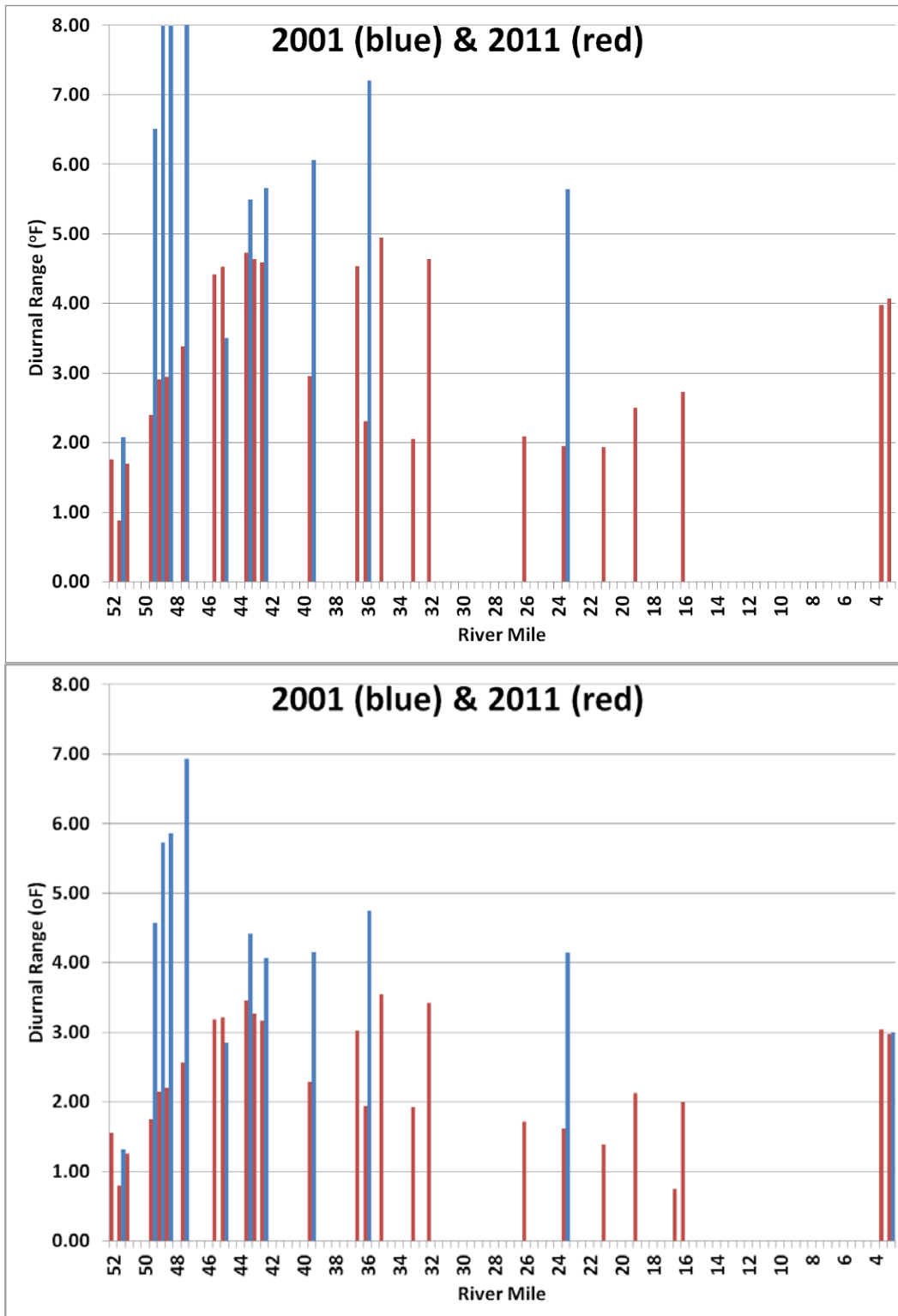


Figure 5.3-15. Comparison of 2011 and 2001 ranges (top=summer, lower=annual).

6.0 DISCUSSION AND RECOMMENDATIONS

The HEC-RAS model showed the ability to reasonably reproduce the observed temperature conditions in the lower Tuolumne River over the calibration and validation years of 2011 and 2012. The model did have issues at certain locations in 2011 where unexpected changes in diurnal temperature ranges were observed below about RM 40, a pattern observed in historical data, as well (See Attachment A of the Reservoir Temperature Model (TID/MID 2013f)). In 2012, which was a much drier and warmer year than 2011, these diurnal variations were not observed. These limited diurnal temperature variations are currently unexplained. However, groundwater inflows or possibly reemergence of hyporrheic flows may be possible causes. The Districts are proposing to undertake in the summer of 2013 an intensive river temperature investigation at two sites where rapid changes in these diurnal variations occur over short longitudinal distances in an effort to pinpoint the longitudinal extent, and potentially the cause, of the rapid changes. The study plan for this effort is provided as Attachment A to this document.

7.0 STUDY VARIANCES AND MODIFICATIONS

This study was conducted following the methods in Study W&AR-16 that was included in the Districts' Revised Study Plan filed with FERC on November 11, 2011, and approved with modification by FERC in its Study Determination on December 22, 2011. The study was performed in conformance with the FERC-approved study, with one variance. After the SJR5Q model could not produce adequate output to determine the 7DADM, the Districts migrated to the HEC-RAS model platform presented herein.

8.0 REFERENCES

- AD Consultants, Resources Management Associates Inc., Watercourse Engineering, Inc. 2009. San Joaquin River Basin Water Temperature Modeling and Analysis. Prepared for: CALFED ERP-06D-S20. Moraga, CA.
- California Department of Water Resources, 2004. California's Groundwater Bulletin 118: San Joaquin Valley Groundwater Basin, Modesto Subbasin. Sacramento, California.
- Central Valley Regional Water Quality Control Board (CVRWQCB). 1998. The Water Quality Control Plan (Basin Plan) for the Sacramento River Basin and the San Joaquin River Basin. 4th ed. California Regional Water Quality Control Board, Central Valley Region. Revised in October 2011 with the Approved Amendments. Available online at: <http://www.waterboards.ca.gov/centralvalley/water_issues/basin_plans/>.
- McBain & Trush, Inc. 2000. Habitat Restoration Plan for the Lower Tuolumne River Corridor. Arcata, California. Prepared for The Tuolumne River Technical Advisory Committee. March 2000.
- Stanislaus County. 2006. Stanislaus County General Plan. Stanislaus County Board of Supervisors, Modesto, California.
- State Water Resources Control Board (SWRCB). 2010. 2010 Integrated Report Clean Water Act Sections 303(d) and 305(b). Approved August 4, 2010. Board Resolution No. 2010-0040. Sacramento, California. Available online at: <http://www.waterboards.ca.gov/water_issues/programs/tmdl/integrated2010.shtml>
- Turlock Irrigation District and Modesto Irrigation District (TID/MID). 2013a. Lower Tuolumne Temperature Model Progress Report (W&AR-16). Attachment to Don Pedro Hydroelectric Project Initial Study Report. January.
- _____. 2013b. Districts' Responses to Relicensing Participants Comments on the Initial Study Report. Project No. 2299. Filed with FERC on April 9.
- _____. 2013c. Project Operations/Water Balance Model Study Report (W&AR-02). Attachment to Don Pedro Hydroelectric Project Initial Study Report. January 2013.
- _____. 2013d. Reservoir Temperature Model Progress Report (W&AR-03). Attachment to Don Pedro Hydroelectric Project Initial Study Report. January 2013.
- _____. 2013e. Spawning Gravel in the Lower Tuolumne River. Progress Report. Don Pedro Project Relicensing. Prepared by Stillwater Sciences. January.
- _____. 2013f. Reservoir Temperature Model Progress Report (W&AR-03), Attachment A: Water Temperature Dataset. Attachment to Don Pedro Hydroelectric Project Initial Study Report. January 2013.

_____. 2012a. October 26, 2012 Consultation Workshop Notes

_____. 2012b. November 14, 2012 Consultation Workshop Notes

_____. 2011a. Tuolumne River water temperature modeling study. Final Report. Prepared by Stillwater Sciences, Berkeley, California for Turlock Irrigation District and Modesto Irrigation District, California, March 2011.

_____. 2011b. Lower Tuolumne Temperature Model Study Plan (W&AR-16). Attachment to Don Pedro Hydroelectric Project Revised Study Plan. November 2011.

USACE 2001. HEC-HMS for the Sacramento and San Joaquin Comprehensive Study. Chapter 2: Digital Elevation Model Construction. August.

_____. 2010. HEC-RAS. River Analysis System. User's Manual. Version 4.1. January 2010.

**STUDY REPORT W&AR-16
LOWER TUOLUMNE RIVER
TEMPERATURE MODEL**

ATTACHMENT A

**STUDY PLAN W&AR-16
IN - RIVER DIURNAL TEMPERATURE VARIATION STUDY**

**TURLOCK IRRIGATION DISTRICT & MODESTO IRRIGATION DISTRICT
DON PEDRO PROJECT
FERC NO. 2299
WATER & AQUATIC RESOURCE WORK GROUP**

**Study Plan W&AR-16
In - River Diurnal Temperature Variation Study
May 2013**

1.0 Project Nexus

Turlock Irrigation District's (TID) and the Modesto Irrigation District's (MID) (collectively, the Districts) continued operation and maintenance (O&M) of the Don Pedro Project (Project) will affect reservoir storage levels in Don Pedro Reservoir, reservoir releases, and stream flow in the Tuolumne River downstream of Don Pedro Reservoir. Similarly, flow releases from Don Pedro Reservoir will affect the temperature of waters downstream of Don Pedro Dam and may contribute to the cumulative effects to resources in the lower Tuolumne River.

2.0 Resource Agency Management Goals

The Districts believe that two agencies have resource management goals related to water temperature in Don Pedro Reservoir and in the lower Tuolumne River: (1) the California Department of Fish and Wildlife (CDFW)¹, and (2) the State Water Resources Control Board, Division of Water Rights (SWRCB). Each of these agencies and their management goals, as understood by the Districts at this time, is described below.

CDFW's goal is to preserve and protect the habitats necessary to support native fish, wildlife and plant species.

SWRCB is the state agency that administers the federal Clean Water Act (CWA) (33 U.S.C. §11251-1357) as applies to California waters with the responsibility to maintain the chemical, physical, and biological integrity of the state's waters and to protect the beneficial uses of stream reaches consistent with Section 401 of the federal CWA, the Regional Water Quality Control Board Basin Plans, State Water Board regulations, California Environmental Quality Act, and other applicable state law. On October 11, 2011, the U.S. Environmental Protection Agency (EPA) issued its decision that the lower Tuolumne River, the reach covered by the study plan, was impaired for temperature.

¹ In this document, the California Department of Fish and Wildlife is referred to by the acronyms "CDFW" and "CDFG".

3.0 Study Goals

The objective of this study is to more precisely identify and define the occurrence of and, if possible the reasons for, significant changes in diurnal temperature fluctuations in the lower Tuolumne River observed at multiple locations.

This detailed investigation will examine the local complexity of in-river temperatures at key locations to understand the potential role of groundwater accretions, special run pools, and/or river geometry in moderating diurnal temperature fluctuations in the lower Tuolumne River.

This information will be used (1) to better understand the geographic extent of the groundwater inflow temperature signatures captured by the Lower Tuolumne Temperature Model and (2) identify and define some of the local in-river temperature complexities that may not be predicted by the one-dimensional model. It is expected that results of this study will assist in the interpretation of output from scenarios run using the lower Tuolumne River Temperature Model (TID/MID 2013a).

4.0 Existing Information and Need for Additional Information

The Lower Tuolumne Temperature Model (WA&R-16) uses measured flows and temperatures obtained immediately below the Don Pedro powerhouse as the upstream boundary condition (TID/MID 2013a). TID and MID withdrawals occur at La Grange diversion dam at RM52.2. Flow enters at RM16.3 from Dry Creek and the Dry Creek flows and temperatures are estimated based on measurements. In the model, groundwater accretion along the river is estimated based on the results of accretion surveys completed in 2012 and 2013 (TID/MID 2013b). Boundary information is summarized in Table 1. Tuolumne River water temperature monitoring locations, special run pool (SRP) locations, irrigation canal operational spill locations, and 2012 accretion field measurement locations are provided by river mile in Table 2.

Table 1. Tuolumne River water temperature monitoring boundary condition locations

Site Locations	Source	Tuolumne River Mile	Coordinates (Decimal °)		Period of Record		Notes
			Latitude	Longitude	Start Date	End Date	
BOUNDARY CONDITION TEMPERATURES							
Tuolumne River below Don Pedro Powerhouse	MID/TID	54.3	37.6929	-120.4216	5/19/10	12/6/12	
Tuolumne River above La Grange Dam	MID/TID	52.2	37.6725	-120.4438	8/25/11	12/6/12	
Groundwater accretion	--	To be determined	To be determined	To be determined	--	--	Groundwater inflow measured during three field streamflow measurement events
Dry Creek above Tuolumne River	CDFG	--	37.6398	-120.9848	2/3/06	4/27/12	

-- = not applicable

CDFG = California Department of Fish and Game

MID = Modesto Irrigation District

TID = Turlock Irrigation District

Following the completion of the 2012 relicensing studies, the following observations were made:

- Accretion measurements taken in the lower Tuolumne River in 2012 and 2013 show that the river is generally a gaining stream. In June 2012, October 2012, and February 2013, the influence of groundwater inflows was first observed at RM 43.4 and then inflows seemed to become more noticeable as measurements were taken further downstream (Table 2; Figure 1).
- During calibration of the Lower Tuolumne River Temperature Model, summer river temperatures were not consistently reproducible around RM 33 or between RM 26 and RM 16.1 (Table 2; see TID/MID 2013a). Actual diurnal temperature ranges were significantly smaller than predicted by the model in these reaches. See Attachment A to the Don Pedro Reservoir Model Report (WA&R-03) for all available historical data (TID/MID 2013c).
- A review of data collected from 2001 through 2010 finds similar abrupt changes in diurnal ranges; however, the pattern was not observed in 2012.
- The reduction in the diurnal temperature range was primarily observed at and below RM 33 (below SRP11). The downstream limit of Chinook spawning habitat is thought to be about RM 24. See Spawning Gravel Study Report (W&AR-04) (TID/MID 2013d).

Based on these observations, it appears that groundwater flows either into or out of the lower Tuolumne River or other local physical processes are influencing river temperatures under summer conditions.

Table 2. Tuolumne River water temperature monitoring locations, special run pool locations, agricultural return flow locations, and 2012 accretion field measurement locations

Location ¹	Source	Tuolumne River Mile	Coordinates (Decimal °)		Period of Record		Notes
			Latitude	Longitude	Start Date	End Date	
DOMINANT SALMON SPAWNING REACH—RM 52.0 to RM 46.6 (Over half of all Chinook spawning occurs in this reach²)							
Tuolumne River at La Grange USGS Station	Stillwater	51.8	37.6669	-120.4418	1/8/77	12/5/12	--
Tuolumne River at Riffle A1	CDFG	51.6	37.6694	-120.4438	6/18/01	1/15/13	--
Tuolumne River at La Grange gage house—accretion field measurement	TID/MID	51.5	--	--	6/2012 10/2012 2/2013		--
Special Run Pool 1 (SRP1)	--	51	--	--	--	--	--
Tuolumne River at Rifle A7	Stillwater	50.7	37.6652	-120.4567	11/14/01	12/5/12	--
Tuolumne River at Riffle C1	CDFG	49.7	37.6671	-120.4764	6/14/01	1/22/13	--
Tuolumne River at Riffle 3B	Stillwater	49.1	37.6627	-120.4820	1/18/90	12/5/12	--
Tuolumne River at Basso Pool—accretion field measurement	TID/MID	49.1	--	--	6/2012 10/2012 2/2013		--
Tuolumne River at Riffle D2	CDFG	48.8	37.6595	-120.4874	6/14/01	1/22/13	--
Tuolumne River at Basso Bridge	CDFG	47.5	37.6507	-120.4946	7/29/03	1/22/13	--
DREDGER TAILING REACH—RM 46.6 to RM 40.3							
Tuolumne River at Riffle 13B	Stillwater	45.5	37.6290	-120.5205	11/14/01	12/5/12	--
Tuolumne River at Zanker property—accretion field measurement	TID/MID	45.5	--	--	10/2012 2/2013		
Tuolumne River at Riffle G3	CDFG	45	37.6289	-120.5208	6/15/01	1/22/13	--
Special Run Pool 2 (SRP2)	--	45	--	--	--	--	--
Special Run Pool 3 (SRP3)	--	44	--	--	--	--	--
Tuolumne River at Bobcat Flat—accretion field measurement	TID/MID	43.4	--	--	6/2012 10/2012 2/2013		Groundwater influence first observed
Tuolumne River at Riffle I2	CDFG	43.2	37.6319	-120.5611	6/15/01	1/22/13	--
Tuolumne River	Stillwater	42.9	37.6323	-120.5635	5/27/04	12/5/12	---

Location ¹	Source	Tuolumne River Mile	Coordinates (Decimal °)		Period of Record		Notes
			Latitude	Longitude	Start Date	End Date	
at Rifle 21							
Tuolumne River at Riffle K1	CDFG	42.6	37.6315	-120.5829	6/16/01	1/23/13	--
Special Run Pool 4 (SRP4)	--	41	--	--	--	--	--
GRAVEL MINING REACH—RM 40.3 to RM 34.2							
Tuolumne River at Roberts Ferry Bridge	Stillwater	39.5	37.6366	-120.6153	8/11/98	12/5/12	--
Tuolumne River at Roberts Ferry Bridge—accretion field measurement	TID/MID	39.5	--	--	6/2012 10/2012 2/2013		--
Tuolumne River at 7-11 Gravel Company	CDFG	38	37.6272	-120.6401	6/16/01	1/23/13	--
Tuolumne River at Santa Fe Aggregates—accretion field measurement	TID/MID	37.1	--	--	6/2012 10/2012 2/2013		--
Tuolumne River at Ruddy Gravel	Stillwater	36.5	37.6405	-120.6659	4/1/87	12/5/12	--
Tuolumne River at Sante Fe Gravel	CDFG	36.5	37.6405	-120.6657	5/31/02	1/23/13	--
Special Run Pool 11 (SRP11)	--	36.5	--	--	--	--	--
Tuolumne River at Riffle Q3	CDFG	35	37.6444	-120.6991	5/31/02	1/23/13	--
IN-CHANNEL GRAVEL MINING REACH—RM 34.2 to RM 24							
Tuolumne River above Hickman Spill	CDFG	33	37.6361	-120.7317	3/9/05	1/23/13	Diurnal temperature range reduced.
Special Run Pool 5 (SRP5)	--	33	--	--	--	--	--
Waterford Main (MID)	MID	33.0	--	--	--	--	--
Hickman Spill (TID)	TID/MID	33.0	--	--	--	--	--
Tuolumne River below Hickman Spill	CDFG	32	37.6352	-120.7478	3/9/05	1/23/13	Diurnal temperature range expands back towards upstream range.
Tuolumne River at Waterford—	TID/MID	31.5	--	--	6/2012 10/2012		--

Location ¹	Source	Tuolumne River Mile	Coordinates (Decimal °)		Period of Record		Notes
			Latitude	Longitude	Start Date	End Date	
accretion field measurement					2/2013		
Tuolumne River at Hickman Bridge	CDFG	31	37.636	-120.7593	7/15/02	12/13/12	--
Special Run Pool 6 (SRP6)	--	30.5	--	--	--	--	--
Tuolumne River at Delaware Road—accretion field measurement	TID/MID	30.5	--	--	6/2012 10/2012 2/2013		Groundwater influence observed
Special Run Pool 7 (SRP7)	--	28.5	--	--	--	--	--
Special Run Pool 8 (SRP8)	--	27	--	--	--	--	--
Tuolumne River near Fox Grove Bridge	CDFG	26	37.6178	-120.8455	9/9/05	1/1/13	Diurnal temperature range reduced.
Tuolumne River at Fox Grove Park—accretion field measurement	TID/MID	26.0	--	--	10/2012 2/2013		--
Special Run Pool 9 (SRP9)	--	25.9	--	--	--	--	--
Special Run Pool 10 (SRP10)	--	25.2	--	--	--	--	--
UPPER SAND-BEDDED REACH—RM 24 to RM 19.3 (Downstream extent of Chinook spawning habitat²)							
Tuolumne River at Hughson	Stillwater	23.6	37.6281	-120.8717	12/10/97	12/5/12	Diurnal temperature range reduced.
Tuolumne River above Santa Fe Bridge	CDFG	21	37.623	-120.8987	8/12/05	1/15/13	Diurnal temperature range reduced.
Faith Home Spill (TID)	TID	20.0	--	--	--	--	
URBAN SAND-BEDDED REACH—RM 19.3 to RM 10.5							
Tuolumne River at Mitchell Road Bridge	CDFG	19	37.6172	-120.9382	8/12/05	4/27/12	Diurnal temperature range reduced.
Lateral No. 1 (MID)f	MID	18.0	--	--	--	--	--
Tuolumne River at Legion Park—accretion field measurement	TID/MID	17.2	--	--	6/2012 10/2012 2/2013		Groundwater influence observed
Mouth of Dry Creek—accretion field	TID/MID	16.4	--	--	6/2012 10/2012 2/2013		--

Location ¹	Source	Tuolumne River Mile	Coordinates (Decimal °)		Period of Record		Notes
			Latitude	Longitude	Start Date	End Date	
measurement							
Tuolumne River above Dry Creek	CDFG	16.3	37.6271	-120.9811	7/25/06	1/15/13	Diurnal temperature range reduced.
Tuolumne River at Modesto 9th St. Bridge	TID/MID	16.2	--	--	6/2012 10/2012 2/2013		
Tuolumne River at 9th Street Bridge	CDFG	16	37.6274	-120.987	8/12/05	8/22/12	Diurnal temperature range reduced.
Tuolumne River at Carpenter Road Bridge	CDFG	12	37.6098	-121.0319	8/12/05	8/22/12	Diurnal temperature range expands again.
Lateral 1 (TID)	TID	11.0	--	--	--	--	
LOWER SAND-BEDDED REACH—RM 10.5 to RM 0							
Tuolumne River near Riverdale Park—accretion field measurement	TID/MID	10.0	--	--	10/2012 2/2013		Groundwater influence observed
Tuolumne River at Shiloh Bridge—accretion field measurement	TID/MID	3.7	--	--	6/2012 10/2012 6/2012		--
Tuolumne River at Shiloh Bridge	Stillwater	3.5	37.6027	-121.1315	4/2/87	12/5/12	--
Tuolumne River at Shiloh Bridge	CDFG	3.4	37.6027	-121.1313	2/16/05	1/6/13	--
Lateral No. 5 (MID)	MID	2.0	--	--	--	--	--

-- = not available or not applicable.

¹ Temperature monitoring locations included herein are limited to those that include data collection in 2011 and 2012.

² per W&AR-04 Report (TID/MID 2013d).

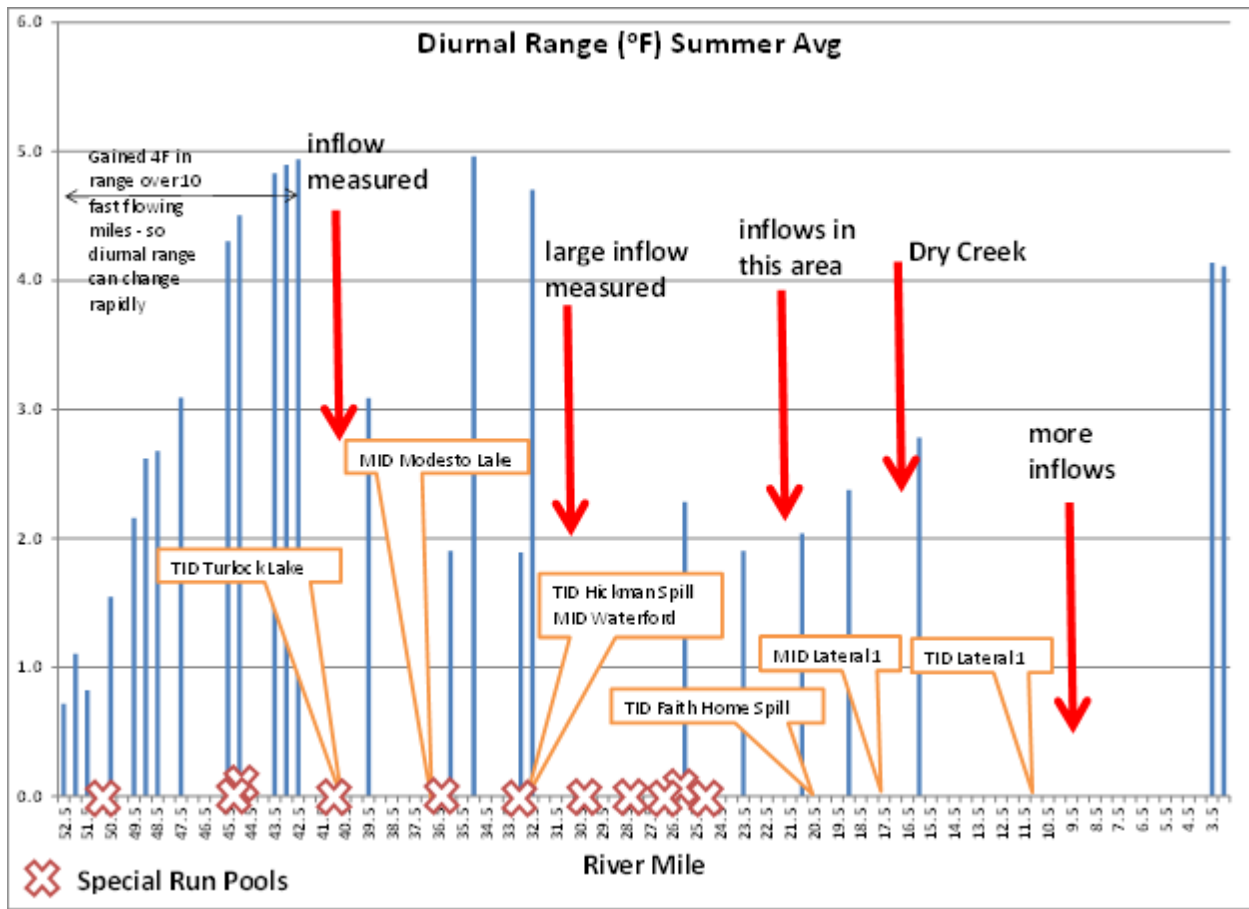


Figure 1. Diurnal range of lower Tuolumne River temperature data, 2011

5.0 Study Methods

5.1 Study Area

The study area includes specific reaches in the lower Tuolumne River as described below.

5.2 Study Methods

The study consists of four steps:

Step 1 – Install High Density Grid of Temperature Loggers

Loggers will be placed in areas such that a variety of in-river temperature conditions are monitored—at multiple depths in deeper areas (e.g. selected special run pools), habitats of interest, large eddies, and/or suspected points of groundwater inflow for a continuous two months of monitoring during summertime flow conditions. The high density grid of temperature data loggers will be installed at the following locations shown in Table 3.

Table 3. Locations of high intensity water temperature monitoring.

Location	Reason
RM 52.5 to RM 36.6	No high density monitoring.
RM 36.5 to RM 34.5	Within Gravel Mining Reach. Area of suspected groundwater inflow. SRP 11 in study area. Riffle Q3 in Study Area. Upstream of where reduction in diurnal temperature variation first observed. Downstream of both Turlock and Modesto lakes.
RM 33.5 to RM 32	Within In-Channel Gravel Mining Reach. Area of suspected groundwater inflow. SRP 5 in study area. Diurnal temperature range low in this area; normalizes downstream of this study site. Hickman spill is located in this study area.
RM 24 to RM 23	Within Upper Sand Bedded Reach. Located in area of suspected groundwater inflow. Diurnal temperature variation reduced.
RM 10 to RM 9	Within Lower Sand Bedded Reach. Area of suspected groundwater inflow.

RM = River Mile
SRP = Special Run Pool

The density of temperature loggers shall be one per quarter mile unless an SRP spans a greater distance than one-quarter mile in which case the loggers will be located above and below the SRP. Loggers shall be placed on both sides of the river and in the thalweg. The loggers shall be operational from July 1 to September 30 and record temperatures at one hour intervals.

The stream water temperature recorders in the active flow channel will have 12-bit resolution with a minimum accuracy of +/- 0.2° C (i.e., Onset or equivalent). Each stream recorder will be contained in a durable protective housing that permits the active flow of water in and around the unit. Each stream recorder will be secured by a cable to a stable root mass, tree trunk or man-made structure, or secured using embedded rebar where necessary such that the recorder will be secured in the channel during high flow periods. The stream recorders will be installed in the location of interest, and the housing and cable will be disguised as much as possible while ensuring the ability to retrieve the unit for future downloads. A GPS coordinate will be taken and recorded at each installation point, along with any waypoints that may prove valuable for future retrieval, especially where there is not a defined trail leading to the access point. Photographs of the recorder site, including installation configuration, will be taken. Recorders will be downloaded at least monthly.

Prior to installation, each recorder will be numbered and calibrated to manufacturer's recommended specifications. During each visit, data will be downloaded into an optic shuttle or directly to a personal computer. Immediately after the data are safely downloaded, back-ups will be recorded on compact disc (CD) or other suitable medium. Only after the raw water temperature data are safely backed-up will the optic shuttle be cleared or the data analyzed.

Prior to each download of data, a National Institute of Standards and Technology (NIST) traceable digital thermometer will be used to determine the water temperature at the recorder. The water temperature reading from the NIST-traceable thermometer will be compared to the last logger reading to check for accuracy drift of the recorder.

In addition, during each site visit, any faulty recorder will be replaced or repaired. Any recorder or optic shuttle that fails to download will be returned to the manufacturer for possible data recovery.

During each visit, equipment operation/calibration will be verified, battery life checked, and instruments calibrated to manufacturer's specifications. After the recorder is removed from the water, it will be cleaned and visually inspected. A record of all recorder installations and data downloads will be maintained for a comparison between the NIST-traceable thermometer and recorder water temperature readings, as will a record of any problems encountered in the field.

Step 2 – Collect Water Temperature Profiles in SRP 11 and SRP 5

Once in early August and once in early September, temperature profiles will be collected to examine the temperature conditions occurring in SRP 11 and SRP 5 using a Hydrolab® DataSonde 5® multi-parameter water quality monitoring system (or equivalent) ($\pm 0.2^\circ \text{C}$). Generally, measurements will be taken at three (3) foot vertical increments where the change in temperature with respect to depth is small ($< 0.5^\circ \text{C}$). Where the temperature gradient is greater or where measuring an apparent zone of interflow or an underflow, one (1) foot or smaller vertical increments will be used. At each sample depth, the temperature readings will be allowed to stabilize before water temperature will be recorded on the data sheet. The profile location in each SRP will be taken at what is believed to be the deepest point of the pool, using existing bathymetry data and a hand held depth sounder. A GPS receiver will be used during each successive sampling occasion to locate the geographical coordinates of each sample site. Care will be taken to identify the same site for successive profiles where water conditions and GPS accuracy allow.

Step 3 – Data Quality Assurance and Processing

In addition to the field quality assurance procedures, following data collection the Districts will subject all data to a quality assurance/quality control (QA/QC) procedures including, but not limited to (1) checking field data sheets (*e.g.*, comparison of NIST-traceable thermometers and recorder readings) to determine if corrections are needed, (2) spot-checking data, and (3) reviewing recorder readings and electronic data for completeness. The datasets will also be reviewed graphically to check for errors. If any datum seems inconsistent during the QA/QC procedure, the problem will be further investigated. Values that are determined to be anomalous will be removed from the database if the reason for the reading cannot be identified. All such deleted anomalous data will be reported as well as the justification for deletion.

If data are unavailable for brief periods of the record (*i.e.* less than 6 consecutive hours), the missing data will be synthesized into the record using a straight line interpolation method, and the data will be indicated as “synthesized” in the record and all subsequent summaries. Data gaps greater than six consecutive hours will not be synthesized and will appear in the data set and related graphs as a gap.

The raw data files will be retained in their unaltered state for future QA/QC reference. Any data modified in the final record will be so indicated in the record.

Step 4 – Prepare report

A report will be prepared that includes the following: (1) Study Goals; (2) Study Methods; (3) Results; (4) Conclusions; and (5) Description of Variances from the study plan, if any. A

narrative description of each site will be prepared and logger site photos and field notes be provided as appendices to the report. The report and temperature data, both usable and deemed unusable, will be provided to relicensing participants upon completion.

6.0 Schedule

The Districts anticipate the schedule to complete the study as follows:

Install temperature logger grids and monitor (Step 1).....	June -September 2013
Collect SRP temperature profiles (Step 2).....	August-September 2013
Data Quality Assurance and Processing (Step 3)	June-November 2013
Prepare Report (Step 4).....	December 2013

7.0 Consistency of Methodology with Generally Accepted Scientific Practices

The field methods presented in this study plan incorporate those used in recent relicensings in California.

8.0 Deliverables

Products from this study will be the above mentioned report.

9.0 Level of Effort and Cost

The estimated cost to complete this study is \$50,000.

10.0 References

- Turlock Irrigation District and Modesto Irrigation District (TID/MID). 2013a. Lower Tuolumne Temperature Model. Progress Report for Study W&AR-16. Don Pedro Project. FERC No. 2299. Prepared by HDR. January.
- _____. 2013b. Accretion Flow Measurements for June 2012, October 2012, and February 2013. Attachment 5 to W&AR-02 Hydrology Workshop 2. Filed with FERC on March 19.
- _____. 2013c. Reservoir Temperature Model. Progress Report for Study W&AR-03. Don Pedro Project. FERC No. 2299. Prepared by HDR. January.
- _____. 2013d. Spawning Gravel in the Lower Tuolumne River. Progress Report for Study W&AR-04. Don Pedro Project. FERC No. 2299. Prepared by Stillwater Sciences. January.

Doody, Andrew

From: Staples, Rose
Sent: Wednesday, June 26, 2013 10:11 AM
To: Alves, Jim; Amerine, Bill; Asay, Lynette; Barnes, James; Barnes, Peter; Barrera, Linda; Blake, Martin; Bond, Jack; Borovansky, Jenna; Boucher, Allison; Bowes, Stephen; Bowman, Art; Brenneman, Beth; Buckley, John; Buckley, Mark; Burke, Steve; Burt, Charles; Byrd, Tim; Cadagan, Jerry; Carlin, Michael; Charles, Cindy; Colvin, Tim; Costa, Jan; Cowan, Jeffrey; Cox, Stanley Rob; Cranston, Peggy; Cremeen, Rebecca; Damin Nicole; Day, Kevin; Day, P; Denean; Derwin, Maryann Moise; Devine, John; Donaldson, Milford Wayne; Dowd, Maggie; Drake, Emerson; Drekmeier, Peter; Edmondson, Steve; Eicher, James; Fargo, James; Ferranti, Annee; Ferrari, Chandra; Findley, Timothy; Fleming, Mike; Fuller, Reba; Furman, Donn W; Ganteinbein, Julie; Giglio, Deborah; Gorman, Elaine; Grader, Zeke; Gutierrez, Monica; Hackmack, Robert; Hastreiter, James; Hatch, Jenny; Hayat, Zahra; Hayden, Ann; Hellam, Anita; Heyne, Tim; Holley, Thomas; Holm, Lisa; Horn, Jeff; Horn, Timi; Hudelson, Bill; Hughes, Noah; Hughes, Robert; Hume, Noah; Jackson, Zac; Jauregui, Julia; Jennings, William; Jensen, Art; Jensen, Laura; Johannis, Mary; Johnson, Brian; Jones, Christy; Jsansley, Justin; Keating, Janice; Kempton, Kathryn; Kinney, Teresa; Koepele, Patrick; Kordella, Lesley; Le, Bao; Levin, Ellen; Linkard, David; Loy, Carin; Lwenya, Roselynn; Lyons, Bill; Madden, Dan; Manji, Annie; Marko, Paul; Marshall, Mike; Martin, Michael; Martin, Ramon; Mathiesen, Lloyd; McDaniel, Dan; McDevitt, Ray; McDonnell, Marty; Mein Janis; Mills, John; Morningstar Pope, Rhonda; Motola, Mary; Murphey, Gretchen; Murray, Shana; O'Brien, Jennifer; Orvis, Tom; Ott, Bob; Ott, Chris; Paul, Duane; Pavich, Steve; Pool, Richard; Porter, Ruth; Powell, Melissa; Puccini, Stephen; Raeder, Jessie; Ramirez, Tim; Rea, Maria; Reed, Rhonda; Richardson, Daniel; Richardson, Kevin; Ridenour, Jim; Riggs T; Robbins, Royal; Romano, David O; Roos-Collins, Richard; Rosekrans, Spreck; Roseman, Jesse; Rothert, Steve; Sandkulla, Nicole; Saunders, Jenan; Schutte, Allison; Sears, William; Shakal, Sarah; Shipley, Robert; Shumway, Vern; Shutes, Chris; Sill, Todd; Slay, Ron; Smith, Jim; Staples, Rose; Stapley, Garth; Steindorf, Dave; Steiner, Dan; Stender, John; Stone, Vicki; Stork, Ron; Stratton, Susan; Taylor, Mary Jane; Terpstra, Thomas; TeVelde, George; Thompson, Larry; Tmberliner; Ulibarri, Nicola; Ulm, Richard; Vasquez, Sandy; Verkuil, Colette; Vierra, Chris; Wantuck, Richard; Welch, Steve; Wenger, Jack; Wesselman, Eric; Wetzell, Jeff; Wheeler, Dan; Wheeler, Dave; Wheeler, Douglas; White, David K; Wilcox, Scott; Williamson, Harry; Willy, Allison; Wilson, Bryan; Winchell, Frank; Wooster, John; Workman, Michelle; Yoshiyama, Ron; Zipser, Wayne

Subject: Don Pedro Draft Notes for Review - June 4, 2013 Reservoir-River Model Workshop and Training

Attachments: 2013-01 Ops Model_AttA to AppB_Lower T Accretion.pdf; 2013-0625 Tuolumne River Geometry Data Sources.pdf; 2013-0604 Temp Model June 4 Wkshp Draft Notes_130625.pdf

Please find attached the draft notes from the June 4, 2013 Don Pedro Reservoir and Lower Tuolumne River Model Workshop and Training, for your review and comment. In addition to the draft notes, we are also providing two other documents for comment: (1) The Operations Model Lower Tuolumne River Accretion (La Grange to Modesto) Estimated Daily Flows (1970-2010), a document which was previously provided as part of the January 2013 Initial Study Report, and (2) a detailed write-up of the geometry data sources used for the lower Tuolumne River temperature model.

These draft notes, and the accompanying documents, are also being uploaded to the Don Pedro website (www.donpedro-relicensing) under the June 4 CALENDAR date and under Announcements.

Please forward your comments to me (rose.staples@hdrinc.com) by Friday, July 26.

If you have any difficulties in accessing / downloading these documents, please let me know. Thank you.

**Don Pedro Project Relicensing
Don Pedro Reservoir & Lower Tuolumne River Model Workshop & Training Session
(W&AR-03 and W&AR-16)**

DRAFT Meeting Notes

June 4, 2013

HDR Offices in Sacramento

Attendees

Scott Lowe, HDR and Manhattan College
Tom Holly, NOAA
Peter Barnes, SWRQB
Amber Villalobos, SWRCB
Ramon Martin, USFWS
Jenna Borovansky, HDR
Bill Johnston, MID

John Devine, HDR
Zachary Jackson, USFWS
Bob Hughes, CDFW
Annie Manji, CDFW
John Wooster, NOAA
Ellen Levin, CCSF/SFPUC
Carin Loy, HDR

On June 4, 2013, the Districts hosted a meeting at HDR's offices in Sacramento, California, to present to and discuss with Relicensing Participants (RPs) the MIKE3 reservoir model and HECRAS river hydraulic/temperature model developed for the Don Pedro relicensing studies W&AR-3 Reservoir Temperature Model and W&AR-16 Lower Tuolumne Temperature Model. Scott Lowe of HDR conducted the presentation in which the following topics were covered:

- Review of agenda
- Reservoir model credential sign-up for use of the MIKE3 model
- Temperature model studies schedule update and relicensing update
- Model calibration and validation
- Logistics of running each model

Because model calibration and validation had not been complete in January 2013 when the Initial Study Report (ISR) was published, model calibration and validation were presented at this meeting.

Meeting Materials

Meeting materials are:

- (1) Draft reports for both the reservoir and river models (distributed to the RPs prior to the Workshop on the Don Pedro website www.donpedro-relicensing.com and also available, on disc, at the workshop).
- (2) Agenda (provided both on the website and at the meeting).
- (3) Disc containing all model input data identified as "available upon request" in the model reports.
- (4) Thumb drive containing the HECRAS river model.
- (5) Credentials to access the Districts' reservoir model (there was a demonstration at the meeting on using the website link to access the model). Instructions on how to receive credentials are also provided on the Don Pedro website. Credentials are necessary because, due to its size, the reservoir model is run remotely by credentialed users on an HDR server.

Action Items

Three action items were identified during the meeting:

- Dr. Lowe will provide Workshop attendees the calibration and validation working running files with excel files. These files are located with the MIKE3 model, which is accessible via the Don Pedro website http://www.donpedro-relicensing.com/water_model.aspx.
- The Districts will reissue the accretion flow memo that is part of the operations model's documentation. It details how accretion flows between the Modesto and La Grange gages are accounted for in the operations model. These same flows are included in the temperature model. This description is attached.
- The Districts will distribute a detailed description of the river geometry data sources used in the lower Tuolumne river temperature model. This description is attached.

Meeting Summary

The lower Tuolumne temperature model was discussed in the morning and the reservoir temperature model was discussed in the afternoon. Discussing the models in this order allowed HDR to more efficiently sign up RPs for reservoir model credentials.

Lower Tuolumne Temperature Model

The ISR Report distributed in January 2013 included a discussion of the extent of calibration conducted by the Districts using the SJR5Q model platform. CDFW was still performing its quality assurance/quality control (QA/QC) review for its last 6 months of 2012 temperature data, so these data were not yet available. In addition, as detailed in the ISR, the Districts had by that time migrated to the HECRAS model platform. The model report distributed in May 2013 includes both the calibration and validation of the HECRAS model.

Dr. Lowe discussed the boundary conditions, calibration, validation, and long term data sets used for the lower Tuolumne River model

- Write-ups describing each data dataset are provided as attachments to the Reservoir Temperature Model and all of the data are available upon request.
- Since river geometry can have a significant influence on temperatures predicted by the model, the lower Tuolumne River transect data were discussed. A more detailed write-up of the lower Tuolumne dataset is attached.
- The Districts pointed out that the "Base Case" is defined in the Operations Model. A description of the Base Case was part of the meeting materials distributed to the RPs in support of the May 30 Operations Modeling Consultation Workshop No. 5. The Ops Model base case is also run through the reservoir and river temperature models.

Dr. Lowe presented figures that compared calibration and validation model results. These figures showed:

- The recorded temperatures of the calibration (2011) and validation (2012) years were very different.
- The model predicts the observed daily maximum temperatures well but, during the calibration year of 2011, the diurnal variation is not predicted well at all temperature stations with the minimum daily temperatures not being well predicted where these variations are observed.

- Historical data also exhibits less variation than the model predicts at some locations and times of the year.
- The Districts have developed a study plan to study the range of diurnal temperature variations in two reaches of the upper sections of the lower Tuolumne in 2013. It is attached to the draft river model report distributed for this meeting. The Districts have asked for RP comments.

Following the review of the model's calibration and validation, Dr. Lowe provided hands-on HECRAS training to RPs. Key points included:

- Run "hydraulics" first and then run "water quality", i.e. temperature
- Specifically run "unsteady flow" then "water quality"
- There are two main ways to look at temperature results – spatial and temporal: spatial is the whole river at a point in time (time can be advanced, reversed or animated); temporal gives time series of data at a point on the river – these are how the calibration/validation plots were made
- All data is accessed via "edit" screen

A discussion of Base Case took place in the morning. Base Case consists of a depiction of recent Don Pedro and CCSF operations applied over the model hydrologic period. The draft and/or final license applications will include the results of scenarios that are modeled for water temperatures. These scenarios will assess potential future operations different than the Base Case. The "Base Case" is developed within the Operations Model.

- Peter Barnes, SWRCB asked that the draft license application include a discussion of the FERC Base Case and SWRCB's baseline and how they may differ between CEQA and NEPA. The Districts agreed.
- John Wooster, NOAA, asked if the 2005-2009 Base Case matches up with current operations. John Devine answered that the model is not intended to replicate exact historical water use. The model relies on repeatable equations and algorithms. Irrigation patterns are different every month and every year based on real time weather and hydrologic conditions. In addition, CCSF has been implementing construction projects on their system, so the very recent past would not be appropriate for modeling purposes. CSSF has funded construction for several facets of the Water System Improvement Program (WSIP) yet to be implemented, but will be implemented by 2014, and are therefore included in the Base Case.
- John Wooster, NOAA, asked if the Districts would be reissuing temperature validation reports, after the operations model is final. John Devine answered no, calibration was performed on 2011 data and validation was performed using 2012 data. No operational assumptions were made for calibration or validation.

The Districts note that the Base Case description was part of the meeting materials distributed to the RPs in support of the May 30, 2013 Operations Modeling Consultation Workshop No. 5.

Reservoir Temperature Model

The ISR Report distributed in January 2013 included calibration of MIKE3 model but not the validation. CDFW was still performing its QA/QC review for its last 6 months of 2012 data, and they were not yet available. The model report distributed in May 2013 includes both the calibration and validation of MIKE3 model.

Dr. Lowe discussed the boundary, calibration, validation, and long term data sets used for the reservoir model. The same datasets were used for the lower Tuolumne temperature model, which is discussed above. Base Case was also mentioned; it, too, had been discussed in the morning session.

Dr. Lowe presented figures that compared calibration and validation model results. These figures showed:

- Calibration year and validation year reservoir thermal behaviors were similar
- The reservoir model reproduces the temperature structure in the reservoir quite well
- To reproduce the rate at which the reservoir destratifies the model uses different winter (Nov-Feb) heat constants

Following the review of the model's calibration and validation, Dr. Lowe initiated hands-on MIKE3 training for RPs. Credentials were distributed, but as users accessed the server, the system froze. Hence, a demonstration of the MIKE3 model was performed, which closely followed the report, which can also serve as a user's manual.

Eventually users were able to access the server and the MIKE3 model, although the number of users trying to access the system at the same time caused problems. As the number of active users of the system decreased, some users could run the model successfully. The lessons learned from the training were that (a) the bandwidth of the HDR Guest network (the HDR onsite network access) is limited and cannot support a lot of simultaneous users at the HDR office and data transfer (b) user computers' firewalls when logged into the HDR Guest network may present problems, and (c) the number of active users on the MIKE3 model at any one time will be limited to three to four, but it is unlikely that this will be a problem. More hands-on use of the model was deferred until the next day in the Integrated Model Training meeting. HDR, on behalf of the Districts, committed to troubleshooting RP access to the models.

**Lower Tuolumne River Accretion (La Grange to Modesto)
Estimated daily flows (1970-2010) for the Operations Model
Don Pedro Project Relicensing**

1.0 Objective

Using available data, develop a daily time series representing the total accretion and/or depletion flows between La Grange Dam and the Modesto gage on the Tuolumne River. These data will serve as input into the relicensing operations model. Accretion or depletion in this context is defined as the full inflow or outflow, respectively, contributed by or to the local drainage basin, incorporating both groundwater/baseflow and surface runoff considerations.

2.0 Existing Information

As shown in Table 1, there are three permanent flow gages currently installed in the lower Tuolumne River: (1) the Modesto gage, operated by the USGS (USGS 11290000); (2) the gage below La Grange Dam, operated by Turlock Irrigation District and calibrated to USGS standards (USGS 11289650); and (3) the Dry Creek at the Tuolumne River gage, operated by the California Department of Water Resources (DWR; Gage Code DCM on the California Data Exchange Center) on Dry Creek.

Table 1. Historical flow data for the lower Tuolumne River.

River Mile	Location	Gage Identifier	Period of Analysis	Data Quality	Notes
TUOLUMNE RIVER					
51.5	Tuolumne River at La Grange	USGS: 11289650	October 1 1970 – September 30 2010	Records are “good” with expected accuracy to about 5%. ²	La Grange gage is located 0.5 miles downstream of La Grange Dam.
16.2	Tuolumne River at Modesto	USGS: 11290000	October 1 1970 – September 30 2010	Records are “fair”, except for estimated daily discharges which are “poor”. About 3% of the daily values since 1970 are estimated. ²	The flood control flow objective for the lower Tuolumne River is 9,000 cubic feet per second (cfs) at the Modesto Gage (RM 16.2). As Dry Creek confluences with the lower Tuolumne River just upstream of the Modesto gage, inflows from Dry Creek are accounted for the this management objective.
DRY CREEK					
--	Dry Creek at Tuolumne River Confluence	DWR: B04130/CDEC: DCM	October 1 1970 – September 30 2010	Qualifiers are provided: Good data, Estimated Data or Missing Data. About 1.2% of the daily values are estimated or missing.	Dry Creek is a tributary to the Tuolumne River at RM 16.2. Dry Creek operations changed substantially in 1987. Prior to 1987, substantially greater flows were diverted at LaGrange into the Modesto Canal in fall (October-December) months, with a portion being returned back to the Tuolumne River through Dry Creek.

USGS = US Geological Survey

DWR = Department of Water Resources

² USGS defines fair as having accuracy to approximately 8%, and poor as greater than 8% (Turnipseed, 2010). Typically natural bottomed streamflow measurements are considered “good” if accurate to about 5% (Turnipseed, 2010).

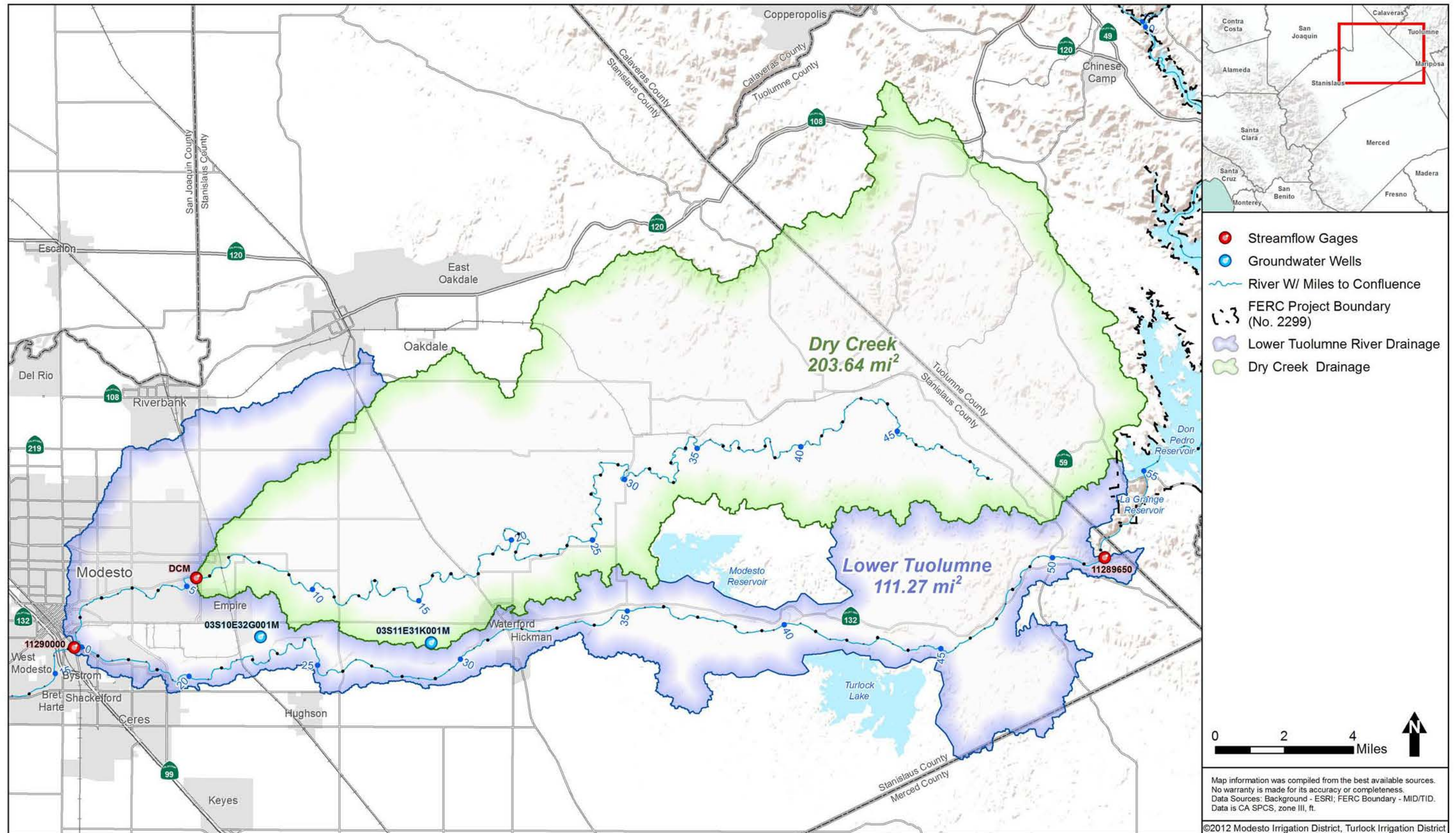


Figure 1. Map of lower Tuolumne drainage, Dry Creek drainage, and gages.

Using data collected at the three gages, accretion was calculated for the lower Tuolumne through the following equation:

$$\text{Accretion flow (cfs)} = \text{Flow at the Modesto gage (cfs)} - \text{Flow at La Grange gage (cfs)} - \text{Flow at Dry Creek gage (cfs)}$$

Average daily accretions in the Lower Tuolumne range from 40 cfs to 200 cfs, with an annual average accretion of 218 cfs from water year 1970-1987 and 103 cfs from water year 1988-2010, resulting in a water year 1970-2010 average of 152 cfs (calculated daily accretion data are provided in Attachment B). Deviations from the average are highest in the winter months; as the flows increase, so does the uncertainty in the gage rating. The largest difference in flow observed was during the January 1997 storm; it has been determined that the computations are not reliable during large storm events due to the cumulative gage rating uncertainty associated with the calculation.

A review of the historical gage data from these three locations indicates a higher degree of variability of accretions than would be expected to naturally occur. For example, as shown in Figure 2, when calculated accretions¹ are graphed without any data smoothing or other adjustment, values are erratic and frequent negative flows are observed.

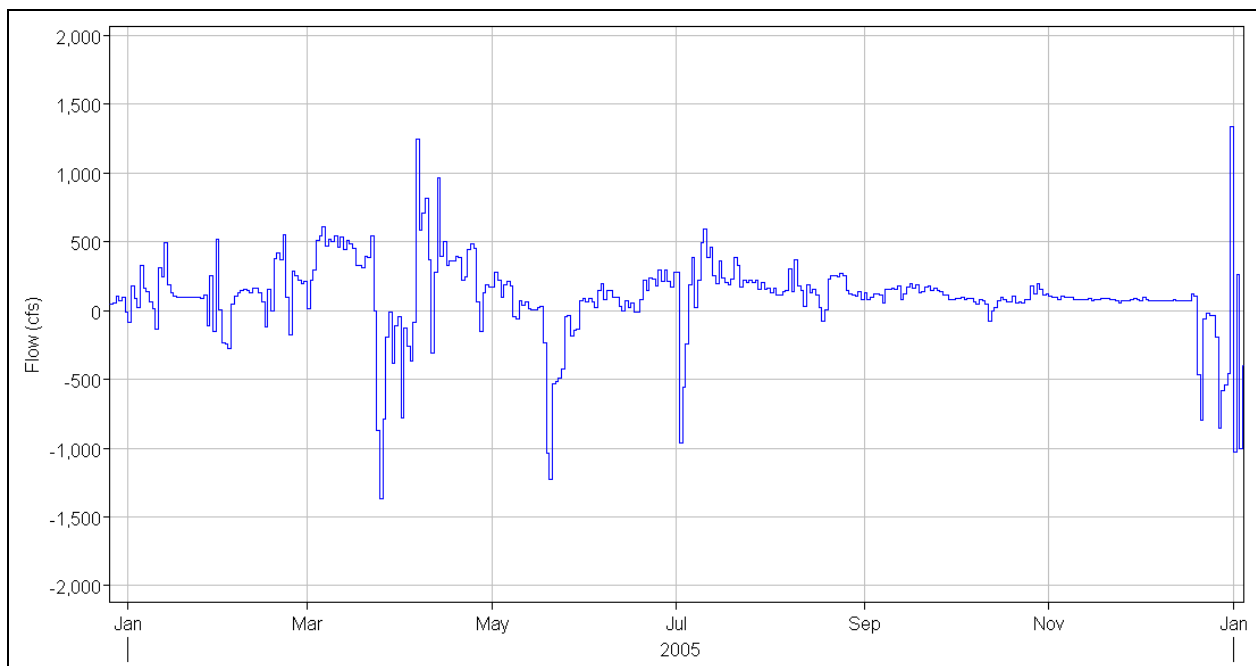


Figure 2. Sample computation of daily Lower Tuolumne accretion (flows at Modesto gage less La Grange gage and Dry Creek gage).

This variability is likely due to the relatively small magnitude of accretions compared to the actual gaged flow; relatively small errors and hydrograph timing differences and would explain much of the variability in accretions determined through a strict mathematical interpretation of

¹ It should be noted that this calculation does not allow for any travel time between locations; at the typical flow rates in the lower Tuolumne River, travel time would be expected to be on the order of hours rather than days.

USGS and DWR gage data. Additionally there may be agricultural withdrawals and return flows that are not being accounted for, as well as some interaction with the groundwater.

Inclusion of these data “as is” into the operations model will introduce variability that is distracting to the planning process, and at times invalid. A synthetic daily time series that represents the total accretion flow between La Grange Dam and the Modesto gage (including the contributions of Dry Creek) is therefore necessary to provide a reasonable estimate for modeling and planning purposes.

3.0 Methods

Due to the nature and quality of data, slightly different approaches were followed for synthesizing Dry Creek accretion and the lower Tuolumne accretion data sets. In addition, the total accretion calculations were split into two separate approaches for estimation of groundwater baseflow and surface runoff contributions. The two approaches are then aggregated to provide an estimate of total accretion.

3.1 Dry Creek

There are several locations within Dry Creek where accretion and depletion may occur. The gage on Dry Creek located about 5.6 miles upstream of the confluence with the Tuolumne River, is the best available approximation of the total flow at the mouth of Dry Creek.

Monthly synthetic baseflow values were then estimated using the average monthly flow rate in months that had less than $\frac{3}{4}$ inches of rain, representing periods with minimal expected surface runoff.

Surface runoff was estimated for Dry Creek manually using baseflow separation techniques. The entire period of record of the gage was examined graphically to determine if the flows recorded were likely to be surface runoff, baseflow, or return flow from irrigation canals. The synthetic baseflow values were then used to fill in all hydrograph values judged to be baseflow, or return flow.

Attachment A contains the synthetic flow record for Dry Creek for the period of 1970-2010, using the methods described above. Attachment B provides all the data files used to derive the synthetic flow record.

3.2 Lower Tuolumne

An estimate of total accretion for the 35.3 mile reach between the La Grange and Modesto gages was developed from the available gage data. Methods were separated into independent baseflow and surface runoff estimates, similar to the approach used to estimate Dry Creek accretion.

For the lower Tuolumne, the long-term daily median demonstrates the annual trend more clearly than the daily calculation using observed data, due to erratic swings in the daily calculation

between large values and negative values. Long-term daily median in this case is the 50% exceedance of each individual date across all years in the record (e.g. the 50% exceedance of all October 1st daily values from 1988 to 2010 is used to represent a single October 1st estimate). During periods of agricultural return flows, rainfall, or high flow, the values can be especially erratic, so the yearly median was examined for comparison to the yearly average.

The long-term daily median datasets were restricted to synthesized values from water year 1988-2010 because the pre-1987 Dry Creek flows from irrigation sources significantly impacted the gage calculation. A piece-wise linear synthetic time series was developed using visual inflection points from the yearly median, while honoring the annual volume estimate derived from the long-term daily median. This piece-wise linear estimation of the median annual accretion curve was then applied to the whole period (1970 to 2010). Figure 3 shows the annual median and resulting synthetic accretion. Attachment B contains the results of this computation.

The gage calculation was too erratic to be useful for surface runoff estimation. Therefore, a simple drainage area proration was applied to estimate surface runoff for the lower Tuolumne natural runoff accretion. This was done using the Dry Creek gage hydrographs, separated from baseflows as described in Section 3.1 above.

4.0 Results

4.1 Baseflow Calculations

Calculated daily time step accretions are provided in the accompanying Attachment B, along with supporting measured gage data.

Synthetic baseflow values² for Dry Creek are developed in Attachment B and summarized, by month, in Table 2. These values were inserted into the daily accretion series, provided in Attachment B.

Table 2. Synthetic baseflow rates for Dry Creek by month in cubic feet per second (cfs).

Jan	Feb	Mar	Apr	May	Jun	Jul	Aug	Sep	Oct	Nov	Dec
10	30	30	40	45	50	55	70	65	30	3	1

Synthetic baseflow accretion values for the lower Tuolumne reach between La Grange and Modesto gages are developed in Attachment B and summarized by month in Figure 3.

² The observed base flow in Dry Creek likely includes agricultural return flows during the typical growing season of April through October. Flows typically recede sharply in November, suggesting the elimination of seasonal return flows.

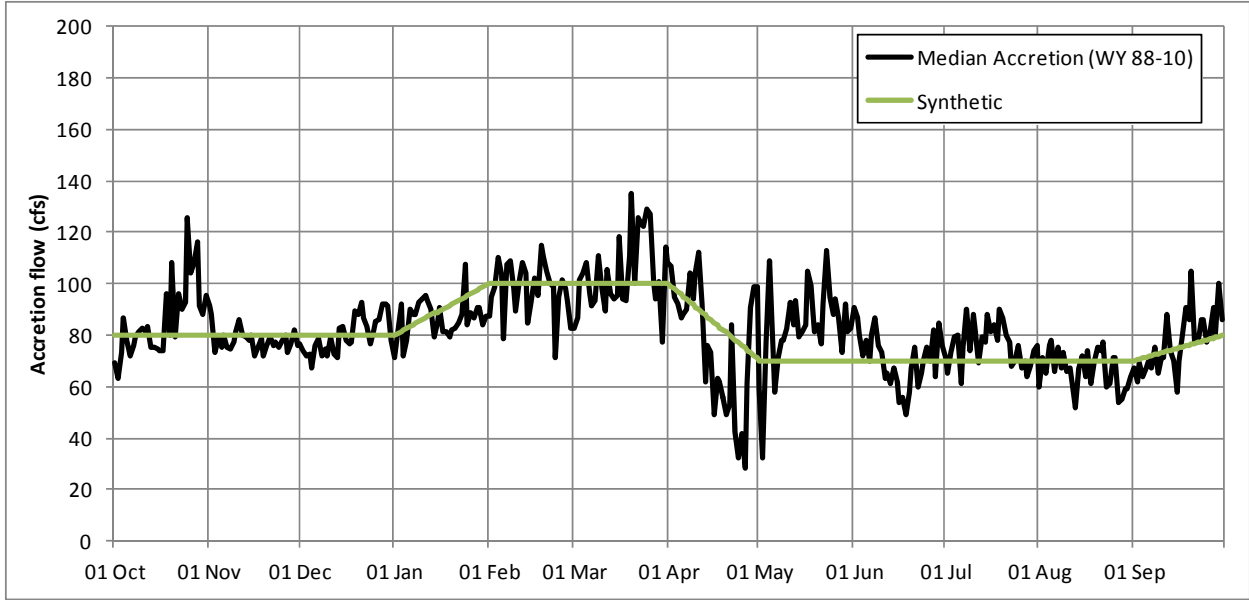


Figure 3. Synthetic accretion flow rates for lower Tuolumne in cubic feet per second (cfs).

4.2 Surface Runoff Calculations

The drainage area to the Dry Creek gage was measured to be 203.6 mi², and the accretion drainage area of the lower Tuolumne was measured to be 111.3 mi². This yields a proration factor of 0.5464, therefore all of the hydrographs separated for use in the Dry Creek synthetic time series were multiplied by 0.5464. A visual examination of the gage computation and synthetic time series for the lower Tuolumne demonstrated that erratic swings in the gage computation are coincident with runoff events in Dry Creek. An example of this phenomenon is shown in Figure 4.

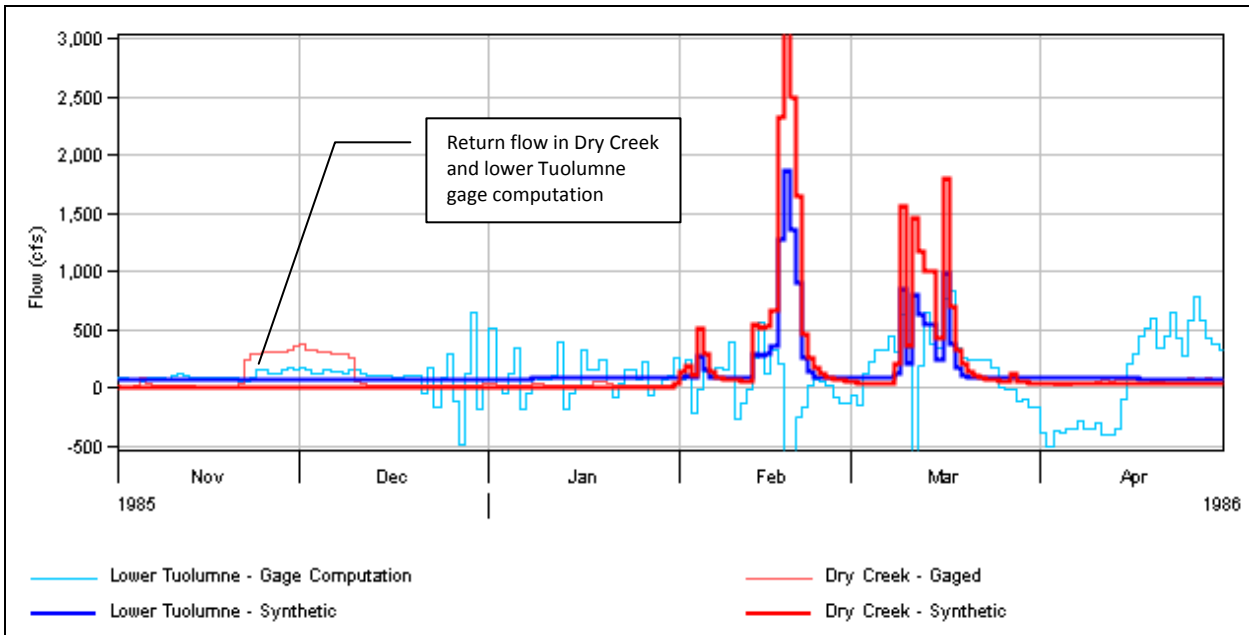


Figure 4. Sample synthetic and gaged data for lower Tuolumne accretion and Dry Creek.

5.0 Discussion

5.1 Dry Creek Accretion

From 1987 to 2011, the period for which Dry Creek operations have been relatively consistent, the volume of synthetic baseflow with observed surface runoff hydrographs is compared to the volume of the unaltered gage data in Figure 5, which indicates the synthetic baseflow values are an appropriate substitute for the gaged data.

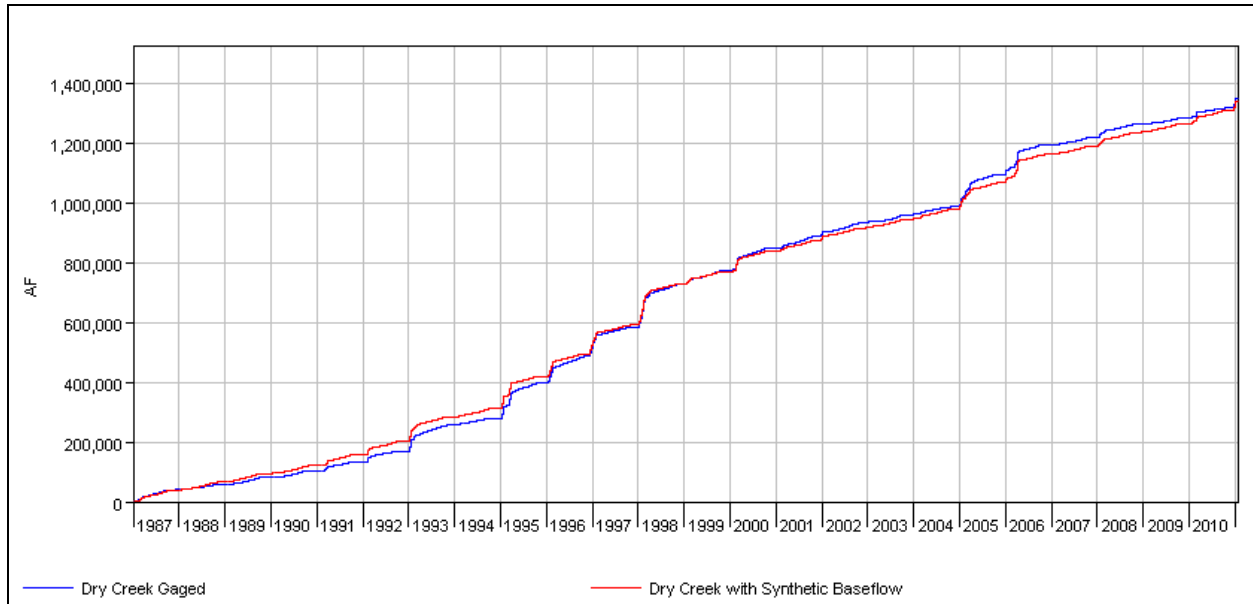


Figure 5. Dry Creek synthetic baseflow and gaged flow, cumulative volumes 1987-2010.

This comparison provides excellent validation in both the annual and long-term volumetric approach to accretion estimates in Dry Creek.

5.2 Lower Tuolumne Accretion

Below, the influence of groundwater synthetic baseflow volume is examined, followed by a comparison of the synthetic accretion dataset to the unaltered gage computation.

5.2.1 Groundwater Influence

The influence of groundwater interactions with the river on computed lower Tuolumne accretions (Modesto flows, less La Grange and Dry Creek) is further examined in Figure 6. The purpose of this examination is to explore the extreme variability in the accretion computation – whether it's due to gage errors, gage re-rating (Modesto gage has been at four different locations during this time³), or interactions with the groundwater. The location of two representative groundwater wells relative to the basin can be seen in Figure 1.

³ United States Geologic Survey (USGS), 2010. *Water-Data Report 2010. 11290000 Tuolumne River at Modesto, CA.*
<<http://wdr.water.usgs.gov/wy2010/pdfs/11290000.2010.pdf>>

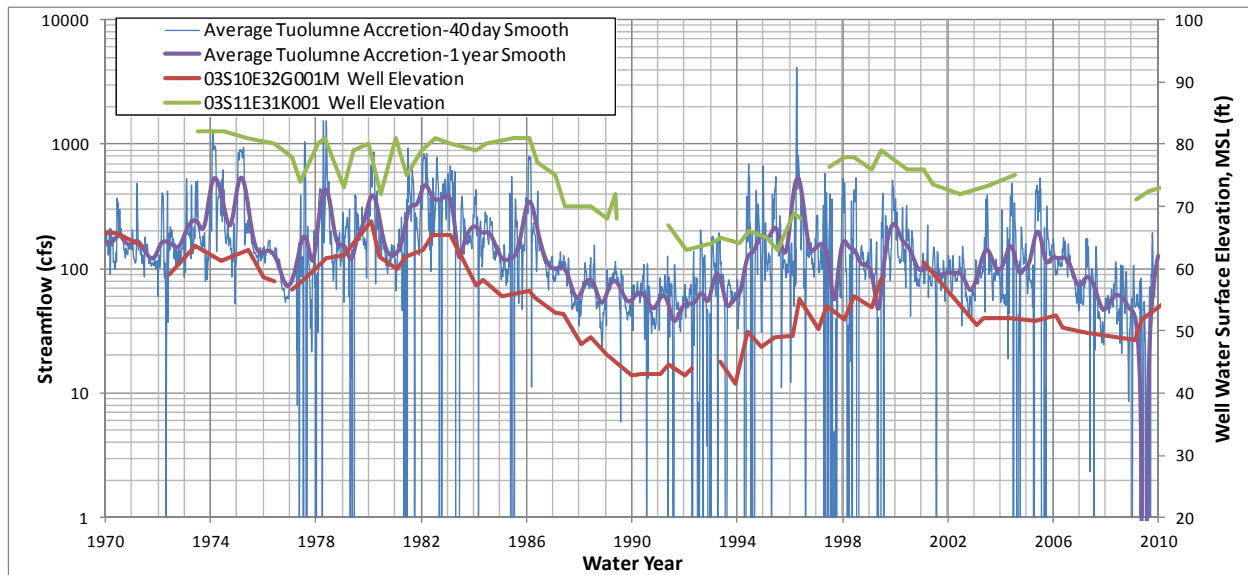


Figure 6. Relationship between lower Tuolumne accretion and groundwater wells 1970-2010.

It can be seen that baseflow and groundwater level roughly correspond to one another. Even though 1977 is the driest year in this period of record, it is a relatively short drought period, and groundwater levels do not have a chance to respond, but in the six-year drought period of 1987-1992, groundwater levels drop dramatically, and accretions respond accordingly.

Given that there is a demonstrated relationship between groundwater level and accretion, this leaves several factors that can cause the extreme variation in the daily time series.

- Gage lag-time and inaccuracy
- Local rainfall runoff
- Agricultural return flows and withdrawals
- Agricultural irrigation and M&I withdrawals from groundwater

Quantifying these factors would require many assumptions, as available information is highly uncertain and/or unavailable. It is possible that the periods of depletion in the time series are actually during groundwater pumping or they could be due to something else. Accounting for all of these factors in development of the synthetic accretion values would require many additional assumptions. Given the accuracy and precision of the input data, it could not be reported with any additional confidence.

5.2.2 Comparison to synthetic accretion

The synthetic accretion data set for the lower Tuolumne (Section 4.0) is checked against period of consistent hydrology (1987-2008) in Figure 7. In other words, Figure 7 shows the computed accretion volumes for the reach between the La Grange and Modesto gages compared to synthetic values.

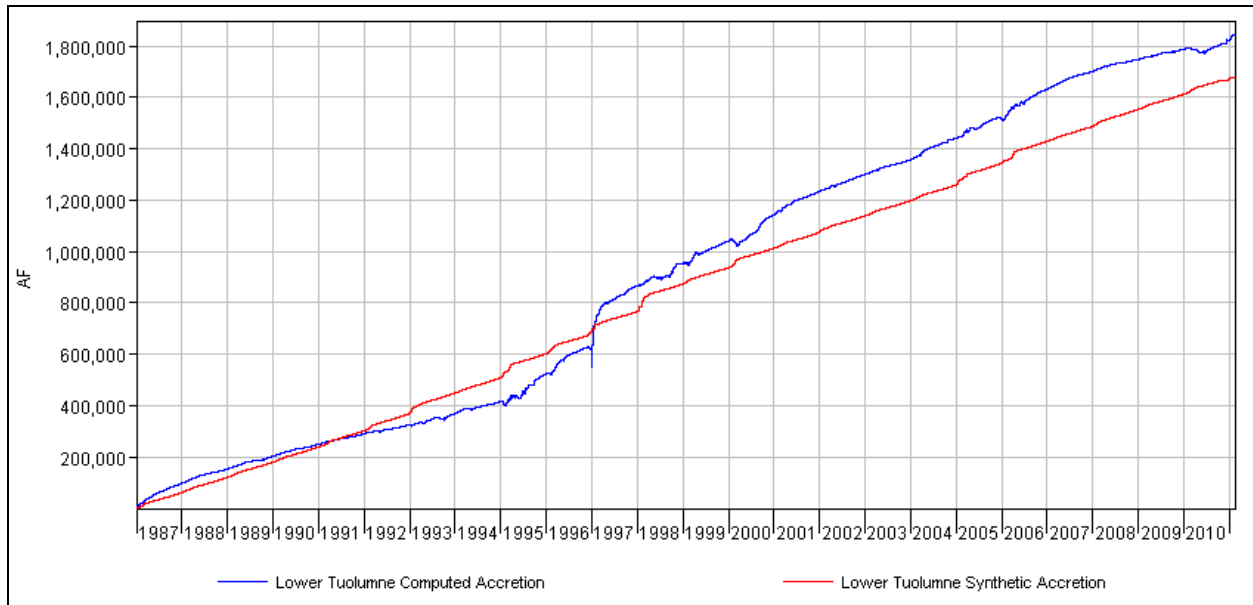


Figure 7. Lower Tuolumne River accretion, synthetic and computed, cumulative volumes (1987-2010).

A significant discontinuity can be seen following the New Years Day 1997 storm. Upon closer examination, it was found that following the 1997 flood, the gage at La Grange had to be re-rated, making its measurements during the storm unreliable. Further, the average accretion between Jan 2nd to Jan 10th 1997 from the gage calculation is about 4,000 cfs, which is just 7% of the peak flow observed at Modesto of 55,800 cfs, well within the margin or error for a three-gage calculation at high flow. If the discontinuity following the New Years Day storm is ignored, the cumulative volume of the synthetic accretion appears to match the cumulative volume of the computed accretion.

5.2.3 Comparison to Accretion Flows Measured in June 2012

On June 25, 2012, Modesto Irrigation District and Turlock Irrigation District collected flow information for the lower Tuolumne River between the La Grange Gage and the San Joaquin River confluence, as well as within Dry Creek. Table 3 presents the results of the measurement.

Table 3. Measured and gaged discharge on the Tuolumne River and Dry Creek.

Location	Measured Discharge (cfs)	Gaged Discharge (cfs)	Percent Difference (%)
Tuolumne at La Grange	114.9	130	12
Tuolumne at Modesto	208.2	219	5
Dry Creek ^a	55.5	38 ^b	46
Lower Tuolumne Accretion	55.3 ^c	-	-

^a Measured at confluence with Tuolumne River, 5.3 miles downstream of the gage.

^b Value from CDEC (DCM), not yet available on Water Data Library (B04130).

^c Using Dry Creek gaged discharge, rather than measured.

It is important to note that the Dry Creek measurement was not taken at the gage. The lower Tuolumne accretion calculation discussed herein uses values from the gage on Dry Creek, and does not attempt to subtract any accretions below the Dry Creek gage. The accretions in Dry Creek, below the gage, are therefore included in the lower Tuolumne accretion numbers. Another distinction to make is that the Dry Creek gage values are published twice, first in real time on CDEC (DCM), and later on the Water Data Library (B04130) after some quality control procedures by the California Department of Water Resources. The computations in this report used the Water Data Library values when available, and CDEC values only to fill in gaps in the record, and the values are often considerably different.

The synthetic baseflow value for Dry Creek in June is 50 cfs, which is in the range of values estimated by the measurement. The synthetic accretion for the lower Tuolumne in June (including accretion below the Dry Creek gage) is 70 cfs. In this case the synthetic accretion is more than the measured accretion (55 cfs), which could be due to lower groundwater levels in 2012. The lower amount could also be due to efforts to minimize all operational spills into the Tuolumne River during the measurement. Using the gaged measurements alone, the accretion would be estimated to be 51 cfs.

The Dry Creek gage has been deemed to provide the most reliable data for estimation for surface runoff-based accretion in the entire lower Tuolumne River drainage. Other elements of accretion estimation, such as groundwater contributions, have been estimated by honoring as much of the source data as possible in the lower Tuolumne. The resulting synthetic, aggregate hydrograph provides a reasonable estimate for both long-term and rainfall event-driven contributions to the lower Tuolumne River from the La Grange gage to the Modesto gage.

6.0 Attachments

The following attachments to this memo are available on <http://www.donpedro-relicensing.com>.

- AttachmentA.pdf
- AttachmentB.dss

Attachment A contains the final time series data for Dry Creek, lower Tuolumne (excluding Dry Creek), and total accretion from La Grange to Modesto gage.

A brief description of each of the DSS tables that comprise Attachment B is provided as Table 3.

Table 3. Attachment B Contents, final datasets indicated with bold font.

Name - /LOWER TUOLUMNE/B/C//E/F/	Contents
//DRY CREEK/FLOW//1MON/BASEFLOW/	A time series containing averaged monthly baseflow values in months with less than 0.75" of precipitation (cfs)
//DRY CREEK/FLOW//1DAY/DCM_ADJUSTED/	Gaged flow at Dry Creek DWR record B04130 , combined with CDEC DCM, for missing days (cfs)
//DRY CREEK/FLOW//1DAY/HYD_ONLY/	Dry creek gaged flow, with baseflow deleted (cfs)
//DRY CREEK/FLOW//1DAY/SYNTHETIC/	Synthetic time series using BASEFLOW_EST in all places that HYD_ONLY is missing data (cfs)
//DRY CREEK 87/ACCUM//1DAY/DCM_ADJUSTED/	1987-2010 cumulative volume for gaged dry creek flow (acre-ft)
//DRY CREEK 87/ACCUM//1DAY/SYNTHETIC/	1987-2010 cumulative volume for SYNTHETIC dry creek

Name - /LOWER TUOLUMNE/B/C//E/F/	Contents
	dataset (acre-ft)
//TUOLUMNE ACCRETION/FLOW//1DAY/COMPUTED/	Time series of computation: Modesto [11290000] minus La Grange [11289650] and Dry Creek [DCM_ADJUSTED] (cfs)
//TUOLUMNE ACCRETION/FLOW//1DAY/BASEFLOW/	Generalized median of COMPUTED values from 1988 to 2010 (cfs)
//TUOLUMNE ACCRETION/FLOW//1DAY/HYD_ONLY/	//DRY CREEK///HYD_ONLY/ times the drainage area proration of 0.5464 (cfs)
//TUOLUMNE ACCRETION/FLOW//1DAY/SYNTHETIC/	Synthetic time series using greater of HYD_ONLY and BASEFLOW (cfs)
//TUOLUMNE ACCRETION 87/ACCUM//1DAY/COMPUTED/	1987-2010 cumulative volume of COMPUTED daily accretion (acre-ft)
//TUOLUMNE ACCRETION 87/ACCUM//1DAY/SYNTHETIC/	1987-2010 cumulative volume of SYNTHETIC daily accretion (acre-ft)

7.0 References

Durbin, T.J., 2003, *Turlock Groundwater Basin Water Budget 1952-2002*. Turlock Groundwater Basin Association. <ftp://ftp.water.ca.gov/uwmp/completed-plans/Ceres/2.pdf>

TID/MID 2012. Study W&AR 2 Operations Model Action Item from April 9, 2012, Hydrology Workshop Proposed Lower Tuolumne Flow Accretion and Depletion Measurement Locations. Memo to Relicensing Participants. June 6.

Turnipseed, D.P., and Sauer, V.B., 2010, *Discharge measurements at gaging stations*: U.S. Geological Survey Techniques and Methods book 3, chap. A8, 87 p.
<<http://pubs.usgs.gov/tm/tm3-a8/>>

Tuolumne River Geometry Data Sources

The table below lists the geometry data sources used for the Don Pedro Relicensing’s Lower Tuolumne River Temperature Model (Table 1).

Table 1. Lower Tuolumne River geometry data sources.

RM	Source	Original reason for collection
0-12	USACE 2001	Flood plain survey performed in 1999. ACOE transects were 100 ft apart. Transect elevations used for model were 0.5 miles apart.
14-31.5	HDR (2012)	Field survey in December 2012 at approximately 235 cfs in support of HEC-RAS temperature model; transects collected every 0.5 mile
RM 33.6 to 39.9	HDR (2003-2006)	Developed from the Ruddy Segment (RS 177300-21074) data developed by HDR for the Tuolumne River restoration program HEC-RAS model. Survey files included stitched TIN surfaces originating from Lidar and ground truthed bathymetric soundings from a licensed surveyor. More than 100 transects were measured, anywhere from 50 to 100 feet apart. (AD Consultants et al 2009). Transect elevations created for model at 0.5 mile intervals.
40-45.5	Extrapolated	Extrapolated from upstream and downstream transects, as well bank LiDAR (flown at about 300 cfs in March 2012). Transects pulled from model 0.5 miles apart.
45.5-51.5	TID/MID 2013e. W&AR-4, Spawning Gravel in the Lower Tuolumne River.	ADCP performed at 2000 cfs in 2013. A combination of LiDAR and overbank surveys. Transects pulled from model 0.5 miles apart.
52.3-54.3	Meridian Surveying Engineering (2012)	Hydrographic Survey for TID. Transects pulled from model 0.5 miles apart.

ADCP = Acoustic Doppler Current Profiler
 cfs = cubic feet per second
 ACOE = Corps of Engineers
 ft = feet
 LiDAR = Light Detection and Ranging
 MID = Modesto Irrigation District
 RM = River Mile
 SJRB = San Joaquin River Basin
 TID = Turlock Irrigation District

Based on the bathymetric data from sources summarized in Table 1, cross sections were generated approximately every 0.5 miles along the river using GIS. In HECRAS further cross section are created by interpolating between these 0.5 mile sections. The calibrated model uses 1/6 mile cross section intervals below La Grange dam as shown in Figure 1.

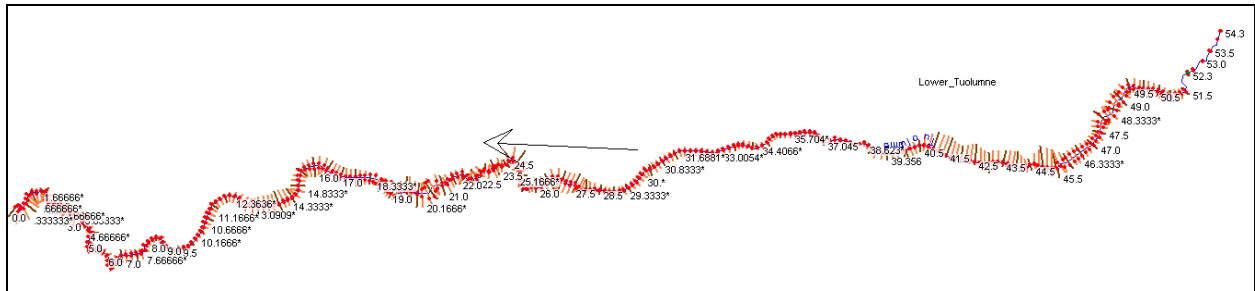


Figure 1. HEC-RAS schematic of Tuolumne River below Don Pedro to San Joaquin confluence.

Over the years, river geometry has been measured several times; however, not all data sources were used to develop the HECRAS model. Only the most up-to-date data were used for the lower Tuolumne River temperature model. Below, a brief description of each geometry data source used, by river mile, is described, followed by descriptions of two sources that were not used.

RM 0 to RM12

Geometry data for this reach was excerpted from a flood plain survey performed in 1999. US Army Corps of Engineers (ACOE) transects were 100 feet (ft) apart. Transect elevations used for model were 0.5 miles apart (USACE 2001)

RM 14 to 31.5

In December 2012, HDR collected transects approximate every 0.5 mile in this reach. Flows were approximately 170 cubic feet per second (cfs), as measured at La Grange. Measurements were collected using two methods. The first method used a GPS and an echo sounder to record position and depth into a computer. Position was recorded using a Trimble GeoXH 6000 series Centimeter Edition GPS unit with Zephyr2 antennae using a real-time kinematic (RTK) realtime correction from Virtual Reference Station (VRS) network. Depths were collected using an Echotrac CVM single beam echosounder. Location and depth information were then combined and recorded using Hypack bathymetry software to an estimated accuracy of 4-10 centimeters (cm). The second method involved the manual survey of points along a transect perpendicular to the flow using an auto-level and stadia rod. Under this second method, the two person team recorded measurements in the field notebook. Temporary benchmarks were established and recorded using the same Trimble system used in the first method.

RM 33.6 to 39.9

These data were derived from the Tuolumne River Restoration Program 1999 - 2006 (HDR 2003-2006). HDR measured channel geometry for the Ruddy Segment restoration project. The survey files included stitched TIN surfaces originating from Lidar and ground truthed bathymetric soundings from a licensed surveyor. Lidar Data were collected by Aerial Photomapping Services of Clovis, California on March 19, 1998. Instream Bathymetry Data were collected by Kjeldsen, Sinnock, and Neudeck Inc. of Stockton California between 2003 and 2006. The resultant HECRAS modeling and channel geometry outputs (i.e. CAD related survey files, digital terrain models (DTM), TINs, and contours) were used for the HECRAS model development.

RM 40-45.5

The geometry in this reach was extrapolated from upstream and downstream transects within ARC GIS, as well bank LiDAR (flown at about 300 cfs in March 2012). Transects pulled from model 0.5 miles apart.

RM 45.5-51.5

The 2012 Digital Terrain Model (DTM) was developed using updated LiDAR, bathymetric, and terrestrial topographic data collected from RM 52.1 to RM 45.5. All survey data is reported in California State Plane Coordinate System, Zone III, NAD 1983 (epoch 2002.00) horizontal datum. Hybrid geoid model GEOID09 was used to convert NAD83 ellipsoidal heights to the NAVD88 vertical datum. Updated LiDAR data was acquired on March 30, 2012 at a discharge of approximately 320 cfs at [USGS #11289650](#). Post-processed LiDAR data provided by the contractor as class 8 model key points (a subset

of bare earth ground points) was used to represent topography at the desired scale and resolution. The LiDAR accuracy assessment reports that a root mean square of 0.15 feet was achieved when comparing elevations from the LiDAR bare-earth DTM to surveyed ground control points.

Bathymetry and terrestrial topographic surveys to characterize channel bed elevations in areas below water during LiDAR data acquisition were conducted during two separate field efforts in 2012. Bathymetric surveys were conducted 8–12 May, 2012 at flows ranging from 650 to 2,100 cfs as measured at [USGS #11289650](#). Sounding data was collected with a Teledyne RDI 1200 kHz Workhorse Rio Grande acoustic doppler current profiler (ADCP) and an Ohmex Sonarmite echosounder mounted to a 15 ft Lowe Jon boat. Position and elevation were surveyed with Trimble R8 GNSS (GPS) survey equipment operating in RTK survey mode. Positions measured by the bottom tracking function of the ADCP were used to fill position gaps that occurred when the GPS antenna was obstructed by dense overhead vegetation or bridges. The GPS rover antenna was mounted at a fixed height directly above the ADCP or echosounder transducer. The GPS rover was configured to output standard National Marine Electronics Association (NMEA 0183) format GGA (positioning), VTG (heading), and ZDA (time-stamp, clock syncing) data strings and connected to a field laptop that simultaneously processed ADCP, GPS, and echosounder data in WinRiver II (ver 2.08) software. At transects where the ADCP was not deployed for safety considerations, continuous RTK GPS survey points and echosounder readings were recorded in a Trimble TSC2 field data controller. Bathymetric surveys were also conducted between June 2–7, 2012 at flows ranging from 125 to 150 cfs to characterize channel bed elevations in areas not covered by LiDAR or the high-flow bathymetry survey. During the low flow bathymetry survey, ADCP and GPS rover equipment were mounted to a small tethered trimaran. Supplementary terrestrial and shallow water surveys were conducted with a GPS rover and a Trimble S6 robotic total station.

ADCP data was initially processed with WinRiver II (Version 2.08) software and screened for erroneous positions and depth measurements that occur due to turbulent flow or dense aquatic vegetation. The WinRiver II data was exported to ASCII format files and imported into the beta Velocity Mapping Software (VMS) for further processing. VMS allows for simultaneous review of multiple ADCP transects, as well as processing of the four individual ADCP beam depth and position solutions. The multi-beam data was imported into ESRI ArcGIS software for final editing and DTM generation. GPS rover and total station survey data was processed in Trimble Business Center software and exported to ESRI Geodatabase format. Raw GPS base station files were submitted to the NOAA NGS Online Positioning User Service (OPUS) for processing and the solutions used to adjust base station coordinates.

A 2012 DTM surface was generated in budget cell 1 from RM 51.5 to RM 45.5 by combining the processed LiDAR, bathymetry, and terrestrial survey data using ESRI ArcGIS 3D Analyst software. A Triangulated Irregular Network (TIN) was generated from the survey data as mass points. Longitudinal profile and cross-section data were extrapolated from the TIN surface. The TIN was converted to a raster with a three foot cell size for surface differencing.

RM 52.3-54.3

In 2012, Meridian Survey Engineering performed a hydrographic survey of the La Grange Reservoir according to Class 1 hydrographic survey methods and accuracies outlined in the Army Corp of Engineers' manual (EM 1110-2-1003) with a sounding precision of 0.5' and a sounding interval of 5-10 feet. The maximum interval between survey lines was less than 200 feet. Measurements were collected to the edge of the water, assisted by the following equipment (1) a 12' survey vessel; an Innerspace Model 455 single beam, dual frequency echosounder; a Trimble R8 RTK GPS, Base and Rover; a Panasonic Toughbook with Hypack Max Hydrographic Surveying Software; and a Trimble TSC2 data collector with Trimble Survey Controller software.

The horizontal control was perpetuated from an extensive geodetic survey performed by CH2MHILL in March of 1997. The horizontal component was based on the California State Plane Coordinate System, Zone 3 (0403), NAD83. The vertical control component was based on existing Turlock Irrigation District benchmarks which were established upon the National Geodetic Datum of 1929 (NGVD29). Work was performed meeting or exceeding Second-Order, Class 1 accuracies. TID staff perpetuated existing survey control for use with the bathymetric survey performed by Meridian Survey Engineering. In addition, TID staff took surface elevation shots and noted current flows on several locations along the river channel. Shots were taken where accessible.

Older Data

Two additional reports were reviewed, but their data were not used for the HECRAS model. More up-to-date data were available for the reaches studied in these reports:

Coarse Sediment Management Plan for the Lower Tuolumne River 2003

Data collected for and presented within TID/MID 2013 updated the data provided in McBain and Trush (2004). For coarse sediment augmentation design purposes, McBain and Trush (2004) surveyed the channel and bank topography, and bathymetry at four sites in February 2002, using a combination of total station, ADCP, and RTK GPS unit. These sites included Riffle A3/4 (RM 51.6), Riffle 1B/C (RM 50.3), Riffle 3A (RM 49.6), and the Zanker site (RM 45.8). These surveys were used to produce DTM of existing topography for each site at one-foot contour intervals. The DTM was then used as the basis for developing the proposed design contours and estimating coarse sediment augmentation volumes for these sites. The DTMs provide detailed topographic information, useful for monitoring short-term trends in bed aggradation and degradation. Site topography is shown in the site design drawings in Appendix B of the report.

CalFed San Joaquin River Basin model (SJR5Q)

The data compiled for the SJR5Q were not used for the HECRAS model because, in general, more recent datasets were available and/or the data were directly available through another source or contact, e.g. HDR 2003-2006.

Stream representation in the SJR5Q includes representation of system geometry and flow representations (AD Consultants et al 2009). A brief description of each of the six SJR5Q reach geometry data sources is provided below.

- Confluence (river mile (RM) 0) to RM 23.8. The geometry was based on Reach 21 and 23 in the Corps' UNET model.
- RM 23.8 to 24.3. The geometry for this short reach was achieved by interpolating between the upstream and downstream adjacent reaches.
- RM 24.3 to 26.1. The geometry for this reach is excerpted from data developed by HDR for the Tuolumne River restoration program HERAS model, some time before 2005
- RM 26.1 to 33.6. The geometry for this reach was synthesized. Cross sections were generated at 500-foot intervals by interpolating between adjacent reaches. To mimic the range of mean channel velocities observed in adjacent reaches, the bottom of approximately 2/3 of the sections were either lowered or raised to achieve a ripple and pool effect.

- RM 33.6 to 37.9. The geometry for this reach was developed from the Ruddy Segment (RS 177300-21074) data developed by HDR for the Tuolumne River restoration program, sometime before 2005
- RM 37.9 to 51.5. Geometry for this reach was developed from 142 cross sections at 500-foot intervals generated from preliminary Light Detection and Ranging (LIDAR) and bathymetry data provided by McBain & Trust, some time before 2005

References

AD Consultants, Resource Management Associates, Inc., and Watercourse Engineering, Inc. 2009. San Joaquin River Water Temperature Model and Analysis. Section 2.3.1.2. Prepared for CALFED ERP-06D-S20, October.

HDR 2003-2006. HECRAS modeling and channel geometry (i.e. mostly CAD related survey files, dtms, TINs, and contours). Transmitted from M. Garelo, HDR, to C. Loy, HDR, June 20, 2012.

McBain & Trush 2004. Coarse Sediment Management Plan for the Lower Tuolumne River. Revised Final. Section 4.2.3 Conceptual Design Sites. Arcata California. July 20.

Meridian Surveying Engineering. 2012. La Grange Bathymetric Survey 2012. Collected for Turlock Irrigation District.

TID/MID 2013. Spawning Gravel in the Lower Tuolumne River. Progress Report. Don Pedro Project Relicensing. Prepared by Stillwater Sciences. January.

USACE 2001. HEC-HMS for the Sacramento and San Joaquin Comprehensive Study. Chapter 2: Digital Elevation Model Construction. August. A background slide show is provided here: http://www.cwemf.org/workshops/SJRModel_files/frame.htm#slide0224.htm



State of California – Natural Resources Agency
DEPARTMENT OF FISH AND WILDLIFE
Central Region
1234 East Shaw Avenue
Fresno, California 93710
(559) 243-4005
www.wildlife.ca.gov

EDMUND G. BROWN JR., Governor
CHARLTON H. BONHAM, Director



July 19, 2013

Via Electronic Submission

Kimberly D. Bose, Secretary
Federal Energy Regulatory Commission
888 First Street, NE
Washington, D.C. 20426

Steven Boyd
Turlock Irrigation District
Post Office Box 949
Turlock, California 95381

Greg Dias
Modesto Irrigation District
Post Office Box 4060
Modesto, California 95352

Subject: California Department of Fish and Wildlife Comments on Meeting Notes of the Workshops regarding Water & Aquatic Resources (W&AR) Studies Nos. 2, 3 and 16 (Project Operations/Water Balance, Don Pedro Reservoir and Lower Tuolumne River Water Temperature Modeling), Don Pedro Hydroelectric Project No. 2299, Tuolumne River

Dear Secretary Bose and Messrs. Boyd and Dias:

The California Department of Fish and Wildlife¹ (CDFW) has reviewed meeting notes from a June 4, 2013 modeling workshop posted on the Don Pedro Hydroelectric Project (Project) relicensing website (www.donpedro-relicensing.com). This workshop was hosted by the Turlock Irrigation District and Modesto Irrigation District (collectively, the Districts) at the HDR Engineering Inc., headquarters in Sacramento. The Districts also hosted a workshop the following day, June 5, 2013, for parties interested in using three related modeling tools in sequence (the Districts' Project Operations/Water Balance Model, Reservoir Temperature Model, and River Temperature Model). By this letter, CDFW respectfully provides comments on the modeling workshops and associated meeting notes.

¹ Please note that as of January 1, 2013, our new name is the California Department of Fish and Wildlife (CDFW).

Secretary Bose
Steven Boyd
Greg Dias
July 19, 2013
Page 2

The CDFW acknowledges the Districts' outreach to demonstrate the interrelated operations/water balance and water temperature modeling tools. Unfortunately due to a combination of server security issues and computing demands, the ability for hands-on experimentation by more than one user at a time was extremely limited. Given the complexity of linking three modeling tools and a lack of familiarity with the Districts' models (particularly the MIKE3 platform), CDFW staff cannot at this time provide specific comments on the utility of the subject modeling tools. As workloads permit, CDFW staff will attempt to independently assess the modeling tools and run test scenarios. Once we have the opportunity to perform test runs and assess outputs, CDFW staff will contact the Districts' representatives if there are questions or concerns.

At this point, CDFW reiterates the concern over a lack of validation comparing the Operations Model Base Case rules with current project operations. The Districts maintain the Operations Model is not intended to replicate actual water use and the recent past would not be appropriate for modeling purposes. As such, the Operations Model Base Case does not attempt to represent current operations and is simply a starting point for future alternative analyses. The Districts have also referred CDFW staff to an Operations Model Draft Validation Report issued in December 2012.

It is important to note that subsequent to the December 2012 Draft Validation Report, the Districts made several significant changes to the Operations Model, including:

1. New model logic regarding the management of reservoir releases during early-July;
2. New model logic that differentiates between base flow releases and pulse flow releases below LaGrange Dam and that implements current October attraction flow requirements;
3. Inclusion of the new hydrologic data set presented at the March 27, 2013 workshop, which includes "daily shaping of the sub-basin runoff" and the occasional rebalance between the sub-basins "to rectify historically computed negative volumes";
4. Refinement of canal operational assumptions such as "the addition of a component of canal water supply that was previously not recognized in the data set" and the refinement of "monthly turnout delivery factors"; and
5. Changes to the water supply factor based on changes to estimated canal demands and underlying hydrology and a review of **projected operations**.

These changes are described in further detail in Enclosure A – Don Pedro Project Operations/Water Balance Model Study Report Attachment B – Model Description and User's Guide, Addendum 1 Revised 5-20-2013. These model refinements may be

Secretary Bose
Steven Boyd
Greg Dias
July 19, 2013
Page 3

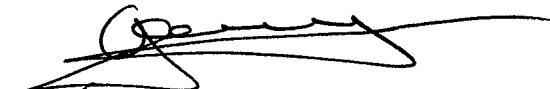
reasonable, but they should be validated against recent historic operation of the project. Given this information, it would appear that "Base Case" is a misnomer, with the subject set of repeatable equations and algorithms and anticipated improvements being more of a "Planning Case" than an actual baseline condition.

Moving beyond concerns over the validation of a Base Case, one aspect that became evident during the workshops is that the interrelated models are constructed to begin with project operational scenarios. One submits a scenario request form (see Enclosure B); the Districts then run the test scenario through the operations model and input the resulting hydrology into the water temperature models. If desired water temperature objectives are not achieved by a test scenario, another set of operational rules must be developed, creating an iterative and somewhat labor intensive process.

Going forward, CDFW is interested in a set of modeling tools that will allow interested parties to start with water temperature objectives and explore subsequent impacts on project operations. CDFW respectfully notes a recently released HEC-5Q model for the San Joaquin River basin has the ability to run such "bottom-up" analyses. Using this tool one can begin with desired temperature conditions (for example, the Environmental Protection Agency (EPA) criteria for salmonids (EPA, 2003)), and then direct the model to develop operational scenarios capable of meeting the selected temperature objectives. The supporting HEC-5Q technical documentation is publically available at: www.rmanet.com/CDFW/HEC5Q-June-13.zip. CDFW encourages interested parties to download this material and become familiar with this modeling tool as it has the potential to provide valuable insight into the development of future mitigation measures.

CDFW appreciates the opportunity to provide comments on the proposed modeling efforts on the Don Pedro Reservoir and Lower Tuolumne River. If you have any questions regarding CDFW's comments provided in this letter, please contact Annie Manji, Staff Environmental Scientist at (530) 224-4924 or Annie.Manji@wildlife.ca.gov.

Sincerely,



Jeffrey R. Single, Ph.D.
Regional Manager, Central Region

Enclosures

cc: See Page Four

Secretary Bose
Steven Boyd
Greg Dias
July 19, 2013
Page 4

cc: Jim Hastreiter
Office of Energy Projects
805 SW Broadway
Fox Tower - Suite 550
Portland, Oregon 97205

Secretary Bose
Steven Boyd
Greg Dias
July 19, 2013
Page 5

Reference

Environmental Protection Agency. 2003. Guidance for Pacific Northwest State and Tribal Temperature Water Quality Standards. EPA 910-B-03-002. Region 10 Office of Water, Seattle, WA. 57 pp.

Don Pedro Project
Project Operations/Water Balance Model Study Report
Attachment B – Model Description and User’s Guide, Addendum 1
Revised 5-20-2013

1.0 INTRODUCTION

The Turlock Irrigation District (TID) and Modesto Irrigation District (MID) (collectively, the Districts) have developed a computerized Tuolumne River Daily Operations Model (Model) to assist in the relicensing of the Don Pedro Project (Project) (FERC Project 2299). The Model is fully described in the User’s Guide submitted to FERC as part of the Initial Study Report (ISR), January 2013 (Model version 1.01). The purpose of the User’s Guide is to describe the structure of the Model, the interfaces available for operation of the Model, and methods available for reviewing Model results. Procedures for development of input files for running scenarios for alternative future Project operations are also described and illustrated. The data presented in the ISR document referenced a “Test Case” simulation of operations for illustrative purposes. The test case was presented at a Workshop held with relicensing participants on December 7, 2012 for the purpose of training interested relicensing participants in the use of the Model.

Subsequent to the ISR submittal, the Districts proceeded to develop the “Base Case” which depicts the operation of the Don Pedro Project in accordance with the current FERC license, ACOE flood control management guidelines, and the Districts’ irrigation and M&I water management practices. Under FERC policy, the Base Case represents the “No Action” alternative for purposes of evaluating future operation scenarios under NEPA. Future scenarios are compared to the Base Case to assess their impacts. As a result of the effort, including a collaborative refinement of the underlying hydrology of the Model completed at a Workshop held on March 27, 2013, several refinements and modifications to the Model have been implemented. The purpose of this Addendum 1 is to describe the refinements and modifications that have been made to the revised Model (Model Version 2.0) since the ISR submittal.

The Tuolumne River Daily Operations Model provides a depiction of the Don Pedro Project and City and County of San Francisco water operations consistent with the FERC-approved W&AR-02 study plan. The Model portrays operations that can be described systematically by various equations and algorithms. Actual project operations may vary from those depicted by the Model due to circumstantial and real-time conditions of hydrology and weather, facility operation, and human intervention. The FERC-approved study plan has identified a number of user-controlled variables. The fact that the Model provides these user-controlled inputs is not an indication that either the Districts or CCSF endorse or support any specific operational alternative developed by manipulating these inputs.

2.0 MODEL LOGIC AND EXECUTION MODIFICATIONS

Several Model logic routines were modified to provide a better or more adaptable depiction of Project operations. The specific areas of Project operations that were modified included the depiction of the current minimum flow requirements of the Don Pedro Project for the lower Tuolumne River and the reservoir operation logic during June and early July when Don Pedro Reservoir is filling. The simulation of power generation from the Project has also been revised as mentioned in the December 7, 2012 Workshop.

2.1 Don Pedro Reservoir Snow-melt Management

User's Guide reference: Section 5.12: "DonPedro" Worksheet, Section 5.12.3 Snow-melt Management

The Model computes a daily operation of Don Pedro Reservoir. Each day Don Pedro Reservoir inflow is computed from upstream CCSF System operations and unregulated inflow. The minimum stream flow requirements and the MID and TID canal diversions are assumed as the release from Don Pedro Reservoir. The prior day's reservoir evaporation is included in the calculation. If the computation produces a Don Pedro Reservoir storage value in excess of a preferred storage target, an "encroachment" is computed. If an encroachment occurs, a "check" release is computed. It is assumed that a constant supplemental "check" release (in excess of minimum releases) will be initiated. This protocol repeats itself periodically, reestablishing the level of check release each time. The end result of this procedure will allow encroachment of storage space above the preferred storage target and not require unrealistic "hard" releases of water to exactly conform to the target reservoir level.

A second check release is made during the April through June period for management of anticipated snow-melt runoff. Model Version 1.01 provided logic that on the first day of each of these months a forecast is made of anticipated runoff into the reservoir and minimum releases and losses from the reservoir from the date of forecast through the end of June (the assumed target date of reservoir filling). These forecasts determine the snow-melt "check" release volume of water (if any) that will require release in excess of minimum releases and losses and storage gain by the end of June. The snow-melt check release is evenly distributed across the days of the month. The release made in a day is the greater of the two check releases or the minimum release. At no time is the maximum capacity of the reservoir (2,030,000 acre-feet, elevation 830 ft) allowed to be exceeded, and if necessary a release, regardless of magnitude, will be made by the Model to not exceed this storage capacity.

Through testing of alternative Model scenarios it was discovered that Version 1.01 logic could produce erratic reservoir release results during early July, whereby a relatively constant release through the end of June could be followed by an erratic large release during the first part of July. The cause of the circumstance was the result of requiring the "filling" date of the reservoir to be the end of June. The assumption could lead to a full reservoir at the end of June while substantial inflow could subsequently occur. With no empty reservoir space remaining the Model would essentially pass inflow without modulation and in some circumstances large releases in excess of downstream flood control objectives. To remedy this outcome the Model was modified to extend

the June snow-melt release check logic through July 7. All computational procedures for June remained the same except the time period upon which hydrologic information was known or assumed extends through July 7. Figure 2.1-1 illustrates the location of the revised logic within the DonPedro Worksheet, within the June computation section and designated by notes concerning the June through July 7 computational period.

Also newly incorporated into the snow-melt logic routine for the entire April through July 7 period is release change “smoothing” logic which can lessen the occurrence of modeled erratic release reductions that would otherwise sometimes occur during the transition from one month’s computed release to the next month’s computed release. During periods when the snow-melt release computation is controlling reservoir releases, user-defined values can be specified for a threshold and a rate of change that can occur from one day to the next. The threshold (C 1.13, “Control” Worksheet) defines the level of flow of the previous day for which a constraint to a next-day release reduction will occur, and the fraction (C 1.14, “Control” Worksheet) defines the reduced flow rate that can occur the next day. By illustration, if a previous day’s flow is 2,500 cfs or greater, the next day’s flow cannot be less than 0.75 of the previous day’s flow. This logic does not represent any known “ramping” constraints, but the protocol provides additional guidance to Model release decisions and produces reasonable results.

AR	AS	AT	AU	AV	AW	AX	AY	AZ	BA	BB	BC	BD	BE	BF	BG	BH	BI	BJ	BK	BL	BM	BN	BO
1																							
2	Unit Title																						
3	Parameter Title																						
4																							
5	Acre-foot to CFS conversion																						
6	divide by:	1.983471																					
7																							
8																							
9																							
10																							
11																							
12																							
13																							
14																							
15																							
16																							
17	Month																						
18	Index																						
19																							
20	1970.10	10/1/1970	T	31																			
21	1970.10	10/2/1970	F	31																			
22	1970.10	10/3/1970	S	31																			
23	1970.10	10/4/1970	S	31																			
24	1970.10	10/5/1970	M	31																			
25	1970.10	10/6/1970	T	31																			
26	1970.10	10/7/1970	W	31																			
27	1970.10	10/8/1970	T	31																			
28	1970.10	10/9/1970	F	31																			
29	1970.10	10/10/1970	S	31																			

Figure 2.1-1. Snow-melt management section.

2.2 Don Pedro Current Minimum Flow Requirement

User’s Guide reference: Section 5.17: “LaGrangeSchedule” Worksheet, Section 5.17.1 Minimum Flow Requirement Options, Section 5.17.2 April-May Daily Parsing of Flow Requirements, and Section 5.17.3 Computation of 1995 FERC Minimum Flow Requirement

The FERC license for the Don Pedro Project requires flow releases from Don Pedro Reservoir to the lower Tuolumne River. These flows are measured at the USGS gage downstream of the La Grange diversion dam. To keep the Don Pedro Reservoir required flow releases distinct from Don Pedro Reservoir releases in general the model designates “LaGrangeSchedule” Worksheet for assemblage of the minimum flow requirement for the lower Tuolumne River. By user specification (UI 1.10) either the current 1995 FERC schedule is selected (UI 1.10 = 0) or the

user defined minimum flow requirement is selected (UI 1.10 = 1). If the current 1995 FERC schedule is selected the computation of the schedule is computed in this worksheet.

When using current 1995 FERC minimum flow requirements, Version 1.01 (Switch C 1.60, “Control” Worksheet) allowed the user to direct the daily shape of release for pulse flows during April and May. Version 2.0 continues to allow the shaping of April-May migration flows to the lower Tuolumne River and also allows a shaping of October attraction flows. Figure 2.2-1 illustrates the parsing of the monthly flow requirements into daily flow requirements. The structure of this section of the worksheet is mostly the same as before, except the monthly/daily flow requirements have now been defined by “base” and “pulse” components. Also, a computational procedure has been added for October to prescribe current FERC-defined attraction flows.

Figure 2.2-1. Daily parsing of FERC flow requirement from Don Pedro Reservoir.

Figure 2.2-2 illustrates the area for entry of data to parse monthly-designated migration and attraction flow requirements into daily patterns during April, May and October. The “Control” Worksheet designates which parsing pattern is to be used for April and May. The examples illustrate the entry for an evenly distributed pattern of migration flow volume during the April-May 61-day period, and a pattern for which the migration flow volume (by daily fraction of the volume) has been divided between April (16 days) and May (15 days). The migration flow volume for each month has been evenly distributed during each day of the partial month period. These daily migration flows are added to the base flow component of each month. The parsing of the attraction flow volume during the month of October is similarly defined. In this example the attraction flow volume (by daily fraction of the volume) for October is distributed evenly over a two-day period beginning October 15.

Figure 2.2-3 illustrates the section of the worksheet that defines the current 1995 FERC flow requirement from Don Pedro Reservoir. Several elements of information provided in this worksheet and from the “Control” Worksheet provide the computation of flow requirement based on 1995 FERC Settlement procedures and flow rates. The basis of the year type flow requirements is the SWRCB San Joaquin River Basin 60-20-20 index. The annual flow

schedules are assumed to be on an April through March year, with the interpolation water of the schedules applied to April and May pulse flows. For modeling convenience the explicit FERC requirements for October base and attraction flows have been slightly modified to adapt into the evenly daily distributed base flow component of the Model.

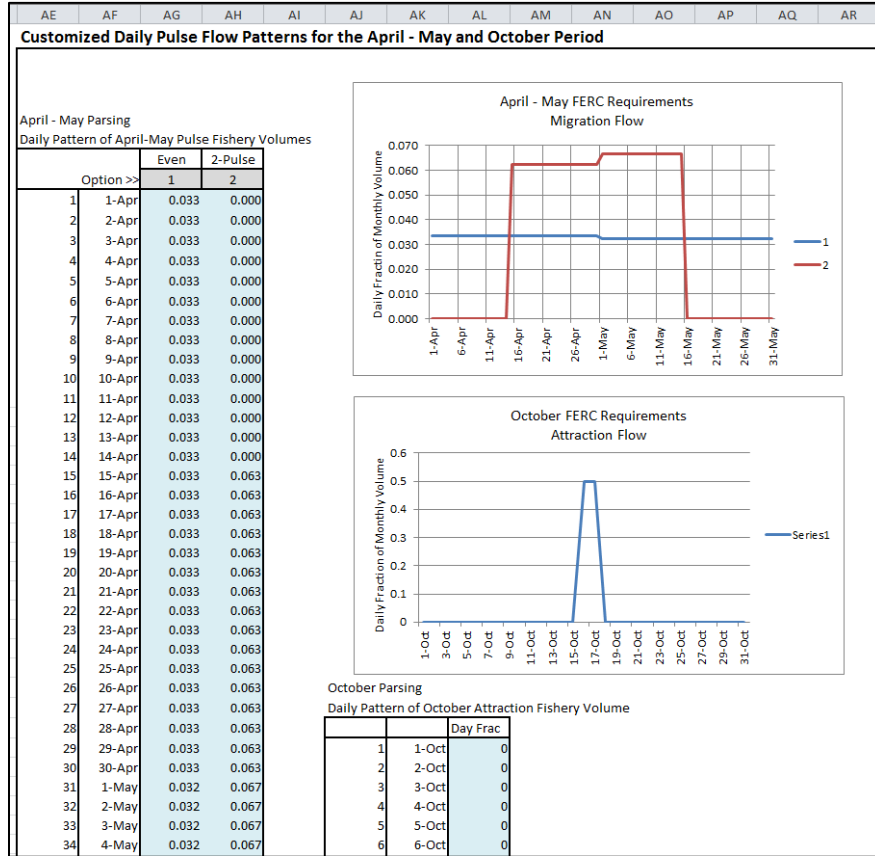


Figure 2.2-2. Daily parsing of FERC migration and attraction flow.

	BK	BL	BM	BN	BO	BP	BQ	BR	BS	BT	BU	BV	BW
FERC Flow Schedules													
													Adapted October
Year Type	1	2	3	4	5	6	7	6					
Oct 1-15 (CFS)	100	100	150	150	180	200	300	188	<i>October has been modified from explicit FERC Schedule for modeling simplicity. Split-month base flow has been leveled.</i>				
Oct 16-31 (CFS)	150	150	150	150	180	175	300	188					
Total Base (AF)	7,736	7,736	9,223	9,223	11,068	11,504	18,447	11,560					
Attraction (AF)	0	0	0	0	1,676	1,736	5,950	1,680					
Total Oct (AF)	7,736	7,736	9,223	9,223	12,744	13,240	24,397	13,240					
Nov (CFS)	150	150	150	150	180	175	300						
AF	8,926	8,926	8,926	8,926	10,711	10,413	17,852						
Dec (CFS)	150	150	150	150	180	175	300						
AF	9,223	9,223	9,223	9,223	11,068	10,760	18,447						
Jan (CFS)	150	150	150	150	180	175	300						
AF	9,223	9,223	9,223	9,223	11,068	10,760	18,447						
Feb (CFS)	150	150	150	150	180	175	300						
AF	8,331	8,331	8,331	8,331	9,997	9,719	16,661						
Mar (CFS)	150	150	150	150	180	175	300						
AF	9,223	9,223	9,223	9,223	11,068	10,760	18,447						
Apr (CFS)	150	150	150	150	180	175	300						
AF	8,926	8,926	8,926	8,926	10,711	10,413	17,852						
May (CFS)	150	150	150	150	180	175	300						
AF	9,223	9,223	9,223	9,223	11,068	10,760	18,447						
Migration Flow													
AF	11,091	20,091	32,619	37,060	35,920	60,027	89,882						
Jun (CFS)	50	50	50	75	75	75	250						
AF	2,975	2,975	2,975	4,463	4,463	4,463	14,876						
Jul (CFS)	50	50	50	75	75	75	250						
AF	3,074	3,074	3,074	4,612	4,612	4,612	15,372						
Aug (CFS)	50	50	50	75	75	75	250						
AF	3,074	3,074	3,074	4,612	4,612	4,612	15,372						
Sep (CFS)	50	50	50	75	75	75	250						
AF	2,975	2,975	2,975	4,463	4,463	4,463	14,876						
Total Annual	94,001	103,001	117,017	127,508	142,503	165,004	300,926						

Figure 2.2-3. 1995 FERC minimum flow requirement schedule.

Figure 2.2-4 illustrates the revised computational section of the “LaGrangeSchedule” Worksheet that computes the components of base and total required schedule annual volumes, October attraction flow volume, and April-May migration flow volume. Other sections of the worksheet have been revised to define the monthly distribution of annual volumes for incorporation into the daily parsing routines shown above.

AU	AV	AW	AX	AY	AZ	BA	BB	BC	BD	BE	BF	BG	BH	BI
Current FERC Requirements														
Tuolumne River Flow Interpolation - Year 2011 Revised Distribution														
Flow Year Type		SJR Basin Index				Flow Requirement						October		
										Base		Attraction		
1	<	1510									94000	82,910	0	
2		1510	- <	2000		0.0286 x (Index - 1510) +					103000	82,910	0	
3		2000	- <	2190		0.0552 x (Index - 2000) +					117016	84,398	0	
4		2190	- <	2440		0.0600 x (Index - 2190) +					127507	90,448	0	
5		2440	- <	2720		0.0804 x (Index - 2440) +					142502	104,907	1,676	
6		2720	- <	3180		0.2955 x (Index - 2720) +					165002	103,297	1,680	
7		3180	and Greater								300923	205,094	5,950	
Option >>														
1	<<Option	Ave	219,421	146,114	70,146			Actual	90% Exc.	75% Exc.	Med.	10% Exc.		
SJR		TR	Tuolumne	Tuolumne	Pulse	Base	SJR	Apr SJR						
Index	Year	October	River	River	Flow	Year	Index	Index	Index	Index	Index	Index		
602020	Class	Year	Attraction	Require	Base	Calc	Type	602020	Fcast	Fcast	Fcast	Fcast		
4,543,729	Wet	1922	5,950	300,923	205,094	89,879	7	4,543,729	2,424,373	2,561,322	2,674,495	2,921,846		
3,549,358	Above	1923	5,950	300,923	205,094	89,879	7	3,549,358	1,765,568	1,897,976	2,007,411	2,246,643		
1,419,746	Critical	1924	0	94,000	82,910	11,090	1	1,419,746	799,642	853,197	957,737	1,186,335		
2,929,617	Below	1925	1,680	226,944	103,297	121,967	6	2,929,617	2,042,878	2,179,628	2,292,637	2,539,632		
2,300,567	Dry	1926	0	134,141	90,448	43,693	4	2,300,567	1,256,470	1,387,014	1,494,917	1,730,818		
3,558,955	Above	1927	5,950	300,923	205,094	89,879	7	3,558,955	2,147,110	2,284,156	2,397,408	2,644,932		
2,632,407	Below	1928	1,676	157,972	104,907	51,388	5	2,632,407	1,934,163	2,068,826	2,180,117	2,423,380		
2,004,815	Critical	1929	0	117,282	84,398	32,884	3	2,004,815	1,140,712	1,270,277	1,377,372	1,611,521		

Figure 2.2-4. 1995 FERC flow requirements from Don Pedro Reservoir.

2.3 Don Pedro Project Generation

User’s Guide reference: Section 5.12: “DonPedro” Worksheet, Section 5.12.5 Don Pedro Project Generation and River Flows

The hydroelectric generation characteristics of any modeled Project operation scenario are modeled incidental to Project hydrologic operations. The power generation of the Project is computed from the simulation of daily time step operations and is incorporated into the “DonPedro” Worksheet. Input to the power component includes daily average flow past Don Pedro Dam (flow through the dam and through the spillway, if any) and Don Pedro Reservoir storage. The power component computes gross and net head, flow through turbines, efficiency and power output based on a group of reservoir rating, tailwater rating and manufacturer’s performance characteristic curves, and generalized equations for head losses.

Figure 2.3-1 illustrates the components of computational procedure that derives power output of the Project. The power characteristics of the turbine generators are defined for a range of head and flow combinations. “Cutoff” of generation that would otherwise be indicated by the performance curves is provided through user defined switches entered in the “Control” Worksheet. Switch C 1.20 defines the minimum reservoir storage level at which generation occurs, and Switch C 1.22 defines the maximum flow through the powerplant. In this illustration generation will not occur when Don Pedro Reservoir storage is less than 308,960 acre-feet (elevation 600 ft). The performance curves indicate that generation may occur up to a flow rate of approximately 5,500 cfs. Switch C 1.22 has been set higher than this value to not impede the computation.

	A	B	C	D	DK	DL	DM	DN	DO	DP	DQ	DR	DS	DT	DU	DV	DW	DX	DY	DZ
1			1		CFS															
2	Unit Title				Total Dam Release															
3	Parameter Title																			
4																				
5	Acre-foot to CFS conversion																			
6	divide by: 1.983471																			
7																				
8					TEST															
9					11/21/1977	289	361,955	614.3	298.0	316.3	316.2	310	325	0		3	1	10	4550	289
10																				
11					308,960 (C 1.20) Cutoff of generation, DP Storage (sets available units to zero)															
12					Penstock Loss: 9.66E-07 ft/cfs ² Scheduled Maintenance? (1) Yes, (0) No: 0															
13	39-year Ave or Max				Max	67,039	830	298	532	527	530	525			3	1	10	5,655	5,500	
14	Min				Min	207	614	298	316	316	310	325			3	1	10	4,550	207	
15					Don Pedro Power Generation															
16																				
17	Month				Don Pedro Release	Don Pedro Storage	Don Pedro Elevation	Approx Tailwater Elevation	Gross Head	Approx Net H	Net H Look-up Units 1-3	Net H Look-up Unit 4	Sched Outage	Unsched Outage / Bypass	Number Available Units 1-3	Number Available Unit 4	Min Plant Flow	Max Plant Flow	Potential Plant Flow	
18	Index	Date	Day	Days	CFS	Ave-AF	FT elev	FT elev	FT	FT	FT	FT	unit #	unit #			CFS	CFS	CFS	
19																				
20	1970.10	10/1/1970	T	31	2,037	1,669,232	800.0	298.0	502.0	498.0	490	500	0		3	1	10	5500	2,037	
21	1970.10	10/2/1970	F	31	1,288	1,666,644	799.7	298.0	501.7	500.1	510	500	0		3	1	10	5500	1,288	
22	1970.10	10/3/1970	S	31	1,209	1,664,882	799.6	298.0	501.6	500.2	510	500	0		3	1	10	5500	1,209	
23	1970.10	10/4/1970	S	31	1,718	1,662,698	799.4	298.0	501.4	498.6	490	500	0		3	1	10	5500	1,718	
24	1970.10	10/5/1970	M	31	1,378	1,660,351	799.2	298.0	501.2	499.4	490	500	0		3	1	10	5500	1,378	
25	1970.10	10/6/1970	T	31	1,502	1,658,222	799.0	298.0	501.0	498.8	490	500	0		3	1	10	5500	1,502	
26	1970.10	10/7/1970	W	31	1,322	1,656,151	798.8	298.0	500.8	499.1	490	500	0		3	1	10	5500	1,322	
27	1970.10	10/8/1970	T	31	728	1,654,638	798.7	298.0	500.7	500.2	510	500	0		3	1	10	5500	728	
28	1970.10	10/9/1970	F	31	827	1,653,407	798.5	298.0	500.5	499.8	490	500	0		3	1	10	5500	827	
29	1970.10	10/10/1970	S	31	898	1,652,016	798.4	298.0	500.4	499.6	490	500	0		3	1	10	5500	898	

	A	B	C	D	EA	EB	EC	ED	EE	EF	EG	EH	EI	EJ	EK	EL			
1			1		CFS											kWh			
2	Unit Title				Total Plant Flow											Modeled			
3	Parameter Title																		
4																			
5	Acre-foot to CFS conversion																		
6	divide by: 1.983471																		
7																			
8																			
9					1	289	0	0	289	315.9	60.0%	0.0%	4,648	0	4,648	111,544			
10																			
11																			
12					39-yr Annual Ave (AF): 1,501,380											39-yr Annual Ave (MWh): 603,718			
13	39-year Ave or Max				3	1	1,000	5,500	525	0.90	0.92	172,991	38,653	208,219	4,997,256				
14	Min				1	0	0	207	316	0.60	0.00	3,333	0	3,333	80,003				
15																			
16					Flow											Plant			
17	Month				Operation	Through	Operation	Through	Plant	Net	Effic	Effic	Power	Power	Plant	Daily			
18	Index	Date	Day	Days	Units 1-3	Units 1-3	Unit 4	Unit 4	Flow	Head	%	%	Units 1-3	Unit 4	Units 1-3	Unit 4	Power	Generation	
19					Count	CFS	CFS	CFS	CFS	FT			kW	kW	kW	kWh	kW	kWh	
20	1970.10	10/1/1970	T	31	3	679	0	0	2037	495.0	77.2%	0.0%	65,942	0	65,942	1,582,609			
21	1970.10	10/2/1970	F	31	3	429	0	0	1288	498.2	65.2%	0.0%	35,423	0	35,423	850,156			
22	1970.10	10/3/1970	S	31	3	403	0	0	1209	498.3	63.9%	0.0%	32,602	0	32,602	782,449			
23	1970.10	10/4/1970	S	31	3	573	0	0	1718	496.0	73.4%	0.0%	53,001	0	53,001	1,272,019			
24	1970.10	10/5/1970	M	31	3	459	0	0	1378	497.3	67.8%	0.0%	39,381	0	39,381	945,135			
25	1970.10	10/6/1970	T	31	3	501	0	0	1502	496.5	70.3%	0.0%	44,432	0	44,432	1,066,359			
26	1970.10	10/7/1970	W	31	3	441	0	0	1322	497.1	67.0%	0.0%	37,296	0	37,296	895,105			
27	1970.10	10/8/1970	T	31	2	364	0	0	728	499.0	60.0%	0.0%	18,467	0	18,467	443,214			
28	1970.10	10/9/1970	F	31	3	276	0	0	827	498.5	60.0%	0.0%	20,971	0	20,971	503,311			
29	1970.10	10/10/1970	S	31	3	299	0	0	898	498.3	60.0%	0.0%	22,759	0	22,759	546,222			

Figure 2.3-1. Project power computational procedure.

A validation of the computational process was made by comparing Model-produced generation to historically reported generation. Table 2.3-1 shows a comparison between computed and reported generation for a 2002 – 2009 period of record. The results show that Project generation is well depicted with the computational procedures, with minimal annual differences. This period of record includes a dry (reduced reservoir and releases) to wet (full reservoir and large releases) range of hydrologic conditions. Figure 2.3-2 illustrates the comparison of Model-produced daily generation and historically reported generation for calendar year 2003, which had a range of reservoir storage and release conditions.

Table 2.3-1. Modeled and reported Project power.

Reported Generation (MWh)													
	Jan	Feb	Mar	Apr	May	Jun	Jul	Aug	Sep	Oct	Nov	Dec	Annual
2002	5,079	4,259	38,044	61,819	54,412	54,341	66,448	52,811	28,790	18,760	6,073	7,005	397,840
2003	5,395	11,275	25,076	39,599	51,964	68,313	75,800	61,667	32,692	33,135	8,343	6,261	419,520
2004	7,509	12,122	62,985	72,157	58,301	58,788	68,904	54,145	25,452	23,118	4,565	4,402	452,449
2005	12,339	48,759	98,233	137,057	143,777	137,291	122,689	84,793	43,861	22,203	9,831	33,044	893,877
2006	111,669	72,155	125,741	110,498	131,217	124,759	97,387	80,643	46,356	26,152	11,631	8,204	946,413
2007	12,597	15,207	45,088	48,189	54,255	57,216	64,531	53,546	22,957	15,461	7,032	3,780	399,859
2008	3,184	5,562	37,289	43,158	58,312	45,852	54,811	46,690	22,417	11,467	4,647	6,114	339,501
2009	4,912	5,326	21,733	41,084	55,267	56,222	67,625	53,082	28,388	18,051	7,781	5,495	364,965
Average	20,335	21,833	56,774	69,195	75,938	75,348	77,274	60,922	31,364	21,043	7,488	9,288	526,803
Ann Dist	4%	4%	11%	13%	14%	14%	15%	12%	6%	4%	1%	2%	100%

Modeled Generation (MWh)													
	Jan	Feb	Mar	Apr	May	Jun	Jul	Aug	Sep	Oct	Nov	Dec	Annual
2002	4,692	4,343	36,119	63,521	54,701	56,249	69,864	53,614	27,334	17,457	5,765	6,422	400,081
2003	5,104	10,231	23,762	39,691	51,839	67,021	80,295	64,791	31,953	31,070	7,742	5,434	418,932
2004	6,696	11,128	62,972	75,770	60,036	59,137	70,224	55,786	24,403	21,785	5,131	4,488	457,555
2005	13,839	50,180	109,404	139,619	146,930	147,343	132,278	89,284	44,552	21,561	10,306	35,026	940,321
2006	102,499	71,293	130,498	108,499	113,092	111,410	102,790	82,253	45,051	24,484	11,237	7,320	910,425
2007	11,023	13,343	43,437	47,548	54,298	59,601	67,647	56,301	22,600	14,898	6,724	4,165	401,585
2008	3,820	5,733	37,688	43,469	59,007	45,476	56,320	49,154	21,603	10,833	4,542	6,150	343,795
2009	4,985	5,740	21,720	40,985	55,636	58,102	72,166	56,015	28,577	16,255	7,465	5,421	373,066
Average	19,082	21,499	58,200	69,888	74,443	75,542	81,448	63,400	30,759	19,793	7,364	9,303	530,720
Generation	4%	4%	11%	13%	14%	14%	15%	12%	6%	4%	1%	2%	100%

% Deviation ((Reported-Actual)/Actual)													
	Jan	Feb	Mar	Apr	May	Jun	Jul	Aug	Sep	Oct	Nov	Dec	Annual
2002	-8%	2%	-5%	3%	1%	4%	5%	2%	-5%	-7%	-5%	-8%	1%
2003	-5%	-9%	-5%	0%	0%	-2%	6%	5%	-2%	-6%	-7%	-13%	0%
2004	-11%	-8%	0%	5%	3%	1%	2%	3%	-4%	-6%	12%	2%	1%
2005	12%	3%	11%	2%	2%	7%	8%	5%	2%	-3%	5%	6%	5%
2006	-8%	-1%	4%	-2%	-14%	-11%	6%	2%	-3%	-6%	-3%	-11%	-4%
2007	-12%	-12%	-4%	-1%	0%	4%	5%	5%	-2%	-4%	-4%	10%	0%
2008	20%	3%	1%	1%	1%	-1%	3%	5%	-4%	-6%	-2%	1%	1%
2009	1%	8%	0%	0%	1%	3%	7%	6%	1%	-10%	-4%	-1%	2%
Average	-6%	-2%	3%	1%	-2%	0%	5%	4%	-2%	-6%	-2%	0%	1%

Modeled generation includes assumptions for historical outages of units.

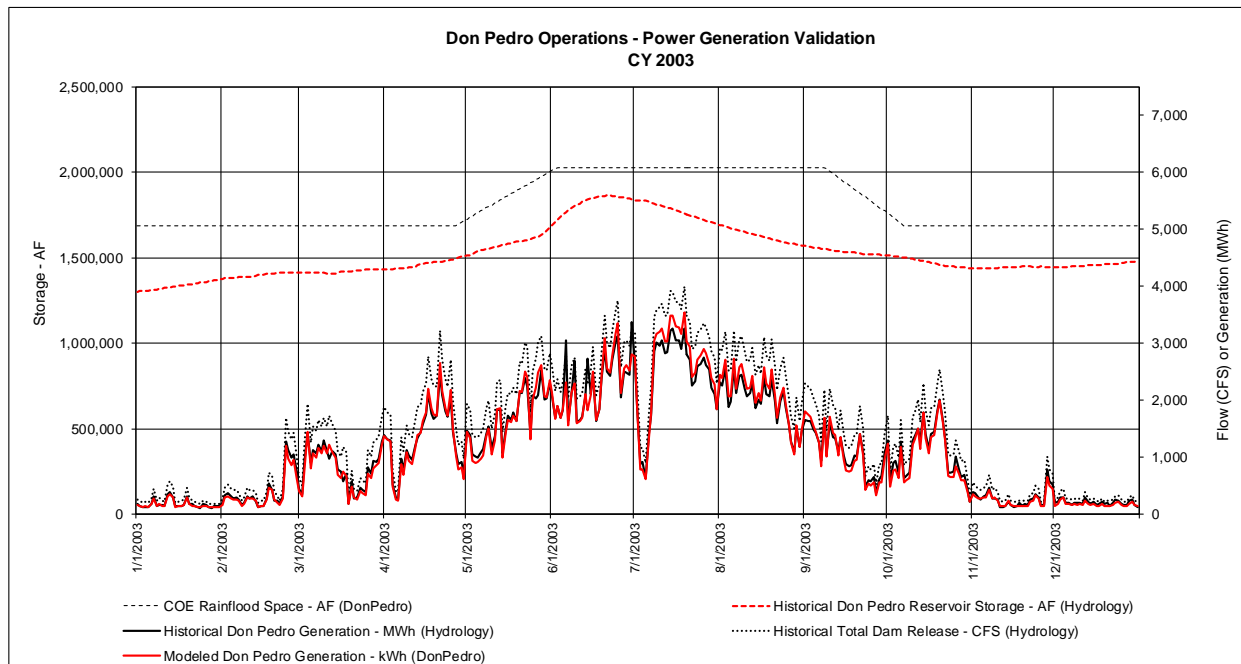


Figure 2.3-2. Project power daily generation.

3.0 INPUT AND HYDROLOGY MODIFICATIONS

Several changes to underlying hydrology and data assumptions have been implemented in the Model (Version 2.0).

3.1 Unimpaired Runoff

User’s Guide reference: Section 5.22: “Hydrology” Worksheet

Concern was raised regarding the sometimes erratic daily pattern of computed unimpaired runoff for various components of the historical record, and the occasional computation of a “negative” value of flow. Although the use of the historically computed data are known to not adversely affect Model results, the Districts forwarded an approach to developing a hybrid gauge summation/gage proration hydrologic record for Tuolumne River unimpaired flow that would provide a “smoother” hydrograph. At a Workshop on March 27, 2013, RPs and the Districts worked through the approach and came to a consensus on an acceptable record of unimpaired flow for the Tuolumne River. It was clearly stated that the Districts and CCSF will not change their historical methods for calculating their respective water supplies from the Tuolumne River or the historical record of water bank operations. This modified data set will only be used to estimate unimpaired flow for the FERC relicensing.

Modified sub-basin hydrology was implemented for Hetch Hetchy Reservoir inflow, Cherry/Eleanor inflow, and the unregulated inflow to Don Pedro Reservoir. With only one month of exception, the historically computed monthly volumes of total runoff above La Grange were maintained in the modified data set. However, the daily shaping of the sub-basin runoff was modified, and on occasion rebalanced between the sub-basins to rectify historically computed negative volumes. Figure 3.1-1 illustrates the location and an example of the modified hydrology implemented in the “Hydrology” Worksheet.

	A	B	C	D	E	F	G	H	I	J	K	L	M																						
1			1		Hydrology																														
2			2		CFS	CFS	CFS	CFS	CFS		CFS	CFS	CFS																						
3			3		Unimpaired	Unimpaired	Unimpaired	Revised Ur	Unregulated Inflow to	Dry Creek		Total LTR Ac	Modesto to																						
6					Read by	Read by	Read by		Read by		Read by	Read by	Read by																						
7					Model	Model	Model		Model		Model	Model	Model																						
13					March 26, 2013 Prorated Hydrology						<table border="1"> <thead> <tr> <th colspan="3">LTR Accretions</th> </tr> <tr> <th>Nov 2012</th> <th>Nov 2012</th> <th></th> </tr> </thead> <tbody> <tr> <td>Dry Creek</td> <td>Lower</td> <td>Modesto</td> </tr> <tr> <td>Flow @</td> <td>Tuolumne</td> <td>to</td> </tr> <tr> <td>Modesto</td> <td>River</td> <td>Confluence</td> </tr> <tr> <td>HDR est.</td> <td>Acc abv</td> <td></td> </tr> <tr> <td>CFS</td> <td>CFS</td> <td>CFS</td> </tr> </tbody> </table>				LTR Accretions			Nov 2012	Nov 2012		Dry Creek	Lower	Modesto	Flow @	Tuolumne	to	Modesto	River	Confluence	HDR est.	Acc abv		CFS	CFS	CFS
LTR Accretions																																			
Nov 2012	Nov 2012																																		
Dry Creek	Lower	Modesto																																	
Flow @	Tuolumne	to																																	
Modesto	River	Confluence																																	
HDR est.	Acc abv																																		
CFS	CFS	CFS																																	
14					1,934,193	762,930	487,867		683,396																										
15					Unimpaired Flow			Computed Flow																											
16					La Grange	Hetch Hetchy	Cherry/Eleanor		Unregul blw SF																										
17	Month				CFS	CFS	CFS		CFS																										
18	Index	Date	Day																																
19																																			
20	1970.10	10/1/1970	T		125	4	14		107		30	80	32																						
21	1970.10	10/2/1970	F		130	4	14		111		30	80	32																						
22	1970.10	10/3/1970	S		129	4	14		111		30	80	32																						
23	1970.10	10/4/1970	S		133	4	15		115		30	80	32																						
24	1970.10	10/5/1970	M		135	4	15		117		30	80	32																						
25	1970.10	10/6/1970	T		137	4	15		118		30	80	32																						
26	1970.10	10/7/1970	W		139	4	15		119		30	80	32																						
27	1970.10	10/8/1970	T		142	4	15		122		30	80	32																						
28	1970.10	10/9/1970	F		144	4	15		124		30	80	32																						
29	1970.10	10/10/1970	S		149	4	16		130		30	80	32																						

Figure 3.1-1. Unimpaired runoff data set.

3.2 District Canal Operation Assumptions

User’s Guide reference: Section 5.18: “DailyCanalsCompute” Worksheet, Section 5.18.3 Daily Canal Operation Assumptions

The “DailyCanalsCompute” Worksheet performs the computation of the daily canal demands of the MID and TID. The computation of canal demands incorporate the PDAW and canal operations practices of the Districts. Canal operation assumptions include regulating reservoir operation, seepage and losses, nominal groundwater pumping and canal operational spills. Since the initial development of data for the Model, a recent review of the Districts’ operation records associated with the Districts’ preparation and filing of their 5-year Agricultural Water Management Plans has led to the refinement of certain canal operations assumptions. Model (Version 2.0) assumptions for each District are shown Figure 3.2-1.

Modesto Irrigation District												
Month	Turnout Delivery Factor	Nominal Private GW Pumping	Canal Operational Spills Critical	Canal Operational Spills Non-crit	System Losses below Modesto Res	Intercepted Flows	Nominal MID GW Pumping	Modesto Res and Upper Canal Losses/Div	Municipal Delivery from Modesto Res	Modesto Res Target Storage	Modesto Res Target Storage Change	
	%	TAF	TAF	TAF	TAF	TAF	TAF	TAF	TAF	TAF	TAF	
January	35.0	0.0	2.0	2.0	0.1	0.0	0.0	0.0	2.3	17.0	2.0	
February	35.0	0.0	2.0	2.0	0.1	0.0	0.0	0.0	2.3	18.0	1.0	
March	65.0	1.0	1.0	3.0	0.6	0.9	1.0	2.0	2.7	18.0	0.0	
April	70.0	2.0	3.0	6.0	0.6	0.9	2.3	2.9	2.7	19.0	1.0	
May	85.0	3.0	4.0	6.5	0.6	1.2	2.3	3.9	3.0	20.0	1.0	
June	85.0	4.0	3.5	6.5	0.6	1.0	2.3	4.3	3.2	20.0	0.0	
July	77.5	4.0	3.5	6.5	0.6	1.0	2.6	4.9	3.3	21.0	1.0	
August	70.0	4.0	4.9	7.0	0.6	1.4	2.4	4.9	3.3	22.0	1.0	
September	65.0	2.0	5.0	7.0	0.6	1.2	2.3	4.2	3.3	20.0	-2.0	
October	40.0	1.0	2.8	6.9	0.6	0.9	2.1	2.0	3.2	17.0	-3.0	
November	30.0	0.0	2.0	2.0	0.1	0.0	0.0	2.0	2.7	15.0	-2.0	
December	35.0	0.0	2.0	2.0	0.1	0.0	0.0	0.0	2.5	15.0	0.0	
Total		21.0	35.7	57.4	5.4	8.5	17.3	31.1	34.5			

MID March TO Factor		TID March TO Factor		MID April TO Factor		TID April TO Factor	
Factor Break Pnt (PDAW-TAF)	Factor %						
0.0	65.0	0.0	65.0	0.0	70.0	0.0	57.5
9.9	65.0	19.8	65.0	10.0	70.0	20.0	57.5
13.2	65.0	27.5	65.0	17.5	70.0	35.0	70.0
20.0	65.0	40.0	65.0	25.0	80.0	50.0	80.0
9999.0	65.0	9999.0	65.0	9999.0	80.0	9999.0	80.0

Turlock Irrigation District												
Month	Turnout Delivery Factor	Nominal Private GW Pumping	Canal Operational Spills Critical	Canal Operational Spills Non-crit	System Losses below Turlock Lk	Intercepted and Other Flows	Nominal TID GW Pumping	Turlock Lk and Upper Canal Losses	Other Delivery from Turlock Lk	Turlock Lk Target Storage	Turlock Lk Target Storage Change	
	%	TAF	TAF	TAF	TAF	TAF	TAF	TAF	TAF	TAF	TAF	
January	30.0	0.0	2.0	2.0	0.8	0.0	0.0	1.0	0.0	18.0	5.0	
February	30.0	0.0	2.0	2.0	0.8	0.0	0.0	1.0	0.0	25.0	7.0	
March	65.0	1.2	3.0	3.0	4.5	0.5	4.1	1.0	0.0	30.0	5.0	
April	57.5	2.4	5.1	6.3	4.5	1.0	8.0	6.6	0.0	30.0	0.0	
May	85.0	3.6	4.6	6.7	4.5	1.3	10.3	7.7	0.0	32.0	2.0	
June	92.5	5.2	4.2	6.7	4.5	1.3	12.4	8.2	0.0	32.0	0.0	
July	75.0	6.4	4.2	6.7	4.5	1.5	14.6	8.7	0.0	32.0	0.0	
August	65.0	6.2	4.0	7.3	4.5	1.5	13.3	9.0	0.0	30.0	-2.0	
September	67.5	3.9	3.2	7.3	4.5	1.0	9.1	5.0	0.0	27.0	-3.0	
October	40.0	2.4	2.3	7.3	4.5	0.5	5.3	2.0	0.0	13.0	-14.0	
November	30.0	0.0	2.0	2.0	0.8	0.0	0.0	1.0	0.0	13.0	0.0	
December	30.0	0.0	2.0	2.0	0.8	0.0	0.0	1.0	0.0	13.0	0.0	
Total		31.3	38.6	59.3	39.2	8.5	77.1	52.2	0.0			

Figure 3.2-1. Districts’ canal demand components.

The change that has occurred to the data set is the estimation of “intercepted and other flows” for the TID canal system. The change reflects the addition of a component of canal water supply that was previously not recognized in the data set. Also refined in the data set and computational process for both Districts were several of the monthly turnout delivery factors. The turnout delivery factors are unique to each District and represent a modeling mechanism to adjust the PDAW for irrigation practices that are not included in the estimation of the CUAW, such as irrigation that provides for groundwater recharge. Data identified in this worksheet are entered through the Control Worksheet.

3.3 Don Pedro Water Supply Factor

User’s Guide reference: Section 5.20: “DPWSF” Worksheet

The “DPSWF” Worksheet computes the Don Pedro Water Supply Factor (WSF). The premise of the WSF factor is to reduce the amount of water diverted to the canals during years when lack of carryover storage at Don Pedro Reservoir becomes a concern. The modeling mechanism used to reduce canal diversions is a factor applied to the PDAW of the canal demand. This mechanism results in a reduction to the amount of water “turned out” to the customers. Changes to estimated canal demands and underlying hydrology, in combination with the review of projected operations has led to a change in the WSF to be used for the Base Case. Figure 3.3-1 illustrates the Base Case WSF components in the Model (Version 2.0). The values are entered in the “Control” Worksheet.

Don Pedro Reservoir Inflow Forecast for Diversion of Water Supply				
Reservoir Index Method - Active Matrix				
	M/T NDP Stor + Infl Index	M/TID WS Factor	+1	+1
	kaf	%		
Enter	0	0.75	1090	0.75
Values	1090	0.75	1090	0.875
From	1090	0.875	1700	0.875
C1.90	1700	0.875	1700	1
	1700	1	2300	1
	2300	1	9999	1
	9999	1		

(Water (S)upply (F)actor is established by forecasting upcoming water supply, based on antecedent storage and anticipated inflow to Don Pedro Reservoir.

*Forecast begins for February:
EO-January storage + Feb-July UF - Feb-July US adj - Feb-Mar minimum river*

*March Forecast:
EO-February storage + Mar-July UF - Mar-July US adj - Mar minimum river*

*April Forecast: (final)
EO-March storage + Apr-July UF - Apr-July US adj*

*Factor Table is April Forecast based
February and March Forecasts act as adjustments to estimate April 1 state.*

Figure 3.3-1. Don Pedro water supply forecast factors.

3.5 Lower Tuolumne River Accretions below Modesto

The Model (Version 1.0) incorporated a synthesized data set for lower Tuolumne River accretions above the “Modesto” gage and estimated flow from Dry Creek. These data sets inform the Model of flow that could influence Don Pedro Reservoir releases during flood control operations. Recent, actual field measurements for flow in the Tuolumne River and for Dry Creek have confirmed general assumptions of the data sets. Also acquired during these field measurements has been flow data for the reach of the lower Tuolumne River below the “Modesto” gage and above the confluence with the San Joaquin River. Based on these measurements, an accretion of 32 cfs has been assumed to occur below the USGS “Modesto” gage. This data set has been added to the “Hydrology” Worksheet, Column M (“Modesto to Confluence”), incorporated into computations of river flow in the “DonPedro” Worksheet,

Column CP (“TR at Confluence”), and the projected flow at the confluence is reported in the “Output” Worksheet, Column AR (“Flow-Confluence”).

3.5 Miscellaneous Reference Case Data Revisions

As the result of defining a Base Case in the Model (Version 2.0), several data sets required update or revision to facilitate automated comparisons between the Base Case results and alternative scenario results. Changes to Base Case reference values occurred in table values or time series sets for:

“UserInput” Worksheet

- Existing FERC Flow Requirements at La Grange Bridge Gage
- Base Case MID Canal Diversion
- Base Case TID Canal Diversion
- Base Case Supplemental Releases

“WaterBankRel” Worksheet

- Water Bank Supplemental Release (Column T)

“DonPedro” Worksheet

- Base Case Full Diversion Demand (Column I – Column L)

“SFWaterBankRel” Worksheet

- Water Bank Supplemental Release (Column AN)

“DailyCanalsCompute” Worksheet

- DP Water Supply Factor Base Case (Column F)

“DailyCanals” Worksheet

- Base MID Canal Diversion (Column L)
- Base TID Canal Diversion (Column N)

4.0 MODEL EXECUTION

To aid in the execution, completion and recording of an alternative operation scenario, several “macro” tools have been incorporated into the Model.

4.1 Water Bank Supplemental Release Macro

A variation from Base Case Don Pedro Reservoir operation assumptions will normally cause a change in results to the CCSF Water Bank Account Balance. If needing revision from Base Case conditions (e.g., revised supplemental releases to maintain a positive Water Bank Account Balance) supplemental releases can be automatically computed by use of a macro implemented for the “WaterBankRel” Worksheet. This macro will replicate the manual action of the user to provide the day-by-day supplemental release exactly needed to maintain no less than a zero Water Bank Balance.

Figure 4.1-1 illustrates the location of the macro button in the “WaterBankRel” Worksheet. To “run” the macro the user simply “clicks” on the button identified by the label “Supplemental Release”. By invoking the macro, values will be automatically placed into Column T to maintain a positive Water Bank Account Balance. The macro will iterate computations up to 24 times to complete the process. It is advised to initialize Column T with zeroes prior to invoking the macro. It is also advised to set the Excel worksheet “Options” to a manual calculation mode prior to invoking the macro.

The screenshot shows the 'WaterBankRel' worksheet with the following data tables:

SF Water Bank Account Balance Calculation																
Month	Index	Date	Day	Days	DP Inflow CFS	La Grange UF CFS	Fourth Agree Check CFS	Daily Districts' Entitle CFS	SF Credit/Debit CFS	SF C/D w/ Credit Adj AF	SF Gross WB Balance AF	SF WB Evap Losses AF	SF Net WB Balance AF	SF Share RFlood DP AF	SF Max WB Balance AF	WB Neg Flag AF
1970.10	10/6/1970	T	31		438	137	2,416	137	301	598	570,598	48	570,000	0	570,000	0
1970.10	10/7/1970	W	31		439	139	2,416	139	300	596	570,596	48	570,000	0	570,000	0
1970.10	10/8/1970	T	31		227	142	2,416	142	85	169	570,169	48	570,000	0	570,000	0
1970.10	10/9/1970	F	31		229	144	2,416	144	85	169	570,169	48	570,000	0	570,000	0
1970.10	10/10/1970	S	31		235	149	2,416	149	86	171	570,171	48	570,000	0	570,000	0

Supplemental Release and Storage Check					
WB Supp Release AF	1st Call Lloyd Release AF	2nd Call HH Release AF	Lloyd Storage AF	HH Storage AF	DP Storage AF
0	0	0	199,997	245,204	1,657,096
0	0	0	199,998	244,404	1,655,205
0	0	0	199,998	243,605	1,654,071
0	0	0	199,998	242,806	1,652,744
0	0	0	200,000	242,006	1,651,288

Figure 4.1-1. Water bank supplemental release macro.

4.2 Copy Output Worksheet Macro

The “Output” Worksheet provides an interface between Model computations and summary and analysis tools. It also provides a formatted set of information usable for exchange into an HEC-DSS database file. Results provided in the worksheet are directly linked to the computational and input worksheets of the Model. As such, any change to model assumptions or data which causes a recalculation by the Model will automatically update the values in the worksheet. To preserve or store the results of a particular study a copy of the worksheet should be created with a unique tab name and its contents converted to values. The user can either use Excel keystroke or menu commands to create the worksheet copy, or can invoke a macro. Figure 4.2-1 illustrates the

location of the macro button in the “Output” Worksheet. To “run” the macro the user simply “clicks” on the button identified by the label “Copy Sheet / Values”. By invoking the macro, the worksheet will be “copied” as “values” into an adjacent worksheet and given a name identified by Switch UI 1.00 in the “UserInput” Worksheet. The user must save the entire workbook to not lose the new worksheet.

	A	B	C	D	E	F	G	H	I	J	K	L	M
1	1	TUOLUMNE	TUOLUMNE	TUOLUMNE	TUOLUMNE	TUOLUMNE	TUOLUMNE	TUOLUMNE	TUOLUMNE	TUOLUMNE	TUOLUMNE	TUOLUMNE	TUOLUMNE
2	2	TUOLUMNE	TUOLUMNE	TUOLUMNE	TUOLUMNE	TUOLUMNE	DONPEDRO	DONPEDRO	DONPEDRO	DONPEDRO	DONPEDRO	DONPEDRO	DONPEDRO
3	3	FLOW-LAGRANGE	FLOW-HHUNIMP	FLOW-LLOYDUNI	FLOW-ELEANORU	FLOW-UNREGUNI	FLOW-TOTINFLO	FLOW-SUP1INFLO	FLOW-SUP2INFLO	FLOW-INFLOWHH	FLOW-INFLOWLL	FLOW-INFLOWEL	STORAGE
4	4	2	3	4	5	6	7	8	9	10	11	12	13
5	5	1DAY	1DAY	1DAY	1DAY	1DAY	1DAY	1DAY	1DAY	1DAY	1DAY	1DAY	1DAY
6	6	Base_Case 4	Base_Case 4	Base_Case 4	Base_Case 4	Base_Case 4	Base_Case 4	Base_Case 4	Base_Case 4	Base_Case 4	Base_Case 4	Base_Case 4	Base_Case 4
7	Save study results	1-Oct-70	1-Oct-70	1-Oct-70	1-Oct-70	1-Oct-70	1-Oct-70	1-Oct-70	1-Oct-70	1-Oct-70	1-Oct-70	1-Oct-70	1-Oct-70
8	as unique	2400	2400	2400	2400	2400	2400	2400	2400	2400	2400	2400	2400
9	worksheet by	30-Sep-09	30-Sep-09	30-Sep-09	30-Sep-09	30-Sep-09	30-Sep-09	30-Sep-09	30-Sep-09	30-Sep-09	30-Sep-09	30-Sep-09	30-Sep-09
10	clicking button	2400	2400	2400	2400	2400	2400	2400	2400	2400	2400	2400	2400
11	↓	CFS	CFS	CFS	CFS	CFS	CFS	AF	AF	CFS	CFS	CFS	AF
12	CopySheet / Values	PER_AVER	PER_AVER	PER_AVER	PER_AVER	PER_AVER	PER_AVER	PER_AVER	PER_AVER	PER_AVER	PER_AVER	PER_AVER	PER_AVER
13	10/1/1970	125	4	10	4	107	427	0	0	90	220	10	1,667,564
14	10/2/1970	130	4	10	4	111	431	0	0	90	220	10	1,665,724
15	10/3/1970	129	4	10	4	111	431	0	0	90	220	10	1,664,041
16	10/4/1970	133	4	10	5	115	435	0	0	90	220	10	1,661,355
17	10/5/1970	135	4	10	5	117	437	0	0	90	220	10	1,659,348
18	10/6/1970	137	4	10	5	118	438	0	0	90	220	10	1,657,096
19	10/7/1970	139	4	10	5	119	439	0	0	90	220	10	1,655,205
20	10/8/1970	142	4	10	5	122	227	0	0	90	5	10	1,654,071
21	10/9/1970	144	4	10	5	124	229	0	0	90	5	10	1,652,744
22	10/10/1970	149	4	11	5	130	235	0	0	90	5	10	1,651,288

Figure 4.2-1. “Output” Worksheet copy values macro.

FOR HDR USE ONLY	
Run #	

DRAFT SCENARIO SHEET
Operations Model Run Request

Originator:
 Relicensing Participant Group:

Date Requested:
 Needed By:

Instructions: Complete this entire form, including a brief narrative description of your request. The narrative description should include specific questions you think this model run will answer and/or be specific how flow requirements should be modified. Empty scenario values will be assumed to be equal to Base Case.

Decription: _____

Section 1—Minimum Flow Requirements at La Grange Bridge	
<input type="checkbox"/> Existing 1995 FERC Requirement <input type="checkbox"/> Alternative, provided as daily time series _____ <input type="checkbox"/> Alternative, provided as Year Type Schedule _____ <input type="checkbox"/> Alternative, previous Run # _____ <input type="checkbox"/> Shared CCSF/Districts Responsibility	<i>Instructions: Attach alternative flow requirements or provide location of file containing alternative flow requirements</i>
Section 2—Canal Diversions of Modesto Irrigation District and Turlock Irrigation District	
<input type="checkbox"/> Base Case Diversions <input type="checkbox"/> Alternative diversions, volume by month <input type="checkbox"/> Alternative, previous Run # _____	<i>Instructions: Attach alternative diversions or provide location of file containing alternative diversions</i>
Section 3—Supplemental Releases to Water Bank from San Francisco	
<input type="checkbox"/> "WaterBankRel" Worksheet <input type="checkbox"/> Alternative releases, volume by month, add to Base Case <input type="checkbox"/> Alternative releases, volume by month, replace Base Case <input type="checkbox"/> Alternative, previous Run # _____	<i>Instructions: Attach alternative diversion, worksheet, or provide location of file containing alternative diversions</i>
Section 4—San Joaquin Pipeline Diversions of San Francisco	
<input type="checkbox"/> Base Case San Joaquin Pipeline Diversions <input type="checkbox"/> Alternative diversions, volume by month <input type="checkbox"/> Alternative, previous Run # _____	<i>Instructions: Attach alternative diversions or provide location of file containing alternative diversions</i>
Section 5—Additional Operational Objectives	



October 4, 2013
E-Filing

Don Pedro Project
FERC No. 2299-075

Honorable Kimberly D Bose, Secretary
Federal Energy Regulatory Commission
Mail Code DHAC PJ-12.3
888 First Street NE
Washington DC 20426

Subject: Districts' Reply Comments to California Department of Fish and Wildlife
Comments on the Meeting Notes of the June 4, 2013 W&AR-03 and W&AR-16
Consultation Workshop

Dear Secretary Bose:

On July 19, 2013, California Department of Fish and Wildlife ("CDFW") filed a letter with the Federal Energy Regulatory Commission ("FERC" or "Commission") providing comments on a Consultation Workshop held by Turlock Irrigation District and Modesto Irrigation District (collectively, the "Districts") on June 4, 2013. The Workshop conducted by the Districts on June 4, 2013 covered topics related to W&AR-03: Reservoir Temperature Model Study and W&AR-16: Lower Tuolumne River Temperature Model. CDFW's letter also provides comments related to the Districts' study W&AR-02: Tuolumne River Operations Model for which the Districts held Consultation Workshop No. 5 on May 30, 2013.

CDFW's July 19 letter provides comments primarily directed at the Districts' Tuolumne River Operations Model. CDFW expresses a concern over "a lack of validation comparing the Operations Model Base Case rules with current project operations." CDFW's July 19 letter also asserts that, according to the Districts' own statements, the Operations Model is "not intended to replicate actual water use and the recent past would not be appropriate for modeling purposes." Based on these statements attributed to the Districts, CDFW goes on to conclude that "the Operations Model Base Case does not attempt to represent current operations and is simply a starting point for future alternatives analyses."

These comments and conclusions by CDFW are simply incorrect. The Operations Model Base Case **does** depict the current demands, regulatory requirements, and operational policies of the Districts' and CCSF's Hetch Hetchy water storage and delivery systems. CDFW states in its July 19 letter that "the Districts maintain the Operations Model is not intended to **replicate actual water use**" [emphasis added]. Here, CDFW seriously mischaracterizes a statement made by the Districts. The

Kimberly D Bose

Page 2

October 4, 2013

actual statement made by the Districts, as reproduced in the Workshop meeting notes reviewed by CDFW and submitted to FERC, reads as follows: “the model is not intended to **replicate exact historical water use**” (see page 3 of the June 4th Workshop notes).

The Districts have explained on numerous occasions to all relicensing participants, including CDFW, that a daily operations model that involves irrigation and municipal water demand and supply could not possibly replicate or duplicate the **exact** patterns and magnitude of water use over time because those patterns and magnitudes occur by virtue of differing regulatory requirements, operating policies, maintenance needs, and the decisions of thousands of water users with different water demands making decisions in real time. In fact, no model has been or should be held to a standard of *duplicating* historical conditions and we doubt that CDFW would hold its own models to that standard. Consistent with FERC’s long standing policy, the Tuolumne River Operations Model base case represents the “no action” alternative; that is, the continuation of Tuolumne River water system operations under current and authorized license terms and operating conditions. This is also consistent with SWRCB’s request to use existing in- river conditions as the baseline for comparison of alternative operating scenarios.

CDFW also attributes to the Districts a statement to the effect that “the recent past would not be appropriate for modeling purposes.” Here, CDFW must be referring to these same June 4th Workshop notes where the phrase “so the very recent past would not be appropriate for modeling purposes” is found. However, it is necessary to include the first part of that sentence to truly understand its meaning related to the Operations Model. The full sentence reads: “**CCSF has been implementing construction projects on their system, so the very recent past would not be appropriate for modeling purposes**” (page 3 of the June 4th Workshop notes). This fact about recent CCSF operations was fully explained in the W&AR-02 Operational Modeling Workshop held on May 30 and fully captured in those Workshop notes (see page 4 of the May 30th notes) where Ms. Ellen Levin, Deputy Manager of the Water Enterprise for CCSF, described that recent operations of CCSF’s system include a number of “maintenance and construction-related shutdowns that have been occurring since 2005.” These would not be expected to recur any time soon, so while these outages and changes may be reflective of actual recent conditions, it would be highly inappropriate for these conditions to be reflected in the Operations Model base case. This is but one example of why trying to duplicate the very recent past would not be appropriate for modeling purposes. We refer CDFW to the W&AR-02: Operations Model Base Case, Workshop No. 5 meeting notes for the full discussion of this issue.

Given that CDFW has apparently misinterpreted statements made by the Districts in the Workshops and mischaracterized portions of the Workshop notes, it follows that the conclusion arrived at by CDFW that the “Operations Model Base Case does not attempt to represent current operations” is also incorrect. The Districts’ statement that the Operations Model does not “*replicate exact* historical water use” should not be interpreted by CDFW to infer that the Operations Model does not adequately *represent* current operations. To be clear, and contrary to CDFW’s assertions, the Districts and CCSF have both stated for the record that the rules of operation contained in the Operations Model base case accurately represent the current water supply operations and current demands of their respective systems.

We review below the substantial efforts made by the Districts and CCSF to accurately describe and demonstrate the Operations Model to relicensing participants and thereby further rectify the several mischaracterizations contained in CDFW's July 19 letter.

The Districts held W&AR-02: Tuolumne River Operations Model Workshop No. 4 on December 7, 2012 which included considerable time devoted to describing the Operations Model Validation process and results. The Districts issued the full Draft Model Validation Report on January 17, 2013 as part of the Initial Study Report (ISR). Relicensing participants' comments on the report were required to be provided by March 11, 2013. Neither CDFW, nor any other participant, had any comments on the Draft Model Validation Report.

The July 19, 2013 CDFW letter does not raise any concerns about the January 17, 2013 Draft Model Validation Report. Instead, CDFW states that since that time, the Districts have made "several significant changes" to the Operations Model. None of the five changes identified by CDFW in its July 19 letter qualifies as constituting a significant change to the Operations Model rules of operations for either the Districts' or CCSF's systems. The overarching rules of operations contained in the Base Case are substantially the same as described in the January 2013 Validation Report. None of the five items identified by CDFW produce any change to seasonal water releases from the Districts' or CCSF's systems. Each of the items described by CDFW simply represent a refinement of the model to either reflect the latest information available, produce a more efficient model, or more closely reflect actual system operations. During the May 30, 2013 W&AR-02: Operations Model Workshop No. 5, the Districts and CCSF thoroughly described and discussed each of the model adjustments identified by CDFW.

To justify its request that the Districts validate the Base Case model to "recent historic operation of the project", CDFW identifies what it believes are five "significant changes" to the Operations Model subsequent to the December 2012 Workshop No. 4. CDFW's comments demonstrate a lack of understanding of what elements of hydrology and logic are of significance to the Model and the comparative analyses to be performed by the Model. Each of the cited "significant changes" is discussed below:

- **Item 1: New model logic regarding management of reservoir releases in early July.** As explained at Workshop No. 5, the Operation Model logic concerning reservoir release management during early-July was modified to refine the Model's representation of reservoir operation to better depict actual Don Pedro operations during a short period of a few days applicable to only a few years in the 39-year period-of-record when the reservoir should fill within the first couple of weeks of July rather than the previously modeled end-of-June time frame. This refinement made daily releases more representative of current operations and does not in any way affect seasonal release volumes. This change improves the model's simulation of actual practices during wet years.

- **Item 2: Differentiation between base flow and pulse flow releases to the lower Tuolumne River and representation of current October attraction flow requirements.** This item concerns modeling current fish flow requirements. The refined logic provides better construction of the daily hydrograph assumed for monthly flow requirements as set forth under the current FERC license terms. Previously, the Model did not provide a daily pulse component during October. The revised logic allows a user-specified pattern of release. Again, both of these refinements to Model logic simply depict current operations more closely and are consistent with CDFW's desire to "attempt to represent current operations."
- **Item 3: Inclusion of new hydrologic data to eliminate negative daily reservoir inflows.** This item refers to the revisions to model hydrology made to eliminate negative daily inflows to the Don Pedro Reservoir. This revised hydrologic data set was presented at the March 27, 2013 Hydrology Workshop held with CDFW and State Water Resources Control Board (SWRCB). The model hydrology was revised to respond to a specific request made by CDFW to eliminate the occurrence of negative daily inflows to Don Pedro Reservoir while still keeping the same monthly volumes in the model in order to maintain overall water balance consistent with conservation of mass requirements. This change has the full support of CDFW and SWRCB. The entire process of modifying the model hydrology was documented in the Districts' April 9, 2013 filing with FERC: *Response to Relicensing Participants Comments on the Initial Study Report*. Section III of this filing provides a full description of the consensus approach to the model hydrology and Appendix 2 provides the Workshop meeting notes which reflect that consensus was reached. The changes made to the original model hydrology to reflect the consensus approach amounted to a "smoothing" of the underlying unimpaired flow that occurs within the Tuolumne River basin upstream of Don Pedro Reservoir. As discussed on several occasions previously, the smoothing and occasional minor rebalancing of unimpaired flow volumes within the basin does not affect Don Pedro Reservoir operations and does not constitute a change in the model's representation of either Don Pedro or Hetch Hetchy operations.
- **Item 4: Refinements to canal diversions.** This item deals with the model's depiction of the Districts' canal diversions. As discussed on numerous occasions with relicensing participants, to represent the Districts' canal demands, a methodology utilizing estimates of recent agricultural land use within the Districts and current MID municipal and industrial water demands has been employed. This methodology was chosen because it is consistent with California's statewide water plan modeling practices. An initial comparison of the Model's results to history was illustrated in the December 2012 Workshop. CDFW's July 19, 2013 letter states that one of the "significant changes" made to the Model since the December Workshop was refinements to the Districts' canal operations, including the "addition of a component to canal water supply that was previously not recognized in the data set" and "refinement of monthly turnout delivery factors." CDFW extracts these statements from the

Districts' Attachment B (revised May 20, 2013) of the Operations Model Study Report (see Section 3.2, page 3-3). A full reading of that Section 3.2 explains the reason for the model refinement (see page 3-2). As clearly explained on page 3-2, subsequent to the December 7 Workshop, both TID and MID filed with the State of California their 2012 *Agricultural Water Management Plans* as required by state regulations. These water management plans provide more recent historical operational records which led to the refinement of Model logic that depicts current water demands and canal operations of the Districts. If CDFW's true concern is for the Operations Model to "represent current operations," then CDFW should be fully supportive of these Model refinements which use the latest information available to represent the Districts' practices.

- **Item 5: Changes to the water supply factor based on changes to estimated canal demands and underlying hydrology and a review of projected operations.** During development of the Operations Model Base Case, additional effort was focused on development of a reservoir management plan for drought to be used for Model simulation purposes. Recent operations of the Districts coincide well with the Model's assumptions; however, a recent long-duration drought to use for validation purposes has fortunately not occurred. However, this limits the confirmation of the Model's overall operation during drought. Comparing the current Model results to the operations that occurred over 20 years ago during the last significant drought (1987 – 1992) would be inappropriate because of the many changes in both CCSF's and Districts' operations. For non-drought years, the Operation Model's Base Case depiction of canal diversions was specifically refined to depict recent operations, with professional judgment used to best fit the many components affecting the annually-varying projected canal diversions.

As summarized above and discussed in detail in the March 27, 2013 Hydrology Workshop, the April 9, 2013 response to comments on the ISR, the May 30, 2013 Operations Model Workshop, and the June 4, 2013 Reservoir and River Temperature Modeling Workshop, each of the five items identified by CDFW represent minor refinements to the Operations Model in an effort to use the most recent water use data and the consensus on hydrology reached on March 27, 2013 with CCSF, CDFW, SWRCB, and the Districts. Additionally, using this most recent information, the Model's logic was refined to better fit actual recorded and estimated data concerning recent canal operations, and the data are consistent with reports submitted to the State of California. Concerning the Model's assumptions for reservoir management during drought (inferred by the "water supply factor"), as also discussed above, there is no metric to validate. The operating rules incorporated into the Model produce an operation during drought that is viable when using historical hydrology as the template for future events.

One additional item raised by CDFW in its July 19 letter is a curious reference to the recently released HEC-5Q model for the San Joaquin River system. CDFW states that it is "interested in a set of modeling tools that will allow interested parties to start with water temperature objectives and explore subsequent impacts to project operations." CDFW states that the HEC-5Q basin-wide model

allows a “bottom-up” analysis, while implying that the suite of site-specific Tuolumne River modeling tools developed by the Districts under the approved FERC study plans do not. The Districts are currently reviewing the HEC-5Q and SALSIM models released by CDFW, and at this point we limit our comments to two general observations:

- As a starting point, the HEC-5Q model is inherently incapable of exploring “impacts to *project* operations” simply because it does not even attempt to model the affects of temperature-driven releases on the City and County of San Francisco’s “project operations.” This is a serious limitation and essentially prevents the HEC-5Q model from informing overall water supply project impacts on the Tuolumne River. Given CDFW’s deep concerns about a model being able to adequately represent “current operations”, ignoring even the existence of CCSF and the potential impacts to CCSF water supply operations should be a serious concern to CDFW.
- At best the HEC-5Q model is a flow rate calculator based on an assumed starting outflow temperature from Don Pedro Reservoir. The HEC-5Q model neither represents current operations of the Districts (nor CCSF) nor can it predict changes in reservoir outflow temperature under conditions of deep drawdowns during drought events due to its over-simplified representation of the thermal structure of the Don Pedro Reservoir. Therefore, any results obtained by using the basin-wide HEC-5Q model would have to be completely re-analyzed by evaluating the same scenario with the river- and project-specific Tuolumne River Operations Model and the Don Pedro Reservoir Temperature Model.
- The scope of the HEC-5Q model – the entire San Joaquin river basin – is inherently broad. FERC directed the Districts to perform studies based upon their capacity to identify and isolate effects associated with existing project operations, thereby demonstrating a capability to inform potential license requirements for the project. As a result, the Districts have prepared a variety of studies, models and analyses that are specific to conditions on the Tuolumne River and in the Don Pedro Reservoir, including bathymetry data, a three-dimensional reservoir temperature model, a river-specific downstream temperature model, and a fully transparent Tuolumne River operations model inclusive of CCSF Hetch Hetchy water supply operations. While the Districts acknowledge that the HEC-5Q model has been used in a variety of efforts concerning regional conditions within the San Joaquin River basin, its broad scope and lack of site-specific detail prevents it from being used to isolate project effects on the Tuolumne River, particularly in light of the Tuolumne and project specific models and studies that have been prepared and conducted.

Use of the HEC-5Q model is unlikely to inform potential license conditions for the Don Pedro Project. The Districts intend to provide further comments on the HEC-5Q and SALSIM models once its reviews are complete.

Kimberly D Bose

Page 7

October 4, 2013

The Districts remain concerned that CDFW's July 19 letter seriously mischaracterizes direct statements made by the Districts in Workshops and in subsequent Workshop meeting notes that have been previously reviewed by relicensing participants. Conclusions based on statements taken out of context are not helpful to the extensive and thorough consultation process undertaken by the Districts and relicensing participants in support of the cooperative development of the Tuolumne River Operations Model. The Districts continue to maintain that in the context of this FERC proceeding and the comparative analyses being performed, the Operations Model represents a reasonable depiction of current operations across the overall 1971-2009 modeling period. Both the Districts and CCSF have stated for the record that the base case rules of operation track closely with actual operations, and believe the Model is fit.

The Districts have recently decided to expand the model period-of-record through 2012 as we approach the filing of the Draft and Final License Application. As such, the Districts are extending both the base case model and model validation through 2012. The Districts will provide both the expanded base case and model validation to relicensing participants in the near future.

Sincerely,



Steven Boyd
Turlock Irrigation District
P.O. Box 949
Turlock, CA 95381-0949
(209) 883-8364
seboyd@tid.org



Greg Dias
Modesto Irrigation District
P.O. Box 4060
Modesto, CA 95352
(209) 526-7566
gregd@mid.org

cc: James Hastreiter, Office of Energy Projects, 805 SW Broadway, Fox Tower-Suite 550, Portland OR 97205
cc: Jeffrey R Single, Ph.D., Regional Manager, Central Region, State of California Natural Resources Agency, Department of Fish & Wildlife, 1234 E Shaw Avenue, Fresno CA 93710